BioMed Research International

From Micro- to Macroscopic Brain Connectivity Using Multiple Modalities

Guest Editors: Ni Shu, Yasser Iturria-Medina, and Roberto C. Sotero

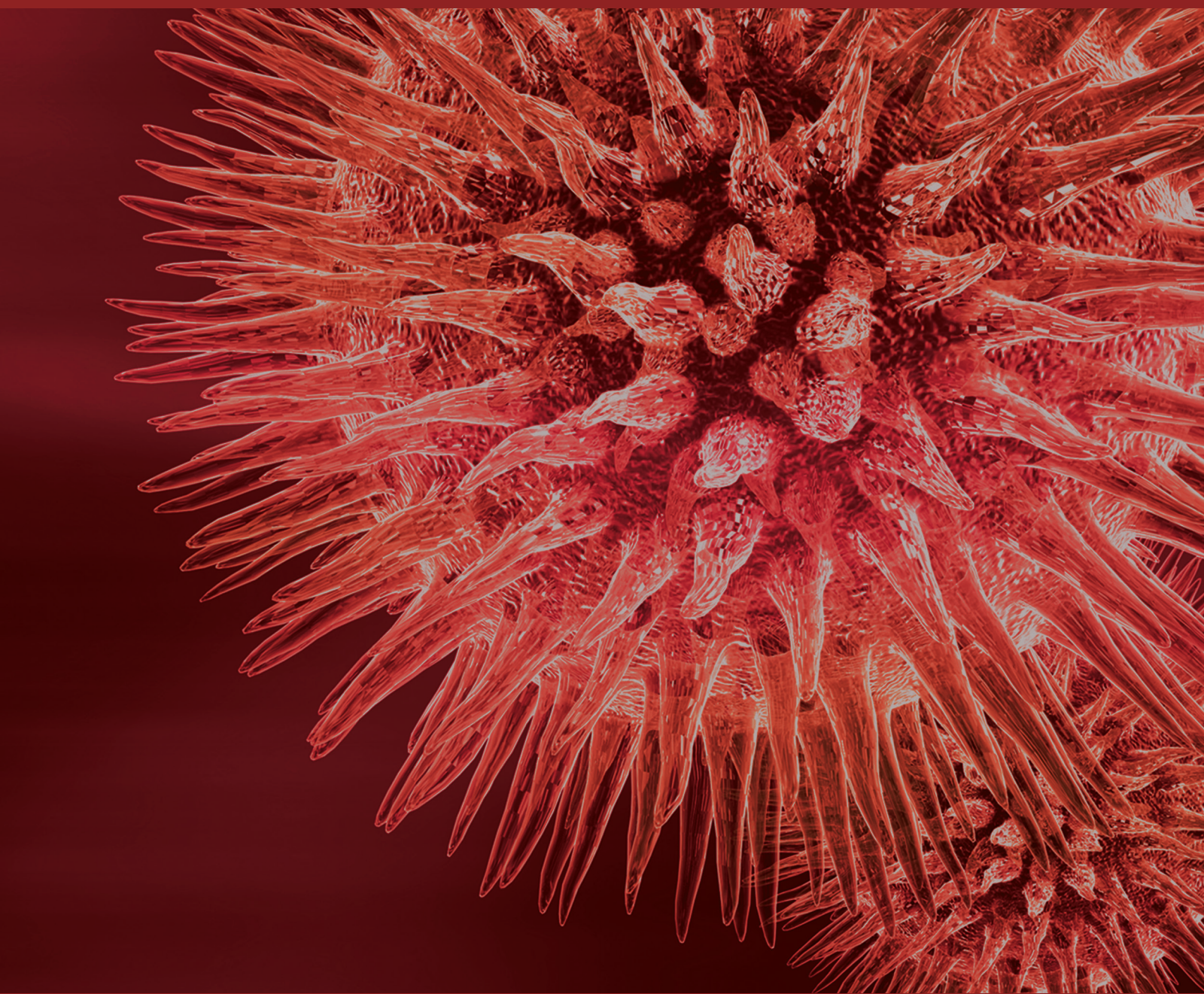

From Micro- to Macroscopic Brain Connectivity Using Multiple Modalities

BioMed Research International

From Micro- to Macroscopic Brain Connectivity Using Multiple Modalities

Guest Editors: Ni Shu, Yasser Iturria-Medina, and Roberto C. Sotero

Contents

Hindawi Publishing Corporation
BioMed Research International
Volume 2016, Article ID 8128095, 2 pages
http://dx.doi.org/10.1155/2016/8128095

Editorial

From Micro- to Macroscopic Brain Connectivity Using Multiple Modalities

Ni Shu,[1,2] Yasser Iturria-Medina,[3] and Roberto C. Sotero[4]

[1] *State Key Laboratory of Cognitive Neuroscience and Learning and IDG/McGovern Institute for Brain Research, Beijing Normal University, Beijing 100875, China*
[2] *Center for Collaboration and Innovation in Brain and Learning Sciences, Beijing Normal University, Beijing 100875, China*
[3] *McConnell Brain Imaging Center, Montreal Neurological Institute, McGill University, Montreal, QC, Canada H3A 2B4*
[4] *Department of Radiology and Hotchkiss Brain Institute, University of Calgary, Calgary, AB, Canada T3A 2E1*

Correspondence should be addressed to Ni Shu; nshu55@gmail.com

Received 24 December 2015; Accepted 24 December 2015

With the advent of brain imaging techniques, the study of human brain connectivity *in vivo* becomes possible and has offered new insights into understanding the structural organization and work mechanisms of the human brain. Using different modalities of neuroimaging, both structural and functional brain connectivity can be mapped. The connectivity analysis has been widely applied into investigating the brain mechanisms of cognitive functions and neuropathology of different brain disorders. However, there are still some challenges when mapping, analyzing, and modeling the brain connectivity at different scales. This special issue aims at reflecting the advances in studies of brain connectivity, including both modeling methods and applications. In this special issue, different imaging techniques, such as structural MRI, diffusion MRI, and functional near-infrared spectroscopy (fNIRS), were employed in the studies of brain connectivity. The applications addressed hemispheric asymmetry, primary insomnia, and motor training. Also, the computational modeling methods and analysis toolbox of brain connectivity were introduced. The types of papers include review articles as well as original research.

For the modeling methods of brain connectivity, R. C. Sotero (2015) reviews computational models of phase-amplitude coupling (PAC) generation ranging from realistic networks of Hodgkin-Huxley neurons to neural mass models (NMMs) describing only the average activity of the neuronal populations involved and showed that NMMs are rich enough to provide a variety of PAC patterns. For the analysis toolbox of brain connectivity, J. Xu et al. (2015) developed a MATLAB software package that facilitates fNIRS-based human functional connectome data-analysis, which will be useful for the resting-state brain functional connectivity (FC) studies. For the application studies of brain connectivity, N. Shu et al. (2015) investigated the hemispheric asymmetry of brain white matter anatomical network which is constructed by diffusion MRI tractography and demonstrated that the topological asymmetries of the anatomical networks might reflect the functional lateralization of the human brain. L. Zhao et al. (2015) investigated the topological alterations of the structural covariance network for patient with primary insomnia, suggesting that insomnia might be related to underlying increase in brain network integration encompassing the sensory to motor networks, the default mode network, and the salience network and decrease in the integration between the sensory regions and the frontoparietal working memory network.

The special issue also contains several review papers: B. Wong et al. (2015) review structural and functional connectivity studies of bilingualism and examined different issues such as whether the language neural network is different for first- (dominant) versus second- (nondominant) language processing; the effects of bilinguals' executive functioning on the structure and function of the "universal" language neural network; the differential effects of bilingualism

on phonological, lexical-semantic, and syntactic aspects of language processing on the brain; and the effects of age of acquisition and proficiency of the user's second language in the bilingual brain, and how these have implications for future research in neurolinguistics. T. D. Ben-Soussan et al. (2015) review the connectivity studies of quadrato motor training and proposed a general model tying cerebellar function to cognitive improvement, via neuronal synchronization as well as biochemical and anatomical changes.

In summary, the papers collected in this special issue cover a wide range of topics that are on the frontier of the methods and applications of brain connectivity.

Authors' Contribution

The three editors contributed equally to the editorial.

Acknowledgment

We thank the authors for their work and hope this special issue will find interested readers in neuroscience and clinical fields.

Ni Shu
Yasser Iturria-Medina
Roberto C. Sotero

Hindawi Publishing Corporation
BioMed Research International
Volume 2016, Article ID 7069274, 22 pages
http://dx.doi.org/10.1155/2016/7069274

Review Article

Neurolinguistics: Structure, Function, and Connectivity in the Bilingual Brain

Becky Wong, Bin Yin, and Beth O'Brien

Education and Cognitive Development Lab, National Institute of Education, Nanyang Technological University, 1 Nanyang Walk, Singapore 637616

Correspondence should be addressed to Becky Wong; nie15661@e.ntu.edu.sg and Beth O'Brien; beth.obrien@nie.edu.sg

Received 27 March 2015; Revised 16 November 2015; Accepted 22 November 2015

Academic Editor: Roberto Sotero

Advances in neuroimaging techniques and analytic methods have led to a proliferation of studies investigating the impact of bilingualism on the cognitive and brain systems in humans. Lately, these findings have attracted much interest and debate in the field, leading to a number of recent commentaries and reviews. Here, we contribute to the ongoing discussion by compiling and interpreting the plethora of findings that relate to the structural, functional, and connective changes in the brain that ensue from bilingualism. In doing so, we integrate theoretical models and empirical findings from linguistics, cognitive/developmental psychology, and neuroscience to examine the following issues: (1) whether the language neural network is different for first (dominant) versus second (nondominant) language processing; (2) the effects of bilinguals' executive functioning on the structure and function of the "universal" language neural network; (3) the differential effects of bilingualism on phonological, lexical-semantic, and syntactic aspects of language processing on the brain; and (4) the effects of age of acquisition and proficiency of the user's second language in the bilingual brain, and how these have implications for future research in neurolinguistics.

1. Introduction

It has been estimated that more than half of the world's population are bilinguals and/or multilinguals [1]. How does this widespread capacity for communicating in two or more languages impact the cognitive and brain systems in humans? For many years, the fields of psychology and neuroscience had limited tools and tended to investigate brain structure and cognitive function separately. However, recent advances in neuroimaging techniques and analytic methods have led to a proliferation of neuroscience findings regarding the impact of bilingualism on the human brain. Here we review these numerous and surprisingly diverse findings in light of current cognitive models, thereby enriching current understandings on the effects of bilingualism through mutual perspectives of linguistics, cognition, and neuroscience. Additionally, in the present review, we overcome the limited perspectives of early work in psychology and neuroscience by spanning the gap between brain structure and cognitive function. Specifically, we systematically examine the structural and functional differences in language networks for domain-general and domain-specific component processes in bilinguals/multilinguals (henceforth referred to as "bilinguals": in this paper, we do not distinguish between findings pertaining to bilinguals versus multilinguals). We also focus on individual-difference factors including age of acquisition and language proficiency that may differentially impact bilingual brain networks. Throughout this review we argue that bilingual cognition is best understood by taking into consideration both structure and function, as well as factors relevant to language learning.

2. Historical Perspective

Early neuroscience perspectives on the relationships between brain structure and cognitive function drew two opposite conclusions from then-available cruder forms of investigation. Brain structure was considered to be organized into localized, isolated areas where pockets of activity serve very specialized function, as in the tradition of Gall and Spurzheim [2] and Fodor [3]. The alternative view was that brain

structure is relatively homogeneous with distributed forms of representation, as in the tradition of Lashley [4] and Hebb [5]. According to this view, brain structure/architecture was related to function in a more holistic way that supports plasticity, whereby functions associated with damaged areas can be picked up by other undamaged areas. The former perspective was supported by myriad functional neuroimaging studies (e.g., [6–8]), while the latter perspective was taken up by connectionist investigations [9–11].

Driven by new technologies and advances in computing power, contemporary approaches to neuroscience have now been able to draw evidence from more sources than in the past, leading to new perspectives placed between these two extremes. Thus, the new evolution of neuroscience investigations is not structurally bound, like the past lesion studies, nor functionally discrete, like the early neuroimaging studies, but can accommodate both perspectives of local specialization with global coordination across areas as self-organized networks that emerge from the individual's experiential history. Current neuroscience-based models can therefore point to a developed neural substrate of networks forged by nature and nurture, which instantiate soft-assembled coordinative structures [12] organized to meet the constraints of the current behavioral task.

As a case in point, language is multifaceted, with oral and written forms as well as receptive and expressive modes, but shows evidence of certain universal properties of brain structures and their interconnections that underlie the behavioral aspects of communicating through speech and/or print in multiple languages. While structure gives clues to the architecture of language networks, function relates to the manner in which networks may be assembled within different contexts or as a result of personal experiences. At present, unresolved questions for bilingualism include the degree to which there is anatomical overlap in the neural networks used for L1 and L2 processing in various language domains.

One possibility is that there is a common neurobiological foundation for different languages (e.g., [13]), addressed below as a "universal language neural network." Although brain networks may be highly constrained across languages and routed to the same cortical circuits [14, 15], this explanation may not be tenable in the case of bilingualism, given that anatomical overlap between language networks could be sensitive to variables such as language proficiency, age of acquisition, and different scripts. A second possibility is that the spatial organization of the neural networks for acts of reading, listening, and speaking is common across one's different languages, only to the extent that a high proficiency is reached for the languages in question. This would indicate that the universal neural network is only accessed at the end of the L2 learning process. Alternatively, a third possibility is that the linguistic brain structures established from L1 acquisition are coopted for L2 learning only during a critical window of chronological development; that is, only early age of L2 acquisition or simultaneous bilingualism would allow for the assimilation of a universal neural network across languages.

In the next section, we briefly introduce advanced neuroimaging techniques and paradigms that have allowed researchers to investigate the impact of bilingualism on brain structure, structural connectivity/physical coupling, brain function, and functional connectivity/statistical coupling.

3. Neuroscience Methodologies

3.1. Techniques Used to Investigate Brain Structure. Magnetic Resonance Imaging (MRI) is a neuroimaging technique that produces high quality images of the internal structure of the living brain by using magnetic fields and radio waves to detect proton signals from water molecules [16]. It provides structural information such as neural volume (total brain volume, gray matter, and white matter volume), cortical thickness, and surface area [17]. Voxel-based morphometry (VBM) is an analysis technique that uses T1-weighted MRI scans and performs statistical tests to identify differences in brain anatomy [18].

3.2. Techniques Used to Investigate Structural Connectivity. Diffusion Tensor Imaging (DTI) is another technique that makes use of the MRI machine to image the neural tracts and fibre pathways that connect brain regions, so as to gauge thickness and density of axonal connections through measures such as fractional anisotropy [19]. Diffusion Spectrum Imaging (DSI) goes one step further in that it was specifically developed to image complex distributions of intravoxel fiber orientation, so as to overcome the inability of DTI to image multiple fibre orientations [20].

3.3. Techniques Used to Investigate Brain Function. Functional Magnetic Resonance Imaging (fMRI) detects the magnetic signal resulting from blood oxygenation and flow that occur in response to neural activity [21, 22]. Functional near infrared spectroscopy (fNIRS) is an optical neuroimaging method that goes beyond fMRI in that the latter simultaneously measures the changes in oxygenated, deoxygenated, and total haemoglobin, is portable, and can be used for both children and infants [23, 24].

Electroencephalography (EEG) measures cortical electrical activity by recording from electrodes placed on the scalp [25]. Researchers typically examine the electrical waveforms for their frequency (e.g., alpha, beta, delta, and theta), intensity and timing, typically seen in event-related potential (ERP) components, and signal coherence/synchrony [26].

Magnetoencephalography (MEG) allows researchers to study neural function in real-time based on the magnetic fields produced by neural electrical activity and, like EEG, is a technique with good temporal resolution [27].

3.4. Techniques Used to Investigate Functional Connectivity. Psychophysiological interactions analysis (PPI) is a method for investigating functional connectivity between different brain areas using fMRI data [28]. Effective connectivity [EC] analysis studies the causal influence that one neural system has on another using fMRI data, so as to allow for a richer understanding of interregional brain connectivity [29, 30].

The review that follows is split into three sections. First, we provide an overview of a "universal" language network

across languages and examine how this network functions in bilinguals. We posit that, upon learning a second language (L2), some of the same structures are engaged, such that first language (L1) and L2 processing show similar patterns of activation across these brain networks (e.g., [31–34]). Additionally, areas besides those closely associated with language function are drawn into the processing of multiple languages and some are correlated with the switching between languages [35, 36]. In the second section, we focus on the specific brain areas and subnetworks that are related to three key aspects of linguistic processing, namely, phonological, lexical, and syntactic components of linguistic processing. Finally, we consider variations to the universal language network in general and to the linguistic component subnetworks in particular, in response to variables of age of acquisition and language proficiency.

4. A Universal Language Neural Network

There is compelling evidence for a "universal" language network of the human brain. Initial insights into this network, from lesion studies, put forth the classical perisylvian language network, consisting of Broca's area (BA44) in the inferior frontal lobe, Wernicke's area (BA22) in the superior posterior temporal lobe, and the arcuate fasciculus connecting the two [37], all left lateralized in most individuals. Additionally, acts of speech draw on the caudate nucleus, superior frontal gyrus, and superior longitudinal fascicle (SLF) [38]; and acts of reading draw on visual association areas, fusiform gyrus, and the angular gyrus [39].

Among languages, including distant ones like Mandarin and English, identical areas of activation are found for speech production tasks. Word generation and rhyming tasks elicit equal activation in L middle frontal cortex and L inferior prefrontal gyrus for both Chinese and English rhyming [40], prefrontal, temporal, and parietal areas, and the supplementary motor area for English and Mandarin word generation [41]. The results of a meta-analysis of 24 studies on word production found no significant differences in hemodynamic activation between L1 and L2 processing on a variety of experimental tasks [42].

With regard to listening, equivalent areas of activation, including the L temporal pole, the superior temporal sulcus, middle temporal gyrus, and hippocampal structures, are found for bilingual individuals in both L1 and L2 [43, 44]. These findings are in line with connectionist theories which see the language network as a single system, with L2 learning being a matter of simply increasing the strength of certain connections within the same network [45, 46].

Across various languages, a common reading network is engaged. This includes dorsal, anterior, and posterior ventral systems [13, 47]. The dorsal system includes the angular gyrus and posterior superior temporal gyrus and is associated with mapping orthography onto phonological and semantic information. The anterior system includes the posterior inferior frontal gyrus and is related to decoding new words. The ventral system, including the left inferior occipitotemporal area, functions as a presemantic word form area.

Each of these linguistic acts (speech, listening, and reading) engages some common areas and requires knowledge represented at different linguistic components, including information about sound structure (phonology), word based meaning (lexical, vocabulary), and word integration (syntax). Given results from behavioral studies, the assemblages of subnetworks related to these different components of linguistic knowledge may show some departure from the common network for bilinguals. Tasks related to these component processes of language have been correlated with activity in the following brain structures.

Phonology. Phonology draws on the auditory input system in Heschl's gyrus [38], auditory association areas in the perisylvian region, including superior temporal gyrus, inferior parietal cortex, inferior frontal gyrus, and the arcuate fasciculus-Broca's area-Wernicke's area pathway [37].

Semantic Vocabulary Knowledge. Semantic vocabulary knowledge draws on amodal association areas such as the middle temporal gyrus, posterior STS, temporoparietal cortex, supramarginal gyrus, anterior inferior frontal cortex, a long-range dorsal fibre tract that connects the temporal lobe with Broca's area, and also the angular gyrus for sentence-level semantics [38, 48].

Syntax. Syntax draws on the L pars opercularis, pars triangularis in Broca's area, and the posterior superior temporal gyrus, connected by the arcuate fasciculus [38, 49].

While the general language network may be similar across languages and even between languages used within a bilingual individual [33, 50–55], there appear to be more variations in the way these subnetworks for the component processes are engaged and assembled. This may partially result from certain features of bilingualism that differentially impact the way that two or more languages are managed. In particular, the age at which one learns a second language affects whether these subnetworks overlap or utilize separate brain areas, implying that language learning is neurophysiologically instantiated in a different manner across development (e.g., [56]).

Further, language proficiency is also differentially related to both structure and activity across brain areas, indicating a similar modification of the way language is instantiated in the brain over the course of learning the language (e.g., [52]). These two factors, age and order of language acquisition plus achieved proficiency, are partially associated and may interact with the overlap versus divergence of neural pathways used for language tasks, such as reading. For instance, simultaneous acquisition of reading in two orthographies lends itself to divergent pathways for reading in each language, whereas sequential reading acquisition gives rise to largely overlapping reading circuits in both languages [57].

In some cases, the type of language (tonal versus nontonal; or logographic versus alphabetic orthographies) involved in bilingualism also results in variation on structural and functional differences in the brain [47, 58, 59]. One area of difference in brain circuitry/function for bilingual compared with monolingual individuals pertains to executive function processes, as described next.

5. What Are the Effects of Bilinguals' Executive Functioning on the Structure and Function of the "Universal" Language Neural Network? Do These Effects Differ from Those of Monolinguals, and If so, How?

The three core aspects of executive functioning that have been identified by Miyake et al. [60] are inhibitory control, shifting, and updating. Inhibitory control refers to the ability to deliberately override a dominant or automatic response [61, 62]. Shifting refers to the ability to move flexibly between multiple tasks or operations [60, 63]. Updating refers to the ability to monitor information that is held in working memory and revising it as appropriate with newer or more relevant information [64, 65].

Many behavioral studies and reviews have found that bilinguals show advantages in tasks of executive functioning (EF) (e.g., [66–68]). EF tasks require the participants to engage in high-level cognitive functions to coordinate their thoughts and actions for goal-directed behaviors [69–71]. It must be noted, however, that this argument of a bilingual advantage in EF has recently been under much scrutiny and debate (e.g., [72–74]). For example, Paap et al. [75] argue that there have been possible methodological issues with and differences among behavioral studies, involving inappropriate baselines and/or questionable use of statistical tests.

In this section, we contribute to the ongoing discussion by examining theoretical models for bilingual language processing and empirical findings from neuroscience studies on the structural, functional, and connective changes in the human brain that ensue from bilingualism and whether this differs from monolinguals, in an effort to clarify the "hazy" differences between bilingual and monolingual brains [72].

Cognitive models of bilingual language processing implicate a specific role for nonlinguistic executive functioning [76]. For example, Green's [77] inhibition control model posits that bilinguals experience a constant competition between the lexical representations of both languages and therefore must use inhibitory control—a domain-general resource—to inhibit the activation from the nontarget language. Similarly, the bilingual interactive activation+ model [78] proposes that there is a decision and response selection mechanism that imposes top-down control in selecting between activated lexical representations. Some consensus has emerged in the literature that bilinguals recruit some measure of domain-general executive control to switch between languages [79, 80]. These models strongly suggest the importance of executive functioning in language processing for bilinguals.

It must be noted, however, that there may be a difference between executive functioning for bilingual language control (e.g., switching between languages and/or inhibiting nontarget lexical representations) versus nonlinguistic executive functioning (e.g., switching between tasks). Preliminary research indicates that bilinguals' advantage for executive functioning might be limited to the former ([79, 81], cf. [82]).

Moving on to the effects of executive functioning and language control on the bilingual brain, neuroscience studies have found structural, functional, and connectivity differences in brain areas associated with domain-general cognition for bilinguals as compared to monolinguals, particularly in the basal ganglia and the frontoparietal brain network.

5.1. Structure. Studies have found differences in brain structure between bilinguals and monolinguals particularly in frontoparietal brain areas traditionally associated with cognitive control and executive functioning. For example, using voxel-based morphometry (VBM), Mechelli et al. [83] found that grey matter density in the inferior parietal cortex was higher in bilinguals than monolinguals and that this effect was sensitive to age of acquisition and proficiency. Specifically, the structural difference was more pronounced in early bilinguals than late bilinguals, as well as bilinguals with a higher L2 proficiency. Using high resolution anatomical MRI, Della Rosa et al. [84] also found that multilingual children had greater grey matter density than monolingual children in the inferior parietal lobe. The authors argued that increased grey matter in the IPL was likely the source of their enhanced attentional and cognitive control.

A number of researchers have also found structural differences in the basal ganglia, particularly the caudate nucleus. For example, using VBM, Zou et al. [85] found that grey matter volume in the left caudate nucleus was higher in bilinguals than monolinguals. The researchers argued that this area was implicated in cognitive control, because functional activation in the caudate nucleus was higher when bilinguals switched between languages, compared to when they did not switch. Hosoda et al. [86] reported that a training intervention for L2 vocabulary in bilinguals resulted in a significant increase in grey matter volume in the caudate nucleus, among other brain areas. A review by Li et al. [87] similarly reported that bilinguals consistently show greater GM volume and density in the caudate nucleus as compared to monolinguals.

Given that the basal ganglia, particularly the caudate nucleus, is known to be part of an anatomical network subserving functions within the dorsolateral prefrontal cortex [88] for goal-directed behavior [89], and since this brain area is implicated in switching between languages in the bilingual brain [90], it is plausible that this brain area, together with the frontoparietal network, might be the locus of the bilingual advantage in executive functioning and language control.

5.2. Structural Connectivity. Using DTI, Grady et al. [91] found stronger connectivity in the frontoparietal control network in bilinguals compared to monolinguals when they were at rest. This network includes the dorsolateral and inferior frontal regions and the inferior parietal lobe and is well-known to be implicated in executive functioning, attention, and cognitive control [92].

5.3. Function. Using fNIRS, Kovelman et al. [93] found that bilinguals activated the dorsolateral prefrontal cortex (DLPFC) and the inferior frontal cortex in a semantic judgment task more strongly than did monolinguals, even though

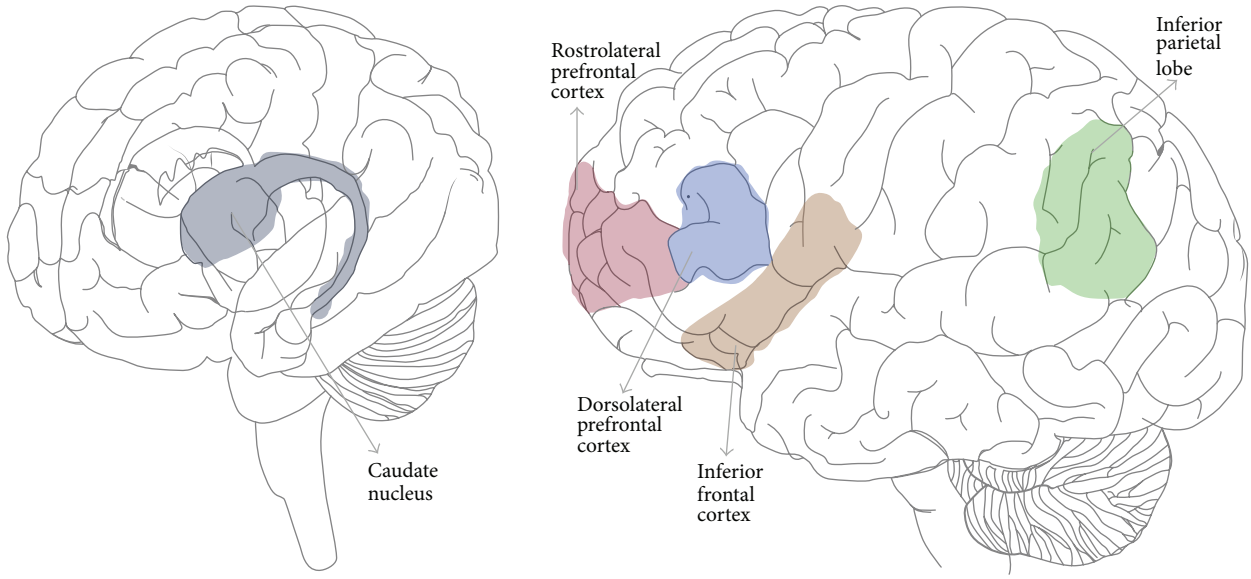

Figure 1: Key brain areas implicated in executive functioning in bilinguals.

both groups had equally good performance in the task. Since previous research has linked the DLPFC with working memory [94, 95], the researchers took this to mean that the ability to process more than one language might have led to functional changes in brain regions that support working memory associated with language processing.

This parallels the findings of a fNIRS study by Jasińska and Petitto [96], where the researchers found that bilinguals activated the classic left hemisphere language areas (L inferior frontal gyrus, superior temporal gyrus) and the domain-general cognitive areas (dorsolateral prefrontal cortex, rostrolateral prefrontal cortex) more strongly than did monolinguals in a reading task. Previous research has found that RLPFC is linked to planning, reasoning, and integrating information [97, 98], and the DLPFC to working memory. As such, the researchers proposed that the bilinguals' experience with monitoring and selecting between two language systems might have been linked to the greater prefrontal cortical activation. The key brain regions implicated in executive functioning in bilinguals as compared to monolinguals are shaded in Figure 1.

In light of the recent debate on the bilingual advantage in EF, then, while we acknowledge that the frequency and effect size of the bilingual advantage in EF may have been inflated by questionable practises among behavioral studies, we argue that existing neuroscience findings paint a consistent picture of the bilingual advantage in EF. Certainly, higher numbers of participants would be ideal for future neuroscience studies to increase statistical power (cf. [72, 73]). However, at our current state of knowledge, current research points to stronger EF in bilinguals, along with increased gray and white matter volume and regional activation in areas associated with cognitive control (specifically, frontoparietal network and basal ganglia, as shown in Figure 1), supporting the notion of a bilingual advantage in executive functions.

Yet another set of findings indicates a bilingual *disadvantage* in specific language abilities/competencies. Friesen and Bialystok [99] frame this disparity in terms of control mechanisms versus representations, or crystallized knowledge. They make the case that while the control mechanisms, such as cognitive control and executive functioning outlined above, seem to be better for bilinguals than monolinguals, the opposite is true for lexical representation. Behaviorally, monolinguals display faster picture naming times than bilinguals in either language [100, 101] and produce more words in verbal fluency tasks [102], particularly in the initial portion of such timed tasks [103]. More specifically, a bilingual disadvantage holds for some forms of crystallized knowledge, such as vocabulary knowledge (e.g., [104]), but not for others, such as metalinguistic skills like phonological and morphological awareness (e.g., [93]).

6. How Is the Differential Effect of Bilingualism on Phonological, Lexical-Semantic, and Syntactic Aspects of Language Reflected in the Structure and Function of the "Universal" Language Neural Network?

Cognitive models help to differentiate these knowledge forms or representations of language further. For instance, Ullman [105, 106] differentiates language processes that involve more declarative memory from more rule-like aspects of language. Vocabulary knowledge and word phonology both involve arbitrary mappings between word labels and their meanings and would draw on declarative memory. Syntax and grammatical knowledge would constitute procedural forms of memory that involve rule-based learning instead of arbitrary mappings.

Kroll and Stewart's [107, 108] model of second language learning makes the further distinction between declarative

memory as word labels and concepts or semantic knowledge. In their model, the former consists of two separate lexical stores, with one store of word labels per language, and the latter is a single store of word meanings that become linked to the word labels from both language lexicons. Word labels are essentially the arbitrary sounds or printed forms associated with the lexical entry and constitute the whole word phonology. For a bilingual, these arbitrary links between lexical labels to semantic features are said to be weaker [109].

How do these cognitive models play out in the brain? Taylor et al.'s [110] meta-analysis of reading studies using neuroimaging found support for Ullman's [105, 106, 111] model with regard to declarative, temporal lobe versus procedural, cortical-subcortical systems function-to-structure links. They reported clusters of activity related to various language tasks, all in the left hemisphere. Cluster-to-function relations included the occipitotemporal cortex related to orthographic analysis; the anterior fusiform and middle temporal gyrus related to lexical/semantic processing and declarative memory; the inferior parietal cortex related to spelling-sound conversion and procedural memory; and the inferior frontal gyrus as related to phonological output resolution and procedural memory.

Thus, while many of the same areas and networks are utilized for both L1 and L2 in bilinguals, even within these shared regions there may be differences in the level of activity (e.g., fMRI) and the degree of connectivity (e.g., DTI) in bilinguals compared with monolinguals. We might expect that relative weakness in semantic/lexical representations (e.g., [104]) and syntactic knowledge (e.g., [112, 113]) for bilinguals is reflected in structural differences as less gray matter volume and white matter connectivity, and functional differences as less activation in areas and subnetworks that are related to lexical and syntactic processing. On the other hand, subnetworks related to metalinguistic processing, such as phonology, may show structural and functional differences in the opposite direction in bilingual individuals, that is, increased gray and white matter and increased activation (following [93, 114]).

In the next sections, we review structural and functional integrity of the respective neural areas and systems related to phonological, lexical, and syntactic processing for bilinguals compared with monolinguals and within-individual differences in processing one's L1 versus L2. In contrast to the universal language network noted above for linguistic acts generally, we show that neural structure and function for these linguistic components are affected by one's linguistic experiences.

6.1. Phonological Processing. Phonological awareness is a metalinguistic skill, which involves the awareness of and ability to discriminate or identify phonological structure of one's language. This includes knowledge of rhyme, syllables, and phonemes (i.e., the smallest units of speech, such as *ba, da*). In alphabetic languages, phonological awareness is a foundational skill for literacy acquisition and also contributes to learning to read nonalphabetic languages [115]. Bilingual exposure facilitates superior phonological awareness [116]. The focus of this section is on brain areas involved in phonological processing for bilinguals and L2 learners.

6.1.1. Structure. Overall, there is evidence for significant differences in brain structure between bilinguals and monolinguals across many of the traditional language areas, including those areas related specifically to phonology. Gray matter volume (VBM) is reported to be significantly greater in bilinguals for Heschl's gyrus [117], the superior temporal gyrus [118–120], left inferior parietal cortex [83, 121, 122], and inferior frontal areas [123].

Functionally, monolingual studies indicate that the superior temporal gyrus is linked to acoustic and phonological processing, while the inferior parietal cortex is linked to semantic/lexical learning [87]. Additionally, increased grey matter volume is found in the caudate nucleus [85], which is associated more with phonemic than semantic fluency [33].

6.1.2. Structural Connectivity. Structural connectivity differs between bilinguals and monolinguals as well. For instance, DTI studies using fractional anisotropy (FA) report that superior bilingual language ability is linked to greater white matter in the arcuate fasciculus [124] and temporoparietal connections [125]. Luk et al. [126] also report higher FA values for early bilinguals compared to monolinguals, for tracts in the right inferior frontooccipital fasciculus, uncinate fasciculus, and the superior longitudinal fasciculus. The arcuate fasciculus connects the temporal cortex with the pars opercularis region of Broca's area (BA 44), and the superior longitudinal fascicle (SLF) also connects superior temporal gyrus to the premotor cortex [127]. The uncinate fasciculus links the anterior temporal lobe with the inferior frontal gyrus, whereas the frontooccipital fasciculus links the frontal lobe to the occipital lobe, as the name implies.

6.1.3. Function. Functional imaging and electrophysiology studies also show variations in activity patterns across similar areas for bilinguals. ERP studies demonstrate that in adults and infants perception of speech phonemes is categorical. For example, there are sharp boundaries between perceiving an acoustic signal as a/p/versus a/b/. This is shown with a mismatch negativity paradigm, and has been localized to the left planum temporale, posterior to the auditory cortex [128].

Similar studies with bilingual participants show that second language speakers of a language also demonstrate this categorical phoneme perception. Using near-infrared spectroscopy (fNIRS), Minagawa-Kawai et al. [129] reported categorical phoneme perception of Japanese vowels in groups of both Japanese L1 and L2 speakers. However, the L2 group showed slower response times, and only the L1 group showed a relation of performance to activity in the left auditory area. Further, Tan et al. [40] found similar activation across L1 and L2 (Chinese and English) on a rhyme task related to L middle frontal cortex and L inferior prefrontal cortex. The authors concluded that the bilinguals used similar phonology networks and transferred their syllable level processing from L1 to L2.

Even in infancy, activation of areas related to a phonetic discrimination task has been found to be similar between

monolinguals and bilinguals [130]. Both groups activate parts of the language network also found in adult studies, including the L superior temporal gyrus (related to phonetic processing in adults) and the L inferior frontal cortex (related to semantic retrieval, syntax, and phonological patterning in adults).

In their study with bilingual adults, Grogan et al. [33] established a link between function and structure with regard to phonological processing for speech production. The authors found that participants with better phoneme fluency than semantic fluency had increased grey matter density in the bilateral presupplementary motor area and the head of the caudate. Importantly, this positive relation of function and structure was strongest for the bilinguals' L2 compared with their L1.

Given the purported role of the caudate nucleus in procedural memory [111] and control processes [90], this finding demonstrates how processing of a second language impacts brain circuitry beyond language areas. In this case, the caudate may be drawn upon to manage activation and suppression between the bilingual's lexicons and to assemble the phonological sequence for articulating a response in the targeted language.

6.1.4. Functional Connectivity. Using psychophysiological interaction analysis in English and Chinese pseudoword rhyming tasks, Cao et al. [47] found differences in functional connectivity during L1 and L2 processing. In the L1 tasks, greater connectivity occurred in the R precentral gyrus and three visuo-orthographic regions (L fusiform gyrus, L middle occipital gyrus, and R middle occipital gyrus), suggesting active sensorimotor processing during Chinese word rhyming. In the L2 tasks, greater connectivity occurred between the L postcentral gyrus and the R middle occipital gyrus, suggesting the importance of somatosensory feedback for this task with foreign phonemes.

Using graph theory in their study of bilingual and monolingual adults, García-Pentón et al. [131] reported two main networks that show stronger connectivity in bilinguals than monolinguals. The first comprises L frontal, parietal, and temporal regions (insula, superior temporal gyrus, pars triangularis and pars opercularis of the inferior frontal gyrus, and medial superior frontal gyrus). This network is potentially involved in phonological, syntactic, and semantic interference between languages. The second network involves the L occipital and parietal-temporal regions (R superior frontal gyrus, L superior occipital gyrus, R superior frontal gyrus, L superior parietal gyrus, L superior temporal pole, and L angular gyrus). This second network is postulated to facilitate visual word recognition, reading, and semantic processing.

Both of these networks were more graph-efficient in bilinguals as compared to monolinguals; that is, they had higher capability of transferring information, as higher efficiency indicates that pairs of nodes "have short communication distances and can be reached in a few steps" [132, page 14]. Further, age of language acquisition also played a role, whereby early acquisition resulted in the development of specialised structural brain networks in terms of higher connection density between regions and more graph-efficient flow of information.

In sum, across the structural, functional, and connectivity investigations, phonological processing areas show some differences between bilinguals compared to monolinguals. As predicted, bilinguals showed increased brain volume in traditional phonology-related areas (temporal, temporoparietal, and frontal areas) and greater connective white matter volume between these areas (AF, SLF, and uncinate fasciculus). At a basic level, these structural differences may correspond to the enhanced phonological awareness that comes with bilingual exposure, supporting the hypothesis that areas related to spelling-sound conversion (IPC) and phonological output (IFG) would show increases in structure and function with bilingualism (following [93, 114]).

Functionally, bilinguals' ERPs were qualitatively similar to monolinguals' for phoneme perception tasks, even though overt behavioral responses were slower and unrelated to temporal brain area activity. This might indicate weaker declarative-knowledge types of representations that may not be consolidated within the temporal brain areas. On the other hand, frontal area activation (L IFC) continued to be elicited with phoneme discrimination by bilingual infants for both L1 and L2 as they grew older (12 months), whereas this frontal engagement for a second language dropped out for monolingual infants. Also, performance on L2 speech production tasks requiring phonemic processing was positively related to increased structural volume in frontal (SMA) and basal ganglia (CN) areas.

With regard to connective networks, bilinguals also showed different assemblages for each language when making rhyme judgements and overall greater estimated processing efficiency within local subnetworks (frontoparietotemporal and occipitoparietal). At the same time, they evidenced less global whole brain network efficiency. These findings suggest that bilingualism may result in the formation of early specialized subnetworks that deal with phonological, as well as semantic and syntactic, information between languages [131]. The key brain areas and connections showing variation in structure and functional activity for bilinguals performing phonological processing tasks are illustrated in Figure 2.

6.2. Lexical-Semantic Processing. Lexical knowledge encompasses both the breadth and depth of the meaning of words, where breadth indicates the number of known words or vocabulary size, while depth indicates the degree of representation of a known word, including its semantic connections to other words (synonyms, antonyms), and morphological and syntactic variations [133]. Vocabulary bears strong relations to reading comprehension, directly and indirectly through conceptual knowledge [134]. Both vocabulary breadth and depth are reduced in bilinguals' languages [104, 135]. The focus of this section is on neural correlates of lexical-semantic processing by bilinguals and L2 learners.

6.2.1. Structure. For monolinguals as well as bilinguals, MRI studies reveal that vocabulary size correlates positively with grey matter volume in the L and bilateral supramarginal gyrus in the left hemisphere [136–138]. As a group, bilinguals show

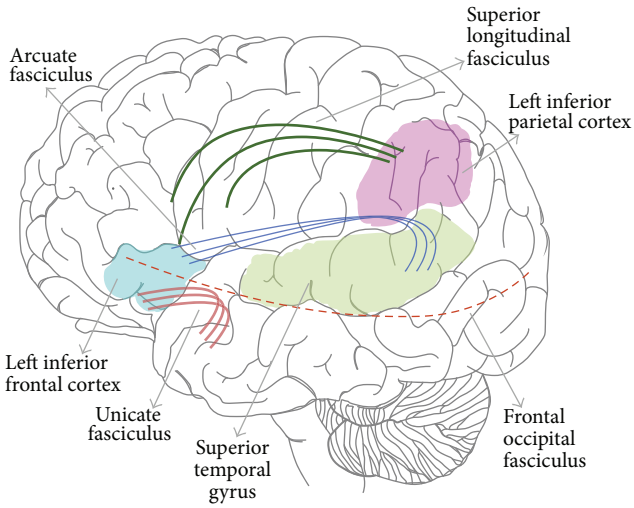

FIGURE 2: Key brain areas and connections showing variation in structure and functional activity for bilinguals performing phonological processing tasks.

greater volume in these areas compared with monolinguals [83, 139].

Grey matter volume in the L pars opercularis of the inferior frontal gyrus is also positively related to speed and accuracy of making lexical decisions, verbal fluency [139], and expressive vocabulary [86].

6.2.2. Structural Connectivity. Studies investigating structural connectivity in lexical-semantic processing similarly implicate supramarginal areas and the IFG. For example, using fractional anisotropy (FA) analysis, Hosoda et al. [86] found that white matter between the IFG-pars opercularis and the supramarginal gyrus and the superior temporal gyrus is related to increased L2 competence. This relation was stronger in the R hemisphere structures and increased after L2 vocabulary training, along with increased connectivity in the R pars opercularis-caudate nucleus pathway. This plasticity was transient, however, and reversed at one-year follow-up [86].

6.2.3. Function. While some findings with functional imaging show overlap in areas activated in bilinguals and monolinguals for lexical-semantic tasks, others show that some disparities exist as well. As with the structural studies, the two main sets of findings pertain to the frontal cortex and temporal cortex.

For frontal areas, Kovelman et al. [140] found that early bilinguals showed different brain activation patterns compared with monolinguals in the prefrontal cortex (DLPFC and IFC), even though they recruited similar language areas (Broca's 44/45). These differences occurred when bilinguals had to use both or either of their languages. When bilinguals had to use one language only, they showed greater signal intensity (as measured by changes in oxygenated hemoglobin) in DLPFC and IFC areas. This finding was taken to suggest neural activity to support working memory and attention associated with bilingual processing.

Similarly, in a visual lexical decision task with morphologically related primes, Bick et al. [141] found that highly proficient Hebrew-English bilinguals activated the L inferior and middle frontal gyri and occipital-temporal regions regardless of language type. However, the degree of activation was modulated by semantic properties for English only, showing cross-language sensitivity to differences in linguistic structure.

Vingerhoets et al. [142] reported that late multilinguals show similar regions of activation regardless of language used (Dutch, French, and English) during covert lexical-semantic processing. However, certain task-specific requirements activated additional areas during L2 processing. Specifically, picture naming involved additional L2 recruitment of L frontal areas, and inferior frontal, lateral, and medial areas (including Broca's), while word generation involved additional recruitment of inferior frontal and L middle temporal gyri for L2 processing.

Yet other studies report differences in functional activation in the temporal cortex for L2 lexical-semantic processing. Jeong et al. [143] manipulated whether L2 Korean words by Japanese learners were learned through situation-based dialogue or from print. They found that the R supramarginal gyrus was active for L2 words learned in the former manner, while the latter manner of learning drew greater activation in the L middle frontal area (WM) during the retrieval test. Further, when words that were learned in one condition were tested in the other condition (e.g., situation-learned, print tested), the L inferior frontal gyrus was activated, supporting the role of IFG in flexible retrieval of L2 vocabulary.

Raboyeau et al. [144] examined fMRI activation patterns during phases of learning new L2 Spanish vocabulary by French speakers (early, first 5 days, and later, 2 weeks). Left inferior frontal and Broca's region activity was associated with early learning, along with anterior cingulate cortex and DLPFC activation, suggesting the role of these areas in effortful lexical retrieval, phonological output, and monitoring, respectively. During the extended learning phase, L premotor cortex and R supramarginal gyrus as well as cerebellum areas were activated.

Finally, Crinion et al. [145] found with a semantic priming task in German-English and Japanese-English bilinguals that L ventral anterior temporal lobe activity was reduced with semantic primes (compared with unrelated primes) regardless of the language and regardless of whether the prime and target were in the same language. In contrast to this language general effect, a whole brain fMRI analysis found language-specific effects in the L head of the caudate nucleus. In this case, only semantically related word pairs that were presented in the same language showed reduced activity; other conditions with different language pairs showed increased activity in the CN. This suggests a role of the CN in lexical-semantic control, which the authors interpreted as a possible mechanism for regulating output given variations in language input.

6.2.4. Functional Connectivity. Ghazi Saidi et al. [146] examined functional connectivity after L2 vocabulary training for Persian-French bilinguals in a picture-naming task. They

reported increased functional connectivity within both networks with increasing L2 proficiency. The two networks included language areas (L temporal, perisylvian, and frontal areas) on the one hand and domain general cognitive control areas (bilateral cingulate, postcentral gyri, R superior parietal and inferior frontal gyri, and L superior frontal gyri) as regions of interest on the other.

In sum, lexical-semantic processing in bilingual and L2 learners is associated with similar areas as in monolinguals and L1, including anterior inferior frontal cortex and supramarginal gyrus. Increased volume and structural connectivity between these areas is reported for bilingual and L2 learners. Additionally, structural connectivity between inferior frontal with superior temporal gyrus, as well as the caudate nucleus, is also related to training induced changes in L2 vocabulary. Activation in these areas of the temporal and frontal "universal reading network" also showed increases in bilinguals or L2 learners when they process lexical-semantic information. While most areas were insensitive to different scripts, there was some indication that task type or learning modes or phases impacted different parts of the network, with frontal areas (e.g., L IFG) relating to early learning phases and flexible retrieval (across modes) of new vocabulary in an L2.

In light of behavioral findings that point to a bilingual disadvantage in lexical knowledge, we had predicted generally lower structural volume and connectivity, as well as lower function-related activity and connectivity for bilingual and L2 lexical-semantic processing. Yet this is not the pattern of the reported results. Instead, we observe apparently divergent findings between structure and function for bilinguals on one hand and behavioral differences between bilinguals and monolinguals on the other. The set of results here, taken in line with the behavioral findings of reduced bilingual lexical knowledge and efficiency, may need to be considered in light of effortful versus efficient processing (e.g., see [110]). In other words, reduced knowledge and efficiency observed behaviorally may be reflected neurally in terms of more volume and activation, characteristics of more effortful processing. This may be the case for the studies examining function, where bilingual compared with monolingual groups showed greater activation during semantic word processing tasks, especially in the prefrontal and inferior frontal cortex—areas outside the language circuits. These areas correspond more closely with general cognitive functions like working memory and may therefore reflect greater effort for bilinguals even when only processing one of their languages (e.g., [93, 114]).

With regard to the structural findings, both gray and white matter volume were greater for bilingual groups and even more so for multilinguals, possibly as a correlate of overall vocabulary size across known languages. These metrics also waxed and waned with second language proficiency after L2 vocabulary training. This suggests a more fluid relation of structure and function compared with our original hypothesis, and the findings above further suggest that the neural substrate assembled for lexical-semantic processing is responsive to both context-specific factors (e.g., [143]) and language-specific contexts (e.g., [145]).

6.3. Morphosyntactic Processing. In this section, we discuss the neural correlates of syntactic representation and processing in bilinguals/L2 learners. Syntax is a module of grammar which can be defined as a system of combinatorial rules that enables the generation of an infinite number of sentences from a finite lexicon. Syntactic knowledge can be characterized by its generative and systematic nature. The rule-based nature of syntax is in contrast with vocabulary, where the form-meaning association in words (i.e., lexical knowledge) is largely arbitrary. As mentioned above, these two types of knowledge are thought to be acquired via different memory systems for monolingual speakers: procedural and declarative, respectively [105, 106, 111]. According to Ullman's model [111], L2 learners employ the declarative system for the learning of both types of linguistic knowledge, especially those at lower proficiency levels. That is because instead of computing morphosyntax information from smaller units in accordance with linguistic rules, such information tends to be remembered as an unanalyzed chunk for second or additional languages. We review studies that discuss L1-L2 differences in the neural aspects of morphosyntactic processing.

6.3.1. Structure. The cerebellum is considered part of the procedural memory network. Its role in syntactic processing has been demonstrated in studies reporting a link between cerebellar damage and grammar impairment (see review in [147]). In their study with whole brain MRI, Pliatsikas et al. [148] report greater GM volume in several cerebellar areas for highly proficient L1 Greek/L2 English bilinguals compared with monolingual controls. Further, cerebellar GM volume was significantly correlated with behavioral performance on an English masked priming morphological task. The negative relationship between response time (i.e., faster, more efficient) and greater cerebellar volume was only evident for the L2 group, not the monolingual controls. The structure-behavior relation was also specific to a rule-based condition with past tense inflection. The conditions that did not involve rule-based morphological application did not show such a correlation, implying the cerebellum is not simply related to word reading or lexical decision tasks.

6.3.2. Structural Connectivity. Most research on the connectivity of morphosyntactic language pathways for bilingual or L2 speakers shows that structural differences covary with L2 grammatical competence and learning. Using DTI, Xiang [149] found that L2 grammar competence was correlated with volume of the BA45 (pars triangularis of the IFG) to posterior temporal lobe pathway. To examine the grammar acquisition process in a more controlled way, other investigators have employed artificial language learning paradigms [150–152].

Of particular interest, Friederici et al. [150] looked at the learning of two types of syntactic information: local transitions (such as $(AB)^n$) and hierarchical structures (such as A^nB^n). While the former information can be learned by both human and nonhuman primates, it is argued that hierarchical structures can only be learned by humans. This position is supported by linguistic theories which take the hierarchical nature of syntax and phonology to

be the hallmark characteristic of human language (e.g., [153, 154]). Friederici et al. [150] postulated that learning of local transitional probabilities ($(AB)^n$) can be mapped to the ventral premotor cortex and the frontal operculum (FOP) while Broca's area is responsible for the computation of complex, hierarchical information (A^nB^n). Participants were assigned to either of the two learning conditions with fMRI data acquired two days after learning and structural data (DTI) acquired from 4 of the participants (2 from each learning group). The authors found that the "local transition" participants showed structural connectivity of the FOP via the fasciculus uncinatus to the temporal lobe. The "hierarchical structure" participants demonstrated the same profile but showed an additional connectivity of Broca's area via the fasciculus longitudinalis superior to the temporal lobe.

Flöel et al. [151] found similar results: participants learning an artificial grammar showed a correlation between grammaticality judgment and white matter integrity in fibers originating from Broca's area. In contrast, Loui et al. [152] posited that R rather than L hemisphere areas implicated in pitch-based grammar learning. Specifically, their study showed that participants' ability to generalize learned rules to novel sequences correlated with the volume of the ventral arcuate fasciculus in the R hemisphere and with white matter integrity underlying the R temporal-parietal junction.

6.3.3. Function. ERP research on the temporal dynamics of language processing yields primary neurolinguistic evidence bearing on L1-L2 syntactic processing differences especially in relation to the D/P model. Of interest are the ELAN (early L anterior negativity) and P600 effects, where the former has been interpreted as reflecting first-pass, automatic parsing, characteristic of native language processing, and the latter reflects a more controlled process of grammatical reanalysis and repair. Here, it has often been found that low-proficiency L2 learners do not evidence ELAN in syntactic/morphological violation judgments (e.g., [155–158]). For such speakers, only the less automatic/more controlled pattern of P600 effect was observed (e.g., [159, 160]). A biphasic pattern of ELAN followed by P600 is only observed in higher-proficiency speakers [160–162].

fMRI studies, in contrast with ERP studies, generally reveal that native and L2 syntactic processing recruit the same or similar regions, indicating a universal language network for syntax. Reported L1-L2 differences in such studies involve the relative degree of activation of these common areas. For instance, in a covert/silent sentence production task administered to native French speakers with moderate proficiency in English, Golestani et al. [163] found that regions such as Broca's area, dorsolateral prefrontal cortex, and R superior parietal cortex were activated in both L1 (French) and L2 (English) but that production in L2 resulted in greater activation in the L prefrontal area.

Unlike the production task in Golestani et al. [163], Wartenburger et al. [54] administered a grammaticality judgment task requiring comprehension to Italian-German bilinguals. For their early, high proficiency group, no differences were detected in brain activation regardless of whether such participants were judging sentences in their L1 or L2. The other lower proficiency groups (one early exposure and one late exposure group) showed more extensive activation involving Broca's region and subcortical areas when processing grammar in L2 versus in L1.

Also utilizing a sentence comprehension task, but varying the level of syntactic complexity, Suh et al. [164] found that processing in either L1 (Korean) or L2 (English) activated mainly the same areas, including the L inferior frontal gyrus (IFG), bilateral inferior parietal gyrus, and occipital lobe including cuneus and lingual gyrus. However, there was an effect of syntactic complexity: more complex structure induced greater activation in the L inferior frontal gyrus when processing L1 but not L2 sentences. Other studies generally support the view of shared cerebral regions for L1/L2 syntactic processing by more proficient learners [52, 165, 166].

Further, the generalization regarding a common syntactic network seems to hold true for low-proficiency L2 learners as well (e.g., [167–169]). For instance, Indefrey et al. [169] administered a grammaticality judgment task to Chinese immigrants in Netherlands after 3, 6, and 9 months of classroom learning of Dutch and found that as early as at 6 months, these L2 learners were shown to recruit areas related to native syntactic processing such as the L inferior frontal gyrus. This is somewhat problematic for the D/P model, since proceduralization and recruitment of L1-like syntax processing areas (such as inferior frontal cortex) is not predicted for beginning and low-proficiency learners.

However, not all findings support the shared network hypothesis, as different areas are found to be activated when processing L1 and L2 for certain types of morphosyntactic tasks. For instance, while Golestani et al. [163] found overlap in activation areas (noted above), covert language production in L2 English, but not in L1 French, activated the L inferior and superior parietal cortices, the R occipital cortex, and the cerebellum. On the other hand, the L putamen was found to be activated in L1 French production only. Thus, syntax may best be considered not as a monolithic module (as is the case for the D/P model) but rather as a set of more fine-grained processes as reviewed in theoretical syntax. Accordingly, contradictory findings may not be surprising given the different methodologies and tasks used in the field.

6.3.4. Functional Connectivity. Dodel et al. [168] investigated "conditional dependent functional interactions" by looking at subject-dependent variables in a group of L1 French/L2 English bilinguals engaged in covert language production tasks (both lexical and syntactic). Findings of note include a more functionally linked network during L2 sentence production than during L1 consisting of the L inferior frontal gyrus, putamen, insula, precentral gyrus, and supplementary motor area. This finding held for participants with higher L2 syntactic proficiency than for those with lower proficiency.

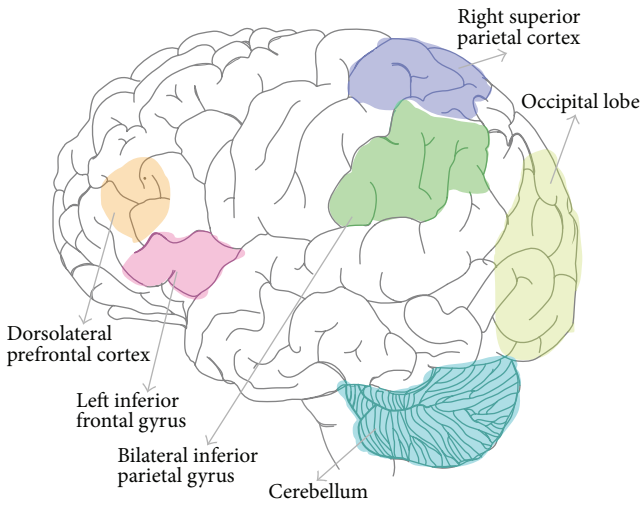

Figure 3: Brain areas showing variation in structure and functional activity for bilinguals performing syntactic processing tasks.

In sum, bilingual individuals had more gray matter volume than monolinguals in areas related to syntactic processing and procedural representation in the cerebellum. Differences were also reported for syntactic processing of bilinguals' L2 compared with their L1, including engagement of L inferior frontal gyrus (IFG), precentral gyrus and SMA, putamen, and SMA. Further, the degree of grammatical proficiency in one's L2 or a learned artificial grammar also corresponded to increased activity in brain areas of overlap, notably Broca's area (BA44) and connecting fibers with Broca's such as the superior longitudinal fasciculus. Structural connectivity involving Broca's area has been demonstrated for L1 learning and processing [170]. Additionally, higher L2 grammatical proficiency corresponded with electrophysiological patterns related to automatic language processing (ELAN) and cerebellar volume. The key brain areas showing variation in structure and functional activity for bilinguals performing L2 syntactic processing tasks are illustrated in Figure 3.

For morphosyntactic processing, the L1-L2 overlap seems less complete compared to lexical semantics. The wider degree of L1-L2 neurolinguistic difference lends at least partial support to the Declarative/Procedural model [111] and captures the insight on a very broad level of other similar (psycho)linguistic models such as the Fundamental Difference Hypothesis [171], Shallow Tree Hypothesis [172], and the Representational Deficit model [173] that point to divergences in representation and processing in L1 versus L2.

One issue to highlight is that the bulk of current morphosyntactic research may be beset by a "Granularity Mismatch Problem (GMP)" [174]. Specifically, the level at which linguistic computation is posed to take place is more fine-grained than the broader conceptual distinctions that form the basis of neuroscientific studies of language. For example, syntactic details concerning phrase structure, movement, and feature checking are central to linguistic theories but have no visible reflexes in current imaging data. With regard to bilingual syntax, a worthwhile pursuit would emphasize differences between "local" and "nonlocal" syntactic properties, where the latter proves more difficult for L2/bilingual learners behaviorally [172, 175, 176].

6.4. Effects of AoA and Proficiency. In this last section, we explore the effects of age of acquisition (henceforth AoA) and proficiency of L2/nondominant language on the location, interconnections, and intensity of activation in the bilingual brain. We also make a distinction between proficiency and task performance [162]. We refer to "proficiency" as baseline/entering/general language competence prior to the study, whereas "task performance" refers to participants' performance in a specific language task (e.g., lexical decision or grammar judgment) in studies that investigate a specific aspect of language processing. These two variables are often considered to be related (e.g., [177]). Indeed, the well-known Critical Period Hypothesis (e.g., [178]) postulates a direct correlation between AoA and ultimate attainment in native-like proficiency within a maturationally constrained time period (e.g., puberty). Therefore it would be important to attempt to disentangle these two factors in understanding how they impact the neural aspects of bilingualism (e.g., [87]). It should be noted that while some of the studies summarized and reviewed here do control for one or the other variable, others examine one factor without controlling for the other. Both types of studies are included here.

A further distinction is made between the structural and functional imaging studies in the effect of these variables. For structural imaging studies, we mainly look at how AoA, proficiency, and performance are related to GM density and WM integrity. For functional imaging studies, we mainly look at how AoA as well as proficiency further modulates the relationship between task performance and brain activation.

6.4.1. Proficiency. Structural studies generally report a positive relationship between task performance and indicators of brain structure like fractional anisotropy and grey matter (e.g., [31, 33, 148]). For example, in Cummine and Boliek's [31] structural connectivity study, Chinese-English bilingual participants' reading performance was found to be positively associated with mean fractional anisotropy values in the parietal-occipital sulcus. In grammar processing, Greek-English bilinguals who performed better in an inflectional processing task were found to have more grey matter in the cerebellum [148]. The same pattern was observed in studies that examine the effect of general language proficiency. Mechelli et al. [83] found that, for their Italian-English bilinguals with varying AoA (2–34), those identified as having high proficiency in English (regardless of AoA) showed more grey matter density in the L inferior parietal region.

In *functional studies*, better task performance is associated with more L1-L2 similarity in functional activation. In a study where participants who all had late AoA listened to stories in different languages while undergoing PET, it was found that

high proficiency Italian-English bilinguals activated similar L hemispheric areas (L temporal pole, the superior temporal sulcus, middle temporal gyrus, and hippocampal structures) whether the stories were in L1 or L2 [43]. In contrast, low proficiency bilinguals showed no activation for L2 English in those regions.

Wartenburger et al. [54] whose study is reported below for AoA effects on grammar processing also examined semantic processing (e.g., *the deer shoots the hunter*). They found this domain of language to be affected by proficiency, but with mixed results: low proficiency L2 speakers showed more activation in Broca's area and the R middle frontal gyrus than high proficiency speakers who in turn showed more activation in the L middle frontal and R fusiform gyrus.

Proficiency also seems to be a more important factor in understanding the neural substrates of lexical processing. Chee et al. [41] examined both early and late Chinese-English bilinguals (<6 yo, >12 yo). Using fMRI, the authors found both groups activated the same areas for both L1 and L2 languages, including the prefrontal, temporal, parietal, and supplementary motor area. There was only a difference in the magnitude of activation for L1 versus L2.

ERP studies, on the other hand, provide evidence that the effect of proficiency depends on the specific language domain in question, as discussed in the section on morphosyntactic processing. While semantic anomalies elicit the similar responses (i.e., N400) in all groups (native controls, low and high proficiency groups) (e.g., [160]), syntactic violation elicits a native-like biphasic pattern of ELAN followed by P600 only in high proficiency learners (and native controls), whether in an artificial language learning paradigm (e.g., [161]) or in natural language learning cases (e.g., [160, 162, 179]).

6.4.2. Age of Acquisition. In general, *structural* imaging results show that AoA is *negatively* associated with grey matter density and white matter integrity [83, 139, 180]. That is, individuals acquiring the second language early in life show increased volumetric changes (grey and white) in the brain. For example, in Mechelli et al. [83], early English-Italian bilinguals (L2 learned before 5 years of age) showed greater increase in grey matter density in the bilateral inferior parietal cortex than late bilinguals (L2 learned between 10 and 15 years of age). In Grogan et al. [139], grey matter density in another area, L pars opercularis, was negatively related to L2 AoA. For structural connection studies, Mohades et al. [180] found that simultaneous bilinguals (considered to have comparatively early AoA) showed higher FA value in the L inferior occipitofrontal fasciculus (IIFOF) than sequential bilinguals (and monolinguals). Such studies therefore seem to provide neuroimaging evidence for the maturational effects in language learning that have been observed in behavioral research.

Functional studies on the other hand present a more mixed picture regarding the effect of AoA, possibly due to the specific aspects of linguistic processing involved in the studies [162]. Studies suggest that AoA *positively* modifies brain activation in grammar processing, meaning that the later a second language is acquired, the more the activation is required/observed. For instance, in Wartenburger et al. [54], while early L1 Italian/L2 German learners (L2 = birth) showed no L1-L2 differences in activation, the late groups (L2 = 19 and 20 years), regardless of their proficiency, showed significantly more activation in Broca's area and subcortical structure when processing L2 grammar. Hernandez et al. [166] likewise found more neural activity in the LIFT 44/45 in later L2 Spanish learners compared with early ones while performing a grammatical gender decision task. Similar patterns were observed in Jasinska and Petitto [181] in L2 syntactic processing, for the classic language neural areas.

On the other hand, L2 AoA appears to *negatively* modify brain activation in reading and phonological processing, indicating that early AoA is related to greater activation. For example, Krizman et al. [182] found that simultaneous bilinguals (early AoA) showed greater amplitude in the auditory brainstem and more consistency in responses to synthesized syllables. In a passage reading task administered to Hindi-English bilinguals, Das et al. [57] found that L2 AoA was negatively related to L inferior parietal lobe activity. Lastly, Archila-Suerte et al.'s [183] study on phonological processing in English-Spanish bilinguals showed mixed results: While later bilinguals were found to show more neural activity than early bilinguals in the bilateral superior temporal gyrus (related to perceptual auditory information) and the Rolandic operculum (related to subvocal rehearsal), indicating a positive relationship between AoA and neural activity, the reverse was true for activity in the R middle frontal gyrus (related to high-order executive function and cognitive control). The authors explain this difference in terms of the unique linguistic environment of bilinguals (who need to manipulate speech sounds from an early age) and how that affects the allocation of brain areas for processing language information.

Finally, we consider the mode of learning by early versus late learners, and how such a difference may account for some of AoA effects reported in the studies reviewed above. It has long been hypothesized in the second language acquisition literature that, unlike monolingual/young learners who learn certain language aspects implicitly (without awareness of what is being learned), late learners adopt a more explicit approach [184, 185] whereby they notice negative evidence and make use of pedagogical grammatical descriptions and analogical reasoning, among other things [185].

In cognitive psychology, there are further proposals mapping these learning modes to different language domains (speech/phonology, syntax, lexical semantics, etc.) and different types of language competence (e.g., "Basic Interpersonal Communication Skills" (BICS) versus "Cognitive and Language Proficiency" (CALP), [186]). Various researchers have associated early (implicit) learning with grammar (e.g., [105, 106]) and speech sounds (e.g., [187]), in contrast with (lexical) semantics which characterize late, explicit learning. Consequently, late learners might adopt a different approach (perhaps more conscious, effortful, and academic-like) to learning language (aspects) than early learners (e.g., [188]).

Some of the studies reported here can be interpreted in terms of such a model. For instance, Wartenburger et al.'s

[54] study found an effect of AoA for grammar processing. It could be that if rule-based knowledge such as grammar is learned at a later stage and via the explicit mode, a different pattern of neural recruitment is observed when processing L2 (e.g., increased intensity in activation, as was reported in the study) which could be neural reflexes of effortful learning. The absence of L1-L2 activation difference for grammar processing in the early group is then perhaps reflective of the absence of such conscious, effortful learning for L2ers.

Likewise, Archila-Suerte et al.'s [183] finding that late bilinguals showed increased activity in the bilateral rolandic operculum when processing L2 speech (as compared with early bilinguals and monolinguals) could also be explained by the differences in the mode of learning. This premotor area has been linked to subvocal rehearsal, which, as the authors point out, is important for L2ers for whom the interconnection of L2 sounds may be less strong than L1 sounds. Therefore, the more effortful learning of L2 speech may be reflected in the increased activation of this brain region. A summary of the studies reviewed in this section is shown in Table 1.

7. Conclusion

We have systematically reviewed studies that employ advanced neuroimaging techniques to study the impact of bilingualism on brain structure, structural connectivity, function, and functional connectivity. The first issue we addressed, whether the language neural network is different for L1 versus L2 processing, revealed evidence that similar brain networks are activated for L1 and L2 in the domains of reading, listening, and speech production. Secondly, on the effects of bilinguals' executive functioning on the structure and function of the "universal" language neural network, the reviewed studies indicate that stronger cognitive control in bilinguals is accompanied by increased gray and white matter volume and regional activation in the frontoparietal network and basal ganglia.

The third issue on the effects of bilingualism on phonological, lexical-semantic, and syntactic aspects of language processing conveyed that bilinguals generally showed increased volume in component language structures and the connective tracts between these brain areas compared to monolinguals. Further, the degree of convergence/divergence in brain regions and networks involved in L1 and L2 processing is related to the linguistic processes involved. Specifically, the largest degree of divergence in structure, function, and/or connectivity is observed in phonology, followed by morphosyntax and semantics. It is likely that the development of these brain regions may parallel language developmental milestones, with phonological development beginning first, followed by semantic development, and finally grammatical/syntax development. In line with the often observed difference in reliability and convergence in language systems (between first and second language acquisition, e.g., Fundamental Difference Hypothesis [112]), sensitive periods do not apply to language broadly, rather different linguistic domains or components are affected in a nonuniform manner, with phonology being most susceptible to age effects and syntax to a lesser degree (around adolescence), while vocabulary has no age constraints at all (e.g., [162, 189]).

With regard to the fourth issue, we found that factors such as age of acquisition and proficiency levels further modify the location, interconnections, and intensity of activation in the bilingual brain, especially when considered with respect to the different component processes. Studies indicate that, generally, the earlier a language is learned and the higher proficiency is attained in L2, the more the grey matter intensity and white matter integrity are observed. Functional results, on the other hand, seem to depend on the specific nature of the component processes. While phonology and syntactic knowledge are generally more sensitive to age effects (earlier AoA = less activation), lexical semantics, on the other hand, is more affected by proficiency levels (higher proficiency = more L1-like activation, generally).

In interpreting the nascent neurolinguistics literature, methodological differences between investigations should be taken into account [73], but at the same time advancement in this scientific area would also benefit from multiple sources of information [190]. Therefore, in this review we included findings from research employing diverse neuroscience methods and we considered their concurrence in light of current cognitive and linguistic models. We did not find obvious alignment of structure and function connectivity within the area of neurolinguistics, but we are optimistic that current methodologies emphasizing dynamic and emergent neural networks can supplement behavioral research to inform bilingual models [191].

There are a number of limitations to the conclusions that can be drawn at present. For instance, we note here that not all studies investigating language proficiency controlled for AoA, and vice versa. Thus, future studies should consider the possibility of holding all other language-related variables constant. Future studies may also consider investigating the factor of AoA longitudinally, by following a population of bilingual children across developmental time, or cross-sectionally, by studying bilingual children of varying age ranges at a single time point.

Other considerations for future research regard the mismatch of "granularity" between the disciplines of linguistics and the neuroscience of language. In the neuroscience of language, the terms "phonology, semantics, and syntax" are used in a very general sense to refer to "sound structure, word meaning, and phrase structure," whereas in contemporary linguistics, each of those subfields necessarily consists of numerous computations and much finer-grained representations [174]. In addition, current understanding of linguistics often emphasizes the interconnections or interfaces of different linguistic submodules as well as nonlinguistic information, instead of treating them as separate, isolated domains [192].

Future consideration of neural correlates, especially in terms of connectivity, could focus on issues like how linguistic interfaces affect completeness of bilingual acquisition and L1 attrition (e.g., [193, 194]). Finally, additional factors not included in our review may also prove relevant in the neurolinguistics of bilingualism, such as language types with two typologically/phonetically similar languages (e.g.,

Table 1: Summary of studies reviewed as related to the variables of age of acquisition and proficiency.

Reference	Nature of task (lexical/phonological/syntactical)	Group differences (age of acquisition/language proficiency/task performance)	Methodology and structural/functional effects on the brain	Details
Mechelli et al., 2004, Nature [83]	—	L2 proficiency (indexed by neuropsychological tests of reading, writing, speech comprehension, and production) AoA (monolinguals versus early bilinguals versus late bilinguals)	Structure: VBM (grey matter density)	L2 proficiency was positively related to grey matter density in L inferior parietal cortex (and negatively related to AoA) L2 AoA was negatively related to grey matter density in L and R inferior parietal cortex
Klein et al., 2014, Brain and Language [123]	—	AoA (simultaneous versus sequential early versus sequential late bilinguals)	Structure: MRI (cortical thickness)	L2 AoA was associated with cortical thickness; positive relationship for L inferior frontal gyrus and L superior parietal lobe, negative relationship for R inferior frontal gyrus The researchers argued that the positive relationship could reflect the growth of new cortical tissue as demanded by the new learning in adolescence/adulthood and the ensuing cortical folding to accommodate new tissue
Mohades et al., 2012, Brain Research [180]	—	AoA (simultaneous bilinguals versus sequential bilinguals versus monolinguals)	Structure: MRI DTI (white matter)	L2 AoA was negatively associated with mean fractional anisotropy values for inferior occipitofrontal fasciculus (IIFOF) tracts negatively associated with AoA L2 AoA was positively associated with mean fractional anisotropy values for the bundle of white matter fibres arising from the anterior part of the corpus callosum projecting to the orbital lobe (AC-OL)
Grogan et al., 2012, Neuropsychologia [139]	Lexical (efficiency)	Task performance (speed and accuracy of lexical decisions, and lexical fluency) AoA	Structure: MRI/VBM	L2 task performance was negatively related to grey matter in the L pars opercularis L2 AoA was negatively related to grey matter in the L pars opercularis

Table 1: Continued.

Reference	Nature of task (lexical/phonological/syntactical)	Group differences (age of acquisition/language proficiency/task performance)	Methodology and structural/functional effects on the brain	Details
Pliatsikas et al., 2014, Cerebellum [148]	Lexical (grammar)	Task performance (speed of processing regular inflections) Years of naturalistic exposure (number of years living in UK)	Structure: VBM	L2 task performance was positively associated with grey matter volume in the cerebellum Years of naturalistic exposure to L2 were positively correlated with grey matter volume in the posterior bilateral putamen
Das et al., 2011, Neuroimage [57]	Lexical (reading proficiency)	Task performance AoA (simultaneous versus sequential bilinguals)	Function: fMRI	L2 task performance (English reading proficiency) was positively related to L inferior temporal gyrus activity L2 AoA was negatively related to left inferior parietal lobe activity
Cummine and Boliek, 2013, Brain Structure and Function [31]	Lexical (reading)	Task performance (response time for a complex reading task) for sequential bilinguals versus monolinguals	Structure: DTI (white matter)	L2 task performance was positively associated with mean fractional anisotropy values in the parietal-occipital sulcus The researchers contended that the parietal-occipital sulcus could be a possible gating system for modulating the contribution of sublexical and lexical stream processes
Grogan et al., 2009, Cerebral Cortex [33]	Lexical + phonological	Task performance (semantic and phonemic fluency scores)	Structure: MRI, VBM	Task performance (phonemic fluency) in L1 and L2 was associated with grey matter in the presupplementary motor area and the head of caudate Task performance (semantic fluency) in L1 and L2 was positively associated with grey matter density in the L inferior temporal cortex

Table 1: Continued.

Reference	Nature of task (lexical/phonological/syntactical)	Group differences (age of acquisition/language proficiency/task performance)	Methodology and structural/functional effects on the brain	Details
Krizman et al., 2015, Neuroscience Letters [182]	Phonological (listening to syllables)	AoA, matched for proficiency (simultaneous versus sequential)	Function: EEG	L2 AoA was negatively associated with amplitude of fundamental frequency response in the auditory brainstem to syllables like "ba" and "ga" L2 AoA was negatively associated with neural consistency of responses to syllable "ba" The researchers argued that bilingualism enhances subcortical auditory processing
Archila-Suerte et al., 2015, Brain and Language [183]	Phonological (processing L2 speech sounds)	AoA (early versus late), matched for proficiency and SES	Function: fMRI	L2 AoA was positively associated with neural activity in the bilateral superior temporal gyrus and the Rolandic operculum The researchers posited that late bilinguals recruit this premotor area to support subvocal rehearsal of L2 sounds learned late in development L2 AoA negatively associated with neural activity in the R middle frontal gyrus
Golestani et al., 2006, Neuropsychologia [163]	Syntax	L2 grammatical (syntactic) proficiency as assessed with TOEFL in late bilinguals	Function: fMRI	L2 task proficiency was positively associated with neural activity in the basal ganglia (particularly left caudate nucleus/putamen) During syntactical production, language proficiency was positively related to the closeness of L1 and L2 activity peaks in L inferior frontal gyrus
Jasinska and Petitto, 2013, Developmental Cognitive Neuroscience [181]	Syntactical (sentence judgment task)	AoA (early versus late)	Function: fNIRS	In children, L2 AoA was positively associated with neural activity in the classic language neural areas (bilateral superior temporal gyrus, Broca's area) and negatively associated with neural activity in domain-general areas (dorsolateral prefrontal cortex, frontopolar cortex)

German and English), as compared to bilinguals with two typologically/phonetically dissimilar languages (e.g., Tamil and English). While this goes beyond the scope of the current review, future work may wish to consider investigating the impact of different language types/pairings on the bilingual brain.

Conflict of Interests

The authors declare that there is no conflict of interests regarding the publication of this paper.

References

[1] European Commission Special Eurobarometer, Europeans and their languages, 2012, http://ec.europa.eu/public_opinion/archives/ebs/ebs_243_en.pdf.

[2] F. J. Gall and G. Spurzheim, *Recherches sur le Système Nerveux en Général et sur Celui du Cerveau en Particuller; Mémoire Présenté à l'Institut de France, le 14 Mars 1808; Suivi D'observations sur le Rapport qui en a Été Fait à Cette Compagnie par ses Commissaires*, Bonset, Amsterdam, The Netherlands, 1967, Reprinted from the 1809 edition.

[3] J. A. Fodor, *Modularity of the Mind*, MIT Press, Cambridge, Mass, USA, 1983.

[4] K. S. Lashley, *Brain Mechanisms and Intelligence: A Quantitative Study of Injuries to the Brain*, Dover Publications, New York, NY, USA, 1929–1963.

[5] D. O. Hebb, *The Organization of Behavior*, Wiley, 1949.

[6] G. A. Ojemann, "Cortical stimulation and recording in language," in *Localization and Neuroimaging in Neuropsychology*, A. Kertesz, Ed., pp. 35–55, Academic Press, San Diego, Calif, USA, 1994.

[7] H. Damasio, T. J. Grabowski, D. Tranel, R. D. Hichwa, and A. R. Damasio, "A neural basis for lexical retrieval," *Nature*, vol. 380, no. 6574, pp. 499–505, 1996.

[8] A. Puce, T. Allison, M. Asgari, J. C. Gore, and G. McCarthy, "Differential sensitivity of human visual cortex to faces, letterstrings, and textures: a functional magnetic resonance imaging study," *The Journal of Neuroscience*, vol. 16, no. 16, pp. 5205–5215, 1996.

[9] D. E. Rumelhart and J. L. McClelland, *Parallel Distributed Processing: Explorations in the Microstructure of Cognition. Volume 1: Foundations*, MIT Press, Cambridge, Mass, USA, 1986.

[10] D. C. Plaut, "Structure and function in the lexical system: insights from distributed models of word reading and lexical decision," *Language and Cognitive Processes*, vol. 12, no. 5-6, pp. 765–805, 1997.

[11] M. S. Seidenberg, "Language acquisition and use: learning and applying probabilistic constraints," *Science*, vol. 275, no. 5306, pp. 1599–1603, 1997.

[12] M. T. Turvey, "Coordination," *American Psychologist*, vol. 45, no. 8, pp. 938–953, 1990.

[13] K. R. Pugh, R. Sandak, S. J. Frost, D. Moore, and W. E. Mencl, "Examining reading development and reading disability in diverse languages and cultures: potential contributions from functional neuroimaging," *Journal of American Indian Education*, vol. 45, pp. 60–76, 2006.

[14] S. L. Bressler and V. Menon, "Large-scale brain networks in cognition: emerging methods and principles," *Trends in Cognitive Sciences*, vol. 14, no. 6, pp. 277–290, 2010.

[15] S. Dehaene, "Reading in the brain revised and extended: response to comments," *Mind & Language*, vol. 29, no. 3, pp. 320–335, 2014.

[16] E. R. Sowell, D. Delis, J. Stiles, and T. L. Jernigan, "Improved memory functioning and frontal lobe maturation between childhood and adolescence: a structural MRI study," *Journal of the International Neuropsychological Society*, vol. 7, no. 3, pp. 312–322, 2001.

[17] K. L. Mills and C. K. Tamnes, "Methods and considerations for longitudinal structural brain imaging analysis across development," *Developmental Cognitive Neuroscience*, vol. 9, pp. 172–190, 2014.

[18] J. L. Whitwell, "Voxel-based morphometry: an automated technique for assessing structural changes in the brain," *The Journal of Neuroscience*, vol. 29, no. 31, pp. 9661–9664, 2009.

[19] S. Mori and J. Zhang, "Principles of diffusion tensor imaging and its applications to basic neuroscience research," *Neuron*, vol. 51, no. 5, pp. 527–539, 2006.

[20] V. J. Wedeen, R. P. Wang, J. D. Schmahmann et al., "Diffusion spectrum magnetic resonance imaging (DSI) tractography of crossing fibers," *NeuroImage*, vol. 41, no. 4, pp. 1267–1277, 2008.

[21] R. B. Buxton, *Introduction to Functional Magnetic Resonance Imaging*, Cambridge University Press, Cambridge, UK, 2002.

[22] S. Bookheimer, "Functional MRI of language: new approaches to understanding the cortical organization of semantic processing," *Annual Review of Neuroscience*, vol. 25, pp. 151–188, 2002.

[23] H. Zhang, Y.-J. Zhang, C.-M. Lu, S.-Y. Ma, Y.-F. Zang, and C.-Z. Zhu, "Functional connectivity as revealed by independent component analysis of resting-state fNIRS measurements," *NeuroImage*, vol. 51, no. 3, pp. 1150–1161, 2010.

[24] J. León-Carrión and U. León-Domínguez, "Functional near-infrared spectroscopy (fNIRS): principles and neuroscientific applications," in *Neuroimaging—Methods*, P. Bright, Ed., chapter 3, pp. 47–74, InTech, Rijeka, Croatia, 2012.

[25] S. J. Luck, *An Introduction to Event-Related Potentials and Their Neural Origins*, MIT Press, 2005.

[26] S. Weiss and H. M. Mueller, "The contribution of EEG coherence to the investigation of language," *Brain and Language*, vol. 85, no. 2, pp. 325–343, 2003.

[27] P. Hansen, M. Kringelbach, and R. Salmelin, *MEG: An Introduction to Methods*, Oxford University Press, Oxford, UK, 2010.

[28] J. X. O'Reilly, M. W. Woolrich, T. E. J. Behrens, S. M. Smith, and H. Johansen-Berg, "Tools of the trade: psychophysiological interactions and functional connectivity," *Social Cognitive and Affective Neuroscience*, vol. 7, no. 5, Article ID nss055, pp. 604–609, 2012.

[29] K. J. Friston, "Functional and effective connectivity in neuroimaging: a synthesis," *Human Brain Mapping*, vol. 2, no. 1-2, pp. 56–78, 1994.

[30] K. Stephan and K. J. Friston, "Analysing effective connectivity with fMRI," *Wiley Interdisciplinary Reviews: Cognitive Science*, vol. 1, no. 3, pp. 446–459, 2011.

[31] J. Cummine and C. A. Boliek, "Understanding white matter integrity stability for bilinguals on language status and reading performance," *Brain Structure and Function*, vol. 218, no. 2, pp. 595–601, 2013.

[32] K. R. Pugh, "A neurocognitive overview of reading acquisition and dyslexia across languages," *Developmental Science*, vol. 9, no. 5, pp. 448–450, 2006.

[33] A. Grogan, D. W. Green, N. Ali, J. T. Crinion, and C. J. Price, "Structural correlates of semantic and phonemic fluency ability in first and second languages," *Cerebral Cortex*, vol. 19, no. 11, pp. 2690–2698, 2009.

[34] M. K. Leonard, T. T. Brown, K. E. Travis et al., "Spatiotemporal dynamics of bilingual word processing," *NeuroImage*, vol. 49, no. 4, pp. 3286–3294, 2010.

[35] A. G. Hervais-Adelman, B. Moser-Mercer, and N. Golestani, "Executive control of language in the bilingual brain: integrating the evidence from neuroimaging to neuropsychology," *Frontiers in Psychology*, vol. 2, article 234, 2011.

[36] J. Abutalebi, P. A. Della Rosa, D. W. Green et al., "Bilingualism tunes the anterior cingulate cortex for conflict monitoring," *Cerebral Cortex*, vol. 22, no. 9, pp. 2076–2086, 2012.

[37] M. Catani, D. K. Jones, and D. H. Ffytche, "Perisylvian language networks of the human brain," *Annals of Neurology*, vol. 57, no. 1, pp. 8–16, 2005.

[38] A. D. Friederici and S. M. E. Gierhan, "The language network," *Current Opinion in Neurobiology*, vol. 23, no. 2, pp. 250–254, 2013.

[39] N. Golestani, "Brain structural correlates of individual differences at low-to high-levels of the language processing hierarchy: a review of new approaches to imaging research," *The International Journal of Bilingualism*, vol. 18, no. 1, pp. 6–34, 2014.

[40] L. H. Tan, H.-L. Liu, C. A. Perfetti, J. A. Spinks, P. T. Fox, and J.-H. Gao, "The neural system underlying Chinese logograph reading," *NeuroImage*, vol. 13, no. 5, pp. 836–846, 2001.

[41] M. W. L. Chee, E. W. L. Tan, and T. Thiel, "Mandarin and English single word processing studied with functional magnetic resonance imaging," *The Journal of Neuroscience*, vol. 19, no. 8, pp. 3050–3056, 1999.

[42] P. Indefrey and W. J. M. Levelt, "The spatial and temporal signatures of word production components," *Cognition*, vol. 92, no. 1-2, pp. 101–144, 2004.

[43] D. Perani, E. Paulesu, N. S. Galles et al., "The bilingual brain: proficiency and age of acquisition of the second language," *Brain*, vol. 121, no. 10, pp. 1841–1852, 1998.

[44] T. M. Snijders, V. Kooijman, A. Cutler, and P. Hagoort, "Neurophysiological evidence of delayed segmentation in a foreign language," *Brain Research*, vol. 1178, no. 1, pp. 106–113, 2007.

[45] M. Gasser, "Connectionism and universals of second language acquisition," *Studies in Second Language Acquisition*, vol. 12, no. 2, pp. 179–199, 1990.

[46] M. E. Sokolik and M. E. Smith, "Assignment of gender to French nouns in primary and secondary language: a connectionist model," *Second Language Research*, vol. 8, no. 1, pp. 39–58, 1992.

[47] F. Cao, S. Young Kim, Y. Liu, and L. Liu, "Similarities and differences in brain activation and functional connectivity in first and second language reading: evidence from Chinese learners of English," *Neuropsychologia*, vol. 63, pp. 275–284, 2014.

[48] A. D. Friederici, "The brain basis of language processing: from structure to function," *Physiological Reviews*, vol. 91, no. 4, pp. 1357–1392, 2011.

[49] S. M. Wilson, S. Galantucci, M. C. Tartaglia et al., "Syntactic processing depends on dorsal language tracts," *Neuron*, vol. 72, no. 2, pp. 397–403, 2011.

[50] M. Brysbaert and W. Duyck, "Is it time to leave behind the revised hierarchical model of bilingual language processing after fifteen years of service?" *Bilingualism: Language and Cognition*, vol. 13, no. 3, pp. 359–371, 2010.

[51] P. Indefrey, "A meta-analysis of hemodynamic studies on first and second language processing: which suggested differences can we trust and what do they mean?" *Language Learning*, vol. 56, no. 1, pp. 279–304, 2006.

[52] S.-A. Rüschemeyer, S. Zysset, and A. D. Friederici, "Native and non-native reading of sentences: an fMRI experiment," *NeuroImage*, vol. 31, no. 1, pp. 354–365, 2006.

[53] D. Perani and J. Abutalebi, "Neural basis of first and second language processing," *Current Opinion in Neurobiology*, vol. 15, no. 2, pp. 202–206, 2005.

[54] I. Wartenburger, H. R. Heekeren, J. Abutalebi, S. F. Cappa, A. Villringer, and D. Perani, "Early setting of grammatical processing in the bilingual brain," *Neuron*, vol. 37, no. 1, pp. 159–170, 2003.

[55] A. E. Hernandez, "Language switching in the bilingual brain: what's next?" *Brain & Language*, vol. 109, no. 2-3, pp. 133–140, 2009.

[56] S. Dehaene, E. Dupoux, J. Mehler et al., "Anatomical variability in the cortical representation of first and second language," *NeuroReport*, vol. 8, no. 17, pp. 3809–3815, 1997.

[57] T. Das, P. Padakannaya, K. R. Pugh, and N. C. Singh, "Neuroimaging reveals dual routes to reading in simultaneous proficient readers of two orthographies," *NeuroImage*, vol. 54, no. 2, pp. 1476–1487, 2011.

[58] C. A. Perfetti and L. N. Harris, "Universal reading processes are modulated by language and writing system," *Language Learning and Development*, vol. 9, no. 4, pp. 296–316, 2013.

[59] W. Sittiprapaporn, C. Chindaduangratn, and N. Kotchabhakdi, "Long-term memory traces for familiar spoken words in tonal language as revealed by the mismatch negativity," *Songklanakarin Journal of Science and Technology*, vol. 26, no. 6, pp. 779–786, 2004.

[60] A. Miyake, N. P. Friedman, M. J. Emerson, A. H. Witzki, A. Howerter, and T. D. Wager, "The unity and diversity of executive functions and their contributions to complex 'frontal lobe' tasks: a latent variable analysis," *Cognitive Psychology*, vol. 41, no. 1, pp. 49–100, 2000.

[61] R. Bull and K. Lee, "Executive functioning and mathematics achievement," *Child Development Perspectives*, vol. 8, no. 1, pp. 36–41, 2014.

[62] A. Miyake and N. P. Friedman, "The nature and organization of individual differences in executive functions: four general conclusions," *Current Directions in Psychological Science*, vol. 21, no. 1, pp. 8–14, 2012.

[63] J. R. Best and P. H. Miller, "A developmental perspective on executive function," *Child Development*, vol. 81, no. 6, pp. 1641–1660, 2010.

[64] K. Lee, S. F. Ng, R. Bull, M. L. Pe, and R. H. M. Ho, "Are patterns important? An investigation of the relationships between proficiencies in patterns, computation, executive functioning, and algebraic word problems," *Journal of Educational Psychology*, vol. 103, no. 2, pp. 269–281, 2011.

[65] H. L. St Clair-Thompson and S. E. Gathercole, "Executive functions and achievements in school: shifting, updating, inhibition, and working memory," *Quarterly Journal of Experimental Psychology*, vol. 59, no. 4, pp. 745–759, 2006.

[66] E. Bialystok, F. I. M. Craik, and G. Luk, "Bilingualism: consequences for mind and brain," *Trends in Cognitive Sciences*, vol. 16, no. 4, pp. 240–250, 2012.

[67] S. M. Carlson and A. N. Meltzoff, "Bilingual experience and executive functioning in young children," *Developmental Science*, vol. 11, no. 2, pp. 282–298, 2008.

[68] E. Bialystok, R. Klein, F. I. M. Craik, and M. Viswanathan, "Bilingualism, aging, and cognitive control: evidence from the Simon task," *Psychology and Aging*, vol. 19, no. 2, pp. 290–303, 2004.

[69] E. K. Miller and J. D. Wallis, "Executive function and higher-order cognition: definitions and neural substrates," in *Encyclopedia of Neuroscience*, vol. 4, pp. 99–104, Academic Press, Oxford, UK, 2009.

[70] K. D. Cicerone, C. Dahlberg, K. Kalmar et al., "Evidence-based cognitive rehabilitation: recommendations for clinical practice," *Archives of Physical Medicine and Rehabilitation*, vol. 81, no. 12, pp. 1596–1615, 2000.

[71] M. D. Lezak, *Neuropsychological Assessment*, Oxford University Press, New York, NY, USA, 1983.

[72] K. R. Paap, "The neuroanatomy of bilingualism: will winds of change lift the fog?" *Language, Cognition and Neuroscience*, 2015.

[73] L. García-Pentón, Y. F. García, B. Costello, J. A. Duñabeitia, and M. Carreiras, "The neuroanatomy of bilingualism: how to turn a hazy view into the full picture," *Language, Cognition and Neuroscience*, pp. 1–25, 2015.

[74] M. Hilchey, R. M. Klein, and J. Saint-Aubin, "Does bilingual exercise enhance cognitive fitness in traditional non-linguistic executive processing tasks?" in *The Cambridge Handbook of Bilingual Processing*, J. Schwieter, Ed., Cambridge University Press, Cambridge, UK, 2015.

[75] K. R. Paap, H. A. Johnson, and O. Sawi, "Bilingual advantages in executive functioning either do not exist or are restricted to very specific and undetermined circumstances," *Cortex*, vol. 69, pp. 265–278, 2015.

[76] J. A. Linck, N. Hoshino, and J. F. Kroll, "Cross-language lexical processes and inhibitory control," *The Mental Lexicon*, vol. 3, no. 3, pp. 349–374, 2008.

[77] D. W. Green, "Mental control of the bilingual lexico-semantic system," *Bilingualism: Language and Cognition*, vol. 1, no. 2, pp. 67–81, 1998.

[78] A. F. Dijkstra and W. J. Van Heuven, "The architecture of the bilingual word recognition system: from identification to decision," *Bilingualism: Language and Cognition*, vol. 5, no. 3, pp. 175–197, 2002.

[79] G. H. Weissberger, T. H. Gollan, M. W. Bondi, L. R. Clark, and C. E. Wierenga, "Language and task switching in the bilingual brain: bilinguals are staying, not switching, experts," *Neuropsychologia*, vol. 66, pp. 193–203, 2015.

[80] M. Hernández, C. D. Martin, F. Barceló, and A. Costa, "Where is the bilingual advantage in task-switching?" *Journal of Memory and Language*, vol. 69, no. 3, pp. 257–276, 2013.

[81] M. Calabria, F. M. Branzi, P. Marne, M. Hernández, and A. Costa, "Age-related effects over bilingual language control and executive control," *Bilingualism: Language and Cognition*, vol. 18, no. 1, pp. 65–78, 2015.

[82] N. Verreyt, E. Woumans, D. Vandelanotte, A. Szmalec, and W. Duyck, "The influence of language-switching experience on the bilingual executive control advantage," *Bilingualism: Language and Cognition*, 2015.

[83] A. Mechelli, J. T. Crinion, U. Noppeney et al., "Neurolinguistics: structural plasticity in the bilingual brain," *Nature*, vol. 431, article 757, 2004.

[84] P. A. Della Rosa, G. Videsott, V. M. Borsa et al., "A neural interactive location for multilingual talent," *Cortex*, vol. 49, no. 2, pp. 605–608, 2013.

[85] L. Zou, J. Abutalebi, B. Zinszer et al., "Second language experience modulates functional brain network for the native language production in bimodal bilinguals," *NeuroImage*, vol. 62, no. 3, pp. 1367–1375, 2012.

[86] C. Hosoda, K. Tanaka, T. Nariai, M. Honda, and T. Hanakawa, "Dynamic neural network reorganization associated with second language vocabulary acquisition: a multimodal imaging study," *The Journal of Neuroscience*, vol. 33, no. 34, pp. 13663–13672, 2013.

[87] P. Li, J. Legault, and K. A. Litcofsky, "Neuroplasticity as a function of second language learning: anatomical changes in the human brain," *Cortex*, vol. 58, pp. 301–324, 2014.

[88] R. Levy, H. R. Friedman, L. Davachi, and P. S. Goldman-Rakic, "Differential activation of the caudate nucleus in primates performing spatial and nonspatial working memory tasks," *Journal of Neuroscience*, vol. 17, no. 10, pp. 3870–3882, 1997.

[89] J. A. Grahn, J. A. Parkinson, and A. M. Owen, "The cognitive functions of the caudate nucleus," *Progress in Neurobiology*, vol. 86, no. 3, pp. 141–155, 2008.

[90] A. Stocco, B. Yamasaki, R. Natalenko, and C. S. Prat, "Bilingual brain training: a neurobiological framework of how bilingual experience improves executive function," *International Journal of Bilingualism*, vol. 18, no. 1, pp. 67–92, 2014.

[91] C. L. Grady, G. Luk, F. I. M. Craik, and E. Bialystok, "Brain network activity in monolingual and bilingual older adults," *Neuropsychologia*, vol. 66, pp. 170–181, 2015.

[92] N. Hon, R. A. Epstein, A. M. Owen, and J. Duncan, "Frontoparietal activity with minimal decision and control," *Journal of Neuroscience*, vol. 26, no. 38, pp. 9805–9809, 2006.

[93] I. Kovelman, S. A. Baker, and L.-A. Petitto, "Age of first bilingual language exposure as a new window into bilingual reading development," *Bilingualism: Language and Cognition*, vol. 11, no. 2, pp. 203–223, 2008.

[94] C. E. Curtis and M. D'Esposito, "Persistent activity in the prefrontal cortex during working memory," *Trends in Cognitive Sciences*, vol. 7, no. 9, pp. 415–423, 2003.

[95] A. Baddeley, "Working memory: looking back and looking forward," *Nature Reviews Neuroscience*, vol. 4, no. 10, pp. 829–839, 2003.

[96] K. K. Jasińska and L. A. Petitto, "Development of neural systems for reading in the monolingual and bilingual brain: new insights from functional near infrared spectroscopy neuroimaging," *Developmental Neuropsychology*, vol. 39, no. 6, pp. 421–439, 2014.

[97] G. Wagner, K. Koch, J. R. Reichenbach, H. Sauer, and R. G. M. Schlösser, "The special involvement of the rostrolateral prefrontal cortex in planning abilities: an event-related fMRI study with the tower of London paradigm," *Neuropsychologia*, vol. 44, no. 12, pp. 2337–2347, 2006.

[98] K. Christoff, V. Prabhakaran, J. Dorfman et al., "Rostrolateral prefrontal cortex involvement in relational integration during reasoning," *NeuroImage*, vol. 14, no. 5, pp. 1136–1149, 2001.

[99] D. Friesen and E. Bialystok, "Control and representation in bilingualism: implications for pedagogy," in *Innovative Research and Practices in Second Language Acquisition and Bilingualism*, vol. 38, pp. 223–240, John Benjamins, Amsterdam, The Netherlands, 2013.

[100] T. H. Gollan, R. I. Montoya, C. Fennema-Notestine, and S. K. Morris, "Bilingualism affects picture naming but not picture classification," *Memory & Cognition*, vol. 33, no. 7, pp. 1220–1234, 2005.

[101] I. Ivanova and A. Costa, "Does bilingualism hamper lexical access in speech production?" *Acta Psychologica*, vol. 127, no. 2, pp. 277–288, 2008.

[102] T. C. Sandoval, T. H. Gollan, V. S. Ferreira, and D. P. Salmon, "What causes the bilingual disadvantage in verbal fluency? The dual-task analogy," *Bilingualism: Language and Cognition*, vol. 13, no. 2, pp. 231–252, 2010.

[103] L. Luo, G. Luk, and E. Bialystok, "Effect of language proficiency and executive control on verbal fluency performance in bilinguals," *Cognition*, vol. 114, no. 1, pp. 29–41, 2010.

[104] E. Bialystok, G. Luk, K. F. Peets, and S. Yang, "Receptive vocabulary differences in monolingual and bilingual children," *Bilingualism: Language and Cognition*, vol. 13, no. 4, pp. 525–531, 2010.

[105] M. T. Ullman, "A neurocognitive perspective on language: the declarative/procedural model," *Nature Reviews Neuroscience*, vol. 2, no. 10, pp. 717–726, 2001.

[106] M. T. Ullman, "The neural basis of lexicon and grammar in first and second language: the declarative/procedural model," *Bilingualism: Language and Cognition*, vol. 4, pp. 105–122, 2001.

[107] J. F. Kroll and E. Stewart, "Category interference in translation and picture naming: evidence for asymmetric connections between bilingual memory representations," *Journal of Memory and Language*, vol. 33, no. 2, pp. 149–174, 1994.

[108] J. F. Kroll, "The bilingual lexicon: an update of Kroll & Dijkstra (2002), the bilingual lexicon," in *Handbook of Applied Linguistics*, R. Kaplan, Ed., Oxford University Press, Oxford, UK, 2nd edition, 2010.

[109] T. H. Gollan and L.-A. R. Acenas, "What is a TOT? Cognate and translation effects on tip-of-the-tongue states in Spanish-English and tagalog-English bilinguals," *Journal of Experimental Psychology: Learning Memory and Cognition*, vol. 30, no. 1, pp. 246–269, 2004.

[110] J. S. H. Taylor, K. Rastle, and M. H. Davis, "Can cognitive models explain brain activation during word and pseudoword reading? A meta-analysis of 36 neuroimaging studies," *Psychological Bulletin*, vol. 139, no. 4, pp. 766–791, 2013.

[111] M. T. Ullman, "Contributions of memory circuits to language: the declarative/procedural model," *Cognition*, vol. 92, no. 1-2, pp. 231–270, 2004.

[112] R. Bley-Vroman, "The logical problem of foreign language learning," *Linguistic Analysis*, vol. 20, pp. 3–49, 1990.

[113] H. Clahsen and U. Hong, "Agreement and null subject in German L2 development: new evidence from reaction–time experiment," *Second Language Research*, vol. 11, pp. 57–58, 1995.

[114] I. Kovelman, S. A. Baker, and L.-A. Petitto, "Bilingual and monolingual brains compared: a functional magnetic resonance imaging investigation of syntactic processing and a possible 'neural signature' of bilingualism," *Journal of Cognitive Neuroscience*, vol. 20, no. 1, pp. 153–169, 2008.

[115] B. W.-Y. Chow, C. McBride-Chang, and S. Burges, "Phonological processing skills and early reading abilities in Hong Kong Chinese kindergarteners learning to read english as a second language," *Journal of Educational Psychology*, vol. 97, no. 1, pp. 81–87, 2005.

[116] L.-J. Kuo and R. C. Anderson, "Effects of early bilingualism on learning phonological regularities in a new language," *Journal of Experimental Child Psychology*, vol. 111, no. 3, pp. 455–467, 2012.

[117] V. Ressel, C. Pallier, N. Ventura-Campos et al., "An effect of Bilingualism on the auditory cortex," *Journal of Neuroscience*, vol. 32, no. 47, pp. 16597–16601, 2012.

[118] N. Golestani, T. Paus, and R. J. Zatorre, "Anatomical correlates of learning novel speech sounds," *Neuron*, vol. 35, no. 5, pp. 997–1010, 2002.

[119] N. Golestani, N. Molko, S. Dehaene, D. LeBihan, and C. Pallier, "Brain structure predicts the learning of foreign speech sounds," *Cerebral Cortex*, vol. 17, no. 3, pp. 575–582, 2007.

[120] N. Sebastián-Gallés, C. Soriano-Mas, C. Baus et al., "Neuroanatomical markers of individual differences in native and non-native vowel perception," *Journal of Neurolinguistics*, vol. 25, no. 3, pp. 150–162, 2012.

[121] S. Elmer, J. Hänggi, M. Meyer, and L. Jäncke, "Differential language expertise related to white matter architecture in regions subserving sensory-motor coupling, articulation, and interhemispheric transfer," *Human Brain Mapping*, vol. 32, no. 12, pp. 2064–2074, 2011.

[122] F. M. Richardson and C. J. Price, "Structural MRI studies of language function in the undamaged brain," *Brain Structure and Function*, vol. 213, no. 6, pp. 511–523, 2009.

[123] D. Klein, K. Mok, J.-K. Chen, and K. E. Watkins, "Age of language learning shapes brain structure: a cortical thickness study of bilingual and monolingual individuals," *Brain and Language*, vol. 131, pp. 20–24, 2014.

[124] C. Lebel and C. Beaulieu, "Lateralization of the arcuate fasciculus from childhood to adulthood and its relation to cognitive abilities in children," *Human Brain Mapping*, vol. 30, no. 11, pp. 3563–3573, 2009.

[125] F. C. K. Wong, B. Chandrasekaran, K. Garibaldi, and P. C. M. Wong, "White matter anisotropy in the ventral language pathway predicts sound-to-word learning success," *The Journal of Neuroscience*, vol. 31, no. 24, pp. 8780–8785, 2011.

[126] G. Luk, E. Bialystok, F. I. M. Craik, and C. L. Grady, "Lifelong bilingualism maintains white matter integrity in older adults," *Journal of Neuroscience*, vol. 31, no. 46, pp. 16808–16813, 2011.

[127] M. Catani and M. T. de Schotten, "A diffusion tensor imaging tractography atlas for virtual in vivo dissections," *Cortex*, vol. 44, no. 8, pp. 1105–1132, 2008.

[128] G. Dehaene-Lambertz and T. Gliga, "Common neural basis for phoneme processing in infants and adults," *Journal of Cognitive Neuroscience*, vol. 16, no. 8, pp. 1375–1387, 2004.

[129] Y. Minagawa-Kawai, K. Mori, and Y. Sato, "Different brain strategies underlie the categorical perception of foreign and native phonemes," *Journal of Cognitive Neuroscience*, vol. 17, no. 9, pp. 1376–1385, 2005.

[130] L. A. Petitto, M. S. Berens, I. Kovelman, M. H. Dubins, K. Jasinska, and M. Shalinsky, "The 'perceptual wedge hypothesis' as the basis for bilingual babies' phonetic processing advantage: new insights from fNIRS brain imaging," *Brain and Language*, vol. 121, no. 2, pp. 130–143, 2012.

[131] L. García-Pentón, A. P. Fernández, Y. Iturria-Medina, M. Gillon-Dowens, and M. Carreiras, "Anatomical connectivity changes in the bilingual brain," *NeuroImage*, vol. 84, pp. 495–504, 2014.

[132] O. Sporns, *Networks of the Brain*, MIT Press, Cambridge, Mass, USA, 2011.

[133] W. E. Nagy and J. A. Scott, "Vocabulary Processes," in *Handbook of Reading Research*, M. Kamil, P. Mosenthal, P. D. Pearson, and R. Barr, Eds., vol. 3, pp. 269–284, 2000.

[134] C. J. Lonigan, "Development, assessment, and promotion of preliteracy skills," *Early Education and Development*, vol. 17, no. 1, pp. 91–114, 2006.

[135] M. Schwartz and T. Katzir, "Depth of lexical knowledge among bilingual children: the impact of schooling," *Reading and Writing*, vol. 25, no. 8, pp. 1947–1971, 2012.

[136] F. M. Richardson, M. S. C. Thomas, R. Filippi, H. Harth, and C. J. Price, "Contrasting effects of vocabulary knowledge on temporal and parietal brain structure across lifespan," *Journal of Cognitive Neuroscience*, vol. 22, no. 5, pp. 943–954, 2010.

[137] G. I. de Zubicaray, K. L. Mcmahon, L. Hayward, and J. C. Dunn, "Pre-experimental familiarization increases hippocampal activity for both targets and lures in recognition memory: an fMRI study," *Journal of Cognitive Neuroscience*, vol. 23, no. 12, pp. 4164–4173, 2011.

[138] H. Lee, J. T. Devlin, C. Shakeshaft et al., "Anatomical traces of vocabulary acquisition in the adolescent brain," *Journal of Neuroscience*, vol. 27, no. 5, pp. 1184–1189, 2007.

[139] A. Grogan, Ō. P. Jones, N. Ali et al., "Structural correlates for lexical efficiency and number of languages in non-native speakers of English," *Neuropsychologia*, vol. 50, no. 7, pp. 1347–1352, 2012.

[140] I. I. Kovelman, M. H. M. Shalinsky, M. S. M. Berens, and L. L. Petitto, "Shining new light on the brain's 'bilingual signature': a functional near infrared spectroscopy investigation of semantic processing," *NeuroImage*, vol. 39, no. 3, pp. 1457–1471, 2008.

[141] A. S. Bick, G. Goelman, and R. Frost, "Hebrew brain vs. English brain: language modulates the way it is processed," *Journal of Cognitive Neuroscience*, vol. 23, no. 9, pp. 2280–2290, 2011.

[142] G. Vingerhoets, J. V. Borsel, C. Tesink et al., "Multilingualism: an fMRI study," *NeuroImage*, vol. 20, no. 4, pp. 2181–2196, 2003.

[143] H. Jeong, M. Sugiura, Y. Sassa et al., "Learning second language vocabulary: neural dissociation of situation-based learning and text-based learning," *NeuroImage*, vol. 50, no. 2, pp. 802–809, 2010.

[144] G. Raboyeau, K. Marcotte, D. Adrover-Roig, and A. I. Ansaldo, "Brain activation and lexical learning: the impact of learning phase and word type," *NeuroImage*, vol. 49, no. 3, pp. 2850–2861, 2010.

[145] J. Crinion, R. Turner, A. Grogan et al., "Language control in the bilingual brain," *Science*, vol. 312, no. 5779, pp. 1537–1540, 2006.

[146] L. Ghazi Saidi, V. Perlbarg, G. Marrelec, M. Pélégrini-Issac, H. Benali, and A.-I. Ansaldo, "Functional connectivity changes in second language vocabulary learning," *Brain and Language*, vol. 124, no. 1, pp. 56–65, 2013.

[147] H. J. De Smet, P. Paquier, J. Verhoeven, and P. Mariën, "The cerebellum: its role in language and related cognitive and affective functions," *Brain and Language*, vol. 127, no. 3, pp. 334–342, 2013.

[148] C. Pliatsikas, T. Johnstone, and T. Marinis, "Grey matter volume in the cerebellum is related to the processing of grammatical rules in a second language: a structural voxel-based morphometry study," *Cerebellum*, vol. 13, no. 1, pp. 55–63, 2014.

[149] H. Xiang, *The language networks of the brain [M.S. dissertation]*, Radboud University, Nijmegen, The Netherlands, 2012.

[150] A. D. Friederici, C. J. Fiebach, M. Schlesewsky, I. D. Bornkessel, and D. Y. Von Cramon, "Processing linguistic complexity and grammaticality in the left frontal cortex," *Cerebral Cortex*, vol. 16, no. 12, pp. 1709–1717, 2006.

[151] A. Flöel, M. H. de Vries, J. Scholz, C. Breitenstein, and H. Johansen-Berg, "White matter integrity in the vicinity of Broca's area predicts grammar learning success," *NeuroImage*, vol. 47, no. 4, pp. 1974–1981, 2009.

[152] P. Loui, H. C. Li, and G. Schlaug, "White matter integrity in right hemisphere predicts pitch-related grammar learning," *NeuroImage*, vol. 55, no. 2, pp. 500–507, 2011.

[153] N. Chomsky, *Syntactic Structures*, Mouton, The Hague, The Netherlands, 1957.

[154] M. D. Hauser, N. Chomsky, and W. T. Fitch, "The faculty of language: what is it, who has it, and how did it evolve?" *Science*, vol. 298, no. 5598, pp. 1569–1579, 2002.

[155] C. M. Weber-Fox and H. J. Neville, "Neural subsystems for open and closed class words differential impacted by delays in second-language immersion: ERP evidence in bilingual speakers," Purdue University, 1998.

[156] A. Hahne, "What's different in second-language processing? Evidence from event-related brain potentials," *Journal of Psycholinguistic Research*, vol. 30, no. 3, pp. 251–266, 2001.

[157] A. Hahne and A. D. Friederici, "Processing a second language: late learners' comprehension mechanisms as revealed by event-related brain potentials," *Bilingualism: Language and Cognitio*, vol. 4, pp. 123–141, 2001.

[158] A. Hahne, J. Muller, and H. Clahsen, "Second language learners' processing of inflected words: behavioral and ERP evidence for storage and decomposition," *Essex Research Reports in Linguistics*, vol. 45, pp. 1–42, 2003.

[159] J. L. Mueller, A. Hahne, Y. Fujii, and A. D. Friederici, "Native and nonnative speakers' processing of a miniature version of Japanese as revealed by ERPs," *Journal of Cognitive Neuroscience*, vol. 17, no. 8, pp. 1229–1244, 2005.

[160] H. W. Bowden, C. Sanz, K. Steinhauer, and M. Ullman, "An ERP study of proficiency in second language," in *Proceedings of the Meeting of the Cognitive Neuroscience Society*, New York, NY, USA, May 2007.

[161] A. D. Friederici, K. Steinhauer, and E. Pfeifer, "Brain signatures of artificial language processing: evidence challenging the critical period hypothesis," *Proceedings of the National Academy of Sciences of the United States of America*, vol. 99, no. 1, pp. 529–534, 2002.

[162] K. Steinhauer, E. J. White, and J. E. Drury, "Temporal dynamics of late second language acquisition: evidence from event-related brain potentials," *Second Language Research*, vol. 25, no. 1, pp. 13–41, 2009.

[163] N. Golestani, F.-X. Alario, S. Meriaux, D. Le Bihan, S. Dehaene, and C. Pallier, "Syntax production in bilinguals," *Neuropsychologia*, vol. 44, no. 7, pp. 1029–1040, 2006.

[164] S. Suh, H. W. Yoon, S. Lee, J.-Y. Chung, Z.-H. Cho, and H. Park, "Effects of syntactic complexity in L1 and L2; an fMRI study of Korean-English bilinguals," *Brain Research*, vol. 1136, no. 1, pp. 178–189, 2007.

[165] K.-K. Luke, H.-L. Liu, Y.-Y. Wai, Y.-L. Wan, and L. H. Tan, "Functional anatomy of syntactic and semantic processing in language comprehension," *Human Brain Mapping*, vol. 16, no. 3, pp. 133–145, 2002.

[166] A. E. Hernandez, J. Hofmann, and S. A. Kotz, "Age of acquisition modulates neural activity for both regular and irregular syntactic functions," *NeuroImage*, vol. 36, no. 3, pp. 912–923, 2007.

[167] K. L. Sakai, K. Miura, N. Narafu, and Y. Muraishi, "Correlated functional changes of the prefrontal cortex in twins induced by classroom education of second language," *Cerebral Cortex*, vol. 14, no. 11, pp. 1233–1239, 2004.

[168] S. Dodel, N. Golestani, C. Pallier, V. ElKouby, D. Le Bihan, and J.-B. Poline, "Condition-dependent functional connectivity: syntax networks in bilinguals," *Philosophical Transactions of the Royal Society of London B*, vol. 360, no. 1457, pp. 921–935, 2005.

[169] P. Indefrey, F. Hellwig, D. Davidson, and M. Gullberg, "Native-like hemodynamic responses during sentence comprehension after six months of learning a new language," in *Proceedings of the 11th Annual Meeting of the Organization for Human Brain Mapping*, Toronto, Canada, 2005.

[170] S. Kennison, *Introduction to Language Development*, Sage Publications, Thousand Oaks, Calif, USA, 2013.

[171] R. Bley-Vroman, "What is the logical problem of foreign language learning?" in *Linguistic Perspectives on Second Language Acquisition*, S. Gass and J. Schachter, Eds., pp. 41–68, Cambridge University Press, New York, NY, USA, 1989.

[172] H. Clahsen and C. Felser, "Grammatical processing in language learners," *Applied Psycholinguistics*, vol. 27, no. 1, pp. 3–42, 2006.

[173] R. Hawkins and C. Y.-H. Chan, "The partial availability of universal grammar in second language acquisition: the 'failed functional features hypothesis'," *Second Language Research*, vol. 13, no. 3, pp. 187–226, 1997.

[174] D. Poeppel and D. Embick, "Defining the relation between linguistics and neuroscience," in *Twenty-First Century Psycholinguistics: Four Cornerstones*, A. Cutler, Ed., pp. 103–118, Lawrence Erlbaum Associates, Mahwah, NJ, USA, 2005.

[175] T. Marinis, L. Roberts, C. Felser, and H. Clahsen, "Gaps in second language sentence processing," *Studies in Second Language Acquisition*, vol. 27, no. 1, pp. 53–78, 2005.

[176] C. Felser, I. Cunnings, C. Batterham, and H. Clahsen, "The timing of island effects in nonnative sentence processing," *Studies in Second Language Acquisition*, vol. 34, no. 1, pp. 67–98, 2012.

[177] R. M. DeKeyser, "Age effects in second language learning," in *The Routledge Handbook of Second Language Acquisition*, S. Gass and A. Mackey, Eds., pp. 442–460, Routledge, London, UK, 2012.

[178] E. H. Lenneberg, *Biological Foundations of Language*, Wiley, 1967.

[179] S. Rossi, M. F. Gugler, A. D. Friederici, and A. Hahne, "The impact of proficiency on syntactic second-language processing of German and Italian: evidence from event-related potentials," *Journal of Cognitive Neuroscience*, vol. 18, no. 12, pp. 2030–2048, 2006.

[180] S. G. Mohades, E. Struys, P. Van Schuerbeek, K. Mondt, P. Van De Craen, and R. Luypaert, "DTI reveals structural differences in white matter tracts between bilingual and monolingual children," *Brain Research*, vol. 1435, pp. 72–80, 2012.

[181] K. K. Jasinska and L. A. Petitto, "How age of bilingual exposure can change the neural systems for language in the developing brain: a functional near infrared spectroscopy investigation of syntactic processing in monolingual and bilingual children," *Developmental Cognitive Neuroscience*, vol. 6, pp. 87–101, 2013.

[182] J. Krizman, J. Slater, E. Skoe, V. Marian, and N. Kraus, "Neural processing of speech in children is influenced by extent of bilingual experience," *Neuroscience Letters*, vol. 585, pp. 48–53, 2015.

[183] P. Archila-Suerte, J. Zevin, and A. E. Hernandez, "The effect of age of acquisition, socioeducational status, and proficiency on the neural processing of second language speech sounds," *Brain and Language*, vol. 141, pp. 35–49, 2015.

[184] R. M. DeKeyser, "Implicit and explicit learning," in *The Handbook of Second Language Acquisition*, C. J. Doughty and M. H. Long, Eds., pp. 313–384, Blackwell Publishing, Oxford, UK, 2003.

[185] R. Ellis, *SLA Research and Language Teaching*, Oxford University Press, New York, NY, USA, 2008.

[186] J. Cummins, "Psychological assessment of immigrant children: logic or intuition?" *Journal of Multilingual and Multicultural Development*, vol. 1, no. 2, pp. 97–111, 1980.

[187] J. F. Werker, J. H. V. Gilbert, K. Humphrey, and R. C. Tees, "Developmental aspects of cross-language speech perception," *Child Development*, vol. 52, no. 1, pp. 349–355, 1981.

[188] A. E. Hernandez, *The Bilingual Brain*, Oxford University Press, Oxford, UK, 2013.

[189] A. Van Hout, "Acquired aphasias in children," in *Handbook of Neuropsychology*, S. J. Segalowitz and I. Rapin, Eds., pp. 631–654, Elsevier Science, Amsterdam, The Netherlands, 2003.

[190] J. F. Kroll and C. Chiarello, "Language experience and the brain: variability, neuroplasticity, and bilingualism," *Language, Cognition and Neuroscience*, vol. 30, pp. 1–4, 2015.

[191] K. Friston, "Causal modelling and brain connectivity in functional magnetic resonance imaging," *PLoS Biology*, vol. 7, no. 2, article e33, pp. 220–225, 2009.

[192] R. Jackendoff, *Foundations of Language: Brain, Meaning, Grammar, Evolution*, Oxford University Press, Oxford, UK, 2002.

[193] A. Sorace and F. Filiaci, "Anaphora resolution in near-native speakers of Italian," *Second Language Research*, vol. 22, no. 3, pp. 339–368, 2006.

[194] A. Sorace and L. Serratrice, "Internal and external interfaces in bilingual language development: beyond structural overlap," *International Journal of Bilingualism*, vol. 13, no. 2, pp. 195–210, 2009.

Hindawi Publishing Corporation
BioMed Research International
Volume 2015, Article ID 908917, 11 pages
http://dx.doi.org/10.1155/2015/908917

Research Article

Hemispheric Asymmetry of Human Brain Anatomical Network Revealed by Diffusion Tensor Tractography

Ni Shu,[1,2] Yaou Liu,[3] Yunyun Duan,[3] and Kuncheng Li[3]

[1]*State Key Laboratory of Cognitive Neuroscience and Learning and IDG/McGovern Institute for Brain Research, Beijing Normal University, Beijing 100875, China*
[2]*Center for Collaboration and Innovation in Brain and Learning Sciences, Beijing Normal University, Beijing 100875, China*
[3]*Department of Radiology, Xuanwu Hospital, Capital Medical University, Beijing 100053, China*

Correspondence should be addressed to Ni Shu; nshu55@gmail.com

Received 27 March 2015; Revised 10 August 2015; Accepted 11 August 2015

Academic Editor: Tianming Liu

The topological architecture of the cerebral anatomical network reflects the structural organization of the human brain. Recently, topological measures based on graph theory have provided new approaches for quantifying large-scale anatomical networks. However, few studies have investigated the hemispheric asymmetries of the human brain from the perspective of the network model, and little is known about the asymmetries of the connection patterns of brain regions, which may reflect the functional integration and interaction between different regions. Here, we utilized diffusion tensor imaging to construct binary anatomical networks for 72 right-handed healthy adult subjects. We established the existence of structural connections between any pair of the 90 cortical and subcortical regions using deterministic tractography. To investigate the hemispheric asymmetries of the brain, statistical analyses were performed to reveal the brain regions with significant differences between bilateral topological properties, such as degree of connectivity, characteristic path length, and betweenness centrality. Furthermore, local structural connections were also investigated to examine the local asymmetries of some specific white matter tracts. From the perspective of both the global and local connection patterns, we identified the brain regions with hemispheric asymmetries. Combined with the previous studies, we suggested that the topological asymmetries in the anatomical network may reflect the functional lateralization of the human brain.

1. Introduction

The brain exhibits asymmetry in both macroscopic structure and microscopic cytoarchitecture. Moreover, many studies have revealed the anatomical asymmetry corresponding with functional lateralization [1–3]. For example, leftward asymmetries in the size of regions are involved in language and auditory processing, such as planum temporale [4–7], sylvian fissure [8], and Heschl's gyrus [4, 9, 10], consistent with left-hemispheric dominance for language [11]. Recently, functional neuroimaging studies have established hemispheric specificity for a range of language, motor, and spatial tasks [12]. Structural MRI studies have revealed the structural asymmetries in the cortical thickness or gray matter volumes of various brain regions [13, 14]. Using diffusion tensor imaging (DTI) techniques, researchers have also identified the leftward asymmetries of some white matter tracts, such as cingulum bundles [15, 16] and arcuate fasciculus [2, 3, 17–21].

These previous studies examined the structural or functional asymmetries of some specific brain regions or the anatomical connections between them. The asymmetries of the gray matter or white matter were analyzed from the local regional attributes. Recently, network model was proposed as a useful tool for investigating the structural organization and functional mechanisms of the human brain [22–31]. Graph theory approaches the analyses of complex network that could provide a new powerful way of quantifying the brain's structural and functional systems. With the network models, more and more studies have revealed that the structural and functional networks of the human brain exhibit small-world attributes [23–26, 28, 30, 32–34] and modular structure

[35–37]. Using diffusion MRI, several studies have proposed different methods to construct the brain anatomical network [25, 32, 33, 36, 38, 39]. All these studies revealed that the cortical networks of the human brain have a "small-world" topology, which is characterized by large clustering coefficients and short average path length [30, 40]. However, few studies have examined the hemispheric asymmetries from the perspective of the cerebral anatomical network, and little is known about the asymmetry of the connection patterns of brain regions, which may reflect the functional integration and interaction between different regions.

In this study, we first constructed the anatomical network for each subject by deterministic diffusion tensor tractography (DTT) technique, and then we applied graph theory approaches to examine the topological properties of bilateral brain regions of the network. To investigate the hemispheric asymmetries of the brain, statistical analyses were performed to reveal the brain regions with significant differences between bilateral topological properties. Furthermore, local structural connections were also investigated to examine the local asymmetries of some specific white matter tracts. From the perspective of both the global and local connection patterns, we identified the brain regions with hemispheric asymmetries.

2. Materials and Methods

2.1. Subjects. This study included 72 healthy adult subjects (42 males; mean age 23.4 ± 3.7 years; mean years of education 13.5 ± 4.7 years). All participants were right-handed according to the Edinburgh handedness inventory [41]. Each participant provided a written informed consent before MRI examinations and this study was approved by the Medical Research Ethics Committee of Xuanwu Hospital of Capital Medical University.

2.2. Data Acquisition. DTI was performed with a 3T Siemens Trio MR system using a standard head coil. Head motion was minimized with restraining foam pads provided by the manufacturer. Diffusion-weighted images were acquired employing a single-shot echo planar imaging (EPI) sequence in alignment with the anterior-posterior commissural plane. Integral Parallel Acquisition Technique (iPAT) was used with an acceleration factor of 2. Acquisition time and image distortion from susceptibility artifacts can be reduced by the iPAT method. The diffusion sensitizing gradients were applied along 12 nonlinear directions ($b = 1000\,\text{s/mm}^2$), together with an acquisition without diffusion weighting ($b = 0\,\text{s/mm}^2$). The imaging parameters were 45 continuous axial slices with a slice thickness of 3 mm and no gap, field of view = 256 mm × 256 mm, repetition time/echo time = 6000/87 ms, and acquisition matrix = 128 × 128. The reconstruction matrix was 256 × 256, resulting in an in-plane resolution of 1 mm × 1 mm. For each participant, a sagittal T1-weighted 3D image was also collected using a magnetization prepared rapid gradient echo (MP-RAGE) sequence. The imaging parameters for this were a field of view of 22 cm, repetition time/echo time = 24/6 ms, flip angle = 35°, and voxel dimensions of 1 mm × 1 mm × 1 mm.

2.3. Data Preprocessing. Eddy current distortions and motion artifacts in the DTI dataset were corrected by applying affine alignment of each diffusion-weighted image to the $b = 0$ image, using FMRIB's Diffusion Toolbox (FSL, version 3.3; http://www.fmrib.ox.ac.uk/fsl). After this process, the diffusion tensor elements were estimated by solving the Stejskal and Tanner equation [42, 43], and then the reconstructed tensor matrix was diagonalized to obtain three eigenvalues (λ_1, λ_2, and λ_3) and eigenvectors. The fractional anisotropy (FA) of each voxel was calculated according to the following formula:

$$\text{FA} = \frac{\sqrt{(\lambda_1 - \lambda_2)^2 + (\lambda_1 - \lambda_3)^2 + (\lambda_2 - \lambda_3)^2}}{\sqrt{2\left(\lambda_1^{\,2} + \lambda_2^{\,2} + \lambda_3^{\,2}\right)}}. \quad (1)$$

DTT was implemented with DTIstudio, Version 2.40, software (http://www.mristudio.org), by using the "fiber assignment by continuous tracking" method [44]. All tracts in the dataset were computed by seeding each voxel with FA greater than 0.2. Tractography was terminated if it turned an angle greater than 50 degrees or reached a voxel with FA less than 0.2 [45].

2.4. Construction of Anatomical Network. We constructed the anatomical network for each subject based on the fiber connectivity from deterministic DTT. The main procedures are as follows: First, the brain was automatically segmented into 90 cortical and subcortical regions (45 for each hemisphere; see Table 1) through AAL template (for details, see [32]). Briefly, the individual T1-weighted images were coregistered to the b0 images in the DTI space. The transformed T1 images were then nonlinearly transformed to the ICBM152 T1 template in the Montreal Neurological Institute (MNI) space. Inverse transformations were used to warp the AAL atlas from the MNI space to the DTI native space. Using this procedure, we obtained 90 cortical and subcortical ROIs, each representing a node of the network. Second, all fibers in the brain were obtained by deterministic fiber tractography. And then two nodes u and v are connected with an edge if there exist at least three fibers with end points in regions u and v; the threshold of three fibers was chosen to ensure that the average size of the biggest connected component of the network keeps 90 across all subjects. The number of fibers between regions was only used to indicate the existence/absence of the edge. Therefore, the binarized anatomical network for each subject was constructed and represented by a symmetric 90 × 90 matrix.

2.5. Network Analysis. We investigated the topological properties of the anatomical network at regional (nodal) levels. Regional properties were described in terms of degree (K_i), shortest path length (L_i), and betweenness centrality (B_i) of the node i. Here, we provide brief, formal definitions of each nodal property used in this study.

Table 1: Cortical and subcortical regions of interest defined in the study.

Index	Regions	Abbr.
(1, 2)	Precentral gyrus	PreCG
(3, 4)	Superior frontal gyrus, dorsolateral	SFGdor
(5, 6)	Superior frontal gyrus, orbital part	ORBsup
(7, 8)	Middle frontal gyrus	MFG
(9, 10)	Middle frontal gyrus, orbital part	ORBmid
(11, 12)	Inferior frontal gyrus, opercular part	IFGoperc
(13, 14)	Inferior frontal gyrus, triangular part	IFGtriang
(15, 16)	Inferior frontal gyrus, orbital part	ORBinf
(17, 18)	Rolandic operculum	ROL
(19, 20)	Supplementary motor area	SMA
(21, 22)	Olfactory cortex	OLF
(23, 24)	Superior frontal gyrus, medial	SFGmed
(25, 26)	Superior frontal gyrus, medial orbital	ORBsupmed
(27, 28)	Gyrus rectus	REC
(29, 30)	Insula	INS
(31, 32)	Anterior cingulate and paracingulate gyri	ACG
(33, 34)	Median cingulate and paracingulate gyri	DCG
(35, 36)	Posterior cingulate gyrus	PCG
(37, 38)	Hippocampus	HIP
(39, 40)	Parahippocampal gyrus	PHG
(41, 42)	Amygdala	AMYG
(43, 44)	Calcarine fissure and surrounding cortex	CAL
(45, 46)	Cuneus	CUN
(47, 48)	Lingual gyrus	LING
(49, 50)	Superior occipital gyrus	SOG
(51, 52)	Middle occipital gyrus	MOG
(53, 54)	Inferior occipital gyrus	IOG
(55, 56)	Fusiform gyrus	FFG
(57, 58)	Postcentral gyrus	PoCG
(59, 60)	Superior parietal gyrus	SPG
(61, 62)	Inferior parietal but supramarginal and angular gyri	IPL
(63, 64)	Supramarginal gyrus	SMG
(65, 66)	Angular gyrus	ANG
(67, 68)	Precuneus	PCUN
(69, 70)	Paracentral lobule	PCL
(71, 72)	Caudate nucleus	CAU
(73, 74)	Lenticular nucleus, putamen	PUT
(75, 76)	Lenticular nucleus, pallidum	PAL
(77, 78)	Thalamus	THA
(79, 80)	Heschl gyrus	HES
(81, 82)	Superior temporal gyrus	STG
(83, 84)	Temporal pole: superior temporal gyrus	TPOsup
(85, 86)	Middle temporal gyrus	MTG
(87, 88)	Temporal pole: middle temporal gyrus	TPOmid
(89, 90)	Inferior temporal gyrus	ITG

Note: the regions are listed in terms of a prior template of an AAL atlas [46].

2.5.1. Degree. The degree K_i of a node i is defined as the number of connections to that node. Highly connected nodes have large degree. The degree K_p of a graph is the average of the degrees of all nodes in the graph:

$$K_p = \frac{1}{N}\sum_{i\in G} K_i, \tag{2}$$

which is a measure to evaluate the degree of sparsity of a network.

2.5.2. Shortest Path Length. The mean shortest path length L_i of a node i is

$$L_i = \frac{1}{N-1}\sum_{i\neq j\in G} L_{i,j}, \tag{3}$$

in which $L_{i,j}$ is the smallest number of edges that must be traversed to make a connection between the node i and the node j. The characteristic path length of a network is the average of the shortest path length between the nodes:

$$L_p = \frac{1}{N}\sum_{i\in G} L_i. \tag{4}$$

L_p quantifies the ability of parallel information propagation or global efficiency (in terms of $1/L_p$) of a network [47].

2.5.3. Betweenness Centrality. Betweenness centrality is widely used to identify the most central nodes in a network, which are associated with those nodes that act as bridges between the other nodes. The betweenness B_i of a node i is defined as the number of shortest paths between pairs of other nodes that pass through the node i [48, 49]. The normalized betweenness b_i was then calculated as

$$b_i = \frac{B_i}{(N-1)(N-2)}. \tag{5}$$

The nodes with the largest normalized betweenness values were considered as pivotal nodes (i.e., hubs) in the network.

2.6. Reconstruction of White Matter Tracts. To further investigate the local asymmetries of the structural connections, we then reconstructed several major white matter tracts connecting different brain regions. Based on the anatomical knowledge of fiber projections, several studies have suggested the tracking protocols for the major white matter tracts [21, 50, 51]. According to the published tracking protocols, we reconstructed bilateral cingulum bundles (CB), optic radiation (OR), inferior frontooccipital fasciculus (IFO), inferior longitudinal fasciculus (ILF), arcuate fasciculus (AF), and uncinate fasciculus (UF) for each subject. Based on the reconstructed tracts for each subject, the mean FA of each fiber tract were calculated by averaging the FA values across the voxels that form the three-dimensional tracts derived from tractography.

2.7. Asymmetry Analysis. To analyze hemispheric differences in topological properties for brain regions, we computed the laterality ratio $\mathrm{LI} = (L - R)/(L + R)$ for each property

(K_i, L_i, and b_i). We tested the nullity of this ratio over the group using a nonparametric one-tailed sign test ($p < 0.05$ after Bonferroni correction for multiple comparisons; i.e., 90/2 = 45 pairs of regions). To analyze the hemispheric differences in structural properties for white matter tracts, we compared mean FA values and fiber numbers of each tract between left and right hemispheres by paired t-tests. For each tract, significant asymmetry of FA or fiber number was defined if $p < 0.05$. All the statistical analyses were performed with Matlab.

3. Results

3.1. Brain Regions with Hemispheric Asymmetries in Node Properties. Based on the binary anatomical network constructed for each subject, we calculated the topological properties (K_i, L_i, and b_i) of each node for each subject. Through statistical analyses for all subjects, we revealed some regions with hemispheric asymmetries in nodal properties (Figure 1). We defined leftward asymmetries with better topological properties in the left hemisphere than in the right, such as larger K_i and b_i and smaller L_i in the left. Similarly, rightward asymmetries were defined as regions with larger K_i and b_i and smaller L_i in the right hemisphere. From the results, we revealed some regions with hemispheric asymmetries in all three topological properties, such as leftward asymmetries in the inferior frontotriangular gyrus, insula, inferior parietal gyrus, and posterior medial cortex (paracentral lobule, precuneus, and posterior cingulate gyrus) and rightward asymmetries in the superior frontal gyrus, hippocampus, superior parietal gyrus, supramarginal gyrus, angular gyrus, and middle temporal pole ($p < 0.05$ after Bonferroni correction).

3.2. Structural Asymmetries of the White Matter Tracts. For each subject, we can successfully reconstruct most of the bilateral white matter tracts (Figure 2(a)). However, the right AF is difficult to be tracked out for some subjects (15 out of 72). From Figure 2(b), we can see that several white matter tracts exhibit hemispheric asymmetries in both the microstructural (FA value) and macrostructural (fiber number) properties, such as CB, ILF, and AF ($p < 0.05$, uncorrected).

4. Discussion

In this study, we investigated the hemispheric asymmetries of the human brain from the perspective of the cerebral anatomical network constructed from DTI data. By comparing bilateral topological properties, we revealed some brain regions with significant leftward or rightward asymmetries, which indicated the asymmetric connection patterns of these regions. Moreover, the structural properties of some local white matter tracts also exhibit hemispheric asymmetries, which indicated the asymmetries of local connections. It suggested that the structural organizations of the human brain are asymmetric from both the global and local connection patterns. Then, the functional meanings of these structural asymmetries should be discussed.

4.1. Hemispheric Asymmetries in Node Properties of the Anatomical Network. Previous studies of hemispheric asymmetries in the human brain focused on the structures or functions of some local regions [1, 2, 20, 52, 53]. In this study, we explored the hemispheric asymmetries from the connection patterns between different brain regions, by comparing the topological properties of nodes between bilateral hemispheres in the anatomical network.

Different nodal properties reflect different aspects of the node in the network. In this study, we chose three topological properties, degree, normalized betweenness centrality, and shortest path length, to analyze the hemispheric asymmetries of the anatomical network. Degree means the number of direct connections to the node. Larger degree means more structural connections to other brain regions in the binary anatomical network. Betweenness centrality reflects the importance of the node, and a node with high centrality is thus crucial to efficient communication [48, 49]. Shortest path length quantifies parallel information propagation or global efficiency (in terms of $1/L_i$) of the node, and smaller L_i means higher global efficiency of the parallel information transfer [47]. Although these three properties interrelated with each other, they reflect different aspects of the node in the network. Therefore, a node with a larger degree, a higher centrality, and a smaller shortest path length will play a more important role in the network. Then we suggested that the asymmetric properties of the regions in bilateral hemispheres indicate the lateralization of these regions in the anatomical network.

Since the regions with hemispheric asymmetries in nodal properties were revealed, we categorized these regions by their functions as follows.

Regions with Leftward Asymmetries

(1) Language and auditory function: middle and inferior temporal gyrus [54, 55], caudate nucleus [56, 57], Heschl's gyrus [58, 59], and triangular and orbital part of inferior frontal gyrus [60, 61].

(2) Visual function: middle and inferior temporal gyrus [62, 63], calcarine fissure, and surrounding cortex [62, 64].

(3) Emotion, sensation, and addiction: insula [65, 66].

(4) Association cortex: paracentral lobule, precuneus, posterior cingulate gyrus, and inferior parietal gyrus.

Regions with Rightward Asymmetries

(1) Spatial attention: angular and supramarginal gyrus [67–69].

(2) Face recognition: fusiform gyrus [70, 71].

(3) Emotion and memory: hippocampus and amygdala [68, 72–74].

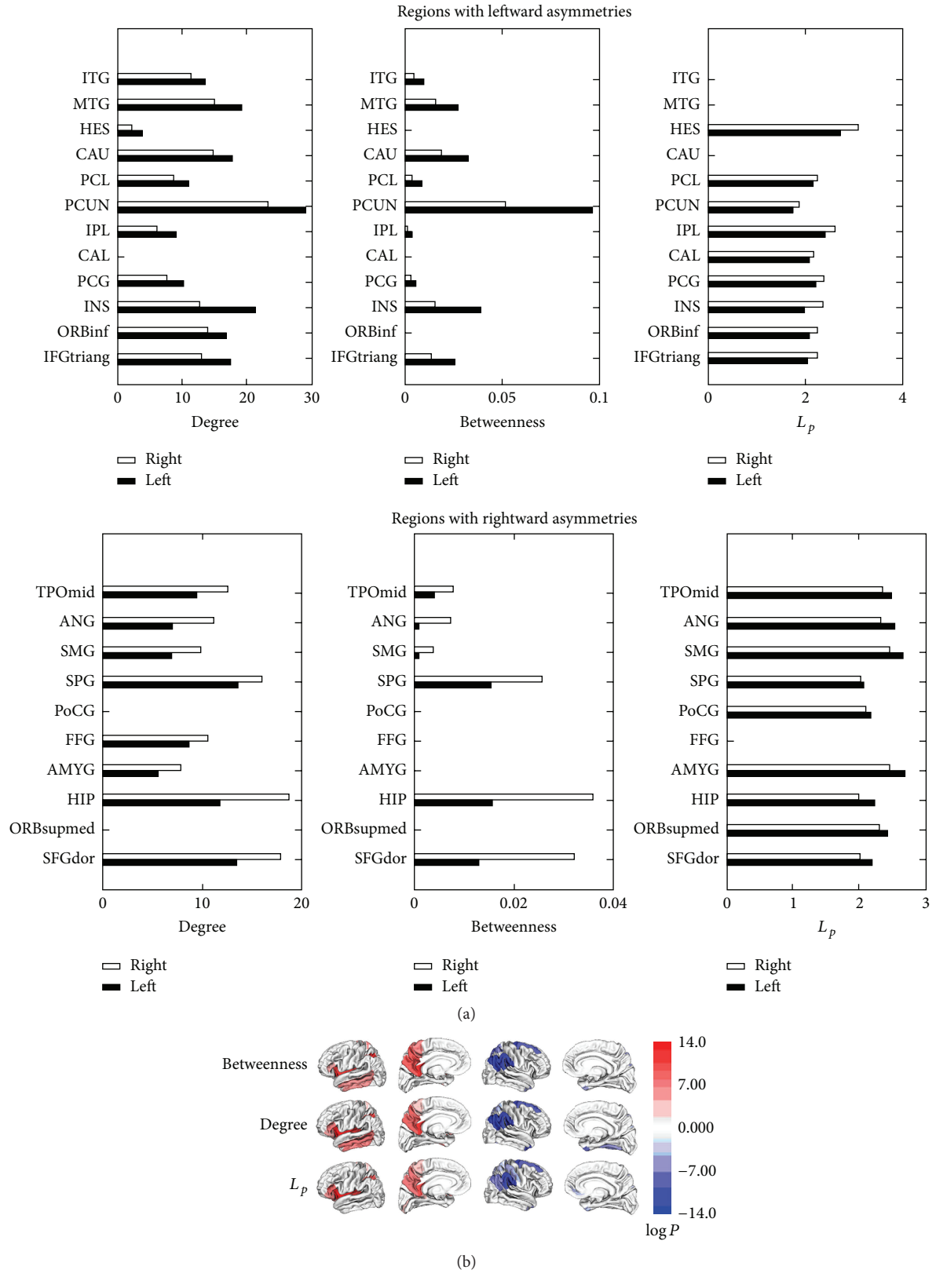

FIGURE 1: Cortical regions with hemispheric asymmetry in node properties. (a) Bars represent the mean values of the nodal property of brain regions with significantly hemispheric asymmetry ($p < 0.05$, corrected) (black: left; white: right). (b) 3D representation of the asymmetric cortical regions overlaid on the cortical surface (red: left > right for betweenness, degree, and $1/L_p$; blue: right > left for betweenness, degree, and $1/L_p$).

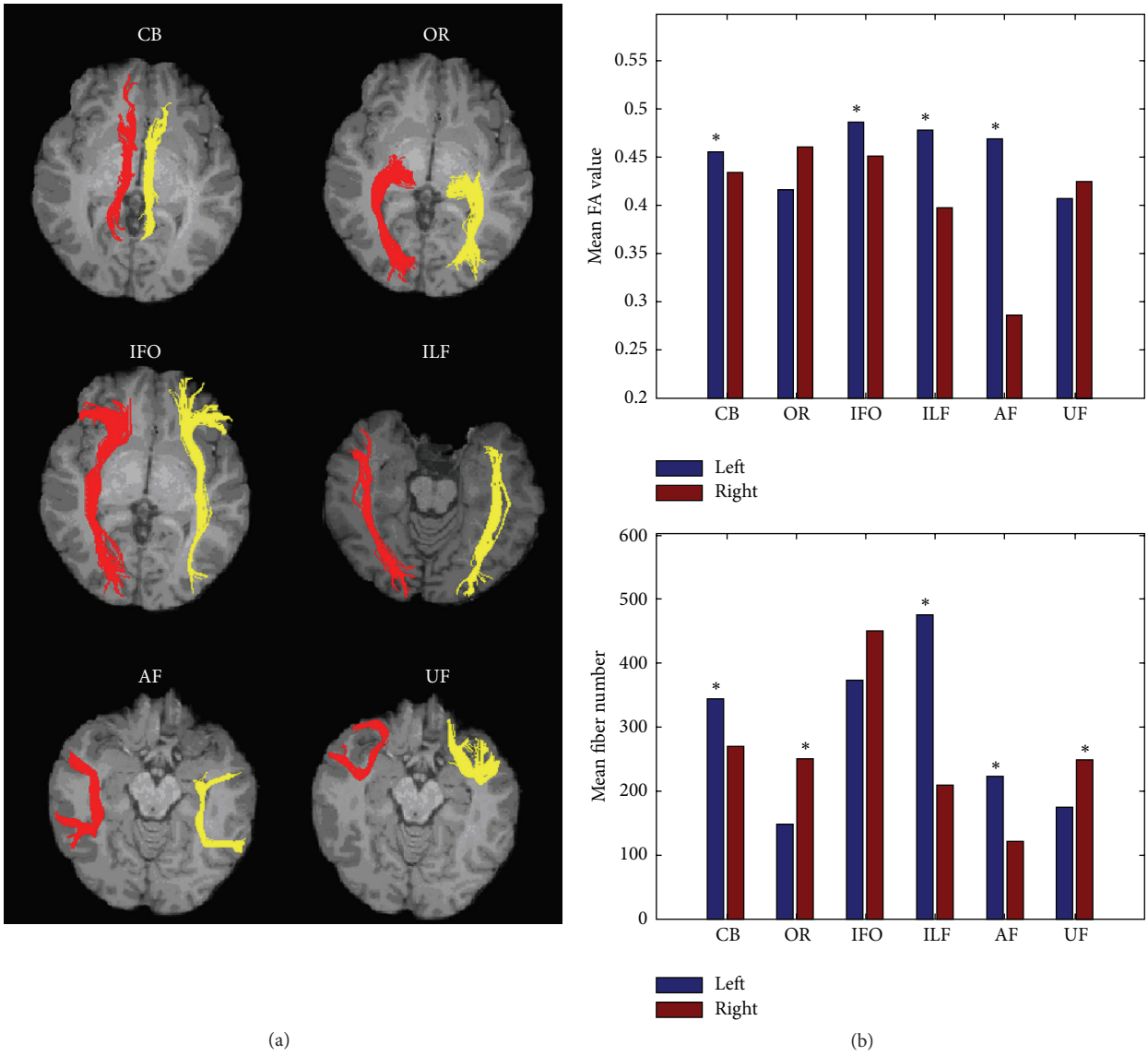

(a) (b)

Figure 2: Structural asymmetries of major white matter tracts. (a) Reconstructed bilateral white matter tracts: cingulum bundles (CB), optic radiation (OR), inferior frontooccipital fasciculus (IFO), inferior longitudinal fasciculus (ILF), arcuate fasciculus (AF), and uncinate fasciculus (UF) (red: left; yellow: right). (b) Between-hemisphere differences for the structural properties of the white matter tracts (∗: significant differences at $p < 0.05$).

(4) Association cortex: superior and middle frontal gyrus, superior parietal gyrus, and middle temporal pole.

From the results, we can see that regions with leftward asymmetries are mainly related to language, visual processing, and sensory functions. Regions with rightward asymmetries are mainly related to the functions of spatial attention, face recognition, emotion, and memory. Some regions in the association cortex with multiple functions also exhibit leftward or rightward asymmetries in the nodal properties.

Combined with the findings of some previous studies, we speculated that the topological asymmetries in the anatomical network are likely to form the structural substrate of different functional principles of information processing in the two hemispheres. Since Paul Broca's discovery in 1861, the notion of left hemisphere specialization for language has been established [11]. Recently, more and more studies revealed the leftward asymmetries in the size of regions involved in language and auditory processing, such as planum temporale [4–7], sylvian fissure [8], and Heschl's gyrus [4, 9, 10], which may supply the anatomic basis of the functional lateralization in the human brain. In this study, the most obvious finding is the leftward asymmetries in several language related regions, such as triangular and orbital areas of inferior frontal gyrus, middle and inferior temporal gyrus, and Heschl's gyrus. The results dovetailed with the prevailing notion that the left hemisphere is the dominant hemisphere for language [75, 76]. It may also suggest that not only the structural asymmetries

of these regions, but also the asymmetric connection patterns of these regions support the functional lateralization of the human brain.

Another finding is the rightward asymmetries of angular and supramarginal gyrus, which located in the temporoparietal junction. The right angular and supramarginal gyrus have been widely implicated in the functions of spatial attention [67–69]. Previous functional MRI studies have also revealed that right temporoparietal junction plays a dominant role in actual implementation of spatial attention by functional connectivity analysis [77, 78]. Therefore, this result corresponded with the right hemispheric specializations for visuospatial functions [75, 79–81].

Some subcortical structures in the limbic system, such as hippocampus and amygdala, were also revealed with rightward asymmetries in the topological properties. Hippocampus plays an important role in memory and spatial navigation [68, 74], and amygdala performs a primary role in the processing of memory and emotion [72, 73]. Then, in this study, the rightward asymmetries in topological properties of hippocampus and amygdala may suggest that the right hemisphere is more prominent in the functions of emotion and memory. It is also consistent with the findings of some structural MRI studies which indicated that the hippocampus and amygdala are rightward asymmetric based on the volume measurements [82].

Besides the above results, we revealed some regions with hemispheric asymmetries in all three topological properties, such as leftward asymmetries in three regions of posterior medial cortex (paracentral lobule, precuneus, and posterior cingulate gyrus), inferior parietal gyrus, and insula and rightward asymmetries in middle temporal pole, superior parietal gyrus, and superior frontal gyrus. Most of these regions are located in the association cortex, which plays a central role in receiving convergent inputs from multiple cortical regions [68]. To be mentioned, three continuous regions in the posterior medial cortex have been revealed as the structure core of the cerebral cortex by a diffusion MRI study [36]. However, no study has examined the functional or structural asymmetries of these core regions yet. Then, in this study, it is the first time to reveal the leftward asymmetries of the core regions in the anatomical network.

Of note, abnormal asymmetric patterns of brain structure or function have been implicated in some psychiatric disorders, such as schizophrenia, and the extent of altered asymmetry is related to the symptoms of the patients [83]. Therefore, we speculated that the asymmetric topology of brain networks would also change under various conditions with mental diseases and may supply as sensitive biomarkers for early disease detection, which should be further investigated.

4.2. Structural Asymmetries of the White Matter Tracts. Based on the tractography results of six major white matter tracts, we analyzed the structural asymmetries of these tracts in mean FA values and fiber numbers. Previous DTI studies have identified the anatomical asymmetries of some fiber tracts, such as leftward asymmetries of the arcuate fasciculus [2, 3, 19–21]. As one of the most important language pathways, arcuate fasciculus starts from Broca's area in inferior frontal gyrus and projects into the middle and inferior temporal gyrus [84]. In this study, we revealed the leftward asymmetries of AF from both the micro- and macrostructural properties. The leftward asymmetry of AF corresponds with the leftward asymmetries of the triangular area of inferior frontal gyrus, middle and inferior temporal gyrus revealed by the topological analysis of the anatomical network. These results suggest that the language related regions exhibit leftward asymmetries from both the global and local anatomical connection patterns. We speculated that these structural asymmetries may provide the anatomical substrate of language related functional lateralization of the human brain. Besides the leftward asymmetries of AF, the CB and ILF are also leftward asymmetric in both mean FA values and fiber numbers. The cingulum bundles have been investigated in several previous DTI studies, and the leftward asymmetries in fiber integrity were identified by different methods [15, 16, 85]. The inferior longitudinal fasciculus, which connects the temporal lobe and occipital lobe, plays an important role in visual memory [86, 87] and is considered as an indirect pathway of language semantic processing [88]. This is the first time leftward asymmetry of ILF is revealed and it may provide new information for future studies. The inferior frontooccipital fasciculus, which connects the posterior occipital areas and the orbitofrontal region, is a direct pathway of language semantic processing [88]. A previous DTI study has reported the leftward asymmetries in the fiber integrity of IFO and has suggested that the structural asymmetries of the tract correspond with the hemispheric dominance for language [21]. Additionally, we found that the optic radiation and uncinate fasciculus are rightward asymmetric in fiber numbers. However, the functional meaning of these asymmetries should be examined in future studies.

As both the global (structural connectome) and local (FA) measures were investigated in the present study, some results can be cross-validated by different measures. For example, we found that both the language related regions and WM tracts exhibited significantly leftward asymmetries. However, global and local measures may represent different physiological meanings. The local measure, such as FA, reflects the white matter integrity or the consistency of fiber orientation at microstructural level, while the nodal properties of brain connectome, such as nodal efficiency, are an integrated metric of global information flow capacity and related to all of the nodal connections, which consist of a specific tract or several tracts together. Therefore, the findings from network analysis can supply more comprehensive information than the traditional regional and local investigations from a system level.

4.3. Methodological Issues. The most essential elements of a network are the nodes and edges. The definition of the nodes and edges has a great effect on the constructed network and the analysis results. Therefore, we need to address some methodological issues about how we carried out the network construction.

First, we applied the AAL template to define the nodes for each subject's network. The AAL template was taken from a MNI single-subject brain [46]. The biggest limitation of this template is the absence of anatomical lateralization of some regions, such as leftward asymmetry of the planum temporale for the vast majority of right-handers [46]. This limitation will affect the results of the topological asymmetries of the anatomical network in this study. In future studies, a more fine parcellation representation, which is defined at a voxel population level rather than a regional level to partition the cerebral cortex into thousands of regions [36], should be employed to investigate the asymmetries of the brain network, in order to localize the asymmetric topological organizations more accurately.

Second, we employed deterministic DTT to define the edges of the anatomical network. However, the "fiber crossing" problem is a limitation of deterministic tractography algorithms, because the tracking always stops when it reaches fiber crossing regions with low factional anisotropy values [89]. This will result in the loss of some existing fibers and hence some edges of the network. Another limitation of deterministic tractography, especially for long-distance fiber bundles, is erroneous tracking results due to noise and resolution limitations [89]. To solve this issue, several researchers have used probabilistic fiber tracking algorithms [90–92]. By modeling a probability distribution of the fiber orientations within a voxel, these statistical methods can identify fiber connections missed by deterministic tracking approaches. However, the number of gradient directions in our diffusion dataset is not sufficient to accurately estimate the probability density function of the fiber orientations. Therefore, future studies with more advanced diffusion imaging techniques or tractography methods could yield a more complete and accurate anatomical network for each subject.

Another issue about the choice of a binary or weighted network needs addressing. For a weighted network, a challenge is to decide on the most representative measure of structural connectivity. Several candidate measures, such as fiber numbers, mean fiber length, fiber density, and mean fraction anisotropy, can be selected as the connectivity measure [25, 38, 39, 93]. But the physiological meaning of these measures is unclear. It is also hard to validate which measure describes the information transfer of neural signals most accurately. In this work, we constructed the binary network by just taking into consideration the existence/absence of regional connections. However, a weighted network with a proper connectivity measure may better reflect the topological asymmetries of the network.

Besides the above methodology limitations, some other important issues should be investigated in the future. First, as the sex effects on the topological organization of brain networks have been suggested [94], the sex differences in the network asymmetry should be examined in the future. Second, due to the relatively small sample size in the present study, other independent datasets with high quality MRI acquisition and larger samples, such as Human Connectome Project (HCP) datasets [95], should be employed to validate the current results.

5. Conclusion

In this study, we have analyzed the hemispheric asymmetries from the perspective of the whole-brain anatomical network and revealed the topological asymmetries of some brain regions, which indicated the asymmetric connection patterns of these regions at the global level. Moreover, we found the structural asymmetries of some local anatomical connections between regions, and the structural asymmetries of the white matter tracts are interrelated with the topological asymmetries of the brain regions. We speculated that the asymmetric connection patterns of brain regions might reflect the functional lateralization of the human brain.

Conflict of Interests

The authors declare that there is no conflict of interests regarding the publication of this paper.

Acknowledgments

This work was supported by the 973 Program (Grant no. 2013CB837300, Ni Shu), the National Natural Science Foundation of China (Grants nos. 81471732, Ni Shu; 81101038 and 30930029, Yaou Liu), the ECTRIMS-MAGNMIS Fellowship from ECTRIMS (Yaou Liu), the Beijing Natural Science Fund (Grant no. 7133244, Yaou Liu), the Beijing Nova Program (Grant no. xx2013045, Yaou Liu), the Beijing New Medical Discipline Based Group (Grant no. 100270569, Ni Shu), and the Fundamental Research Funds for the Central Universities (Grant no. 2013YB28, Ni Shu).

References

[1] T. R. Barrick, I. N. Lawes, C. E. Mackay, and C. A. Clark, "White matter pathway asymmetry underlies functional lateralization," *Cerebral Cortex*, vol. 17, no. 3, pp. 591–598, 2007.

[2] J. Dubois, L. Hertz-Pannier, A. Cachia, J. F. Mangin, D. Le Bihan, and G. Dehaene-Lambertz, "Structural asymmetries in the infant language and sensori-motor networks," *Cerebral Cortex*, vol. 19, no. 2, pp. 414–423, 2009.

[3] M. W. Vernooij, M. Smits, P. A. Wielopolski, G. C. Houston, G. P. Krestin, and A. van der Lugt, "Fiber density asymmetry of the arcuate fasciculus in relation to functional hemispheric language lateralization in both right- and left-handed healthy subjects: a combined fMRI and DTI study," *NeuroImage*, vol. 35, no. 3, pp. 1064–1076, 2007.

[4] R. Dorsaint-Pierre, V. B. Penhune, K. E. Watkins et al., "Asymmetries of the planum temporale and Heschl's gyrus: relationship to language lateralization," *Brain*, vol. 129, no. 5, pp. 1164–1176, 2006.

[5] A. L. Foundas, C. M. Leonard, R. Gilmore, E. Fennell, and K. M. Heilman, "Planum temporale asymmetry and language dominance," *Neuropsychologia*, vol. 32, no. 10, pp. 1225–1231, 1994.

[6] A. M. Galaburda, F. Sanides, and N. Geschwind, "Human brain. Cytoarchitectonic left-right asymmetries in the temporal speech region," *Archives of Neurology*, vol. 35, no. 12, pp. 812–817, 1978.

[7] N. Geschwind and W. Levitsky, "Human brain: left-right asymmetries in temporal speech region," *Science*, vol. 161, no. 3837, pp. 186–187, 1968.

[8] A. B. Rubens, M. W. Mahowald, and J. T. Hutton, "Asymmetry of the lateral (sylvian) fissures in man," *Neurology*, vol. 26, no. 7, pp. 620–624, 1976.

[9] W. C. Loftus, M. J. Tramo, C. E. Thomas, R. L. Green, R. A. Nordgren, and M. S. Gazzaniga, "Three-dimensional quantitative analysis of hemispheric asymmetry in the human superior temporal region," *Cerebral Cortex*, vol. 3, no. 4, pp. 348–355, 1993.

[10] P. Schneider, V. Sluming, N. Roberts et al., "Structural and functional asymmetry of lateral Heschl's gyrus reflects pitch perception preference," *Nature Neuroscience*, vol. 8, no. 9, pp. 1241–1247, 2005.

[11] P. Broca, "Remarques sur le siège de la faculté du langage articulé, suivies d'une observation d'aphémie," *Bulletins de la Société Anatomique de Paris*, vol. 6, pp. 330–357, 1861.

[12] R. J. Davidson and K. Hugdahl, *Brain Asymmetry*, MIT Press, Cambridge, Mass, USA, 1995.

[13] E. Luders, K. L. Narr, P. M. Thompson, D. E. Rex, L. Jancke, and A. W. Toga, "Hemispheric asymmetries in cortical thickness," *Cerebral Cortex*, vol. 16, no. 8, pp. 1232–1238, 2006.

[14] K. E. Watkins, T. Paus, J. P. Lerch et al., "Structural asymmetries in the human brain: a voxel-based statistical analysis of 142 MRI scans," *Cerebral Cortex*, vol. 11, no. 9, pp. 868–877, 2001.

[15] G. Gong, T. Jiang, C. Zhu et al., "Asymmetry analysis of cingulum based on scale-invariant parameterization by diffusion tensor imaging," *Human Brain Mapping*, vol. 24, no. 2, pp. 92–98, 2005.

[16] H.-J. Park, C.-F. Westin, M. Kubicki et al., "White matter hemisphere asymmetries in healthy subjects and in schizophrenia: a diffusion tensor MRI study," *NeuroImage*, vol. 23, no. 1, pp. 213–223, 2004.

[17] C. Büchel, T. Raedler, M. Sommer, M. Sach, C. Weiller, and M. A. Koch, "White matter asymmetry in the human brain: a diffusion tensor MRI study," *Cerebral Cortex*, vol. 14, no. 9, pp. 945–951, 2004.

[18] M. F. Glasser and J. K. Rilling, "DTI tractography of the human brain's language pathways," *Cerebral Cortex*, vol. 18, no. 11, pp. 2471–2482, 2008.

[19] C. Lebel and C. Beaulieu, "Lateralization of the arcuate fasciculus from childhood to adulthood and its relation to cognitive abilities in children," *Human Brain Mapping*, vol. 30, no. 11, pp. 3563–3573, 2009.

[20] P. G. P. Nucifora, R. Verma, E. R. Melhem, R. E. Gur, and R. C. Gur, "Leftward asymmetry in relative fiber density of the arcuate fasciculus," *NeuroReport*, vol. 16, no. 8, pp. 791–794, 2005.

[21] S. Rodrigo, O. Naggara, C. Oppenheim et al., "Human subinsular asymmetry studied by diffusion tensor imaging and fiber tracking," *American Journal of Neuroradiology*, vol. 28, no. 8, pp. 1526–1531, 2007.

[22] S. Achard, R. Salvador, B. Whitcher, J. Suckling, and E. Bullmore, "A resilient, low-frequency, small-world human brain functional network with highly connected association cortical hubs," *Journal of Neuroscience*, vol. 26, no. 1, pp. 63–72, 2006.

[23] D. S. Bassett and E. Bullmore, "Small-world brain networks," *Neuroscientist*, vol. 12, no. 6, pp. 512–523, 2006.

[24] E. Bullmore and O. Sporns, "Complex brain networks: graph theoretical analysis of structural and functional systems," *Nature Reviews*, vol. 10, no. 3, pp. 186–198, 2009.

[25] P. Hagmann, M. Kurant, X. Gigandet et al., "Mapping human whole-brain structural networks with diffusion MRI," *PLoS ONE*, vol. 2, no. 7, article e597, 2007.

[26] Y. He, Z. J. Chen, and A. C. Evans, "Small-world anatomical networks in the human brain revealed by cortical thickness from MRI," *Cerebral Cortex*, vol. 17, no. 10, pp. 2407–2419, 2007.

[27] O. Sporns, D. R. Chialvo, M. Kaiser, and C. C. Hilgetag, "Organization, development and function of complex brain networks," *Trends in Cognitive Sciences*, vol. 8, no. 9, pp. 418–425, 2004.

[28] O. Sporns, G. Tononi, and G. M. Edelman, "Theoretical neuroanatomy: relating anatomical and functional connectivity in graphs and cortical connection matrices," *Cerebral Cortex*, vol. 10, no. 2, pp. 127–141, 2000.

[29] O. Sporns, G. Tononi, and R. Kötter, "The human connectome: a structural description of the human brain," *PLoS Computational Biology*, vol. 1, no. 4, article e42, 2005.

[30] O. Sporns and J. D. Zwi, "The small world of the cerebral cortex," *Neuroinformatics*, vol. 2, no. 2, pp. 145–162, 2004.

[31] C. J. Stam, "Functional connectivity patterns of human magnetoencephalographic recordings: a 'small-world' network?" *Neuroscience Letters*, vol. 355, no. 1-2, pp. 25–28, 2004.

[32] G. Gong, Y. He, L. Concha et al., "Mapping anatomical connectivity patterns of human cerebral cortex using in vivo diffusion tensor imaging tractography," *Cerebral Cortex*, vol. 19, no. 3, pp. 524–536, 2009.

[33] Y. Iturria-Medina, R. C. Sotero, E. J. Canales-Rodríguez, Y. Alemán-Gómez, and L. Melie-García, "Studying the human brain anatomical network via diffusion-weighted MRI and Graph Theory," *NeuroImage*, vol. 40, no. 3, pp. 1064–1076, 2008.

[34] Y. Liu, M. Liang, Y. Zhou et al., "Disrupted small-world networks in schizophrenia," *Brain*, vol. 131, no. 4, pp. 945–961, 2008.

[35] Z. J. Chen, Y. He, P. Rosa-Neto, J. Germann, and A. C. Evans, "Revealing modular architecture of human brain structural networks by using cortical thickness from MRI," *Cerebral Cortex*, vol. 18, no. 10, pp. 2374–2381, 2008.

[36] P. Hagmann, L. Cammoun, X. Gigandet et al., "Mapping the structural core of human cerebral cortex," *PLoS Biology*, vol. 6, no. 7, article e159, pp. 1479–1493, 2008.

[37] D. Meunier, S. Achard, A. Morcom, and E. Bullmore, "Age-related changes in modular organization of human brain functional networks," *NeuroImage*, vol. 44, no. 3, pp. 715–723, 2009.

[38] Y. Li, Y. Liu, J. Li et al., "Brain anatomical network and intelligence," *PLoS Computational Biology*, vol. 5, no. 5, Article ID e1000395, 2009.

[39] A. Zalesky and A. Fornito, "A DTI-derived measure of cortico-cortical connectivity," *IEEE Transactions on Medical Imaging*, vol. 28, no. 7, pp. 1023–1036, 2009.

[40] D. J. Watts and S. H. Strogatz, "Collective dynamics of 'small-world' networks," *Nature*, vol. 393, no. 6684, pp. 440–442, 1998.

[41] R. C. Oldfield, "The assessment and analysis of handedness: the Edinburgh inventory," *Neuropsychologia*, vol. 9, no. 1, pp. 97–113, 1971.

[42] P. J. Basser, J. Mattiello, and D. LeBihan, "Estimation of the effective self-diffusion tensor from the NMR spin echo," *Journal of Magnetic Resonance*, vol. 103, no. 3, pp. 247–254, 1994.

[43] C.-F. Westin, S. E. Maier, H. Mamata, A. Nabavi, F. A. Jolesz, and R. Kikinis, "Processing and visualization for diffusion tensor MRI," *Medical Image Analysis*, vol. 6, no. 2, pp. 93–108, 2002.

[44] S. Mori, B. J. Crain, V. P. Chacko, and P. C. M. Van Zijl, "Three-dimensional tracking of axonal projections in the brain by magnetic resonance imaging," *Annals of Neurology*, vol. 45, no. 2, pp. 265–269, 1999.

[45] S. Mori, W. E. Kaufmann, C. Davatzikos et al., "Imaging cortical association tracts in the human brain using diffusion-tensor-based axonal tracking," *Magnetic Resonance in Medicine*, vol. 47, no. 2, pp. 215–223, 2002.

[46] N. Tzourio-Mazoyer, B. Landeau, D. Papathanassiou et al., "Automated anatomical labeling of activations in SPM using a macroscopic anatomical parcellation of the MNI MRI single-subject brain," *NeuroImage*, vol. 15, no. 1, pp. 273–289, 2002.

[47] V. Latora and M. Marchiori, "Efficient behavior of small-world networks," *Physical Review Letters*, vol. 87, Article ID 198701, 2001.

[48] L. C. Freeman, "A set of measures of centrality based on betweenness," *Sociometry*, vol. 40, no. 1, pp. 35–41, 1977.

[49] M. Girvan and M. E. J. Newman, "Community structure in social and biological networks," *Proceedings of the National Academy of Sciences of the United States of America*, vol. 99, no. 12, pp. 7821–7826, 2002.

[50] K. Hua, J. Zhang, S. Wakana et al., "Tract probability maps in stereotaxic spaces: analyses of white matter anatomy and tract-specific quantification," *NeuroImage*, vol. 39, no. 1, pp. 336–347, 2008.

[51] S. Wakana, A. Caprihan, M. M. Panzenboeck et al., "Reproducibility of quantitative tractography methods applied to cerebral white matter," *NeuroImage*, vol. 36, no. 3, pp. 630–644, 2007.

[52] P. Jung, U. Baumgärtner, P. Stoeter, and R.-D. Treede, "Structural and functional asymmetry in the human parietal opercular cortex," *Journal of Neurophysiology*, vol. 101, no. 6, pp. 3246–3257, 2009.

[53] Y. Otsuka, N. Osaka, and M. Osaka, "Functional asymmetry of superior parietal lobule for working memory in the elderly," *NeuroReport*, vol. 19, no. 14, pp. 1355–1359, 2008.

[54] N. F. Dronkers, D. P. Wilkins, R. D. Van Valin Jr., B. B. Redfern, and J. J. Jaeger, "Lesion analysis of the brain areas involved in language comprehension," *Cognition*, vol. 92, no. 1-2, pp. 145–177, 2004.

[55] C. J. Price, "The anatomy of language: contributions from functional neuroimaging," *Journal of Anatomy*, vol. 197, no. 3, pp. 335–359, 2000.

[56] J. Crinion, R. Turner, A. Grogan et al., "Language control in the bilingual brain," *Science*, vol. 312, no. 5779, pp. 1537–1540, 2006.

[57] D. Ketteler, F. Kastrau, R. Vohn, and W. Huber, "The subcortical role of language processing. High level linguistic features such as ambiguity-resolution and the human brain; an fMRI study," *NeuroImage*, vol. 39, no. 4, pp. 2002–2009, 2008.

[58] Y. Samson, P. Belin, L. Thivard, N. Boddaert, S. Crozier, and M. Zilbovicius, "Auditory perception and language: functional imaging of speech sensitive auditory cortex," *Revue Neurologique*, vol. 157, no. 8-9, pp. 837–846, 2001.

[59] C. Warrier, P. Wong, V. Penhune et al., "Relating structure to function: Heschl's gyrus and acoustic processing," *The Journal of Neuroscience*, vol. 29, no. 1, pp. 61–69, 2009.

[60] F. Aboitiz and R. Garcia, "Merging of phonological and gestural circuits in early language evolution," *Reviews in the Neurosciences*, vol. 20, no. 1, pp. 71–84, 2009.

[61] J. T. Crinion and A. P. Leff, "Recovery and treatment of aphasia after stroke: functional imaging studies," *Current Opinion in Neurology*, vol. 20, no. 6, pp. 667–673, 2007.

[62] J. M. Giménez-Amaya, "Functional anatomy of the cerebral cortex implicated in visual processing," *Revista de Neurología*, vol. 30, no. 7, pp. 656–662, 2000.

[63] L. G. Ungerleider and J. V. Haxby, "'What' and 'where' in the human brain," *Current Opinion in Neurobiology*, vol. 4, no. 2, pp. 157–165, 1994.

[64] C. S. Konen and S. Kastner, "Two hierarchically organized neural systems for object information in human visual cortex," *Nature Neuroscience*, vol. 11, no. 2, pp. 224–231, 2008.

[65] M. Contreras Abarca, F. Ceric, and F. Torrealba, "The negative side of emotions: addiction to drugs of abuse," *Revista de Neurologia*, vol. 47, no. 9, pp. 471–476, 2008.

[66] N. H. Naqvi and A. Bechara, "The hidden island of addiction: the insula," *Trends in Neurosciences*, vol. 32, no. 1, pp. 56–67, 2009.

[67] M. M. Mesulam, "A cortical network for directed attention and unilateral neglect," *Annals of Neurology*, vol. 10, no. 4, pp. 309–325, 1981.

[68] M.-M. Mesulam, "From sensation to cognition," *Brain*, vol. 121, part 6, pp. 1013–1052, 1998.

[69] G. Vallar, "Spatial neglect, Balint-Homes' and Gerstmann's syndrome, and other spatial disorders," *CNS Spectrums*, vol. 12, no. 7, pp. 527–536, 2007.

[70] C. Nagai, "Neural mechanisms of facial recognition," *Brain and Nerve*, vol. 59, no. 1, pp. 45–51, 2007.

[71] M. J. Tovée, "Face processing: getting by with a little help from its friends," *Current Biology*, vol. 8, no. 9, pp. R317–R320, 1998.

[72] I. Ehrlich, Y. Humeau, F. Grenier, S. Ciocchi, C. Herry, and A. Lüthi, "Amygdala inhibitory circuits and the control of fear memory," *Neuron*, vol. 62, no. 6, pp. 757–771, 2009.

[73] B. Roozendaal, B. S. McEwen, and S. Chattarji, "Stress, memory and the amygdala," *Nature Reviews Neuroscience*, vol. 10, no. 6, pp. 423–433, 2009.

[74] L. R. Squire, "Memory and the hippocampus: a synthesis from findings with rats, monkeys, and humans," *Psychological Review*, vol. 99, no. 2, pp. 195–231, 1992.

[75] K. Hugdahl, "Lateralization of cognitive processes in the brain," *Acta Psychologica*, vol. 105, no. 2-3, pp. 211–235, 2000.

[76] K. E. Stephan, J. C. Marshall, K. J. Friston et al., "Lateralized cognitive processes and lateralized task control in the human brain," *Science*, vol. 301, no. 5631, pp. 384–386, 2003.

[77] P. W. Halligan, G. R. Fink, J. C. Marshall, and G. Vallar, "Spatial cognition: evidence from visual neglect," *Trends in Cognitive Sciences*, vol. 7, no. 3, pp. 125–133, 2003.

[78] K. E. Stephan, G. R. Fink, and J. C. Marshall, "Mechanisms of hemispheric specialization: insights from analyses of connectivity," *Neuropsychologia*, vol. 45, no. 2, pp. 209–228, 2007.

[79] F. Lhermitte, F. Chain, F. Chedru, and C. Penet, "A study of visual processes in a case of interhemispheric disconnexion," *Journal of the Neurological Sciences*, vol. 28, no. 3, pp. 317–330, 1976.

[80] R. N. Shepard and J. Metzler, "Mental rotation of three-dimensional objects," *Science*, vol. 171, no. 3972, pp. 701–703, 1971.

[81] J. J. Vogel, C. A. Bowers, and D. S. Vogel, "Cerebral lateralization of spatial abilities: a meta-analysis," *Brain and Cognition*, vol. 52, no. 2, pp. 197–204, 2003.

[82] O. Pedraza, D. Bowers, and R. Gilmore, "Asymmetry of the hippocampus and amygdala in MRI volumetric measurements of normal adults," *Journal of the International Neuropsychological Society*, vol. 10, no. 5, pp. 664–678, 2004.

[83] M. Ke, R. Zou, H. Shen et al., "Bilateral functional asymmetry disparity in positive and negative schizophrenia revealed by resting-state fMRI," *Psychiatry Research*, vol. 182, no. 1, pp. 30–39, 2010.

[84] J. K. Rilling, M. F. Glasser, T. M. Preuss et al., "The evolution of the arcuate fasciculus revealed with comparative DTI," *Nature Neuroscience*, vol. 11, no. 4, pp. 426–428, 2008.

[85] M. Lazar, J. H. Lee, and A. L. Alexander, "Axial asymmetry of water diffusion in brain white matter," *Magnetic Resonance in Medicine*, vol. 54, no. 4, pp. 860–867, 2005.

[86] R. M. Bauer and J. D. Trobe, "Visual memory and perceptual impairments in prosopagnosia," *Journal of Clinical Neuro-Ophthalmology*, vol. 4, no. 1, pp. 39–46, 1984.

[87] N. Shinoura, Y. Suzuki, M. Tsukada et al., "Impairment of inferior longitudinal fasciculus plays a role in visual memory disturbance," *Neurocase*, vol. 13, no. 2, pp. 127–130, 2007.

[88] E. Mandonnet, A. Nouet, P. Gatignol, L. Capelle, and H. Duffau, "Does the left inferior longitudinal fasciculus play a role in language? A brain stimulation study," *Brain*, vol. 130, no. 3, pp. 623–629, 2007.

[89] S. Mori and P. C. M. van Zijl, "Fiber tracking: principles and strategies—a technical review," *NMR in Biomedicine*, vol. 15, no. 7-8, pp. 468–480, 2002.

[90] T. E. J. Behrens, M. W. Woolrich, M. Jenkinson et al., "Characterization and propagation of uncertainty in diffusion-weighted MR imaging," *Magnetic Resonance in Medicine*, vol. 50, no. 5, pp. 1077–1088, 2003.

[91] O. Friman, G. Farnebäck, and C.-F. Westin, "A Bayesian approach for stochastic white matter tractography," *IEEE Transactions on Medical Imaging*, vol. 25, no. 8, pp. 965–978, 2006.

[92] G. J. M. Parker, C. A. M. Wheeler-Kingshott, and G. J. Barker, "Estimating distributed anatomical connectivity using fast marching methods and diffusion tensor imaging," *IEEE Transactions on Medical Imaging*, vol. 21, no. 5, pp. 505–512, 2002.

[93] Y. Iturria-Medina, E. J. Canales-Rodríguez, L. Melie-García et al., "Characterizing brain anatomical connections using diffusion weighted MRI and graph theory," *NeuroImage*, vol. 36, no. 3, pp. 645–660, 2007.

[94] M. Ingalhalikar, A. Smith, D. Parker et al., "Sex differences in the structural connectome of the human brain," *Proceedings of the National Academy of Sciences of the United States of America*, vol. 111, no. 2, pp. 823–828, 2014.

[95] D. C. Van Essen, S. M. Smith, D. M. Barch, T. E. J. Behrens, E. Yacoub, and K. Ugurbil, "The WU-Minn Human Connectome Project: an overview," *NeuroImage*, vol. 80, pp. 62–79, 2013.

Hindawi Publishing Corporation
BioMed Research International
Volume 2015, Article ID 817595, 23 pages
http://dx.doi.org/10.1155/2015/817595

Research Article

Cortical Structural Connectivity Alterations in Primary Insomnia: Insights from MRI-Based Morphometric Correlation Analysis

Lu Zhao,[1] Enfeng Wang,[2] Xiaoqi Zhang,[2] Sherif Karama,[1,3] Budhachandra Khundrakpam,[1] Hongju Zhang,[4] Min Guan,[2] Meiyun Wang,[2] Jingliang Cheng,[5] Dapeng Shi,[2] Alan C. Evans,[1] and Yongli Li[2]

[1]*McConnell Brain Imaging Centre, Montreal Neurological Institute, McGill University, Montreal, QC, Canada H3A 2B4*
[2]*Department of Radiology, Henan Provincial People's Hospital, People's Hospital of Zhengzhou University, Henan 450003, China*
[3]*Douglas Mental Health University Institute, McGill University, Montreal, QC, Canada H4H 1R3*
[4]*Department of Neurology, Henan Provincial People's Hospital, People's Hospital of Zhengzhou University, Henan 450003, China*
[5]*MRI Division, First Affiliated Hospital of Zhengzhou University, Zhengzhou, Henan 450052, China*

Correspondence should be addressed to Dapeng Shi; cjr.shidapeng@vip.163.com, Alan C. Evans; alan.evans@mcgill.ca, and Yongli Li; shyliyongli@126.com

Received 23 March 2015; Revised 25 May 2015; Accepted 28 May 2015

Academic Editor: Enzo Terreno

The etiology and maintenance of insomnia are proposed to be associated with increased cognitive and physiological arousal caused by acute stressors and associated cognitive rumination. A core feature of such hyperarousal theory of insomnia involves increased sensory processing that interferes with the onset and maintenance of sleep. In this work, we collected structural magnetic resonance imaging data from 35 patients with primary insomnia and 35 normal sleepers and applied structural covariance analysis to investigate whether insomnia is associated with disruptions in structural brain networks centered at the sensory regions (primary visual, primary auditory, and olfactory cortex). As expected, insomnia patients showed increased structural covariance in cortical thickness between sensory and motor regions. We also observed trends of increased covariance between sensory regions and the default-mode network, and the salience network regions, and trends of decreased covariance between sensory regions and the frontoparietal working memory network regions, in insomnia patients. The observed changes in structural covariance tended to correlated with poor sleep quality. Our findings support previous functional neuroimaging studies and provide novel insights into variations in brain network configuration that may be involved in the pathophysiology of insomnia.

1. Introduction

Chronic insomnia is the most prevalent sleep complaint, which affects about 20% of adult population worldwide [1]. Insomnia is associated with reduced quality of life [2], cognitive impairments [3], physical complaints [4], and poor social functioning [5]. Moreover, chronic insomnia can increase vulnerability for psychiatric disorders [6, 7] and cardiovascular morbidity and mortality [8] and is associated with increased health care consumption [9]. Despite the huge socioeconomic impact of chronic insomnia, by far, its neurobiological correlates have not been well understood. Insomnia can be classified as an independent psychiatric syndrome, known as primary insomnia (PI), and a common comorbidity associated with a variety of physical and psychiatric disorders, known as secondary insomnia [10]. Approximately 25% of the population with chronic insomnia is considered to have PI [11]. Studying chronic PI may allow investigation of the biology of insomnia in a relatively pure condition, independent of influences attributable to any coexisting comorbid medical or psychiatric disorders [12].

In the past two decades, a number of studies using diverse functional neuroimaging techniques have revealed that central nervous system hyperarousal represents a major

pathophysiologic pathway in the development and maintenance of insomnia [13–16]. A core feature of the hyperarousal theory of insomnia involves increased sensory processing that interferes with the onset and maintenance of sleep. Patients with PI, relative to healthy sleepers, have been found to show greater high frequency electroencephalographic (EEG) activity in the Beta range around sleep onset [17], during non-rapid eye movement (NREM) sleep [18] and even during normal waking [19]. EEG signals in the Beta range have been known to be a main feature of coherent cortical processing of sensory information. Consistently with such hypothesis, increased intrinsic functional connectivity between sensory-motor regions has been observed in patients with PI based on resting-state functional magnetic resonance imaging (fMRI) [20]. In another resting-state fMRI study [21], patients with PI showed increased functional connectivity of the emotional circuit with the premotor and sensory-motor cortex, which were positively correlated with the severity of insomnia. Therefore, insomnia patients may be in a perpetual cycle of hyperarousal and increased sensitivity to sensory stimulation, which may lead to difficulty in initiating or maintaining sleep.

It has been known that the dynamic emergence of coherent physiological activities that span distinct brain regions making up functional networks is supported by complex structural networks constituted by neuronal elements of the brain [22]. Thus, a question arises: are the pathophysiology of insomnia and the deficits in sensory processing associated with alterations in brain structural connectivity in addition to the aberrant functional connectivity? To explore the answer, we investigated the interregional structural networks for patients with PI and healthy sleepers. Interregional structural networks were constructed using covariance analysis of magnetic resonance imaging- (MRI-) based cortical thickness data. Since axonally connected brain regions are believed to have common trophic, genetic, maturational, and functional interaction effects [23–25], correlations in brain morphology can indicate interregional connectivity [26]. Cortical thickness can reflect in vivo intrinsic characteristics of intracortical morphology including cell size, density, and cell arrangement in a topologically and biologically meaningful way [27]. Structural covariance network (SCN) analysis has extensively been used to investigate brain network alterations during normal development [28, 29] and aging [30] and in diseased populations [31–33].

In the present study, the structural covariance of networks involved in sensory processing was investigated by seeding from the primary visual cortex (PVC), the primary auditory cortex (PAC), and the olfactory cortex (OLF). Based on existing functional neuroimaging findings, we hypothesized that patients with PI would show greater sensory-motor connectivity compared with normal sleepers, and such alteration would be correlated with poor sleep quality.

2. Materials and Methods

2.1. Participants. This work studied 35 patients with PI (age = 39.3 ± 8.6 years; range 22–55 years; 5 males; 30 females) and 35 healthy controls (age = 34.9 ± 10.7 years; range 23–54 years; 9 males; 26 females), who were recruited at the Neurology Department of the People's Hospital of Zhengzhou University. All participants were right-handed. Diagnosis was performed according to the DSM-IV inclusion criteria for PI [10]. The questionnaire of Pittsburgh Sleep Quality Index (PSQI) [34] was implemented for all participants to evaluate their sleep quality. Please note that PSQI was not used for PI diagnosis and subject classification. All healthy controls reported restorative and satisfactory sleep and had regular sleep habits and obtained PSQI total scores <5. All participants were also screened to ensure that they had no history of chronic neurological or psychiatric disorders, for example, anxiety, and depression, and had never suffered from other sleep disorders. All procedures were approved by the ethics committee of People's Hospital of Zhengzhou University, and written informed consent was obtained from all participants.

2.2. MRI Image Acquisition. MRI data acquisition was conducted on a Siemens 3.0 T TrioTim whole-body scanner (Siemens AG, Erlangen, Germany) using a 12-channel array coil. High-resolution structural volumes were obtained using a T1-weighted 3-Dimensional Magnetization Prepared Rapid Acquisition GRE (3D-MPRAGE) sequence (TR = 1,950 ms, TE = 2.30 ms, TI = 900 ms, matrix = 248 × 256, slice thickness = 1 mm, no distance, and FOV = 244 × 252).

2.3. MR Image Processing and Cortical Thickness Measurements. The T1-weighted MR images were processed with the CIVET MRI analysis pipeline (version 1.1.12) [35] developed at the Montreal Neurological Institute. First, native MRI images were corrected for intensity nonuniformity using the N3 algorithm [36], and images in the native space were linearly registered into the stereotaxic space [37]. The registered brain volume was segmented into WM, GM, cerebrospinal fluid (CSF), and background [38]. The inner and outer cortical surfaces (each hemispheric surface consisted of 40962 vertices and 81920 triangles) were then automatically extracted using the CLASP algorithm [39]. The obtained cortical surfaces were nonlinearly aligned to a hemisphere-unbiased iterative surface template [40] using a depth-potential function [41] for accurate cross-subject correspondences. Finally, cortical thickness was measured as the Euclidean distance between linked vertices, respectively, on the inner and outer cortical surfaces throughout the cortex with native scaling [27].

2.4. Statistical Analysis. The statistical analysis of SCNs was conducted using the SurfStat toolbox (http://www.math.mcgill.ca/keith/surfstat/) for Matlab (R2014a, The Mathworks, Natick, MA, USA).

2.4.1. Cortical Thickness Analysis. Between-group differences in cortical thickness were assessed using vertex-wise analysis of variance across the whole cortex, controlling for age, gender, and the mean cortical thickness. We also explored whether cortical thickness was associated with the sleep quality, measured as PSQI scores, by computing Pearson's

correlation coefficients removing the effects of age, gender, and global mean cortical thickness.

2.4.2. Structural Covariance Network Construction. SCNs were constructed by seeding from the primary sensory regions, which were delineated using the Automated Anatomical Labeling (AAL) atlas [42]. These seed regions included the PVC, that is, the bilateral calcarine fissure and surrounding cortex (CAL), the PAC, that is, the bilateral Heschl's gyri (HES), and the bilateral OLF (see Figure S1 in Supplementary Material available online at http://dx.doi.org/10.1155/2015/817595). Prior to the network analysis, a linear regression was performed at every cortical vertex to remove the effects of age and gender. The residuals of this regression were used to substitute for the raw cortical thickness measurements. Then, for each group, the averaged adjusted cortical thickness within each of the seed regions was correlated with all other vertices on the entire cortical surface. Significant correlation was interpreted as connectivity. Following previously reported nomenclature [43], the model fitted for the cortical thickness T at a surface point i was

$$T_i = \beta_0 + \beta_1 T_{\text{seed}} + \varepsilon. \quad (1)$$

2.4.3. Between-Group Comparisons in Structural Covariance Networks. To compare the structural covariance in the group of patients with PI and in the group of healthy controls, we used linear interaction models, which contained terms for the *seed thickness* and *group*, together with a *seed thickness* × *group* interaction term. We assessed differences in structural covariance between groups by testing the significance of the interaction term at each vertex [43]. The model fitted for the cortical thickness T at a surface point i was

$$T_i = \beta_0 + \beta_1 T_{\text{seed}} + \beta_2 \text{Group} + \beta_3 \left(T_{\text{seed}} * \text{Group}\right) + \varepsilon. \quad (2)$$

2.4.4. Network Modulations by Sleep Quality. We assessed the modulation of covariance strength by sleep quality that was measured as PSQI score. These models contained terms for *seed thickness* and *PSQI score* as well as a parametric interaction term for *seed thickness* × *PSQI score*. The model fitted for the cortical thickness T at a surface point i was

$$T_i = \beta_0 + \beta_1 T_{\text{seed}} + \beta_2 \text{PSQI} + \beta_3 \left(T_{\text{seed}} * \text{PSQI}\right) + \varepsilon. \quad (3)$$

2.4.5. Correction for Multiple Comparisons. Random field theory (RFT) [44] was utilized to correct for multiple comparisons in our surface-based analyses, which controlled the chance of reporting a familywise error (FWE) to $P < 0.05$. To illustrate trends, surface maps were also shown at an uncorrected threshold of $P < 0.05$.

3. Results

3.1. Demographic Data. Demographic features for the groups of patients with PI and healthy controls are shown in Table 1. The two groups were not significantly different in age and gender proportion ($P > 0.05$, uncorrected). Patients with PI had significantly higher total PSQI score ($P = 4.52e-23$, uncorrected) relative to healthy controls, illustrating that patients had significantly poorer sleep quality.

Table 1: Demographic data of patients with primary insomnia (PI) and healthy controls (HC).

	PI	HC	P value
Number of subjects	35	35	
Gender (male/female)	5/35	9/26	0.23[a]
Age in years (M, SD)	39.3, 8.6	34.9, 10.7	0.067[b]
Total PQSI (M, SD)	12.57, 3.93	2.26, 1.36	$4.52e-23$[c]

M = mean, SD = standard deviation, and PQSI = Pittsburgh Sleep Quality Index.
[a]The P value was obtained with a Chi-square test.
[b]The P value was obtained with a two-tailed two-sample t-test.
[c]The P value was obtained with a one-tailed two-sample t-test.

3.2. Cortical Thickness Analysis. Between-group differences in cortical thickness are illustrated in Figure 1(a). No difference in cortical thickness surpassed the threshold for multiple comparison correction. Analysis of uncorrected differences revealed trends of increased cortical thickness in patients with PI ($P < 0.05$, uncorrected) in the left anterior PAC, the left inferior lateral occipital cortex (LOC), the left the paracentral lobule (PCL), the left anterior cingulate cortex (ACC), the right middle cingulate cortex (MCC), the right cuneus, the right PVC, the right precuneus, and the right parahippocampal gyrus (PHG). In addition, patients with PI also tended to have decreased cortical thickness in the lateral prefrontal cortex (PFC) ($P < 0.05$, uncorrected). Furthermore, correlations between the vertex-wise cortical thickness and the sleep quality (measured as PSQI score, higher PSQI indicates lower sleep quality) are shown in Figure 1(b). The areas showed trends of increased cortical thickness in PI and the left superior parietal cortex (SPC) showed positive correlations ($P < 0.05$, uncorrected) of thickness with PSQI; the areas tended to have decreased thickness in PI and the left inferior parietal cortex (IPC) and the right opercular part of inferior frontal gyrus (IFGoperc) exhibited trends of negative thickness, PSQI correlations ($P < 0.05$, uncorrected).

3.3. Structural Covariance Analysis of Visual Networks. The SCNs seeded from the left and right PVC (CAL) are illustrated in Figures 2(a) and 3(a), respectively. In healthy controls, the left and right PVC anchored similar structural covariance maps that included the SPC, the right pre- and postcentral gyri, the visual areas (the lateral and medial occipital cortex), the precuneus and posterior cingulate cortex (PCC), and the ventral medial prefrontal cortex (vmPFC) ($P < 0.05$, RFT-cluster corrected). The right PVC additionally encompassed the right posterior insula ($P < 0.05$, RFT-cluster corrected).

In patients with PI, the distribution of significant correlations for PVC ($P < 0.05$, RFT-cluster corrected) was similar to that seen in healthy controls, but more widespread

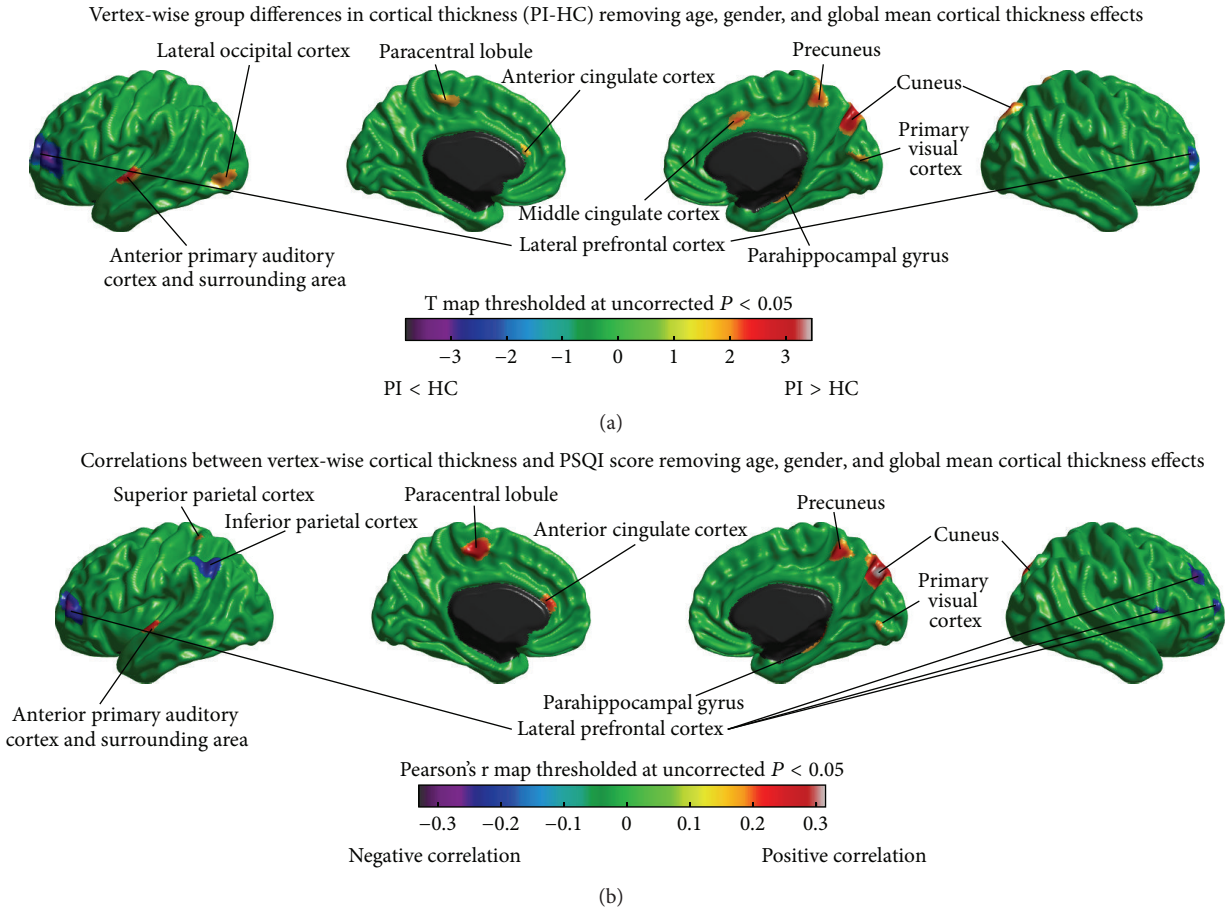

Figure 1: Vertex-wise cortical thickness analysis. (a) Differences in cortical thickness between patients with primary insomnia (PI) and healthy controls (HC), removing effects of age, gender, and global mean cortical thickness. (b) Correlations between vertex-wise cortical thickness and PSQI score removing effects of age, gender, and global mean cortical thickness. No differences and correlations survived the correction for multiple comparisons. Trends ($P < 0.05$, uncorrected) are shown here.

in the medial motor areas (the PCL and the supplementary motor areas (SMA)), the medial temporal cortex (PHG), the left postcentral gyrus, and the right insula and less widespread in the LOC and the left vmPFC.

Figures 2(b), 2(c), 3(b), and 3(c) show the differences in the covariance networks of the PVC between the groups of patients with PI and healthy controls. No difference in the connectivity strength of the left and right PVC surpassed the threshold for multiple comparison correction. Analysis of uncorrected differences revealed trends of increased correlations ($P < 0.05$, uncorrected) between the bilateral PVC and the medial motor areas (PCL/SMA) and the left cuneus, and between the left PVC and the left dorsal parietooccipital region, the right PHG and the right inferior temporal cortex (ITC), and between the right PVC and the right vmPFC and the right posterior insula, in patients with PI. Patients also showed trends of decreased covariance ($P < 0.05$, uncorrected) between the bilateral PVC and the lateral PFC, the IPC, the LOC, the left superior temporal cortex (STC), the dorsal medial prefrontal cortex (dmPFC), and the IFGoperc.

3.4. Structural Covariance Analysis of Auditory Networks. Figures 4(a) and 5(a) show the SCNs seeded from the left and right PAC (HES), respectively. In healthy controls, both the left and right PAC were connected with the bilateral opercular areas (the STC, the posterior insula, and the lower part of the postcentral gyri) ($P < 0.05$, RFT-cluster corrected). The left PAC network additionally included the left and right inferior PFC ($P < 0.05$, RFT-cluster corrected); the right PAC network also included the left and right medial visual areas and the left ITC ($P < 0.05$, RFT-cluster corrected).

The left and right PAC were also connected with the bilateral opercular areas ($P < 0.05$, RFT-cluster corrected) in PI. However, in patients, we observed additional correlations of the left PAC with the lateral PFC, the pre- and postcentral gyri, the lateral temporal and parietal areas, the dmPFC, the vmPFC, and the right superior cuneus; and additional correlations of the right PAC with the left postcentral gyrus, the medial occipital cortex, the medial motor areas (PCL/SMA), the precuneus/PCC, the right dmPFC and vmPFC, and the medial and inferior temporal cortex.

Figures 4(b), 4(c), 5(b), and 5(c) illustrate the differences in the covariance networks of PAC between the groups of patients with PI and healthy controls. In patients, the covariance network of the left PAC showed prominently increased correlations with the left postcentral gyrus and the bilateral

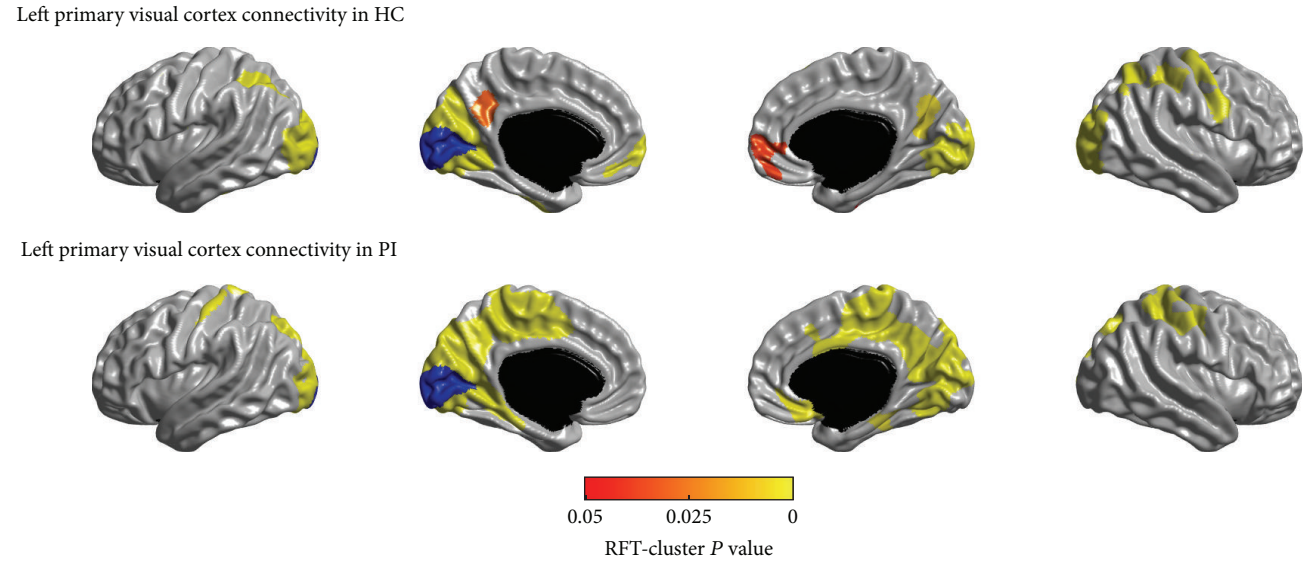

(a)

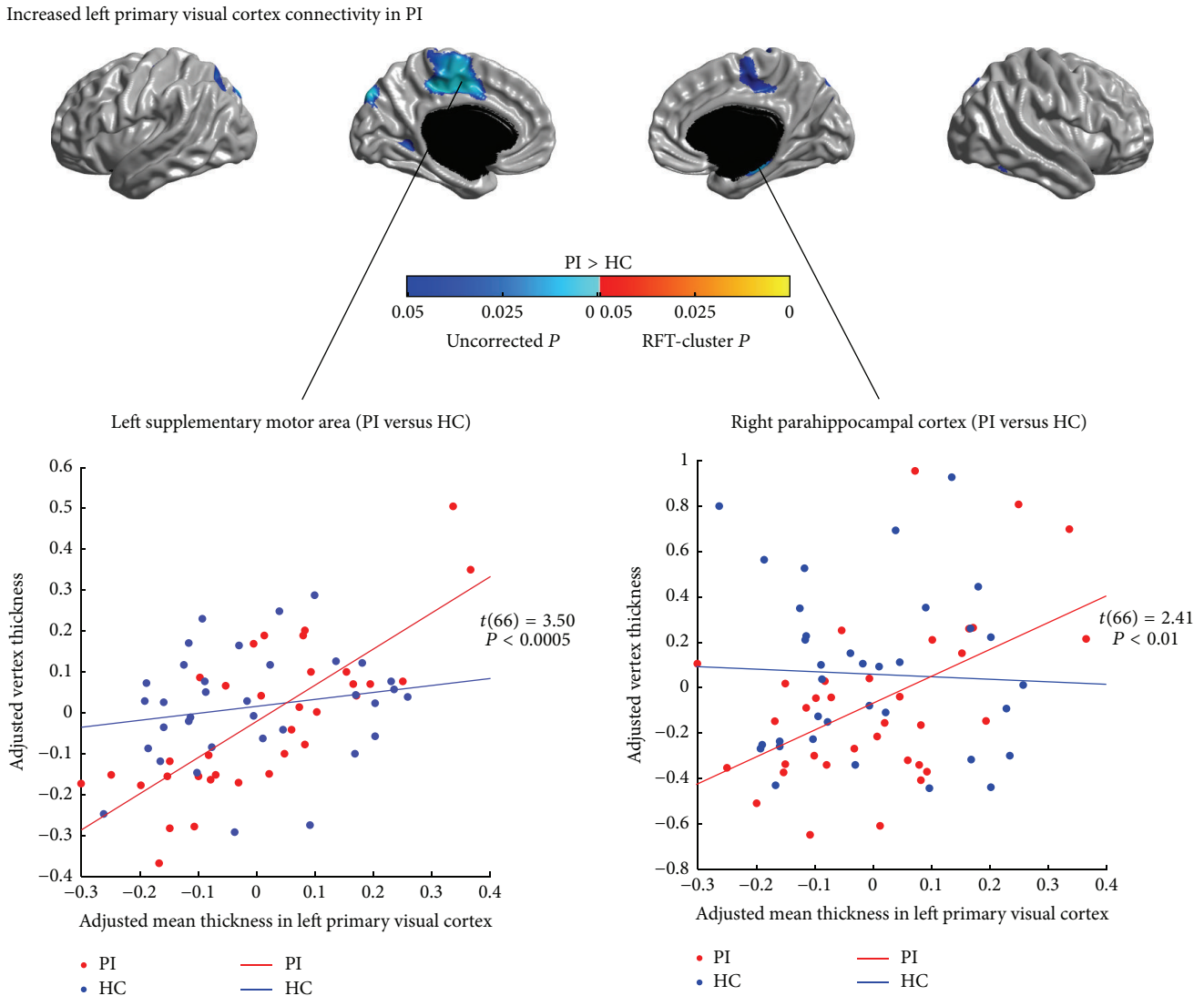

(b)

Figure 2: Continued.

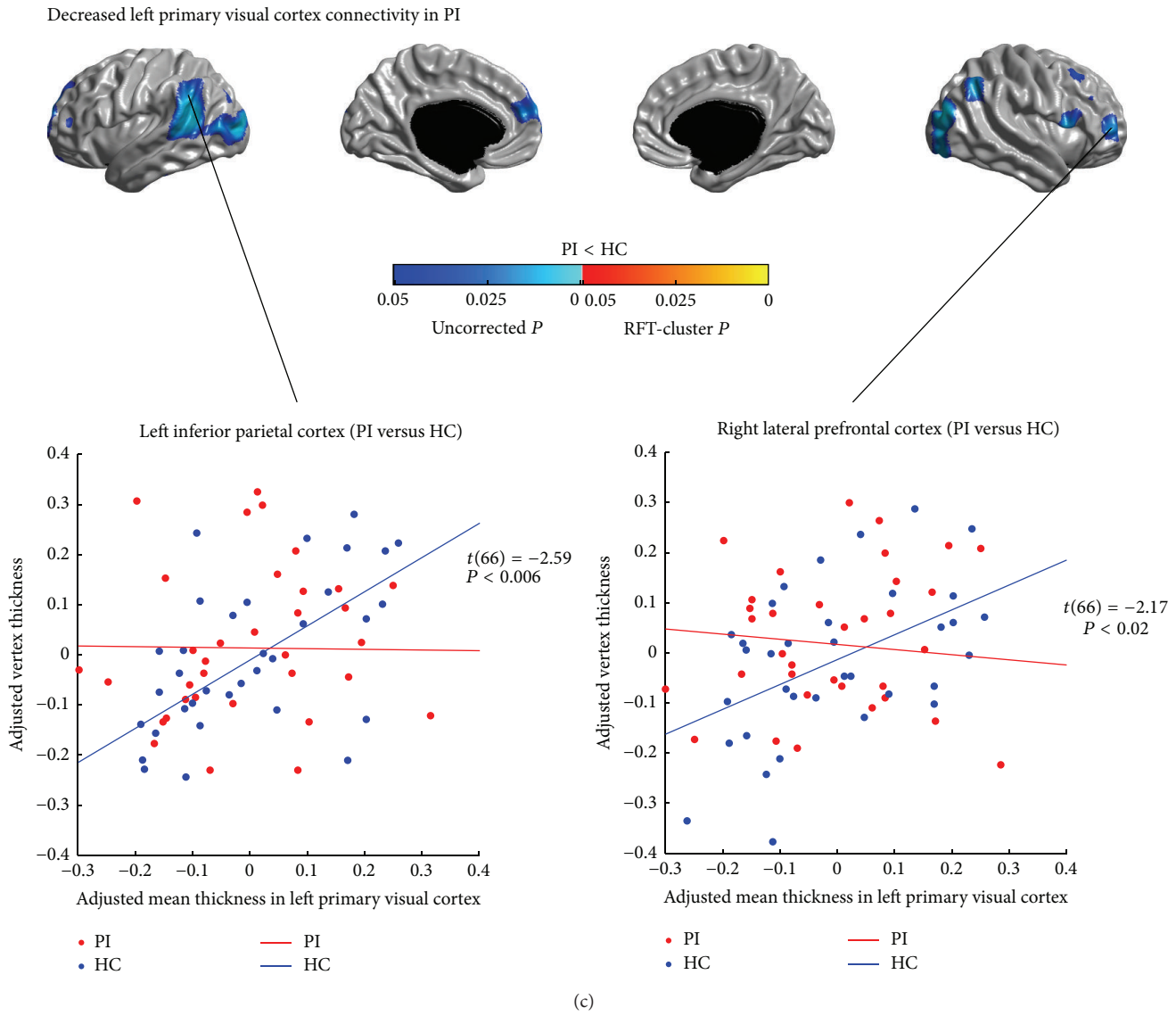

Figure 2: Between-group comparison of structural covariance seeded from the left primary visual cortex (PVC). (a) Structural covariance maps in healthy controls (HC) and patients with primary insomnia (PI). Seed region is colored in blue. (b) Increased left PVC-cortical network covariance in PI. Patients showed trends of increased covariance between the left PVC and the medial motor areas, the left dorsal parietooccipital region, the left cuneus, the right PHG, and the right ITC ($P < 0.05$, uncorrected). (c) Decreased left PVC-cortical network covariance in PI. Patients showed trends of decreased covariance between the left PVC and the lateral PFC, the IPC, the LOC, the left STC, the left dmPFC, and the right IFGoperc ($P < 0.05$, uncorrected). Scatter plots illustrate slope differences in selected vertices, where adjusted cortical thickness values and regression lines are shown in red for patients and in blue for controls.

anterior lateral temporal cortices (LTC) ($P < 0.05$, RFT-cluster corrected), as well as trends of increased correlations with the dorsal and inferior lateral PFC, the bilateral precentral gyri, the right postcentral gyrus, the LTC, the left posterior insula, the lateral parietal cortex, the medial motor areas (PCL/SMA), the dmPFC, the left OLF, the right vmPFC, and the right superior cuneus ($P < 0.05$, uncorrected). Patients' right PAC network showed significantly increased correlation with the right medial motor area (PCL/SMA) ($P < 0.05$, RFT-cluster corrected), and trends of increased correlations with the left postcentral gyrus, the left medial motor area (PCL/SMA), the left cuneus, the precuneus/PCC, the vmPFC, the right MCC, the right OLF, the right ITC, and the right posterior insula ($P < 0.05$, uncorrected). Furthermore, patients showed trends of decreased correlations ($P < 0.05$, uncorrected) between the bilateral PAC and the lateral PFC and the IFGoperc, and between the left PAC and the right ITC (the fusiform gyrus (FFG)), and between the right PAC and the IPC and the LTC.

3.5. Structural Covariance Analysis of Olfactory Networks. The SCNs seeded from the left and right OLF are illustrated in Figures 6(a) and 7(a), respectively. In healthy controls, the left and right OLF were mainly connected with the anterior

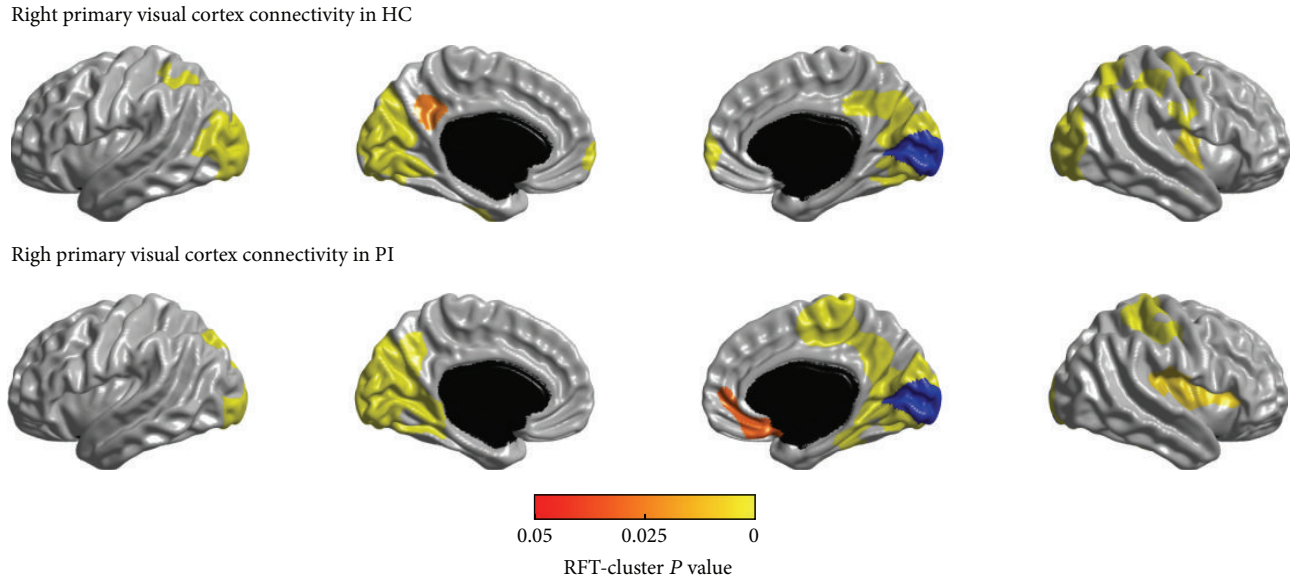

(a)

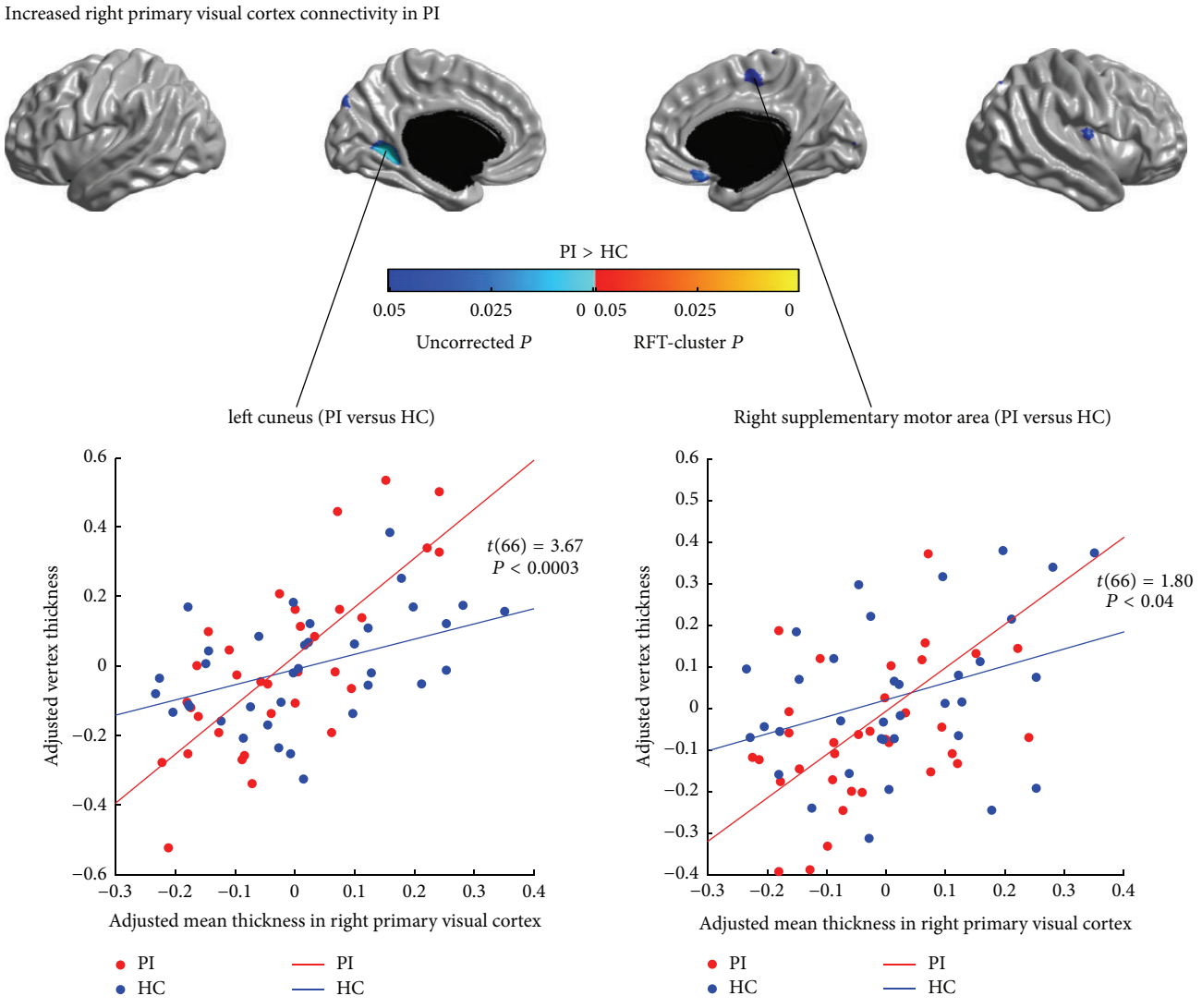

(b)

Figure 3: Continued.

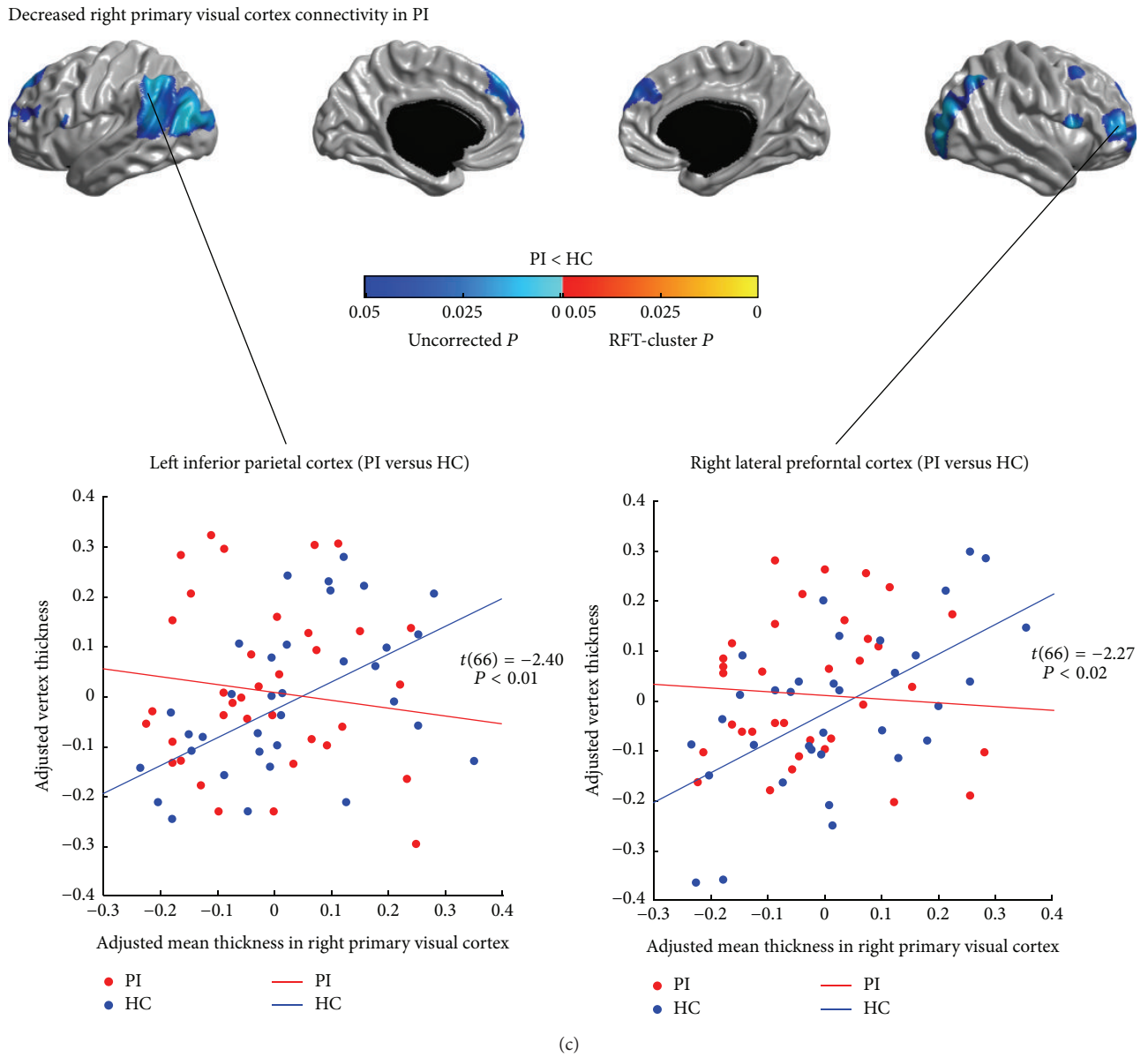

Figure 3: Between-group comparison of structural covariance seeded from the right primary visual cortex (PVC). (a) Structural covariance maps in healthy controls (HC) and patients with primary insomnia (PI). Seed region is colored in blue. (b) Increased right PVC-cortical network covariance in PI. Patients showed trends of increased covariance between the right PVC and the medial motor areas (PCL/SMA) and the left cuneus, the right vmPFC, and the right posterior insula ($P < 0.05$, uncorrected). (c) Decreased right PVC-cortical network covariance in PI. Patients showed trends of decreased covariance between the right PVC and the lateral PFC, the IFGoperc, the IPC, the LOC, the dmPFC, and the left STC ($P < 0.05$, uncorrected). Scatter plots illustrate slope differences in selected vertices, where adjusted cortical thickness values and regression lines are shown in red for patients and in blue for controls.

and inferior PFC, the parietal cortex, and the vmPFC ($P < 0.05$, RFT-cluster corrected). The right PVC additionally encompassed the precuneus/PCC, the ACC and the MCC, the dmPFC, the left lingual gyrus, the right precentral gyrus, and the right posterior insula ($P < 0.05$, RFT-cluster corrected).

Similar to controls, patients' OLF SCNs also included the anterior and inferior PFC, the parietal cortex, and the vmPFC ($P < 0.05$, RFT-cluster corrected). However, in PI, the left OLF network showed additional correlations in the bilateral insula, the temporoparietal regions, the ACC, the right MCC, and the lower parts of the right pre- and post-central gyri. The right OLF network in patients showed more widespread correlations with the dorsal central areas, the superior parietal cortex, the medial motor areas (PCL/SMA), the medial occipital lobes, and the right precuneus, whereas the correlations to the left MCC and the left dmPFC did not reach significance ($P > 0.05$, RFT-cluster corrected).

Figures 6(b), 6(c), 7(b), and 7(c) show the differences in the covariance networks of OLF between the groups of

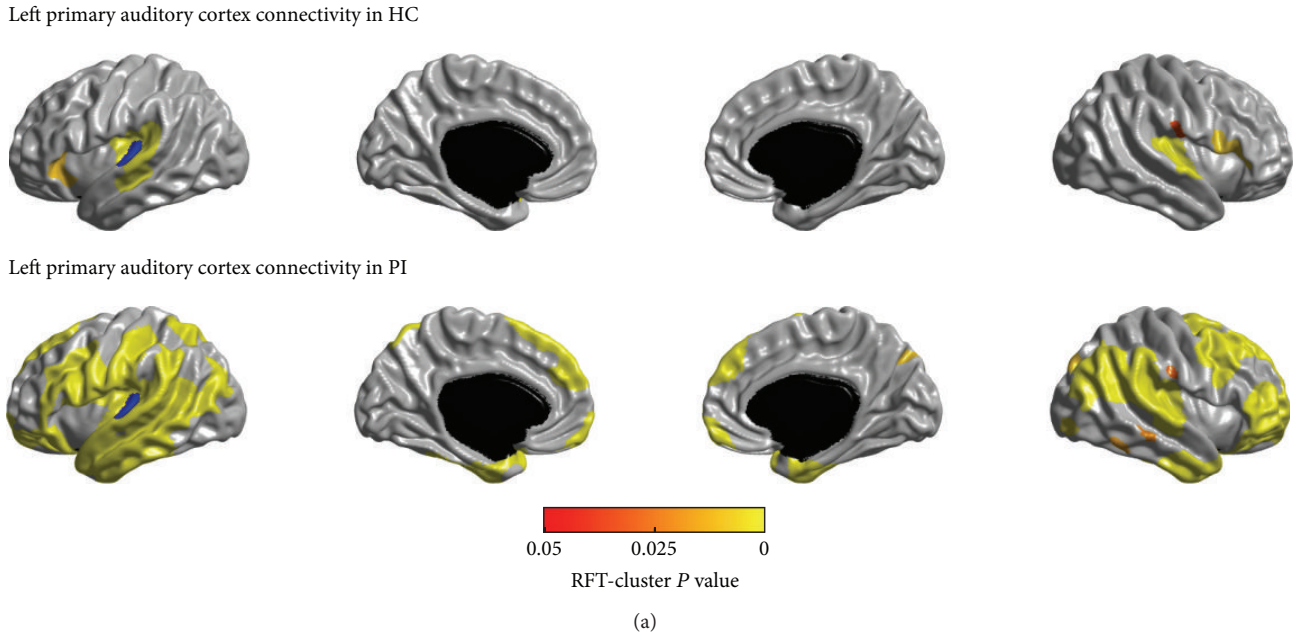

(a)

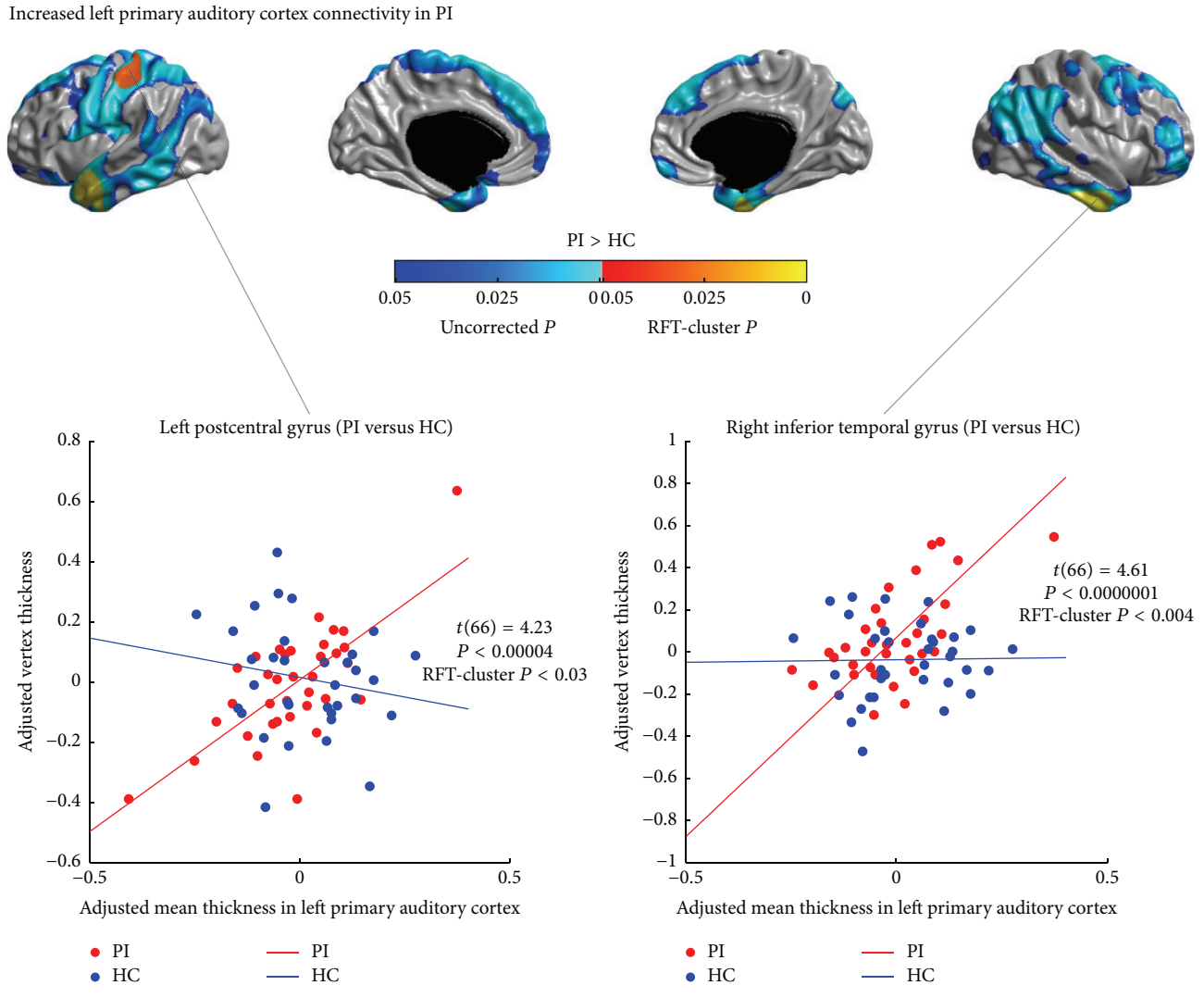

(b)

Figure 4: Continued.

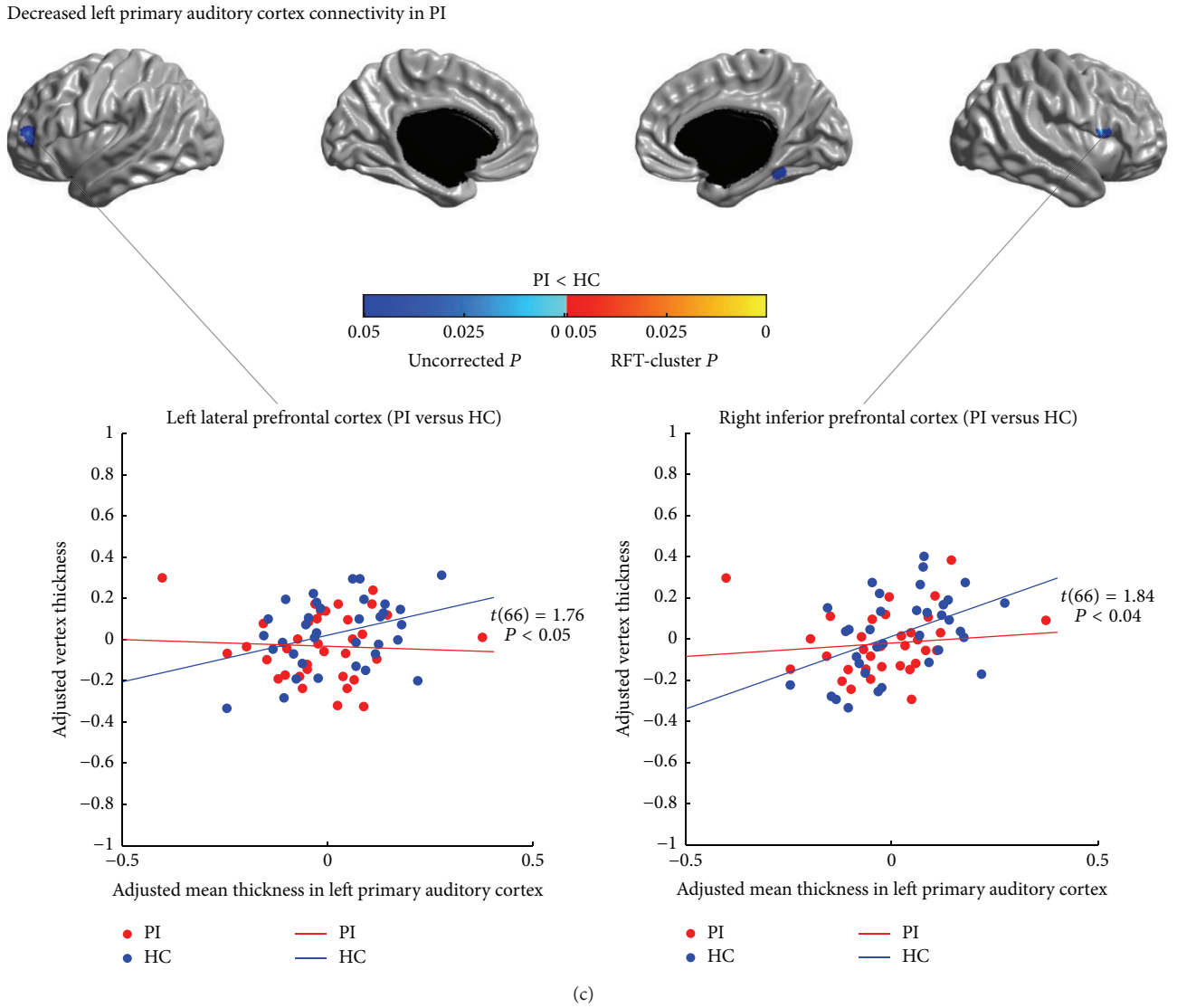

Figure 4: Between-group comparison of structural covariance seeded from the left primary auditory cortex (PAC). (a) Structural covariance maps in healthy controls (HC) and patients with primary insomnia (PI). Seed region is colored in blue. (b) Increased left PAC-cortical network covariance in PI. Patients showed significantly increased correlations of the left PAC with the left postcentral gyrus and the bilateral anterior LTC ($P < 0.05$, RFT-cluster corrected), as well as trends of increased correlations with the dorsal and inferior lateral PFC, the bilateral precentral gyri, the right postcentral gyrus, the LTC, the left posterior insula, the lateral parietal cortex, the medial motor areas (PCL/SMA), the dmPFC, the left OLF, the right vmPFC, and the right superior cuneus ($P < 0.05$, uncorrected). (c) Decreased left PAC-cortical network covariance in PI. Patients showed trends of decreased correlations of the left PAC with the left lateral PFC, the right IFGoperc, and the right FFG ($P < 0.05$, uncorrected). Scatter plots illustrate slope differences in selected vertices, where adjusted cortical thickness values and regression lines are shown in red for patients and in blue for controls.

patients with PI and healthy controls. Compared with healthy controls, patients with PI exhibited markedly increased correlation between the right OLF and the left cuneus ($P < 0.05$, RFT-cluster corrected). Both the left and the right OLF networks in PI also showed trends of increased correlations with the dorsal central areas, the medial motor areas (PCL/SMA), the medial temporal cortex (PHG), and the medial occipital lobes ($P < 0.05$, uncorrected). Additionally, in patients, the left OLF network had trends of increased correlations with the right ACC, the right inferior temporal cortex, the lowermost part of the right postcentral gyrus, the right anterior insula, and the bilateral precuneus/PCC ($P < 0.05$, uncorrected); the right OLF network had trends of increased correlations with the dorsal parietooccipital regions, the right inferior occipital gyrus, and the right PAC (HES) ($P < 0.05$, uncorrected). Moreover, patients showed decreased correlations ($P < 0.05$, uncorrected) between the bilateral OLF and the lateral PFC, the IPC, the LTC, and the dmPFC, and between the right OLF and the bilateral IFGoperc.

3.6. Relationship between Covariance Strength and Sleep Quality. The modulation of SCNs of the primary sensory regions by the sleep quality was assessed by testing the parametric

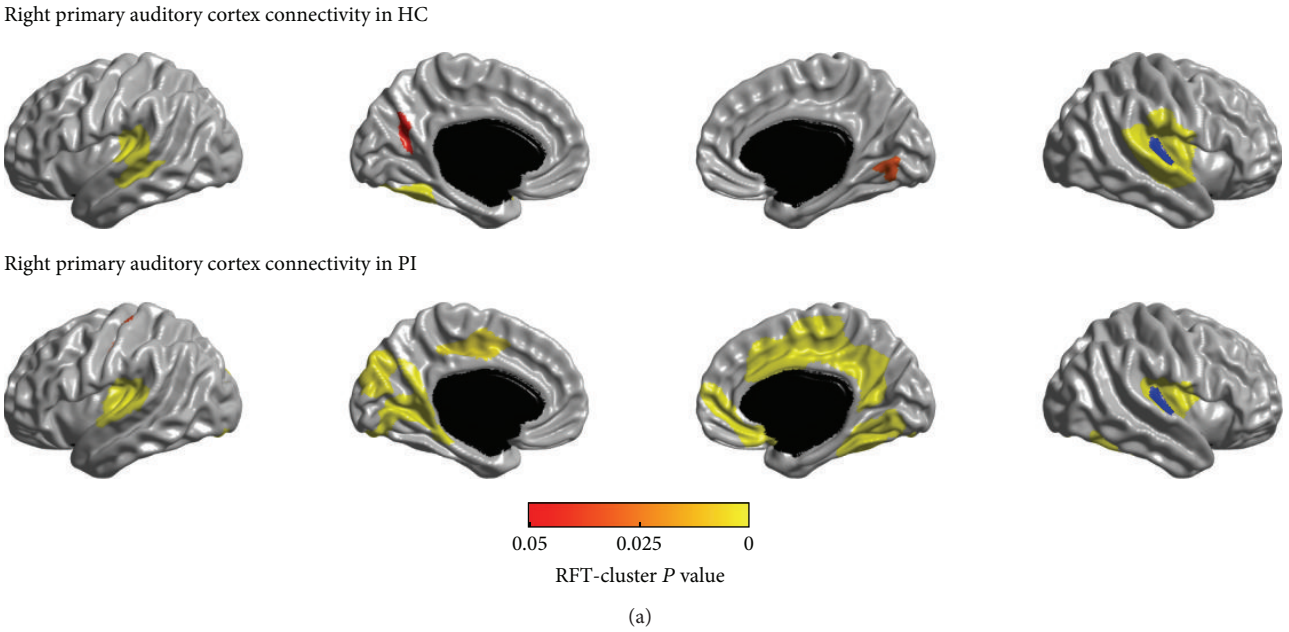

(a)

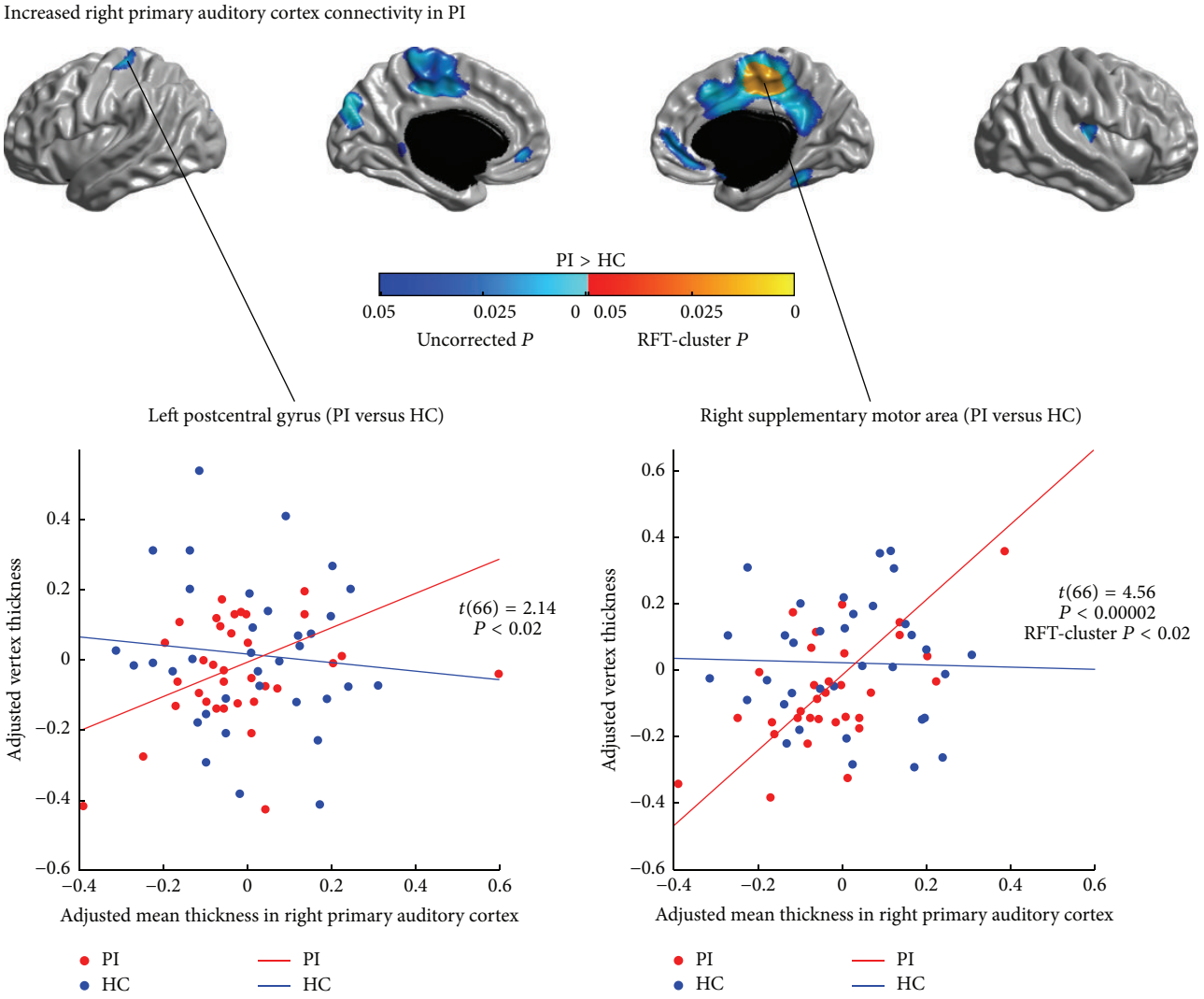

(b)

Figure 5: Continued.

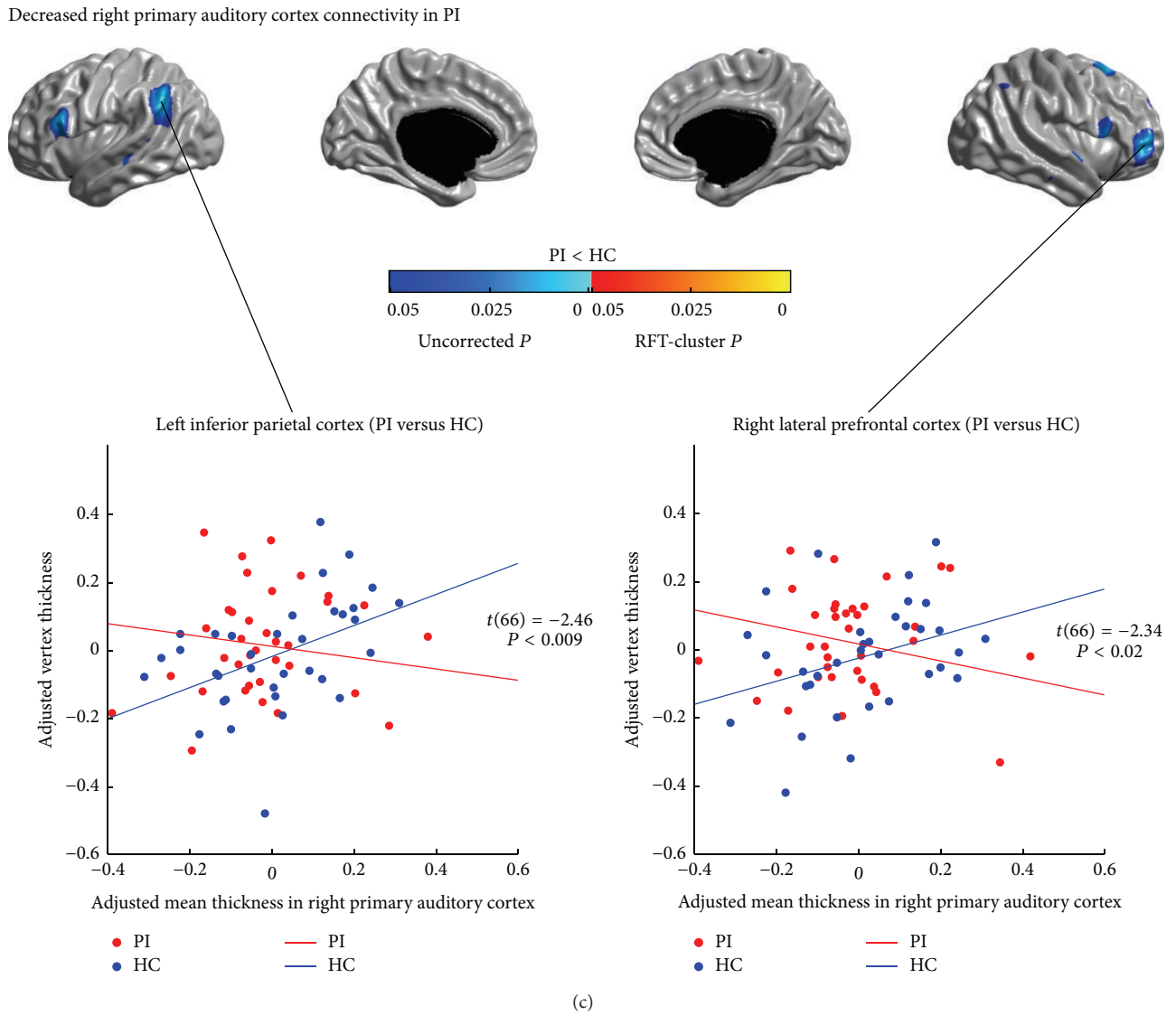

FIGURE 5: Between-group comparison of structural covariance seeded from the right primary auditory cortex (PAC). (a) Structural covariance maps in healthy controls (HC) and patients with primary insomnia (PI). Seed region is colored in blue. (b) Increased right PAC-cortical network covariance in PI. Patients showed significantly increased correlation with the right medial motor area (PCL/SMA) ($P < 0.05$, RFT-cluster corrected); and trends of increased correlations with the left postcentral gyrus, the left medial motor area (PCL/SMA), the left cuneus, the precuneus/PCC, the vmPFC, the right MCC, the right OLF, the right inferior temporal cortex, and the right posterior insula ($P < 0.05$, uncorrected). (c) Decreased right PAC-cortical network covariance in PI. Patients showed trends of decreased correlations of the right PAC with the IFGoperc, the IPC, the LTC, and the right lateral PFC ($P < 0.05$, uncorrected). Scatter plots illustrate slope differences in selected vertices, where adjusted cortical thickness values and regression lines are shown in red for patients and in blue for controls.

interaction between PSQI score and seed covariance strength across all participants. We did not observe any significant modulation for all the studied networks ($P > 0.05$, RFT-cluster corrected). Analysis of the uncorrected modulations identified trends of positive and negative modulatory effects of PSQI score on the sensory networks ($P < 0.05$, uncorrected) (positive and negative modulation trends are shown in Figures 8 and 9, resp.); and it is notable that the patterns of the positive and negative modulation trends were, respectively, consistent with the patterns of uncorrected connectivity increase and reduction in PI (Figures 2–7).

4. Discussion

This work aimed to test the hypothesis that insomnia would be associated with alterations in networks associated with sensory processing, and sleep quality would be associated with such alterations. We measured and analyzed cortical thickness in groups of patients with PI and normal sleepers using a surface-based method that has been validated and applied to the healthy and diseased brains [27]. Compared with healthy controls, patients with PI tended to have increased cortical thickness, as expected, in sensory (PAC, LOC, PVC, and the cuneus) and medial motor areas (PCL

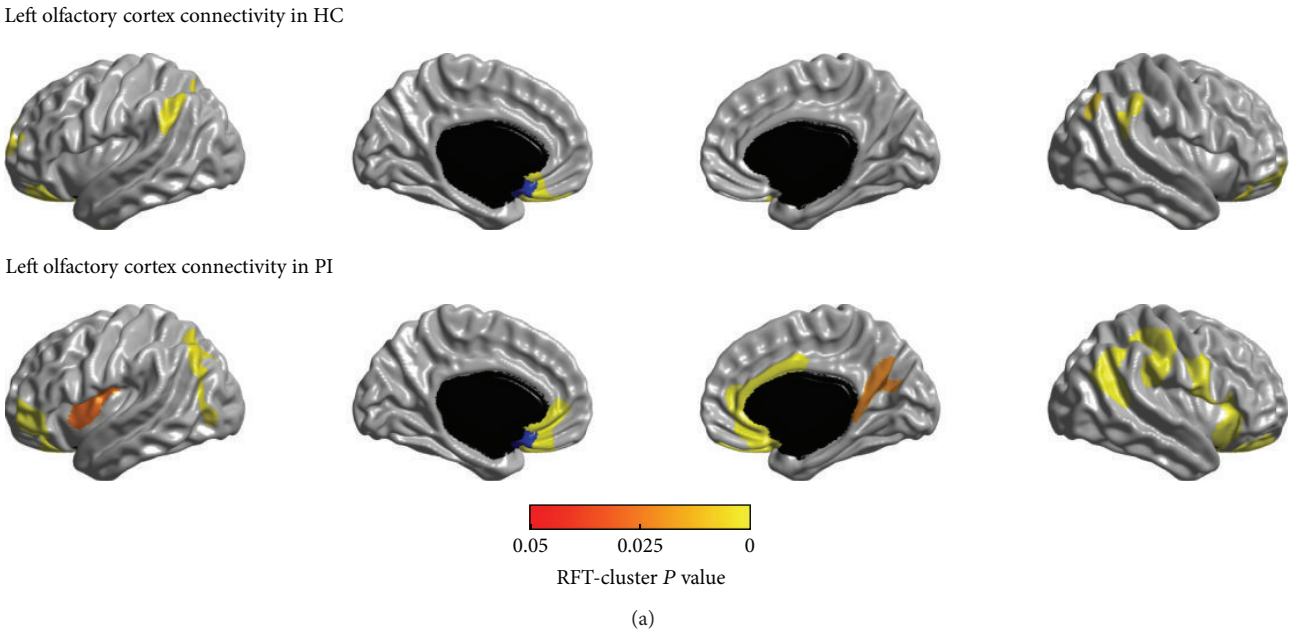

(a)

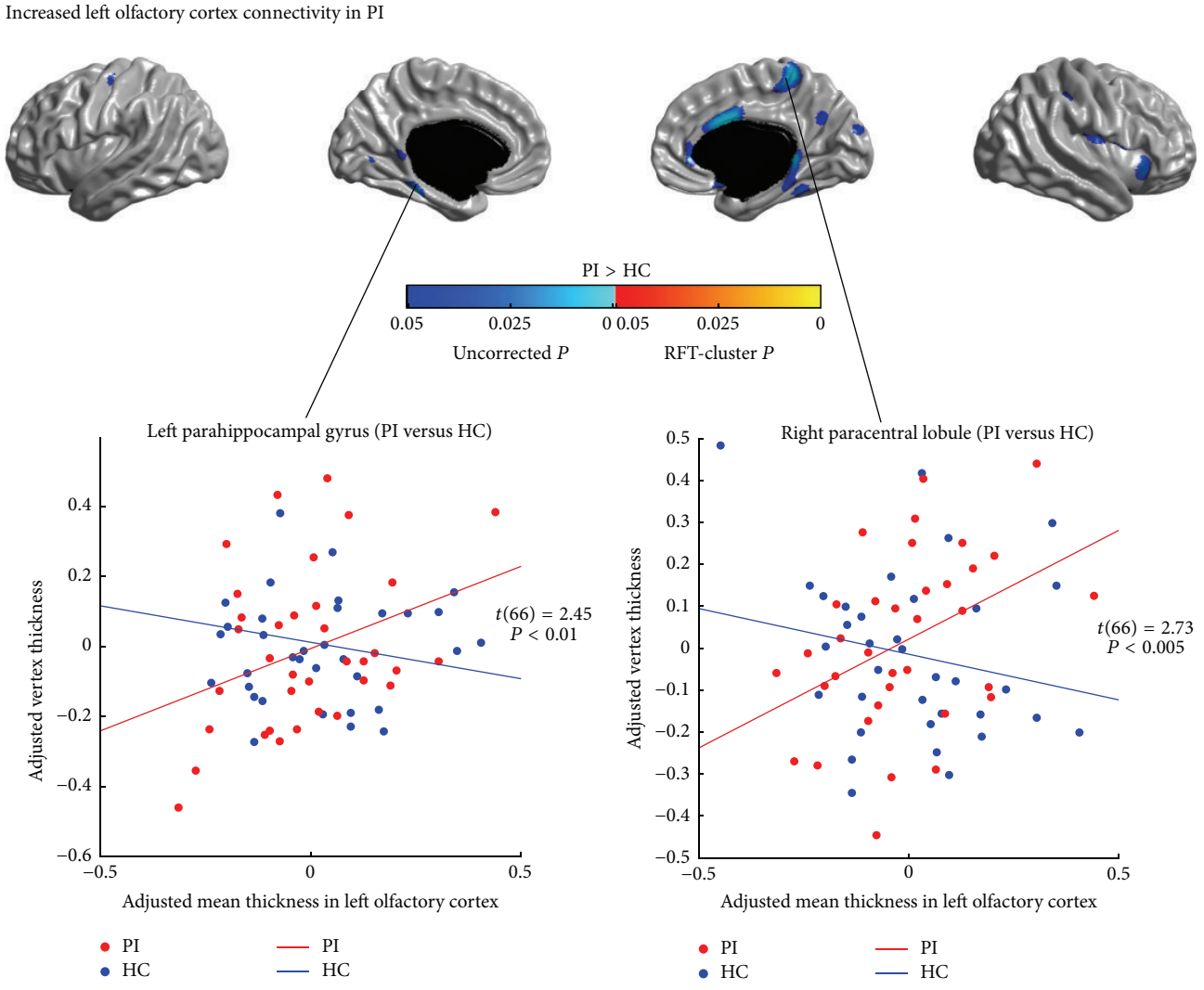

(b)

Figure 6: Continued.

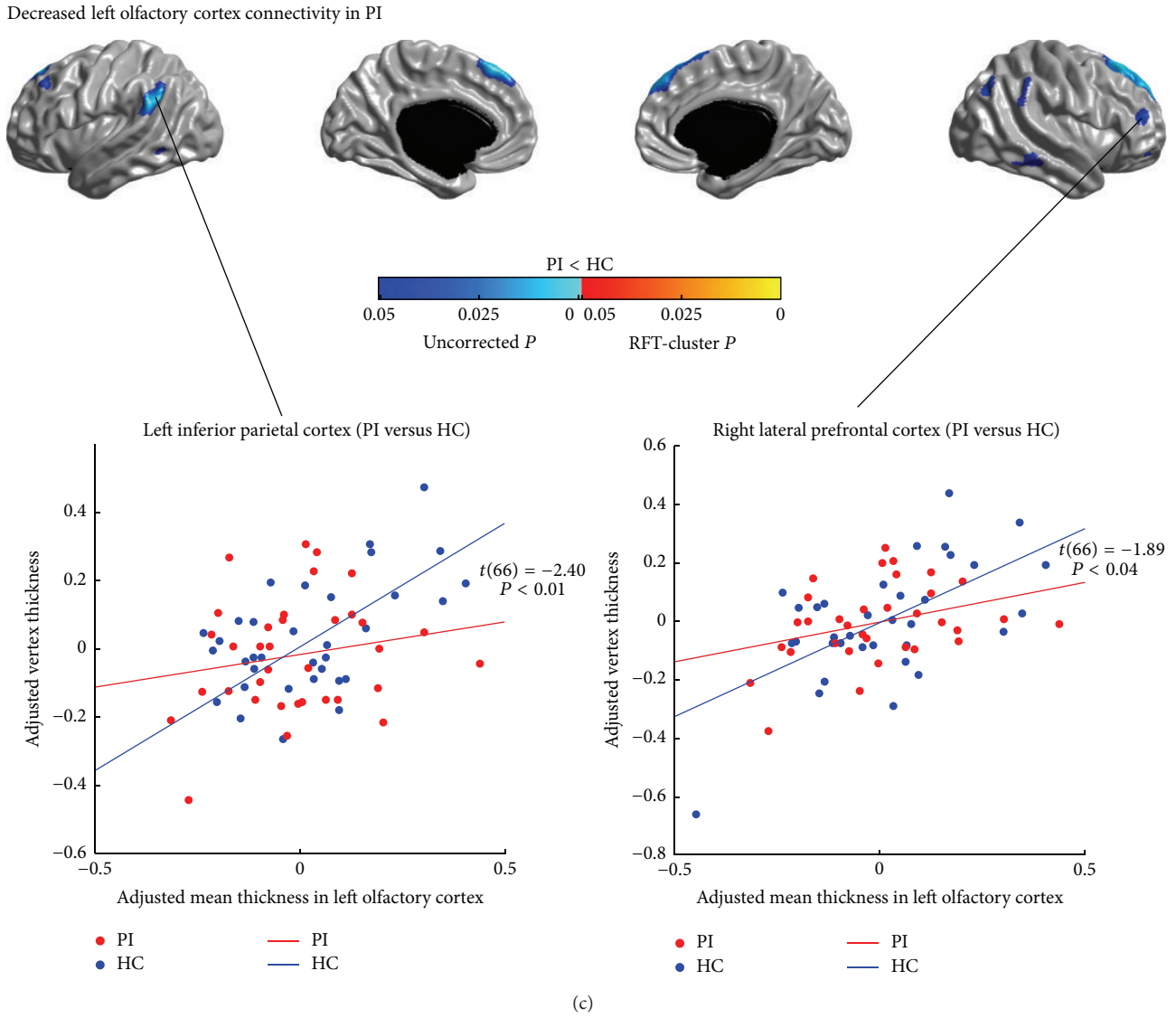

Figure 6: Between-group comparison of structural covariance seeded from the left olfactory cortex (OLF). (a) Structural covariance maps in healthy controls (HC) and patients with primary insomnia (PI). Seed region is colored in blue. (b) Increased left OLF-cortical network covariance in PI. Patients showed trends of increased correlations of the left OLF with the left precentral gyrus, the medial motor areas (PCL/SMA), the PHG, the medial occipital lobes, the right ACC, the right ITC, the lowermost part of the right postcentral gyrus, the right anterior insula, and the bilateral precuenus/PCC ($P < 0.05$, uncorrected). (c) Decreased left OLF-cortical network covariance in PI. Patients showed trends of decreased correlations of the left OLF with the lateral PFC, the IPC, the dmPFC and the LTC ($P < 0.05$, uncorrected). Scatter plots illustrate slope differences in selected vertices, where adjusted cortical thickness values and regression lines are shown in red for patients and in blue for controls.

and MCC) and also in some default-mode network (DMN) (the Precuneus and PHG) and salience network (SN) (ACC) regions. Trends of decreased cortical thickness in PI were also observed in the lateral PFC, which plays a key role in working memory [45]. These cortical structural changes were also found to tend to be positively correlated with poor sleep quality. Mapping cortical thickness alterations alone does not provide sufficient information about the underlying pathological mechanisms leading to such changes. On the other hand, since abnormal interactions between cortical regions may be related to the observed neuroanatomical variations [26], we studied the structural covariance connectivity between the primary sensory regions and the neocortex. Compared with healthy controls, patients with PI showed significantly increased covariance or trends of increase in covariance between the seeds of primary sensory regions (PVC, PAC, and OLF) and the motor regions (PCL/SMA, the pre- and postcentral gyri), and between the sensory regions (PAC, OLF, and the cuneus), and between the sensory regions and DMN (the precuneus/PCC, vmPFC, and the anterior LTC and PHG) and SN regions (ACC and the insula). In addition, patients with PI also showed trends of decreased structural covariance between the seeds of primary sensory regions and the frontoparietal working memory network

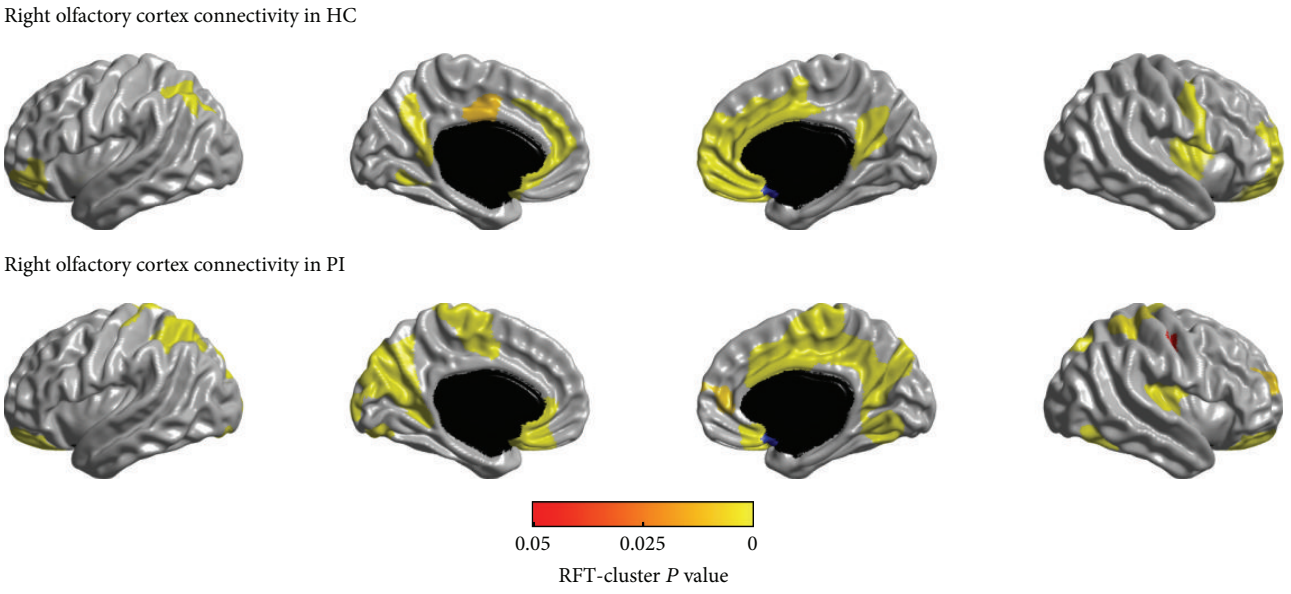

(a)

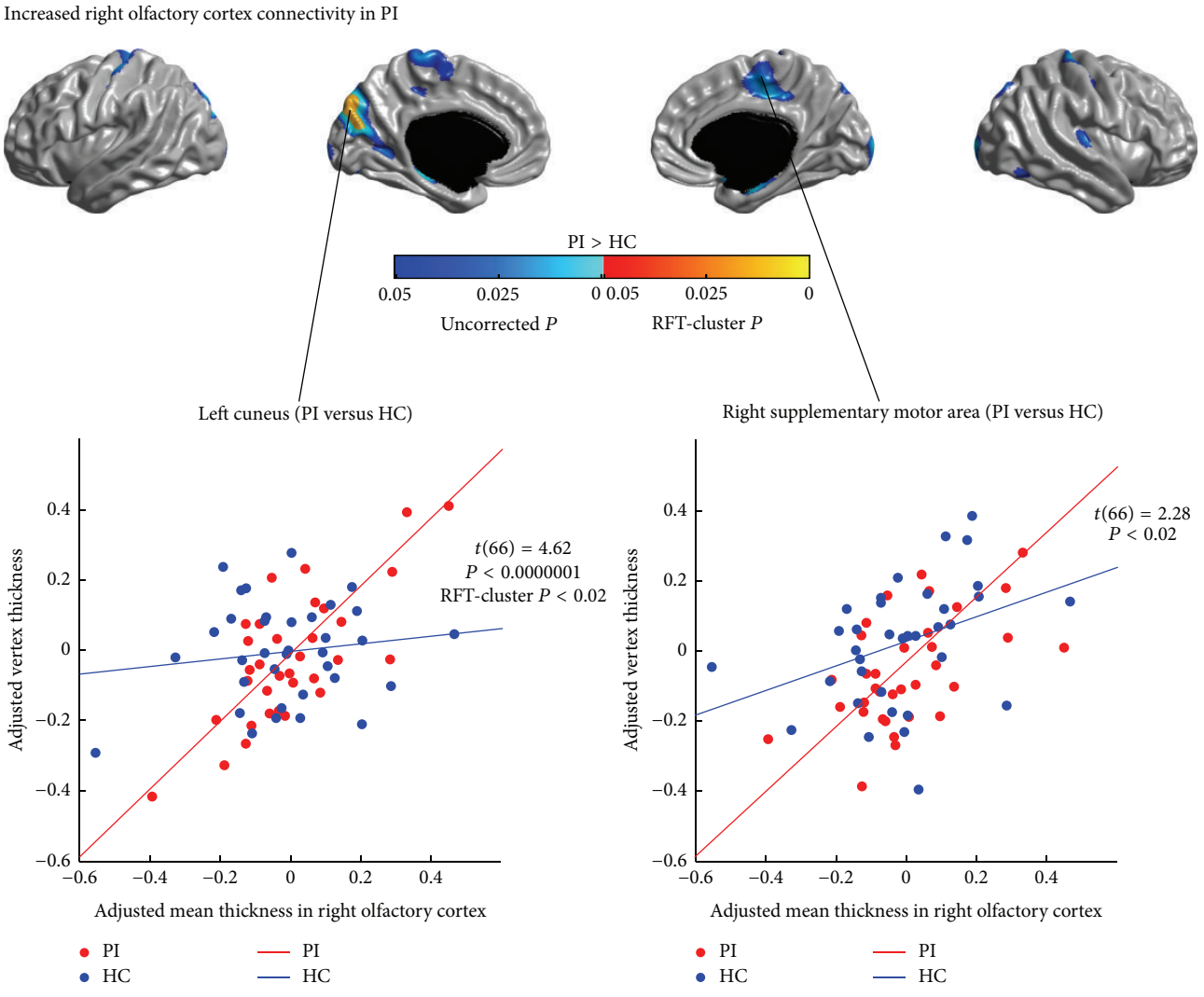

(b)

Figure 7: Continued.

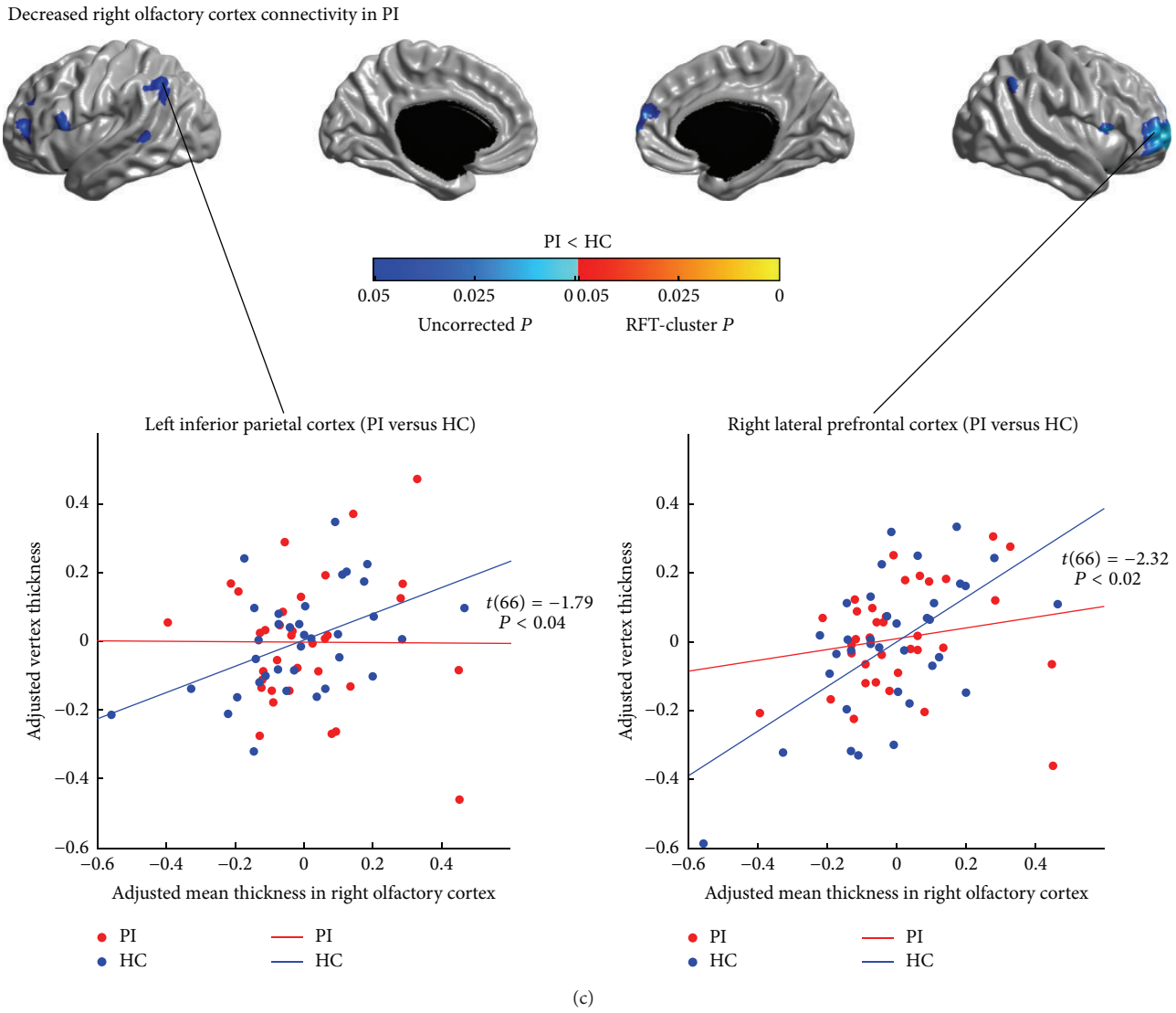

Figure 7: Between-group comparison of structural covariance seeded from the right olfactory cortex (OLF). (a) Structural covariance maps in healthy controls (HC) and patients with primary insomnia (PI). Seed region is colored in blue. (b) Increased right OLF-cortical network covariance in PI. Patients showed significantly increased correlation between the right OLF and the left cuneus ($P < 0.05$, RFT-cluster corrected), and trends of increased correlations with the dorsal central areas, the medial motor areas (PCL/SMA), the PHG, the medial occipital lobes, the dorsal parietooccipital regions, the right inferior occipital gyrus, and the right primary auditory cortex (HES) ($P < 0.05$, uncorrected). (c) Decreased right OLF-cortical network covariance in PI. Patients showed trends of increased correlations between the right OLF and the lateral PFC, the IFGoperc, the IPC, the left LTC, and the right dmPFC ($P < 0.05$, uncorrected). Scatter plots illustrate slope differences in selected vertices, where adjusted cortical thickness values and regression lines are shown in red for patients and in blue for controls.

(lateral PFC, IFGoperc, and IPC). Patterns of trends of positive and negative modulatory effects of poor sleep quality on the SCNs in all the participants were greatly in line with the between-group differences in the corresponding networks. These findings suggest that insomnia might be related to underlying increase in brain network integration encompassing the sensory to motor networks, the DMN and the SN, and decrease in brain networks integration of the sensory regions to the frontoparietal working memory network.

SCN analysis relies on the assumption that related regions covary in brain morphology as a result of mutually trophic influences [46] or from common experience-related plasticity [47, 48]. Furthermore, several existing studies have demonstrated a link between the pattern of structural covariance and the architecture of the intrinsic functional networks [49–51]. Therefore, regions that are associated in cortical thickness may also be a part of the same functional network. In this work, the SCNs were seeded from the key regions involved in sensory processing: the PVC, PAC, and OLF. In healthy sleepers, the SCN of PVC mainly included the superior parietal regions, the pre- and postcentral gyri, the visual areas, the PCC/precuneus, and the vmPFC; the SCN of PAC primarily included the bilateral opercular areas (the superior temporal

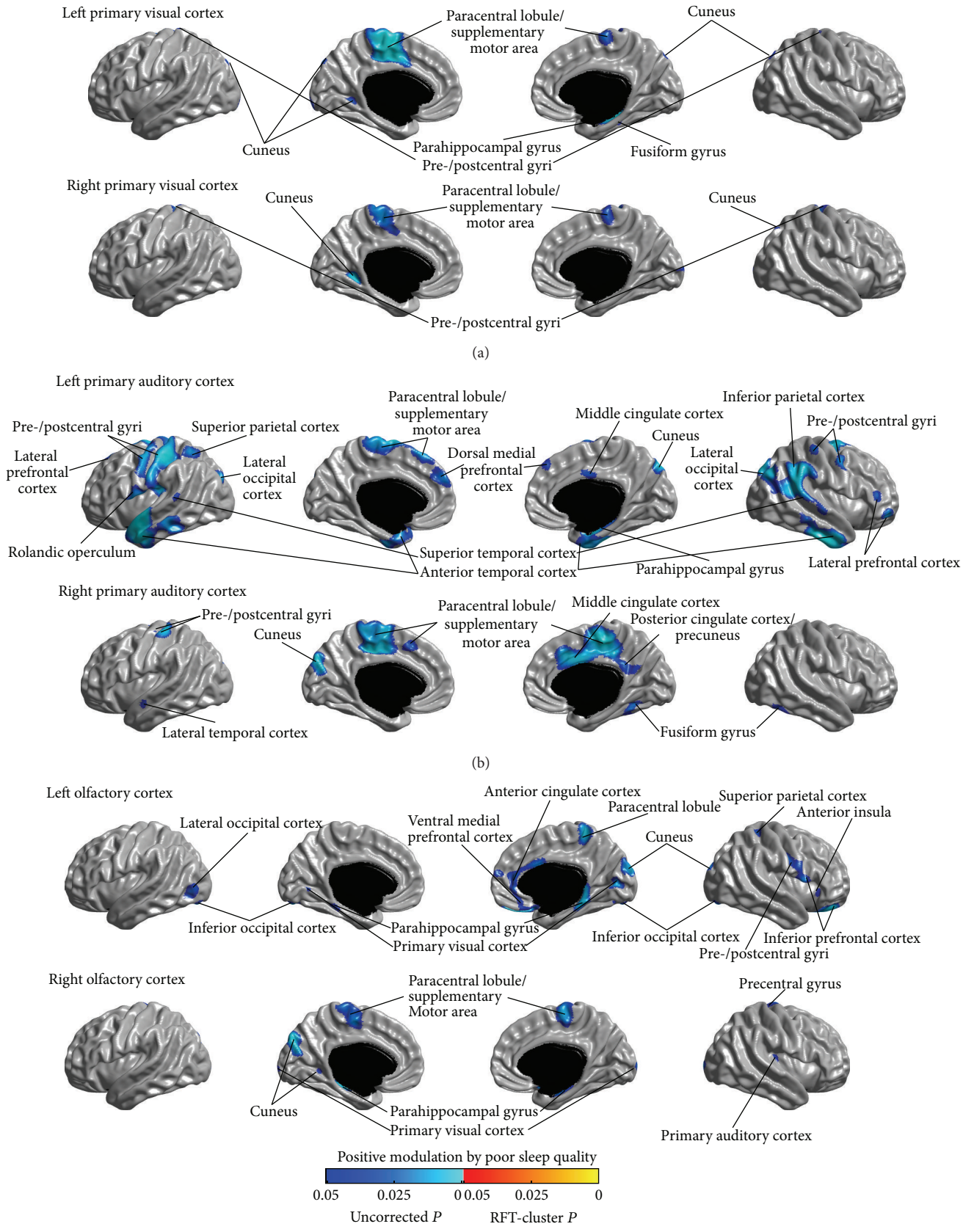

Figure 8: Positive modulations of structural covariance networks by sleep quality, as measured using the Pittsburgh Sleep Quality Index (PSQI) scale. No modulatory effects survived the correction for multiple comparisons. Trends ($P < 0.05$, uncorrected) are shown here.

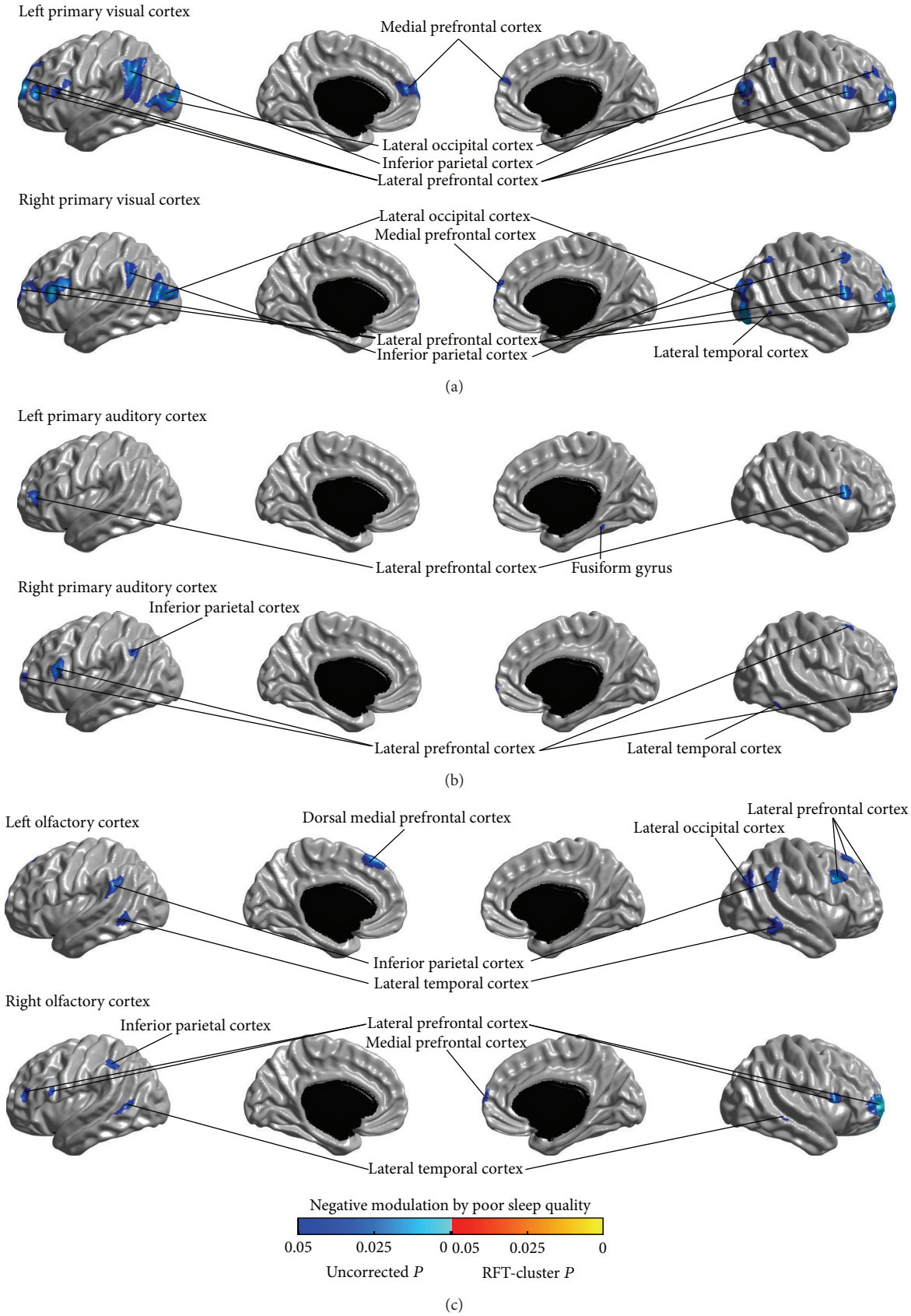

Figure 9: Negative modulations of structural covariance networks by sleep quality, as measured using the Pittsburgh Sleep Quality Index (PSQI) scale. No modulatory effects survived the correction for multiple comparisons. Trends ($P < 0.05$, uncorrected) are shown here.

gyri, the posterior insula, and the lower part of the postcentral gyri); the SCN of OLF predominantly included the anterior and inferior PFC, the parietal cortex, and the vmPFC. These network patterns are in overall agreement with data from previous SCN studies [28, 30] and functional connectivity mapping in normal populations [52–55]. Considering the PI-related cortical thickness alterations in the regions showing abnormal structural covariance, we could speculate that the increased or decreased connectivity may reflect a correlative or inverse cortical thickness changes due to enhanced mutual or inhibitory interregional trophic/functional relationship, as affected by the pathological process of PI.

In the current study, compared with the healthy controls, the primary alterations in SCNs in patients with PI were the increased covariance between the sensory and motor regions. Significantly increased covariance was found between the left PAC and the left primary somatosensory cortex (the postcentral gyrus), and between the right PAC and the right medial motor area (PCL/SMA), and between the right OLF and the left cuneus ($P < 0.05$, RFT-cluster corrected). In addition, we also found trends of increased covariance of PVC with the medial motor area (PCL/SMA) and the left cuneus, and of PAC with the primary motor and somatosensory cortex (the pre- and postcentral gyri), the medial motor area (PCL/SMA), the cuneus visual cortex, and the OLF, and of OLF with the primary motor and somatosensory cortex (the pre- and postcentral gyri), the medial motor area (PCL/SMA), the dorsal visual cortex, and the right PAC. The findings are well in line with data from previous functional connectivity analysis. Killgore and colleagues examined resting-state functional connectivity differences between individuals with or without insomnia-related sleep problems [20]. They observed that difficulty in falling asleep was associated with increased functional connectivity between cuneus and other sensory regions such as the PAC and OLF, and the medial motor area (SMA), and between the PAC and the medial motor area (SMA); and problems with sleep maintenance were associated with greater connectivity between the cuneus and the OLF. Their findings indicated that stimulation of one sensory modality might be associated with increased activation of other sensory and motor regions in insomnia. Therefore, greater connectivity among the sensory and motor regions in insomnia may be conceivably associated with sustained arousal and enhance unwanted sensory awareness, leading to difficulty in sleep initialization or maintenance.

Furthermore, patients with PI also showed increased structural covariance between the sensory regions and the DMN regions, such as the precuneus/PCC, the vmPFC, the anterior LTC, and the PHG. In particular, the increased structural covariance between the right PAC and the bilateral anterior LTC survived correction for multiple comparisons ($P < 0.05$, RFT-cluster corrected). Although there is no full understanding about the functions inherent to DMN, in general, DMN concerns the neural network that is active when the individual is not focused on an external task mobilizing the explicit attentional resources and the brain is at wakeful rest [56]. Studies using resting-state paradigms have revealed that DMN is involved in internal modes of cognition, such as mind wandering, recovery of past memories, planning/projection of future events, and consideration of others' perspectives [57]. Dysfunction in DMN has also been related to the neuropathophysiology of insomnia [58]. Drummond et al. [59] investigated the neural correlates of working memory performance in PI, and found that, during behavioral performance, patients with PI failed to deactivate DMN regions compared to good sleepers. Hasler et al. [60] examined the functional connectivity within DMN in patients with PI and good sleepers in different times of the day and found that both groups were not distinct regarding functional connectivity in the morning period after waking up; however, the patient group showed higher DMN connectivity at evening, during NREM sleep, and after sleep restriction. Therefore, the increased structural covariance between the sensory and DMN regions might be related to a high level of arousal in sensory and DMN regions during the day which tends to persist at night and during sleep stages [13]. Alternatively, such structural covariance increase in PI might also be related to pronounced activation of sensory processing and self-referential processes at bedtime or in the absence of tasks/external stimuli [61].

Patients with PI also tended to have increased structural covariance of the sensory regions, especially the left OLF, with the ACC and the insula that are nodes within SN. SN is thought to recruit relevant brain regions for the processing of sensory information and integrate processed sensory data with visceral, autonomic, and hedonic signals in order to guide behavior [62, 63]. Although the role of SN in the mechanism of insomnia is unclear, increased resting-state functional connectivity in SN has been reported in normal subjects after sleep deprivation [64] and patients with PI [65]. Therefore, the trend of increased structural covariance between sensory and SN regions might be associated with the aberrant neural activity in these regions induced by sleep loss.

Another finding in the current study is that patients with PI showed trends of decreased connectivity of the seeds of primary sensory regions with the frontoparietal working memory network consisting of the lateral PFC, the IFGoperc, and the IPC [45]. Such connectivity decrease is in line with the trends of increased cortical thickness in the sensory regions and the trends of decreased cortical thickness in these frontoparietal working memory network regions in PI, observed in the cortical thickness analysis. In Drummond and colleagues' study investigating the neural correlates of working memory performance in PI [59], compared with good sleepers, patients with PI showed reduced activation of the frontoparietal working memory network and specifically reduced modulation of the lateral PFC with increasing task difficulty, in addition to their failure to deactivate DMN regions. Therefore, our results further demonstrated the impairment of the frontoparietal working memory network in PI, which might account for the reported decline of working memory capacity in sleep disorders [66]. Trends of decreased connectivity with the dmPFC were also observed in the networks of the PVC and OLF. Damage of the dmPFC has been associated with insomnia and was thought to disrupt the propagation of sleep slow waves along the insula-cingulate corridor, resulting in difficulty initiating or

maintaining sleep [67]. In this study, we were unable to test this hypothesis, which requires EEG sleep recording. In addition, trends of decreased connectivity between the sensory regions and the LOC, the LTC and the ITC were also found in PI. However, no PI-related structural or functional changes in these regions were found in this work or previous studies. Therefore, it is unclear whether and how the trends of decreased connectivity in these regions are related to the pathology of PI. Furthermore, we observed an exception that the left PAC showed trends of increased connectivity with the right lateral PFC, the right IPC, the dmPFC, and the LTC in patients with PI. This may suggest a complementary mechanism in patients with PI to compensate for the decreased connectivity within other SCNs.

We assessed the relationship between the structural covariance and sleep quality by testing the parametric interaction between the PSQI score and the structural covariance strength from seed regions across all participants. Although all modulation of structural covariance by PSQI did not survive multiple comparison correction, analysis of the uncorrected modulations found trends of positive and negative modulatory effects of PSQI score on the sensory networks; and it is notable that the patterns of the positive and negative modulation trends were, respectively, consistent with the patterns of uncorrected connectivity increase and reduction in PI. This further illustrated that the structural covariance alterations in patients with PI observed in this work may be related to the pathophysiology of insomnia.

In this work, we noted some asymmetries between the SCN alteration maps of the left and right sensory regions, for example, the increased structural covariance maps of the left and right PAC. Although, by far, there is no clear evidence about asymmetric effects of insomnia on the brain, previous studies have also reported lateralized patterns of brain structural alterations in PI [67–69]. It is plausible that the asymmetric structural changes may be related to the abnormal functional asymmetries in patients with PI during night or sleep [70, 71]. In addition, we also noted that only the SCNs of the primary auditory and olfactory regions showed statistically significant alterations in patients with PI (survived in the multiple comparison correction), but the SCNs of the primary visual cortex. This might indicate that the sleep deprivation of the patients may be mainly related to the heightened arousal induced by auditory or odor stimuli rather than visual stimuli, when they are in the bed. In line with this, previous study examining event-related potentials during sleep reported that patients with insomnia showed reduced sensory gating of auditory stimuli compared with normal sleepers [72]. However, specific functional study is needed to verify this hypothesis.

There are limitations of the current study that should be addressed in future investigations. First, most present results did not survive the correction for multiple comparisons, which might be caused by the relatively small sample size. It is desirable to increase the sample size in the future work to increase the statistical power. Second, although our findings in structural covariance were qualitatively well in line with the data from previous functional connectivity analyses, it is unclear about the quantitative similarity between the observed SCNs and the functional connectivity networks derived from fMRI data. There is still lack of systematic comparison of structural covariance and functional connectivity networks. It should be cautious to generalize the findings of SCNs in PI to other networks. Combinations of multimodal neuroimaging approaches should yield a more comprehensive understanding of how abnormalities in the brain network architecture are associated with functional deficits. Third, the structural network was group-based so that we could not explore the network organization for individual subjects. Furthermore, subcortical regions were not included in this study, as this study concentrated on the structural covariance in cortical thickness. It is desirable to extend the study to subcortical regions to explore their contributions to the disruptions of the SCNs in PI. Some existing studies, that is, [73], attempted to correlate the volume of certain subcortical regions with the cortical thickness across the cortex or in specific cortical regions; however, it might be questionable to correlate structural metrics at distinct exponential scales. Comparable subcortical structural measurements to cortical thickness are expected for such analysis. Finally, utilizing other network analysis methods in the future work, for example, graph theory analysis to assess the topological patterns of the large-scale brain network organization [22], could enhance the understanding of the brain network organization in insomnia.

In summary, we, for the first time, used a seed-based SCN mapping approach to investigate large-scale structural networks in PI. The results demonstrated increased covariance in cortical thickness between sensory and motor regions, and likely between sensory regions and DMN and SN regions, and trends of decreased connectivity between sensory regions and the frontoparietal working memory network regions, in patients with PI. In addition, the observed alterations in structural covariance tended to be correlated with poor sleep quality. Our findings support the aberrant functional activation and connectivity in insomnia reported by previous functional neuroimaging based studies and also provide novel insights into variations in brain network configuration that may be involved in the pathophysiology of insomnia.

Conflict of Interests

All the authors declare no biomedical financial interests or potential conflict of interests regarding the publication of this paper.

Authors' Contribution

Lu Zhao and Enfeng Wang have contributed equally to this work.

Acknowledgments

This work was supported by the Canadian Institutes of Health Research (CIHR-MOP 37754), 2013 Henan Provincial Key Technological Projects of the Department of Science and Technology (no. 132102310063) and 2012 Henan Provincial

Key Technological Projects of the Department of Public Health (no. 201202023), the National Natural Science Foundation of China (no. 81271534), and the National High Technology Research and Development Program of China (863, no. 2012AA011603). The funding organizations had no influence on the design and conduct of the study; collection, management, analysis, and interpretation of the data; and preparation, review, or approval of the paper.

References

[1] D. J. Buysse, "Insomnia," *The Journal of the American Medical Association*, vol. 309, no. 7, pp. 706–716, 2013.

[2] D. Léger, C. M. Morin, M. Uchiyama, Z. Hakimi, S. Cure, and J. K. Walsh, "Chronic insomnia, quality-of-life, and utility scores: comparison with good sleepers in a cross-sectional international survey," *Sleep Medicine*, vol. 13, no. 1, pp. 43–51, 2012.

[3] É. Fortier-Brochu, S. Beaulieu-Bonneau, H. Ivers, and C. M. Morin, "Insomnia and daytime cognitive performance: a meta-analysis," *Sleep Medicine Reviews*, vol. 16, no. 1, pp. 83–94, 2012.

[4] D. J. Buysse, W. Thompson, J. Scott et al., "Daytime symptoms in primary insomnia: a prospective analysis using ecological momentary assessment," *Sleep Medicine*, vol. 8, no. 3, pp. 198–208, 2007.

[5] S. D. Kyle, C. A. Espie, and K. Morgan, "'. . .Not just a minor thing, it is something major, which stops you from functioning daily': quality of life and daytime functioning in insomnia," *Behavioral Sleep Medicine*, vol. 8, no. 3, pp. 123–140, 2010.

[6] K. M. Wright, T. W. Britt, P. D. Bliese, A. B. Adler, D. Picchioni, and D. Moore, "Insomnia as predictor versus outcome of PTSD and depression among Iraq combat veterans," *Journal of Clinical Psychology*, vol. 67, no. 12, pp. 1240–1258, 2011.

[7] C. Baglioni, G. Battagliese, B. Feige et al., "Insomnia as a predictor of depression: a meta-analytic evaluation of longitudinal epidemiological studies," *Journal of Affective Disorders*, vol. 135, no. 1–3, pp. 10–19, 2011.

[8] F. Sofi, F. Cesari, A. Casini, C. Macchi, R. Abbate, and G. F. Gensini, "Insomnia and risk of cardiovascular disease: a meta-analysis," *European Journal of Preventive Cardiology*, vol. 21, no. 1, pp. 57–64, 2014.

[9] A. D. Bramoweth and D. J. Taylor, "Chronic insomnia and health care utilization in young adults," *Behavioral Sleep Medicine*, vol. 10, no. 2, pp. 106–121, 2012.

[10] American Psychiatric Association, *Diagnostic Criteria from DSM-IV-TR*, American Psychiatric Association, Washington, DC, USA, 2000.

[11] M. M. Ohayon, "Epidemiology of insomnia: what we know and what we still need to learn," *Sleep Medicine Reviews*, vol. 6, no. 2, pp. 97–111, 2002.

[12] J. W. Winkelman, D. T. Plante, L. Schoerning et al., "Increased rostral anterior cingulate cortex volume in chronic primary insomnia," *Sleep*, vol. 36, no. 7, pp. 991–998, 2013.

[13] D. Riemann, K. Spiegelhalder, B. Feige et al., "The hyperarousal model of insomnia: a review of the concept and its evidence," *Sleep Medicine Reviews*, vol. 14, no. 1, pp. 19–31, 2010.

[14] C. A. Espie, N. M. Broomfield, K. M. A. MacMahon, L. M. Macphee, and L. M. Taylor, "The attention-intention-effort pathway in the development of psychophysiologic insomnia: a theoretical review," *Sleep Medicine Reviews*, vol. 10, no. 4, pp. 215–245, 2006.

[15] M. L. Perlis, D. E. Giles, W. B. Mendelson, R. R. Bootzin, and J. K. Wyatt, "Psychophysiological insomnia: the behavioural model and a neurocognitive perspective," *Journal of Sleep Research*, vol. 6, no. 3, pp. 179–188, 1997.

[16] M. H. Bonnet and D. L. Arand, "Hyperarousal and insomnia: state of the science," *Sleep Medicine Reviews*, vol. 14, no. 1, pp. 9–15, 2010.

[17] M. L. Perlis, H. Merica, M. T. Smith, and D. E. Giles, "Beta EEG activity and insomnia," *Sleep Medicine Reviews*, vol. 5, no. 5, pp. 363–374, 2001.

[18] K. Spiegelhalder, W. Regen, B. Feige et al., "Increased EEG sigma and beta power during NREM sleep in primary insomnia," *Biological Psychology*, vol. 91, no. 3, pp. 329–333, 2012.

[19] D. Wolyńczyk-Gmaj and W. Szelenberger, "Waking EEG in primary insomnia," *Acta Neurobiologiae Experimentalis*, vol. 71, no. 3, pp. 387–392, 2011.

[20] W. D. S. Killgore, Z. J. Schwab, M. Kipman, S. R. Deldonno, and M. Weber, "Insomnia-related complaints correlate with functional connectivity between sensory-motor regions," *NeuroReport*, vol. 24, no. 5, pp. 233–240, 2013.

[21] Z. Huang, P. Liang, X. Jia et al., "Abnormal amygdala connectivity in patients with primary insomnia: evidence from resting state fMRI," *European Journal of Radiology*, vol. 81, no. 6, pp. 1288–1295, 2012.

[22] E. Bullmore and O. Sporns, "Complex brain networks: graph theoretical analysis of structural and functional systems," *Nature Reviews Neuroscience*, vol. 10, pp. 186–198, 2009.

[23] J. M. Cheverud, "Quantitative genetics and developmental constraints on evolution by selection," *Journal of Theoretical Biology*, vol. 110, no. 2, pp. 155–171, 1984.

[24] K. Zhang and T. J. Sejnowski, "A universal scaling law between gray matter and white matter of cerebral cortex," *Proceedings of the National Academy of Sciences of the United States of America*, vol. 97, no. 10, pp. 5621–5626, 2000.

[25] A. Raznahan, J. P. Lerch, N. Lee et al., "Patterns of coordinated anatomical change in human cortical development: a longitudinal neuroimaging study of maturational coupling," *Neuron*, vol. 72, no. 5, pp. 873–884, 2011.

[26] A. C. Evans, "Networks of anatomical covariance," *NeuroImage*, vol. 80, pp. 489–504, 2013.

[27] J. P. Lerch and A. C. Evans, "Cortical thickness analysis examined through power analysis and a population simulation," *NeuroImage*, vol. 24, no. 1, pp. 163–173, 2005.

[28] B. A. Zielinski, E. D. Gennatas, J. Zhou, and W. W. Seeley, "Network-level structural covariance in the developing brain," *Proceedings of the National Academy of Sciences of the United States of America*, vol. 107, no. 42, pp. 18191–18196, 2010.

[29] B. S. Khundrakpam, A. Reid, J. Brauer et al., "Developmental changes in organization of structural brain networks," *Cerebral Cortex*, vol. 23, no. 9, pp. 2072–2085, 2013.

[30] M. Montembeault, S. Joubert, J. Doyon et al., "The impact of aging on gray matter structural covariance networks," *NeuroImage*, vol. 63, no. 2, pp. 754–759, 2012.

[31] D. S. Bassett, E. Bullmore, B. A. Verchinski, V. S. Mattay, D. R. Weinberger, and A. Meyer-Lindenberg, "Hierarchical organization of human cortical networks in health and schizophrenia," *The Journal of Neuroscience*, vol. 28, no. 37, pp. 9239–9248, 2008.

[32] Y. He, Z. Chen, and A. Evans, "Structural insights into aberrant topological patterns of large-scale cortical networks in Alzheimer's disease," *The Journal of Neuroscience*, vol. 28, no. 18, pp. 4756–4766, 2008.

[33] B. C. Bernhardt, S. L. Valk, G. Silani, G. Bird, U. Frith, and T. Singer, "Selective disruption of sociocognitive structural brain networks in autism and alexithymia," *Cerebral Cortex*, vol. 24, no. 12, pp. 3258–3267, 2013.

[34] D. J. Buysse, C. F. Reynolds III, T. H. Monk, S. R. Berman, and D. J. Kupfer, "The Pittsburgh sleep quality index: a new instrument for psychiatric practice and research," *Psychiatry Research*, vol. 28, no. 2, pp. 193–213, 1989.

[35] Y. Ad-Dab'bagh, O. Lyttelton, J.-S. Muehlboeck et al., "The CIVET imageprocessing environment: a fully automated comprehensive pipeline for anatomical neuroimaging research," in *Proceedings of the 12th Annual Meeting of the Organization for Human Brain Mapping*, M. Corbetta, Ed., Florence, Italy, 2006.

[36] J. G. Sied, A. P. Zijdenbos, and A. C. Evans, "A nonparametric method for automatic correction of intensity nonuniformity in MRI data," *IEEE Transactions on Medical Imaging*, vol. 17, no. 1, pp. 87–97, 1998.

[37] D. L. Collins, P. Neelin, T. M. Peters, and A. C. Evans, "Automatic 3D intersubject registration of MR volumetric data in standardized Talairach space," *Journal of Computer Assisted Tomography*, vol. 18, no. 2, pp. 192–205, 1994.

[38] A. Zijdenbos, R. Forghani, and A. Evans, "Automatic quantification of MS lesions in 3D MRI brain data sets: validation of INSECT," in *Medical Image Computing and Computer-Assisted Interventation—MICCAI'98: First International Conference Cambridge, MA, USA, October 11–13, 1998 Proceedings*, vol. 1496 of *Lecture Notes in Computer Science*, pp. 439–448, Springer, Berlin, Germany, 1998.

[39] S. K. June, V. Singh, K. L. Jun et al., "Automated 3-D extraction and evaluation of the inner and outer cortical surfaces using a Laplacian map and partial volume effect classification," *NeuroImage*, vol. 27, no. 1, pp. 210–221, 2005.

[40] O. Lyttelton, M. Boucher, S. Robbins, and A. Evans, "An unbiased iterative group registration template for cortical surface analysis," *NeuroImage*, vol. 34, no. 4, pp. 1535–1544, 2007.

[41] M. Boucher, S. Whitesides, and A. Evans, "Depth potential function for folding pattern representation, registration and analysis," *Medical Image Analysis*, vol. 13, no. 2, pp. 203–214, 2009.

[42] N. Tzourio-Mazoyer, B. Landeau, D. Papathanassiou et al., "Automated anatomical labeling of activations in SPM using a macroscopic anatomical parcellation of the MNI MRI single-subject brain," *NeuroImage*, vol. 15, no. 1, pp. 273–289, 2002.

[43] J. P. Lerch, K. Worsley, W. P. Shaw et al., "Mapping anatomical correlations across cerebral cortex (MACACC) using cortical thickness from MRI," *NeuroImage*, vol. 31, no. 3, pp. 993–1003, 2006.

[44] K. J. Worsley, M. Andermann, T. Koulis, D. MacDonald, and A. C. Evans, "Detecting changes in nonisotropic images," *Human Brain Mapping*, vol. 8, no. 2-3, pp. 98–101, 1999.

[45] C. Rottschy, R. Langner, I. Dogan et al., "Modelling neural correlates of working memory: a coordinate-based meta-analysis," *NeuroImage*, vol. 60, no. 1, pp. 830–846, 2012.

[46] I. Ferrer, R. Blanco, M. Carulla et al., "Transforming growth factor-alpha immunoreactivity in the developing and adult brain," *Neuroscience*, vol. 66, no. 1, pp. 189–199, 1995.

[47] B. Draganski, C. Gaser, V. Busch, G. Schuierer, U. Bogdahn, and A. May, "Neuroplasticity: changes in grey matter induced by training," *Nature*, vol. 427, pp. 311–312, 2004.

[48] A. Mechelli, J. T. Crinion, U. Noppeney et al., "Neurolinguistics: structural plasticity in the bilingual brain," *Nature*, vol. 431, no. 7010, article 757, 2004.

[49] W. W. Seeley, R. K. Crawford, J. Zhou, B. L. Miller, and M. D. Greicius, "Neurodegenerative diseases target large-scale human brain networks," *Neuron*, vol. 62, no. 1, pp. 42–52, 2009.

[50] M. Clos, C. Rottschy, A. R. Laird, P. T. Fox, and S. B. Eickhoff, "Comparison of structural covariance with functional connectivity approaches exemplified by an investigation of the left anterior insula," *NeuroImage*, vol. 99, pp. 269–280, 2014.

[51] A. Alexander-Bloch, J. N. Giedd, and E. Bullmore, "Imaging structural co-variance between human brain regions," *Nature Reviews Neuroscience*, vol. 14, no. 5, pp. 322–336, 2013.

[52] S. M. Smith, P. T. Fox, K. L. Miller et al., "Correspondence of the brain's functional architecture during activation and rest," *Proceedings of the National Academy of Sciences of the United States of America*, vol. 106, no. 31, pp. 13040–13045, 2009.

[53] J. S. Damoiseaux, S. A. R. B. Rombouts, F. Barkhof et al., "Consistent resting-state networks across healthy subjects," *Proceedings of the National Academy of Sciences of the United States of America*, vol. 103, no. 37, pp. 13848–13853, 2006.

[54] J. Plailly, C. Delon-Martin, and J.-P. Royet, "Experience induces functional reorganization in brain regions involved in odor imagery in perfumers," *Human Brain Mapping*, vol. 33, no. 1, pp. 224–234, 2012.

[55] C. Moessnang, G. Frank, U. Bogdahn, J. Winkler, M. W. Greenlee, and J. Klucken, "Altered activation patterns within the olfactory network in Parkinson's disease," *Cerebral Cortex*, vol. 21, no. 6, pp. 1246–1253, 2011.

[56] M. E. Raichle and A. Z. Snyder, "A default mode of brain function: a brief history of an evolving idea," *NeuroImage*, vol. 37, no. 4, pp. 1083–1090, 2007.

[57] R. L. Buckner, J. R. Andrews-Hanna, and D. L. Schacter, "The brain's default network: anatomy, function, and relevance to disease," *Annals of the New York Academy of Sciences*, vol. 1124, pp. 1–38, 2008.

[58] D. R. Marques, A. A. Gomes, V. Clemente, J. Moutinho dos Santos, and M. Castelo-Branco, "Default-mode network activity and its role in comprehension and management of psychophysiological insomnia: a new perspective," *New Ideas in Psychology*, vol. 36, pp. 30–37, 2015.

[59] S. P. A. Drummond, M. Walker, E. Almklov, M. Campos, D. E. Anderson, and L. D. Straus, "Neural correlates of working memory performance in primary insomnia," *Sleep*, vol. 36, no. 9, pp. 1307–1316, 2013.

[60] B. Hasler, J. James, P. Franzen, E. Nofzinger, A. Germain, and D. Buysse, "Variation in default mode network connectivity across sleep-wake states differs between adults with primary insomnia and good sleepers," *Sleep*, vol. 36, p. 192, 2013.

[61] A. G. Harvey, N. K. Y. Tang, and L. Browning, "Cognitive approaches to insomnia," *Clinical Psychology Review*, vol. 25, no. 5, pp. 593–611, 2005.

[62] W. W. Seeley, V. Menon, A. F. Schatzberg et al., "Dissociable intrinsic connectivity networks for salience processing and executive control," *The Journal of Neuroscience*, vol. 27, no. 9, pp. 2349–2356, 2007.

[63] K. S. Taylor, D. A. Seminowicz, and K. D. Davis, "Two systems of resting state connectivity between the insula and cingulate cortex," *Human Brain Mapping*, vol. 30, no. 9, pp. 2731–2745, 2009.

[64] Z. Fang, A. M. Spaeth, N. Ma et al., "Altered salience network connectivity predicts macronutrient intake after sleep deprivation," *Scientific Reports*, vol. 5, article 8215, 2015.

[65] M. C. Chen, C. Chang, G. H. Glover, and I. H. Gotlib, "Increased insula coactivation with salience networks in insomnia," *Biological Psychology*, vol. 97, no. 1, pp. 1–8, 2014.

[66] M. E. Petrov, K. L. Lichstein, and C. M. Baldwin, "Prevalence of sleep disorders by sex and ethnicity among older adolescents and emerging adults: relations to daytime functioning, working memory and mental health," *Journal of Adolescence*, vol. 37, no. 5, pp. 587–597, 2014.

[67] M. Koenigs, J. Holliday, J. Solomon, and J. Grafman, "Left dorsomedial frontal brain damage is associated with insomnia," *The Journal of Neuroscience*, vol. 30, no. 47, pp. 16041–16043, 2010.

[68] E. Y. Joo, H. J. Noh, J.-S. Kim et al., "Brain gray matter deficits in patients with chronic primary insomnia," *Sleep*, vol. 36, no. 7, pp. 999–1007, 2013.

[69] E. Altena, H. Vrenken, Y. D. Van Der Werf, O. A. van den Heuvel, and E. J. W. Van Someren, "Reduced orbitofrontal and parietal gray matter in chronic insomnia: a voxel-based morphometric study," *Biological Psychiatry*, vol. 67, no. 2, pp. 182–185, 2010.

[70] G. V. Kovrov, S. I. Posokhov, and K. N. Strygin, "Interhemispheric EEG asymmetry in patients with insomnia during nocturnal sleep," *Bulletin of Experimental Biology and Medicine*, vol. 141, no. 2, pp. 197–199, 2006.

[71] G. St-Jean, I. Turcotte, and C. H. Bastien, "Cerebral asymmetry in insomnia sufferers," *Frontiers in Neurology*, vol. 3, article 47, 2012.

[72] I. S. Hairston, L. S. Talbot, P. Eidelman, J. Gruber, and A. G. Harvey, "Sensory gating in primary insomnia," *European Journal of Neuroscience*, vol. 31, no. 11, pp. 2112–2121, 2010.

[73] B. C. Bernhardt, D. A. Rozen, K. J. Worsley, A. C. Evans, N. Bernasconi, and A. Bernasconi, "Thalamo-cortical network pathology in idiopathic generalized epilepsy: insights from MRI-based morphometric correlation analysis," *NeuroImage*, vol. 46, no. 2, pp. 373–381, 2009.

Hindawi Publishing Corporation
BioMed Research International
Volume 2015, Article ID 915606, 12 pages
http://dx.doi.org/10.1155/2015/915606

Review Article

Modeling the Generation of Phase-Amplitude Coupling in Cortical Circuits: From Detailed Networks to Neural Mass Models

Roberto C. Sotero

Department of Radiology and Hotchkiss Brain Institute, University of Calgary, Calgary, AB, Canada T3A 2E1

Correspondence should be addressed to Roberto C. Sotero; roberto.soterodiaz@ucalgary.ca

Received 27 March 2015; Revised 28 July 2015; Accepted 6 August 2015

Academic Editor: Vincenzo Romei

Phase-amplitude coupling (PAC), the phenomenon where the amplitude of a high frequency oscillation is modulated by the phase of a lower frequency oscillation, is attracting an increasing interest in the neuroscience community due to its potential relevance for understanding healthy and pathological information processing in the brain. PAC is a diverse phenomenon, having been experimentally detected in at least ten combinations of rhythms: delta-theta, delta-alpha, delta-beta, delta-gamma, theta-alpha, theta-beta, theta-gamma, alpha-beta, alpha-gamma, and beta-gamma. However, a complete understanding of the biophysical mechanisms generating this diversity is lacking. Here we review computational models of PAC generation that range from detailed models of neuronal networks, where each cell is described by Hodgkin-Huxley-type equations, to neural mass models (NMMs) where only the average activities of neuronal populations are considered. We argue that NMMs are an appropriate mathematical framework (due to the small number of parameters and variables involved and the richness of the dynamics they can generate) to study the PAC phenomenon.

1. Introduction

From the theory of signal processing we know that if an input-state-output system is linear its output will have the same frequency content as its inputs. Conversely, in nonlinear systems, the energy at one frequency in the inputs appears at different frequencies in the outputs. This induces cross-frequency coupling (CFC) between any two sources, when the output of one serves as the input to the other [1]. It has been shown that pyramidal cells produce a varied set of intrinsic dynamics based only on the type and compartmental localization of intrinsic conductances [2]. A combination of sodium, potassium, and calcium conductances produces coexistent gamma (~40 Hz) and theta (~6 Hz) rhythms on tonic depolarization. In contrast, combinations of persistent sodium and potassium channels in the soma produce a use-dependent transition between regular spiking at ~10 Hz and a repetitive, brief burst generation at ~20 Hz [2]. Since cortical columns and brain areas generating different brain rhythms are interconnected, the presence of CFC should not be surprising, even if the exact mechanisms responsible for its generation remain imprecise. The question is then whether CFC is only a mechanistic result of the way the brain is constructed or if it also has a role in brain computations. At least six types of CFC have been documented [3, 4]: amplitude-amplitude coupling (AAC), phase-phase coupling (PPC), frequency-frequency coupling (FFC), phase-amplitude coupling (PAC), phase-frequency coupling (PFC), and frequency-amplitude coupling (FAC). PAC, the type of CFC that occurs when the phase of a low frequency oscillation modulates the amplitude of a higher frequency oscillation, has received a lot of attention in the last decade due to its potential relevance for understanding healthy and pathological brain function [5–11]. PAC has been hypothesized to be the carrier mechanism for the interaction of local and global processes and therefore being directly linked to the integration of distributed information in the brain [12]. For instance, it has been suggested that theta-gamma PAC is used as a coding scheme for multi-item short-term memory in the hippocampus, where different spatial information is represented in different gamma subcycles of a theta cycle [13, 14]. Recent experimental evidence also suggests that PAC

links local blood-oxygen-level-dependent (BOLD) signals to BOLD correlation across distributed networks [15].

In parallel to the experimental study of the PAC phenomenon, computational models have been proposed in order to clarify the neurobiological mechanism underlying its generation [16–23]. Here we review these models, going from the detailed description of each cell (via the Hodgkin-Huxley formalism) in neuronal networks to neural mass models (NMMs), which are a type of mean field description that focuses on the dynamics of the average activity in a neuronal population while neglecting the second-order statistics (variance and covariances) and from models only focusing on generation of the theta-gamma PAC in the hippocampus to the most recent models capable of simultaneously generating several PAC combinations.

This review is structured as follows. First, in Section 2, we show that there is evidence for at least ten different PAC combinations (of a low and a higher frequency oscillation). Computational models of the PAC phenomenon can be divided into two types: detailed and NMMs. The main characteristics of these two types are briefly discussed in Section 3, followed by two sections describing specific models of both types.

2. Experimental Evidence of the Diversity of the PAC Phenomenon

The classic example of PAC was demonstrated in the CA1 region of the hippocampus [24] where the phase of the theta rhythm was found to modulate the power of gamma oscillations. Later studies found that PAC is neither restricted to theta-gamma coupling nor to the hippocampus. For instance, PAC has also been reported in the frontal, posterior, and parietal human cortices during auditory, visual, linguistic, and memory tasks [25–27], in monkey auditory and visual cortices [15, 28, 29] and rodent olfactory bulb [30]. In addition to Bragin et al.'s study [24], other studies have confirmed the existence of theta-gamma coupling in the hippocampus [31–34] and other brain areas [35–44]. Other PAC combinations of low and high frequency rhythms have also been detected: delta-theta [37, 45], delta-alpha [46, 47], delta-beta [44, 46], delta-gamma [34, 35, 38, 41, 44], theta-alpha [46], theta-beta [44, 46], alpha-beta [45], alpha-gamma [15, 26, 27, 35, 46, 48, 49], and beta-gamma [7, 15].

It should be noted that the studies mentioned above do not always use the same frequency values for the boundaries of the different brain rhythms [50] and that sometimes the gamma band is divided into different subbands such as low-gamma, middle-gamma, and fast-gamma, with boundaries that can differ between different studies. Thus, subdivisions of classical bands can potentially increase the number of PAC combinations to be studied. Additionally, a high number of mathematical methods for detecting PAC have been proposed [3, 12, 51–57], each with advantages and caveats, and no gold standard has emerged. Furthermore, those methods are not exempted of spurious results, that is, identifying PAC that is not related to true modulations between neuronal subsystems. These issues (reviewed recently in [58]) are out of the scope of this review, but we mention them here to highlight the fact that the experimental study of the PAC phenomenon is far from being complete and new methods and results in the upcoming years will be necessary to complement, inform, and refine past and future computational models of the phenomenon.

3. Detailed Mathematical Models versus Neural Mass Models

There are two main approaches to modeling the dynamics of neuronal populations. One approach is to realistically model each cell in the network, using multiple compartments for the soma, axon, and dendrites. The most prominent example of this approach is the Blue Brain Project [59], which aims to achieve in the next decade a full simulation of human brain dynamics (a network of approximately 86 billion neurons) in a supercomputer. A practical disadvantage of such realistic modeling is that it requires high computational power. For this reason, simplified versions of such models in which only one compartment is taken into account have been used [16, 60]. However, even in this case, the use of such detailed models makes it difficult to determine the influence of each model parameter on the generated average network characteristics. The second approach is based on the use of NMMs, which constitute a class of biophysical models that captures the average activity of neuronal ensembles, rather than modeling each neuron in the network individually [61, 62]. NMMs are described by nonlinear differential equations and can be rigorously obtained from mean field approaches [63–65] after neglecting the second-order moments. For instance, the Wilson-Cowan neural mass model [61] can be obtained from a mean field approximation of two coupled networks of FitzHugh-Nagumo neurons [63]. An alternative way of constructing the NMM formalism is to consider that each neuronal population performs two mathematical operations [62]. The first is the conversion of postsynaptic potentials (PSP) into an average density of action potentials (AP) which is modeled using a sigmoid function. The second operation is the conversion of AP into PSP, which is done by means of a linear convolution with an impulse response function. The Wilson-Cowan model is obtained when the impulse response function is $g(t) = Ge^{-kt}$, which produces a system of first-order differential equations describing the activity in each population. A more recent neural mass model, the Jansen-Rit model [62], is obtained when the impulse response function has the form $g(t) = Gkte^{-kt}$. This results in a system of second-order differential equations describing the dynamics of PSPs in each population. Computational models based on Wilson-Cowan and Jansen-Rit models have provided the mathematical framework for simulating the generation of electrical activity in the brain during resting state [62, 66–71], stimulation [62, 72–74], and disease [67, 75–77].

4. Detailed Mathematical Models

Detailed mathematical models of PAC generation [16, 18] have focused on the theta-gamma interaction observed in the hippocampus [24]. These models consist of either purely

inhibitory networks [16] or networks with both excitatory and inhibitory cells [18–20] and are based on models previously developed to study the generation of theta and gamma rhythms separately [23].

4.1. Inhibitory-Inhibitory (I-I) Network. A simulated inhibitory network in the hippocampus containing fast and slow interneurons was shown to generate theta-gamma coupling under restricted conditions [16]. The network comprised single compartment neurons modeled with the Hodgkin-Huxley formalism:

$$C\frac{dV_i}{dt} = I_i - I_{\mathrm{Na}} - I_{\mathrm{K}} - I_L - I_S + \eta, \tag{1}$$

where index $i = 1, \ldots, N$, counts the cells in the network, I_i is the applied current, and η is a normally distributed noise. The sodium (I_{Na}), potassium (I_{K}), leak (I_L), and synaptic (I_S) currents are given by

$$\begin{aligned} I_{\mathrm{Na}} &= g_{\mathrm{Na}} m_{\infty}^3 h \left(V_i - V_{\mathrm{Na}}\right), \\ I_{\mathrm{K}} &= g_{\mathrm{K}} n^4 \left(V_i - V_{\mathrm{K}}\right), \\ I_L &= g_L \left(V_i - V_L\right), \\ I_S &= \sum_{j=1}^{N} \frac{g_{s,j}}{N} s_j \left(V_i - V_s\right). \end{aligned} \tag{2}$$

The cell population ($N = 100$) was divided into half on the basis of fast and slow synaptic dynamics. Synaptic conductances $g_{s,j}$ had one of four possible values depending on the types of the cells connected: fast cell to fast cell, fast cell to slow cell, slow cell to slow cell, and slow cell to fast cell. Connectivity was all to all. Equations for the gating variables h, n, and s, as well as parameter values can be found in [16]. The numerical simulations performed in [16] showed that the model can generate PAC under restricted conditions that included strong connections within the same populations, weaker connections between populations (especially from fast to slow populations), and carefully tuned inputs.

4.2. Excitatory-Inhibitory (E-I) Networks. Hippocampal networks producing theta-gamma PAC also have pyramidal cells. To consider this situation, a model comprising three neuronal populations was proposed in [18] and was shown to produce theta-gamma PAC [23]. The three populations are pyramidal cells, fast-spiking basket cells, and oriens lacunosum-moleculare (O-LM) interneurons. The outputs of the O-LM cells are projected as slow inhibitory postsynaptic potentials (IPSP) onto the distal apical dendrites of pyramidal cells [18].

Basket cells were modeled with a single compartment, using the fast-spiking interneuron model proposed in [78], similar to (1) and (2). O-LM cells were also modeled with a single compartment. In addition to sodium, potassium, leak, and synaptic current, two other currents were considered: the h-current and the A current [17, 18]. Pyramidal cells were modeled by 5 compartments: 1 for basal dendrites, 1 for soma, and 3 for apical dendrites. The equation for each compartment k $(1, \ldots, 5)$ is

$$\begin{aligned} C_{E_k}\frac{dV_{E_k}}{dt} = {} & I_{\mathrm{app},E_k} - I_{\mathrm{Na},E_k} - I_{\mathrm{K},E_k} - I_{L,E_k} - I_{h,E_k} - I_{A,E_k} \\ & - I_{\mathrm{syn},E_k} + I_{\mathrm{conn},E_k}, \end{aligned} \tag{3}$$

where I_{conn,E_k} is the current due to electrical coupling between compartments. The expressions for the ionic and synaptic currents as well as the parameter values to simulate the model can be found in the supplementary information section in [18]. Different simulations were performed in [18], but the one with the highest number of cells comprised a total of 180 cells. Their results showed that O-LM cells alone can coordinate cell assemblies and that the same theta rhythm can coordinate different cell assemblies with different frequencies in the gamma range [18, 23].

5. Neural Mass Models

In this section we review three NMMs that are able to generate PAC. The first two studies [21, 22] are based on the works of Wilson-Cowan and Jansen-Rit and only focus on the generation of one PAC combination. The last study [79] is also based on the Jansen-Rit model but is able to simultaneously generate different PAC combinations.

5.1. PAC Generation Using the Wilson-Cowan Model. Onslow et al. [21] used the Wilson-Cowan model to study the generation of theta-gamma PAC in a brain region not necessarily restricted to the hippocampus. The model comprises two coupled populations (Figure 1(a)), one excitatory and one inhibitory. The system of first-order differential equations describing the model is

$$\begin{aligned} \frac{dE(t)}{dt} &= \frac{1}{\tau_E}E + \frac{1}{\tau_E}S\left(p_E + \Gamma_{EE}E - \Gamma_{IE}I\right), \\ \frac{dI(t)}{dt} &= -\frac{1}{\tau_I}I + \frac{1}{\tau_I}S\left(p_I + \Gamma_{EI}E - \Gamma_{II}I\right), \end{aligned} \tag{4}$$

where $E(t)$ and $I(t)$ are the average activity levels of excitatory and inhibitory populations, respectively [61] and p_E and p_I are the external inputs to the two populations. The weight of the connection from the excitatory population to the inhibitory population is Γ_{EI} and from the inhibitory to the excitatory population is Γ_{IE}, and the self-connections are Γ_{EE} and Γ_{II}. τ_E and τ_I are the time constants for each population. The nonlinearity in the model is introduced by means of a sigmoid function:

$$S(x) = \frac{S_0}{1 + e^{r(x - v_0)}}, \tag{5}$$

where parameter r determines the steepness of the sigmoid curve, v_0 determines the position of the sigmoid function, and S_0 determines the amplitude of the response.

System (4) is capable of producing oscillations due to the reciprocal connections between the two populations.

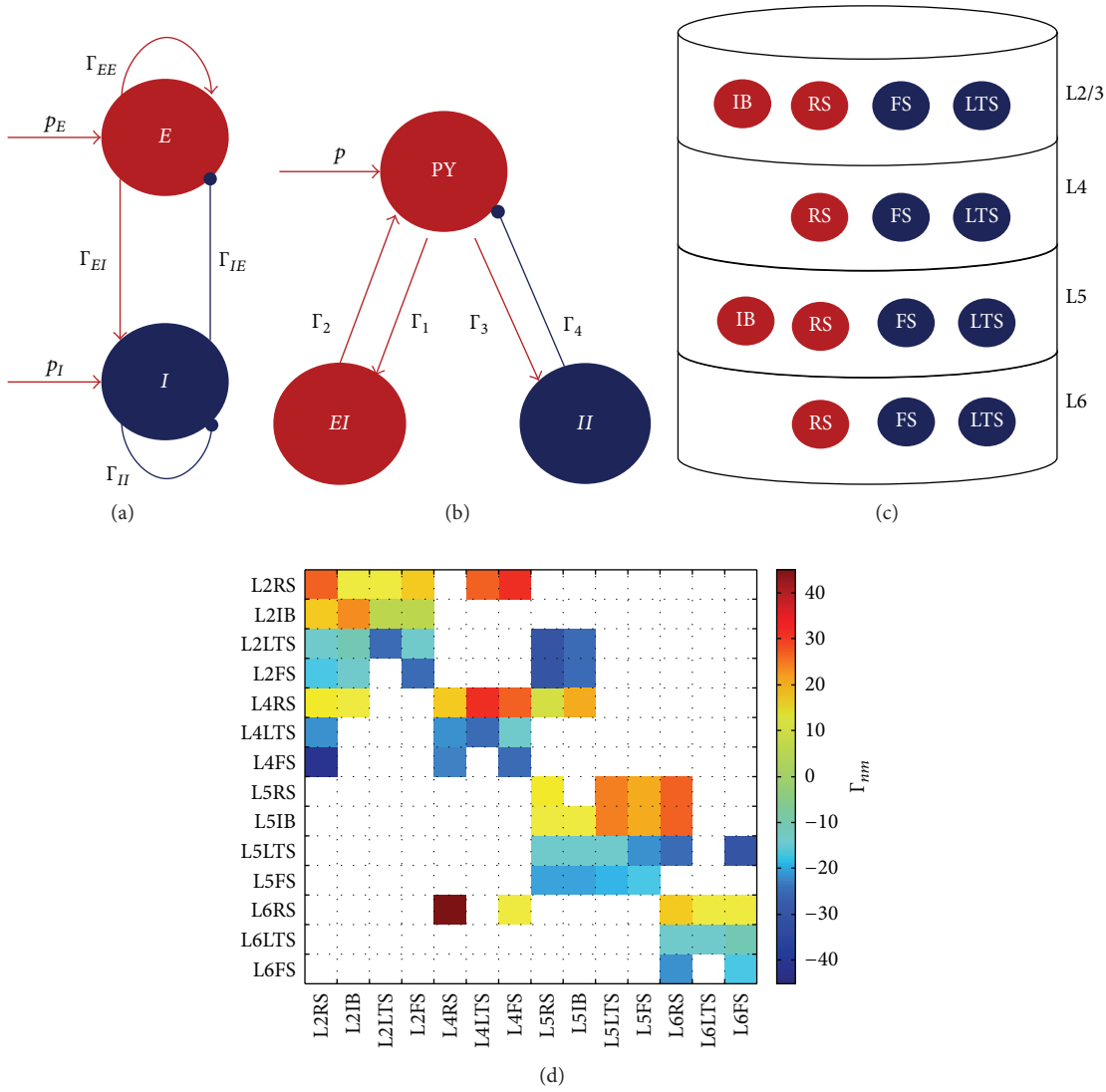

FIGURE 1: Neural mass models. (a) Wilson-Cowan model (Section 5.1) of two coupled populations, one excitatory (E) and one inhibitory (I). External inputs to these populations are p_E and p_I, and the connectivity parameters are Γ_{EI}, Γ_{IE}, Γ_{EE}, and Γ_{II}. (b) Jansen-Rit model (Section 5.2) of a cortical column. Three populations are modeled: pyramidal cells (PY), excitatory interneurons (EI), and inhibitory interneurons. The connectivity parameters are Γ_1, Γ_2, Γ_3, and Γ_4, and the input to the model is p. (c) Neural mass model of the cortical column comprising 14 populations (Section 5.3) distributed across 4 layers. The excitatory populations are the intrinsically bursting (IB) and the regulatory spiking (RS). The inhibitory population are the low-threshold spiking (LTS) and fast-spiking (FS). The connections between the populations are depicted in (d). Any of the 14 populations can be subjected to an external input. In the three models ((a), (b), and (c)), excitatory populations and connections are depicted in red and inhibitory ones in blue. (d) Connectivity matrix values used for coupling the 14 populations are modeled in (c). Negative values correspond to inhibitory connections and positive values correspond to excitatory ones.

Numerical simulations showed [21] that this model generates gamma oscillations that are locked to a certain phase of theta oscillations when considering oscillatory inputs.

Figure 2(a) shows a realization of the model where the phase of a 4 Hz oscillation modulates the amplitude of a 55 Hz oscillation. The parameter values used in this simulation were $\tau_E = 0.0032$ s, $\tau_I = 0.0052$ s, $p_E = 0.6 + 0.1\cos(8\pi t)$, $p_I = 0$, $\Gamma_{EE} = 2.4$, $\Gamma_{EI} = 2$, $\Gamma_{IE} = 2.1$, $\Gamma_{II} = 0$, $r = 4$, $S_0 = 1$, and $v_0 = 1$. Additional simulations showed [21] that the amplitude, frequency, and phase-locking characteristics of the PAC activity generated were dependent on the strength of the connectivity parameters and on the amplitude and mean value of the low frequency input signal. It was possible to tune the parameters of the model to produce different frequencies of activity phase-locked to different phases of the theta rhythm [21].

5.2. The Jansen-Rit Model of a Cortical Column. The Jansen-Rit model of a cortical column [62] comprises three neuronal populations (Figure 1(b)): pyramidal cells, excitatory interneurons, and inhibitory interneurons. The model is

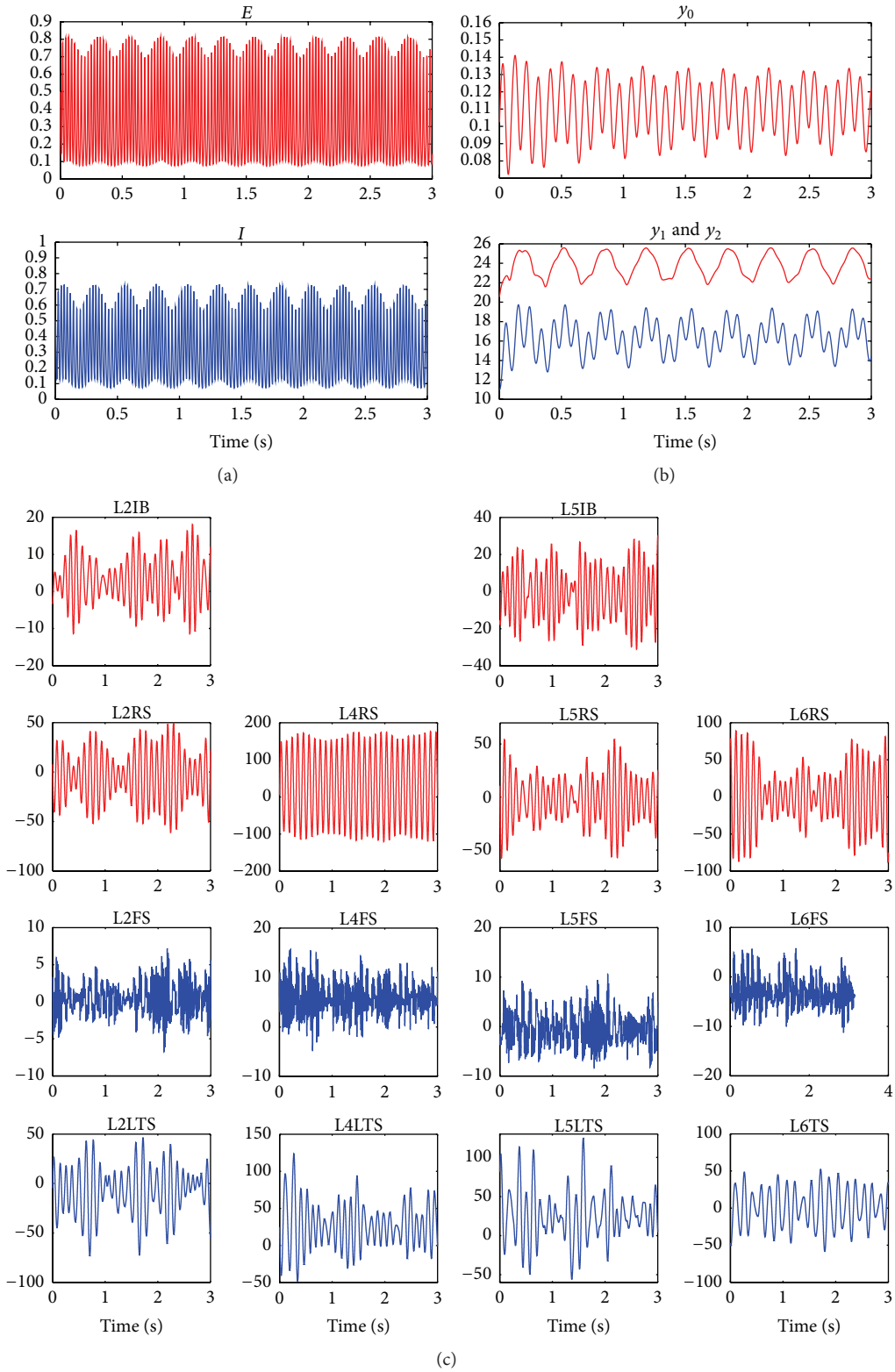

Figure 2: Simulated temporal evolution of the variables of three different neural mass models. (a) Wilson-Cowan model. The phase of a theta oscillation (4 Hz) modulates the amplitude of a gamma oscillation (55 Hz). (b) Jansen-Rit model. The phase of a delta oscillation (3 Hz) modulates the amplitude of an alpha oscillation (11 Hz). (c) Cortical column model. The values of the parameters are given in Tables 1 and 2. Multiple PAC combinations are present (see Figure 3). In all cases, the temporal dynamics of excitatory and inhibitory populations are depicted in red and blue, respectively.

Table 1: Values and physiological interpretation of the parameters.

Parameter (units)	Interpretation	Value
G(mV)	Gain	$G_1 = 3.25$, $G_2 = 3.25$, $G_3 = 30$, $G_4 = 10$, $G_5 = 3.25$, $G_6 = 30$, $G_7 = 10$, $G_8 = 3.25$, $G_9 = 3.25$, $G_{10} = 30$, $G_{11} = 10$, $G_{12} = 3.25$, $G_{13} = 30$, and $G_{14} = 10$
k (s^{-1})	Reciprocal of time constant	$k_1 = 60$, $k_2 = 70$, $k_3 = 30$, $k_4 = 350$, $k_5 = 60$, $k_6 = 30$, $k_7 = 350$, $k_8 = 60$, $k_9 = 70$, $k_{10} = 30$, $k_{11} = 350$, $k_{12} = 60$, $k_{13} = 30$, and $k_{14} = 350$
p	External input	$p_i = 0$ for $i \neq \{5, 7\}$, $p_5 = 500$, and $p_7 = 150$
b	Damping coefficient	$b = 0.06$ for all populations
S_0 (s^{-1})	Maximum firing rate	$e_0 = 5$ for all populations
v_0 (mV)	Position of the sigmoid function	$v_0 = 6$ for all populations
r (mV^{-1})	Steepness of the sigmoid function	$r = 0.56$ for all populations

mathematically described by a system of second-order differential equations:

$$\begin{aligned}
\frac{d^2x_0(t)}{dt^2} &= -2a\frac{dx_0(t)}{dt} - a^2x_0(t) \\
&\quad + AaS\left(x_1(t) - x_2(t)\right), \\
\frac{d^2x_1(t)}{dt^2} &= -2a\frac{dx_1(t)}{dt} - a^2x_1(t) \\
&\quad + Aa\left(p + \Gamma_2 S\left(\Gamma_1 x_0(t)\right)\right), \\
\frac{d^2x_2(t)}{dt^2} &= -2b\frac{dx_2(t)}{dt} - b^2x_2(t) + Bb\Gamma_4 S\left(\Gamma_3 x_0(t)\right),
\end{aligned} \tag{6}$$

where x_0 is the excitatory postsynaptic potential (EPSP) that feeds into the two populations of interneurons and x_1 and x_2 are EPSP and inhibitory postsynaptic potentials (IPSP) that enter into the pyramidal cell population, respectively. Γ_1, Γ_2, Γ_3, and Γ_4 are the connection strengths between the populations. In this model, the electroencephalography (EEG) signal is considered to be proportional to $x_1(t) - x_2(t)$.

Figure 2(b) shows a realization of model (6) where delta (3 Hz)-alpha (11 Hz) PAC is produced when considering an oscillatory input p. The parameter values used in this simulation were $A = 3.25\,\text{mV}$, $B = 22\,\text{mV}$, $p = 200 + 50\cos(6\pi t)$, $a = 100\,\text{s}^{-1}$, $b = 50\,\text{s}^{-1}$, $\Gamma_1 = 135$, $\Gamma_2 = 108$, $\Gamma_3 = 33.75$, $\Gamma_4 = 33.75$, $r = 0.56\,\text{mV}^{-1}$, $S_0 = 5\,\text{s}^{-1}$, and $v_0 = 6\,\text{mV}$.

Alternatively, EEG signals presenting PAC can be obtained by coupling multiple Jansen-Rit models (see Figures 5, 8, and 9 in [67]). In a more recent work [22], several Jansen-Rit models were also coupled and the cross-frequency transfer was studied in a setting where oscillators (generating the different rhythms) were coupled unidirectionally and thus the driving between them was passive. This study showed that this passive driving can also account for CFC in the brain as a result of the complex nonlinear dynamics of the underlying neuronal activity.

5.3. Cortical Column Model Comprising 4 Layers and 14 Neuronal Populations. A more complex neural mass model of the cortical column was recently proposed [79] in which 4 cortical layers and 14 neuronal populations are considered. Figure 1(c) shows the model obtained by distributing four cell classes in four cortical layers (L2/3, L4, L5, and L6). This produced 14 different neuronal populations, since not all cell classes are present in every layer [80]. Excitatory neurons were either regular spiking (RS) or intrinsically bursting (IB) ones, and inhibitory neurons were either fast-spiking (FS) or low-threshold spiking (LTS) neurons.

The model is based on the Jansen-Rit model and the dynamics of the average PSP in each neuronal population x_m is obtained by solving a system of 14 second-order differential equations:

$$\begin{aligned}
\frac{d^2x_m(t)}{dt^2} &= -2k_m b_m \frac{dx_m(t)}{dt} - k_m^2 x_m(t) \\
&\quad + G_m k_m \left(p_m + \sum_{n=1}^{14} \Gamma_{nm} S\left(x_n(t)\right)\right),
\end{aligned} \tag{7}$$

where $n = 1, \ldots, 14$, and $m = 1, \ldots, 14$. The populations are numbered from 1 to 14 following the order: [L2RS, L2IB, L2LTS, L2FS, L4RS, L4LTS, L4FS, L5RS, L5IB, L5LTS, L5FS, L6RS, L6LTS, L6FS]. Layer 2/3 was labelled as 2. As can be seen in (7), neuronal populations interact via the connectivity matrix Γ_{nm} (Figure 1(d)). External inputs are accounted for via p_m which can be any arbitrary function including white noise [62]. The "damping" parameter b_m critically determines the behavior of the system. For $b_m = 1$ (which corresponds to the Jansen-Rit model) an individual population is not capable of oscillating, and it is the presence of interpopulation connections (nonzero Γ_{nm}, $n \neq m$) that produces oscillatory behavior that mimics observed EEG signals. To account for the possibility of an oscillatory population [78, 81] a nonzero value for b_m was used.

Figure 2(c) presents the temporal evolution of the average PSP in each neuronal population. Time series colored in red correspond to excitatory PSP (EPSP) whereas inhibitory PSP (IPSP) are presented in blue. As seen in the figure, both EPSP and IPSP present the characteristic "waxing and waning" (i.e., amplitude modulation) observed in real EEG signals. Parameters values are presented in Tables 1 and 2. To

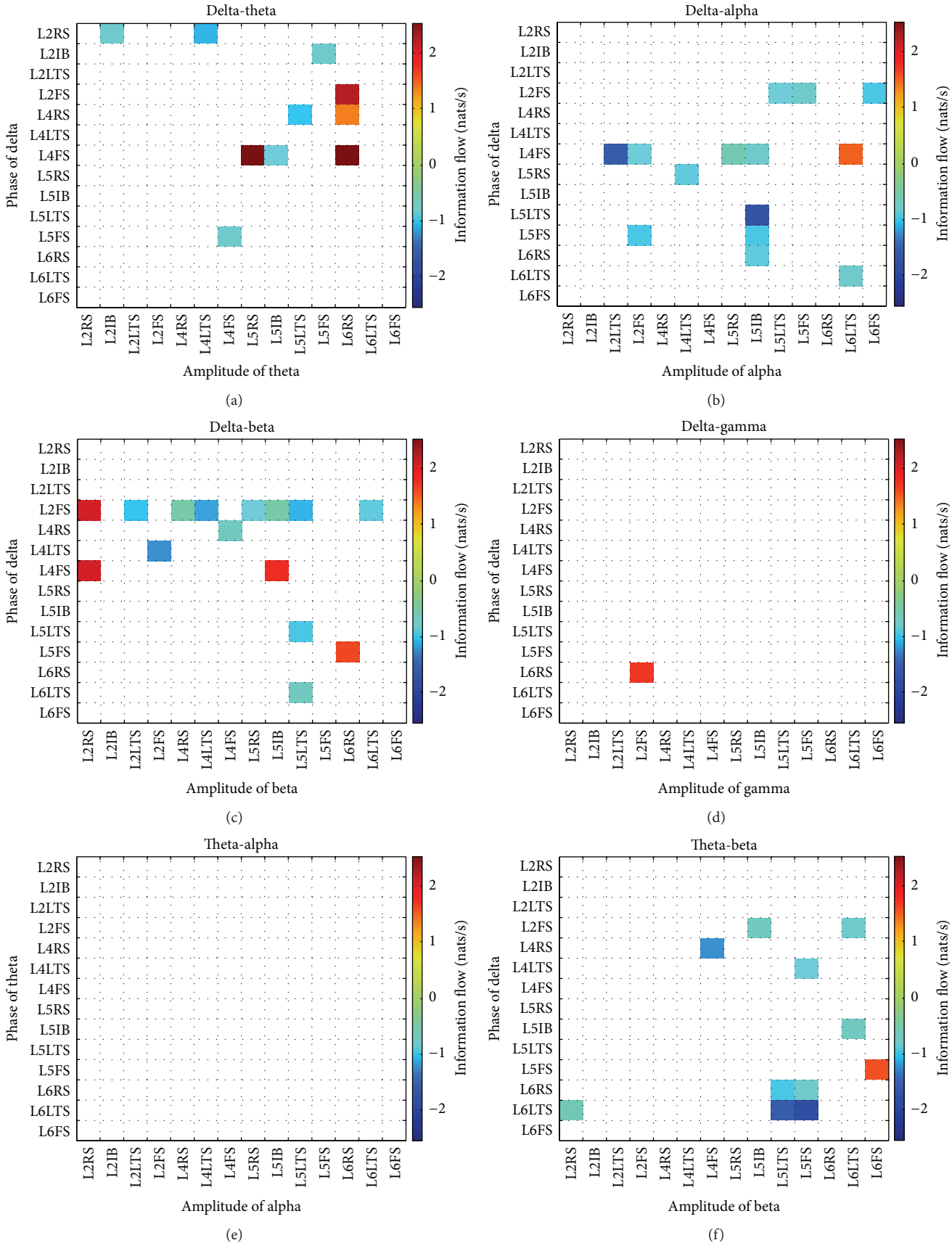

Figure 3: Continued.

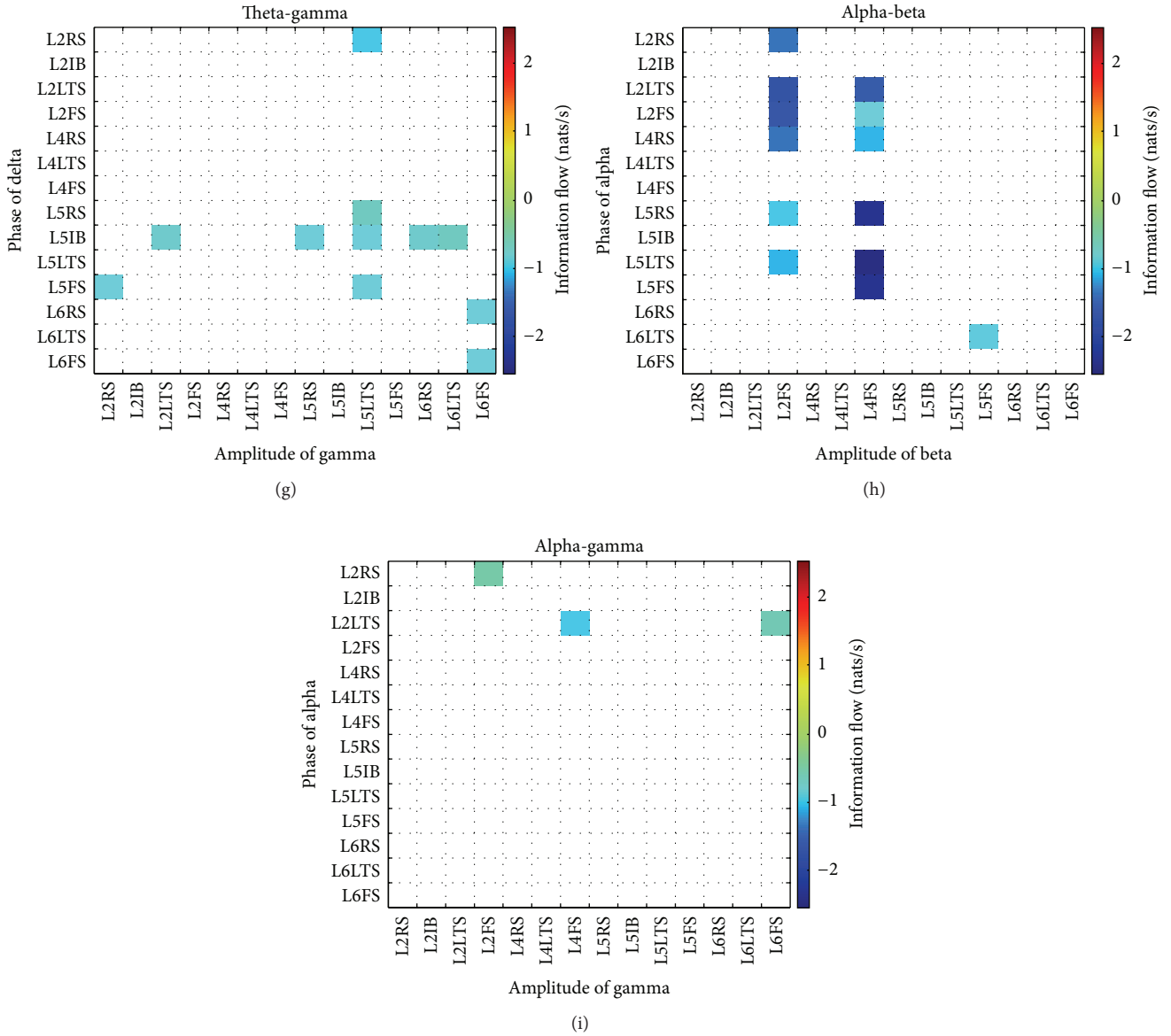

FIGURE 3: Phase-amplitude coupling (PAC) corresponding to the simulation presented in Figure 2(c). Nonsignificant values were set to zero and are depicted in white. (a) Delta-theta, (b) delta-alpha, (c) delta-beta, (d) delta-gamma, (e) theta-alpha, (f) theta-beta, (g) theta-gamma, (h) alpha-beta, and (i) alpha-gamma.

quantify the PAC phenomenon, a causality measure between time series, the information flow [82], was computed using phases and amplitudes of the signals shown in Figure 2(c). Figure 3 shows the information flow from the phase to the amplitude for nine different combinations of phases and amplitudes: delta-theta, delta-alpha, delta-beta, delta-gamma, theta-alpha, theta-beta, theta-gamma, alpha-beta, and alpha-gamma. A negative value of the information flow means that the phase tends to stabilize the amplitude whereas a positive value means that the phase tends to make the amplitude more uncertain. An exploratory analysis of the influence of the parameters on PAC showed that changes in external input and time constants produced theta-gamma PAC values higher than alpha-gamma PAC, whereas changes in connectivity produced higher alpha-gamma PAC values. Additional information can be found in [79].

6. Conclusions

In conclusion, we have shown that PAC is a diverse phenomenon, not restricted to the theta-gamma coupling in the hippocampus. In order to model the complexity of the PAC phenomenon, which is hypothesized to bridge local and global scales in the brain [12, 15], reduced models of neuronal activity such as NMMs are needed, since detailed models are computationally expensive and their results are difficult to interpret due to the high number of variables and parameters

Table 2: Standard values of the connectivity matrix Γ_{nm}.

		L2/3				L4			L5				L6		
		RS	IB	LTS	FS	RS	LTS	FS	RS	IB	LTS	FS	RS	LTS	FS
L2/3	RS	25	10	10	15	0	25	30	0	0	0	0	0	0	0
	IB	10	25	5	5	0	0	0	0	0	0	0	0	0	0
	LTS	−10	−8	−15	−10	0	0	0	−20	−25	0	0	0	0	0
	FS	−15	−10	0	−15	0	0	0	−20	−25	0	0	0	0	0
L4	RS	12	10	0	0	15	30	25	8	18	0	0	0	0	0
	LTS	−20	0	0	0	−20	−25	−10	0	0	0	0	0	0	0
	FS	−42	0	0	0	−22	0	25	0	0	0	0	0	0	0
L5	RS	0	0	0	0	0	0	0	12	0	22	18	25	0	0
	IB	0	0	0	0	0	0	0	10	10	22	18	25	0	0
	LTS	0	0	0	0	0	0	0	−10	−10	−10	−20	−25	0	−30
	FS	0	0	0	0	0	0	0	−19	−19	−17	−15	0	0	0
L6	RS	0	0	0	0	45	0	10	0	0	0	0	15	10	10
	LTS	0	0	0	0	0	0	0	0	0	0	0	−11	−10	−8
	FS	0	0	0	0	0	0	0	0	0	0	0	−20	0	−15

involved. An open problem to be explored with NMMs is how the different PAC combinations are related.

While both types of models reviewed here, detailed models and NMMs, are capable of generating signals reflecting PAC, only in a few studies a quantitative measure of the phenomenon has been provided. This is probably related to the lack of a gold standard for PAC detection, which has resulted in the development of numerous methods.

The computational models summarized here focused on the mechanistic generation of the PAC phenomenon. NMMs are simple (in the sense of the few variables and parameters involved) but complex (in the sense of the richness of the dynamics they can generate) enough to approach important questions related to the functional role of the PAC phenomenon.

Conflict of Interests

The author declares that no conflict of interests exists.

References

[1] C. C. Chen, S. J. Kiebel, and K. J. Friston, "Dynamic causal modelling of induced responses," *NeuroImage*, vol. 41, no. 4, pp. 1293–1312, 2008.

[2] R. D. Traub, E. H. Buhl, T. Gloveli, and M. A. Whittington, "Fast rhythmic bursting can be induced in layer 2/3 cortical neurons by enhancing persistent Na^+ conductance or by blocking BK channels," *Journal of Neurophysiology*, vol. 89, no. 2, pp. 909–921, 2003.

[3] V. Jirsa and V. Müller, "Cross-frequency coupling in real and virtual brain networks," *Frontiers in Computational Neuroscience*, 2013.

[4] O. Jensen and L. L. Colgin, "Cross-frequency coupling between neuronal oscillations," *Trends in Cognitive Sciences*, vol. 11, no. 7, pp. 267–269, 2007.

[5] J. López-Azcárate, M. Tainta, M. C. Rodríguez-Oroz et al., "Coupling between beta and high-frequency activity in the human subthalamic nucleus may be a pathophysiological mechanism in Parkinson's disease," *Journal of Neuroscience*, vol. 30, no. 19, pp. 6667–6677, 2010.

[6] S. A. Shimamoto, E. S. Ryapolova-Webb, J. L. Ostrem, N. B. Galifianakis, K. J. Miller, and P. A. Starr, "Subthalamic nucleus neurons are synchronized to primary motor cortex local field potentials in Parkinson's disease," *Journal of Neuroscience*, vol. 33, no. 17, pp. 7220–7233, 2013.

[7] C. de Hemptinne, E. S. Ryapolova-Webb, E. L. Air et al., "Exaggerated phase-amplitude coupling in the primary motor cortex in Parkinson disease," *Proceedings of the National Academy of Sciences of the United States of America*, vol. 110, no. 12, pp. 4780–4785, 2013.

[8] E. A. Allen, J. Liu, K. A. Kiehl et al., "Components of cross-frequency modulation in health and disease," *Frontiers in Systems Neuroscience*, vol. 5, article 59, 2011.

[9] L. V. Moran and L. E. Hong, "High vs low frequency neural oscillations in schizophrenia," *Schizophrenia Bulletin*, vol. 37, no. 4, pp. 659–663, 2011.

[10] K. Kirihara, A. J. Rissling, N. R. Swerdlow, D. L. Braff, and G. A. Light, "Hierarchical organization of gamma and theta oscillatory dynamics in schizophrenia," *Biological Psychiatry*, vol. 71, no. 10, pp. 873–880, 2012.

[11] V. Miskovic, D. A. Moscovitch, D. L. Santesso, R. E. McCabe, M. M. Antony, and L. A. Schmidt, "Changes in EEG cross-frequency coupling during cognitive behavioral therapy for social anxiety disorder," *Psychological Science*, vol. 22, no. 4, pp. 507–516, 2011.

[12] R. T. Canolty and R. T. Knight, "The functional role of cross-frequency coupling," *Trends in Cognitive Sciences*, vol. 14, no. 11, pp. 506–515, 2010.

[13] J. E. Lisman and M. A. P. Idiart, "Storage of 7+/-2 short-term memories in oscillatory subcycles," *Science*, vol. 267, no. 5203, pp. 1512–1515, 1995.

[14] J. E. Lisman and O. Jensen, "The theta-gamma neural code," *Neuron*, vol. 77, no. 6, pp. 1002–1016, 2013.

[15] L. Wang, Y. B. Saalmann, M. A. Pinsk, M. J. Arcaro, and S. Kastner, "Electrophysiological low-frequency coherence and cross-frequency coupling contribute to BOLD connectivity," *Neuron*, vol. 76, no. 5, pp. 1010–1020, 2012.

[16] J. A. White, M. I. Banks, R. A. Pearce, and N. J. Kopell, "Networks of interneurons with fast and slow γ-aminobutyric acid type A ($GABA_A$) kinetics provide substrate for mixed gamma-theta rhythm," *Proceedings of the National Academy of Sciences of the United States of America*, vol. 97, no. 14, pp. 8128–8133, 2000.

[17] H. G. Rotstein, D. D. Pervouchine, C. D. Acker et al., "Slow and fast inhibition and an H-current interact to create a theta rhythm in a model of CA1 interneuron network," *Journal of Neurophysiology*, vol. 94, no. 2, pp. 1509–1518, 2005.

[18] A. B. L. Tort, H. G. Rotstein, T. Dugladze, T. Gloveli, and N. J. Kopell, "On the formation of gamma-coherent cell assemblies by oriens lacunosum-moleculare interneurons in the hippocampus," *Proceedings of the National Academy of Sciences of the United States of America*, vol. 104, no. 33, pp. 13490–13495, 2007.

[19] X. Zhang, K. M. Kendrick, H. Zhou, Y. Zhan, and J. Feng, "A computational study on altered theta-gamma coupling during learning and phase coding," *PLoS ONE*, vol. 7, no. 6, Article ID e36472, 2012.

[20] E. Spaak, M. Zeitler, and S. Gielen, "Hippocampal theta modulation of neocortical spike times and gamma rhythm: a biophysical model study," *PLoS ONE*, vol. 7, no. 10, Article ID e45688, 2012.

[21] A. C. Onslow, M. W. Jones, R. Bogacz, and A. B. Tort, "A canonical circuit for generating phase-amplitude coupling," *PLoS ONE*, vol. 9, no. 8, Article ID e102591, 2014.

[22] M. Jedynak, A. J. Pons, and J. Garcia-Ojalvo, "Cross-frequency transfer in a stochastically driven mesoscopic neuronal model," *Frontiers in Computational Neuroscience*, vol. 9, article 14, 2015.

[23] N. Kopell, C. Börgers, D. Pervouchine, P. Malerba, and A. Tort, "Gamma and theta rhythms in biophysical models of hippocampal circuits," in *Hippocampal Microcircuits: A Computational Modeler's Resource Book*, V. Cutsuridis, B. P. Graham, S. Cobb, and I. Vida, Eds., Springer, New York, NY, USA, 2010.

[24] A. Bragin, G. Jandó, Z. Nádasdy, J. Hetke, K. Wise, and G. Buzsáki, "Gamma (40–100 Hz) oscillation in the hippocampus of the behaving rat," *The Journal of Neuroscience*, vol. 15, no. 1, pp. 47–60, 1995.

[25] R. T. Canolty, E. Edwards, S. S. Dalal et al., "High gamma power is phase-locked to theta oscillations in human neocortex," *Science*, vol. 313, no. 5793, pp. 1626–1628, 2006.

[26] D. Osipova, D. Hermes, and O. Jensen, "Gamma power is phase-locked to posterior alpha activity," *PLoS ONE*, vol. 3, no. 12, Article ID e3990, 2008.

[27] B. Voytek, R. T. Canolty, A. Shestyuk, N. E. Crone, J. Parvizi, and R. T. Knight, "Shifts in gamma phase-amplitude coupling frequency from theta to alpha over posterior cortex during visual tasks," *Frontiers in Human Neuroscience*, vol. 4, article 191, 2010.

[28] P. Lakatos, C.-M. Chen, M. N. O'Connell, A. Mills, and C. E. Schroeder, "Neuronal oscillations and multisensory interaction in primary auditory cortex," *Neuron*, vol. 53, no. 2, pp. 279–292, 2007.

[29] P. Lakatos, G. Karmos, A. D. Mehta, I. Ulbert, and C. E. Schroeder, "Entrainment of neuronal oscillations as a mechanism of attentional selection," *Science*, vol. 320, no. 5872, pp. 110–113, 2008.

[30] D. Rojas-Líbano and L. M. Kay, "Olfactory system gamma oscillations: the physiological dissection of a cognitive neural system," *Cognitive Neurodynamics*, vol. 2, no. 3, pp. 179–194, 2008.

[31] R. Scheffer-Teixeira, H. Belchior, F. V. Caixeta, B. C. Souza, S. Ribeiro, and A. B. L. Tort, "Theta phase modulates multiple layer-specific oscillations in the CA1 region," *Cerebral Cortex*, vol. 22, no. 10, pp. 2404–2414, 2012.

[32] M. J. Gillies, R. D. Traub, F. E. N. LeBeau et al., "A model of atropine-resistant theta oscillations in rat hippocampal area CA1," *Journal of Physiology*, vol. 543, no. 3, pp. 779–793, 2002.

[33] B. Lega, J. Burke, J. Jacobs, and M. J. Kahana, "Slow-theta-to-gamma phase-amplitude coupling in human hippocampus supports the formation of new episodic memories," *Cerebral Cortex*, 2014.

[34] J. Gross, N. Hoogenboom, G. Thut et al., "Speech rhythms and multiplexed oscillatory sensory coding in the human brain," *PLoS Biology*, vol. 11, no. 12, Article ID e1001752, 2013.

[35] E. Florin and S. Baillet, "The brain's resting-state activity is shaped by synchronized cross-frequency coupling of neural oscillations," *NeuroImage*, vol. 111, pp. 26–35, 2015.

[36] S. Dürschmid, T. Zaehle, K. Kopitzki et al., "Phase-amplitude cross-frequency coupling in the human nucleus accumbens tracks action monitoring during cognitive control," *Frontiers in Human Neuroscience*, vol. 7, article 635, 2013.

[37] P. Lakatos, A. S. Shah, K. H. Knuth, I. Ulbert, G. Karmos, and C. E. Schroeder, "An oscillatory hierarchy controlling neuronal excitability and stimulus processing in the auditory cortex," *Journal of Neurophysiology*, vol. 94, no. 3, pp. 1904–1911, 2005.

[38] J. Lee and J. Jeong, "Correlation of risk-taking propensity with cross-frequency phase-amplitude coupling in the resting EEG," *Clinical Neurophysiology*, vol. 124, no. 11, pp. 2172–2180, 2013.

[39] R. J. McGinn and T. A. Valiante, "Phase-amplitude coupling and interlaminar synchrony are correlated in human neocortex," *Journal of Neuroscience*, vol. 34, no. 48, pp. 15923–15930, 2014.

[40] T. Demiralp, Z. Bayraktaroglu, D. Lenz et al., "Gamma amplitudes are coupled to theta phase in human EEG during visual perception," *International Journal of Psychophysiology*, vol. 64, no. 1, pp. 24–30, 2007.

[41] S. M. Szczepanski, N. E. Crone, R. A. Kuperman et al., "Dynamic changes in phase-amplitude coupling facilitate spatial attention control in fronto-parietal cortex," *PLoS Biology*, vol. 12, no. 8, Article ID e1001936, 2014.

[42] M. van Wingerden, R. van der Meij, T. Kalenscher, E. Maris, and C. M. A. Pennartz, "Phase-amplitude coupling in rat orbitofrontal cortex discriminates between correct and incorrect decisions during associative learning," *The Journal of Neuroscience*, vol. 34, no. 2, pp. 493–505, 2014.

[43] J. Wang, D. Li, X. Li et al., "Phase-amplitude coupling between theta and gamma oscillations during nociception in rat electroencephalography," *Neuroscience Letters*, vol. 499, no. 2, pp. 84–87, 2011.

[44] C. Nakatani, A. Raffone, and C. van Leeuwen, "Efficiency of conscious access improves with coupling of slow and fast neural oscillations," *Journal of Cognitive Neuroscience*, vol. 26, no. 5, pp. 1168–1179, 2014.

[45] R. C. Sotero, A. Bortel, S. Naaman et al., "Laminar distribution of cross-frequency coupling during spontaneous activity in rat area S1Fl," in *Proceedings of the 43rd Annual Meeting of the Society-for-Neuroscience*, San Diego, Calif, USA, 2013.

[46] M. X. Cohen, C. E. Elger, and J. Fell, "Oscillatory activity and phase-amplitude coupling in the human medial frontal cortex during decision making," *Journal of Cognitive Neuroscience*, vol. 21, no. 2, pp. 390–402, 2009.

[47] J. Ito, P. Maldonado, and S. Grün, "Cross-frequency interaction of the eye-movement related LFP signals in V1 of freely viewing monkeys," *Frontiers in Systems Neuroscience*, vol. 7, article 1, 2013.

[48] E. Spaak, M. Bonnefond, A. Maier, D. A. Leopold, and O. Jensen, "Layer-specific entrainment of gamma-band neural activity by the alpha rhythm in monkey visual cortex," *Current Biology*, vol. 22, no. 24, pp. 2313–2318, 2012.

[49] T. Yanagisawa, O. Yamashita, M. Hirata et al., "Regulation of motor representation by phase-amplitude coupling in the sensorimotor cortex," *The Journal of Neuroscience*, vol. 32, no. 44, pp. 15467–15475, 2012.

[50] C. Magri, A. Mazzoni, N. K. Logothetis, and S. Panzeri, "Optimal band separation of extracellular field potentials," *Journal of Neuroscience Methods*, vol. 210, no. 1, pp. 66–78, 2012.

[51] W. D. Penny, E. Duzel, K. J. Miller, and J. G. Ojemann, "Testing for nested oscillation," *Journal of Neuroscience Methods*, vol. 174, no. 1, pp. 50–61, 2008.

[52] A. B. L. Tort, R. Komorowski, H. Eichenbaum, and N. Kopell, "Measuring phase-amplitude coupling between neuronal oscillations of different frequencies," *Journal of Neurophysiology*, vol. 104, no. 2, pp. 1195–1210, 2010.

[53] B. Voytek, M. D'Esposito, N. Crone, and R. T. Knight, "A method for event-related phase/amplitude coupling," *NeuroImage*, vol. 64, no. 1, pp. 416–424, 2013.

[54] D. Dvorak and A. A. Fenton, "Toward a proper estimation of phase-amplitude coupling in neural oscillations," *Journal of Neuroscience Methods*, vol. 225, pp. 42–56, 2014.

[55] B. Pittman-Polletta, W.-H. Hsieh, S. Kaur, M.-T. Lo, and K. Hu, "Detecting phase-amplitude coupling with high frequency resolution using adaptive decompositions," *Journal of Neuroscience Methods*, vol. 226, pp. 15–32, 2014.

[56] T. E. Özkurt, "Statistically reliable and fast direct estimation of phase-amplitude cross-frequency coupling," *IEEE Transactions on Biomedical Engineering*, vol. 59, no. 7, pp. 1943–1950, 2012.

[57] M. A. Kramer and U. T. Eden, "Assessment of cross-frequency coupling with confidence using generalized linear models," *Journal of Neuroscience Methods*, vol. 220, no. 1, pp. 64–74, 2013.

[58] J. Aru, J. Aru, V. Priesemann et al., "Untangling cross-frequency coupling in neuroscience," *Current Opinion in Neurobiology C*, vol. 31, pp. 51–61, 2014.

[59] R. D. Traub, R. Duncan, A. J. C. Russell et al., "Spatiotemporal patterns of electrocorticographic very fast oscillations (> 80 Hz) consistent with a network model based on electrical coupling between principal neurons," *Epilepsia*, vol. 51, no. 8, pp. 1587–1597, 2010.

[60] J. Rinzel, D. Terman, X.-J. Wang, and B. Ermentrout, "Propagating activity patterns in large-scale inhibitory neuronal networks," *Science*, vol. 279, no. 5355, pp. 1351–1355, 1998.

[61] H. R. Wilson and J. D. Cowan, "Excitatory and inhibitory interactions in localized populations of model neurons," *Biophysical Journal*, vol. 12, no. 1, pp. 1–24, 1972.

[62] B. H. Jansen and V. G. Rit, "Electroencephalogram and visual-evoked potential generation in a mathematical-model of coupled cortical columns," *Biological Cybernetics*, vol. 73, no. 4, pp. 357–366, 1995.

[63] H. Hasegawa, "Dynamical mean-field theory of spiking neuron ensembles: response to a single spike with independent noises," *Physical Review E*, vol. 67, no. 4, Article ID 041903, 2003.

[64] H. Hasegawa, "Dynamical mean-field theory of noisy spiking neuron ensembles: application to the Hodgkin-Huxley model," *Physical Review E*, vol. 68, no. 4, Article ID 041909, 2003.

[65] R. Rodriguez and H. C. Tuckwell, "Noisy spiking neurons and networks: useful approximations for firing probabilities and global behavior," *BioSystems*, vol. 48, no. 1–3, pp. 187–194, 1998.

[66] O. David and K. J. Friston, "A neural mass model for MEG/EEG: coupling and neuronal dynamics," *NeuroImage*, vol. 20, no. 3, pp. 1743–1755, 2003.

[67] R. C. Sotero, N. J. Trujillo-Barreto, Y. Iturria-Medina, F. Carbonell, and J. C. Jimenez, "Realistically coupled neural mass models can generate EEG rhythms," *Neural Computation*, vol. 19, no. 2, pp. 478–512, 2007.

[68] M. Zavaglia, L. Astolfi, F. Babiloni, and M. Ursino, "A neural mass model for the simulation of cortical activity estimated from high resolution EEG during cognitive or motor tasks," *Journal of Neuroscience Methods*, vol. 157, no. 2, pp. 317–329, 2006.

[69] P. A. Valdes-Sosa, J. M. Sanchez-Bornot, R. C. Sotero et al., "Model driven EEG/fMRI fusion of brain oscillations," *Human Brain Mapping*, vol. 30, no. 9, pp. 2701–2721, 2009.

[70] F. Cona, M. Zavaglia, and M. Ursino, "Binding and segmentation via a neural mass model trained with hebbian and anti-Hebbian mechanisms," *International Journal of Neural Systems*, vol. 22, no. 2, Article ID 1250003, 2012.

[71] R. C. Sotero and A. Shmuel, "Energy-based stochastic control of neural mass models suggests time-varying effective connectivity in the resting state," *Journal of Computational Neuroscience*, vol. 32, no. 3, pp. 563–576, 2012.

[72] O. David, S. J. Kiebel, L. M. Harrison, J. Mattout, J. M. Kilner, and K. J. Friston, "Dynamic causal modeling of evoked responses in EEG and MEG," *NeuroImage*, vol. 30, no. 4, pp. 1255–1272, 2006.

[73] R. C. Sotero and N. J. Trujillo-Barreto, "Biophysical model for integrating neuronal activity, EEG, fMRI and metabolism," *NeuroImage*, vol. 39, no. 1, pp. 290–309, 2008.

[74] R. C. Sotero, A. Bortel, R. Martínez-Cancino et al., "Anatomically-constrained effective connectivity among layers in a cortical column modeled and estimated from local field potentials," *Journal of Integrative Neuroscience*, vol. 9, no. 4, pp. 355–379, 2010.

[75] F. Wendling, J. J. Bellanger, F. Bartolomei, and P. Chauvel, "Relevance of nonlinear lumped-parameter models in the analysis of depth-EEG epileptic signals," *Biological Cybernetics*, vol. 83, no. 4, pp. 367–378, 2000.

[76] F. Wendling and F. Bartolomei, "Modeling EEG signals and interpreting measures of relationship during temporal-lobe seizures: an approach to the study of epileptogenic networks," *Epileptic Disorders*, vol. 3, no. 1, pp. SI67–SI78, 2001.

[77] B. S. Bhattacharya, D. Coyle, and L. P. Maguire, "A thalamo-cortico-thalamic neural mass model to study alpha rhythms in Alzheimer's disease," *Neural Networks*, vol. 24, no. 6, pp. 631–645, 2011.

[78] X.-J. Wang and G. Buzsáki, "Gamma oscillation by synaptic inhibition in a hippocampal interneuronal network model," *Journal of Neuroscience*, vol. 16, no. 20, pp. 6402–6413, 1996.

[79] R. C. Sotero, "Generation of phase-amplitude coupling of neurophysiological signals in a neural mass model of a cortical column," *BioRxiv*, 2015.

[80] S. A. Neymotin, K. M. Jacobs, A. A. Fenton, and W. W. Lytton, "Synaptic information transfer in computer models of neocortical columns," *Journal of Computational Neuroscience*, vol. 30, no. 1, pp. 69–84, 2011.

[81] L. Tattini, S. Olmi, and A. Torcini, "Coherent periodic activity in excitatory Erdös-Renyi neural networks: the role of network connectivity," *Chaos*, vol. 22, no. 2, Article ID 023133, 2012.

[82] X. S. Liang, "Unraveling the cause-effect relation between time series," *Physical Review E*, vol. 90, no. 5, Article ID 052150, 2014.

Hindawi Publishing Corporation
BioMed Research International
Volume 2015, Article ID 954901, 11 pages
http://dx.doi.org/10.1155/2015/954901

Review Article

From Cerebellar Activation and Connectivity to Cognition: A Review of the Quadrato Motor Training

Tal Dotan Ben-Soussan,[1,2] Joseph Glicksohn,[1,3] and Aviva Berkovich-Ohana[4,5]

[1] *The Leslie and Susan Gonda (Goldschmied) Multidisciplinary Brain Research Center, Bar-Ilan University, Ramat Gan, Israel*
[2] *Research Institute for Neuroscience, Education and Didactics, Patrizio Paoletti Foundation, Rome, Italy*
[3] *Department of Criminology, Bar-Ilan University, Ramat Gan, Israel*
[4] *Department of Neurobiology, Weizmann Institute of Science, Rehovot, Israel*
[5] *Department of Physiology and Pharmacology, University of Rome "La Sapienza", Rome, Italy*

Correspondence should be addressed to Tal Dotan Ben-Soussan; research@fondazionepatriziopaoletti.org

Received 13 February 2015; Accepted 6 May 2015

Academic Editor: Ni Shu

The importance of the cerebellum is increasingly recognized, not only in motor control but also in cognitive learning and function. Nevertheless, the relationship between training-induced cerebellar activation and electrophysiological and structural changes in humans has yet to be established. In the current paper, we suggest a general model tying cerebellar function to cognitive improvement, via neuronal synchronization, as well as biochemical and anatomical changes. We then suggest that sensorimotor training provides an optimal paradigm to test the proposed model and review supporting evidence of Quadrato Motor Training (QMT), a sensorimotor training aimed at increasing attention and coordination. Subsequently, we discuss the possible mechanisms through which QMT may exert its beneficial effects on cognition (e.g., increased creativity, reflectivity, and reading), focusing on cerebellar alpha activity as a possible mediating mechanism allowing cognitive improvement, molecular and anatomical changes. Using the example of QMT research, this paper emphasizes the importance of investigating whole-body sensorimotor training paradigms utilizing a multidisciplinary approach and its implications to healthy brain development.

1. Introduction

In this paper, we suggest a general model tying cerebellum function to cognitive improvement, via neuronal synchronization and multimodal connectivity. We then discuss sensorimotor training effects in humans, specifically the Quadrato Motor Training (QMT) effects on brain connectivity, cognitive function, and structural and molecular changes, supporting such a multimodal cerebellar-cognition relationship.

While the role of the cerebellum was traditionally acknowledged in the field of motor control [1–4], it is increasingly recognized in the last decade in sensory regulation and cognitive learning [5–7]. Particularly, accumulating evidence suggests that the cerebellum serves as a general timing mechanism for both sensorimotor and cognitive processes [8–10]. This may be conducted by the cerebellum's role in regulating the rate, force, rhythm, and accuracy of movements, which are crucial for controlling the speed, capacity, consistency, and appropriateness of cognitive as well as emotional processes [6, 11, 12]. In fact, motor learning studies have long been aware of the cerebellum's oscillatory role in skill acquisition, such as bimanual ability [13–15].

Consistent with its putative role in cognition, the cerebellum forms close connections with neocortical brain regions including the prefrontal cortex, thus providing the neural basis through which the cerebellum contributes to neocortical information processing (for review see [16]). Importantly, both the cerebellum and the prefrontal cortex play a crucial role in the neural network, which is activated when attention

engagement or shifting are required, especially during challenging as well as novel tasks [7]. Indeed, a recent local field potential study has demonstrated the directionality of low frequencies (5–10 Hz) coherence as directed from the cerebellum to frontal areas, playing a role in goal-directed motion [16]. The fact that these anatomical connections are crucial for cognitive development and functions further highlights the importance of moving from the research focusing solely on corticocortical connections to an integrated examination of subcortical regions, and especially the cerebellum [7, 17–19]. The cerebellum has been studied mainly by using animal models (e.g., [20]).

Animals models demonstrate that cerebellar-related deficits are accompanied by cognitive impairment (e.g., memory, attention, and visuospatial abilities), as well as cerebellar microstructural changes as a result of training and exposure to enriched environment (for reviews see [21, 22]). In humans, it is widely accepted that only after the introduction of positron emission tomography (PET) and functional magnetic resonance imaging (fMRI) did it become possible to detect cerebellar activation noninvasively during natural movements (reviewed by [23]). FMRI studies report, for example, cerebellar activation during verbal working memory and finger-tapping tasks [24–26].

While electroencephalographic (EEG) studies have generally avoided studying cerebellar function, due to the fact that the neurons in the cerebellum are arranged in a "closed field" configuration [27], the invention of magnetoencephalography (MEG) provides another possible imaging tool, as electrophysiological signals can be obtained by MEG from the cerebellum, especially the slow rhythms including theta (4–7 Hz) and alpha (8–12 Hz) range [10, 28, 29]. For animal models explaining the possible underlying mechanisms resulting in cerebellar low rhythm oscillations, see [30, 31]. For example, cerebellar activity before a stimulus onset predicts uncued simple reaction time, possibly reflecting cerebellar role in timing, response readiness, prediction, and attention [32]. Thus, new neuroimaging methods in the last 2 decades enabled the noninvasive investigation of the cerebellum in humans. These lines of studies consistently have shown the involvement of the cerebellum in many cognitive functions, and specifically in language and reading [33, 34]. The above accumulating studies support the importance of cerebellar activity and connectivity for higher cognitive functions, including timing, attention, emotion, and cognition.

In the model we present here, the importance of the cerebellar oscillatory activity for higher cognitive function is emphasized possibly mediated through several levels of brain organization, including molecular, anatomical, and neural oscillations (Figure 1). Our model suggests that the importance of cerebellar function for cognition may be based at least partly on two interrelated pathways, the first being alterations in oscillatory activity, leading to changes in functional connectivity [35–37], and the second which takes longer periods to occur is mediated by neurotrophic factors, leading to anatomical changes.

The suggested model is based on the following considerations.

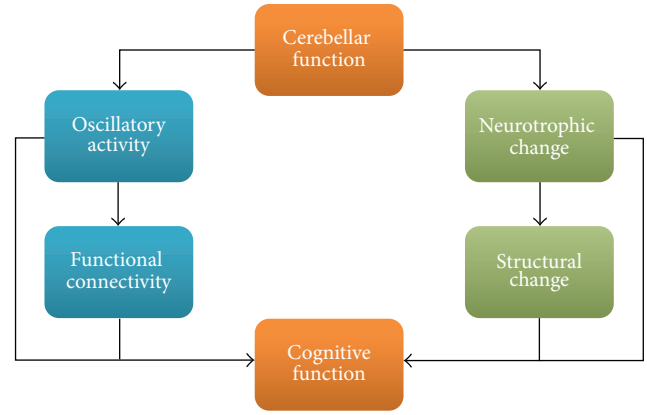

Figure 1: Interconnected relationship between cerebellum and cognitive function. The relationship is mediated via two interrelated routes. The first is slow rhythm oscillations, manifested in functional connectivity. The second is molecular effects on structural changes in structural connectivity.

(1) Electrophysiological Mechanisms Mediating Cerebellar-Cognition Relationship. Cerebellar alpha oscillatory activity has been suggested to be the neural system underlying the planning and execution of movements as well as reading and language comprehension [36–38]. The cerebellum was further found to be the main alpha source of the cerebrocerebellar network that is crucial for speech production, visual recognition and working memory, and coordination [38]. Thus, cerebellar alpha oscillations may mediate both cerebrocerebellar as well as cortical communication, such as the frontoparietal network [35, 38]. This is further in line with previous studies suggesting that sensorimotor-dependent cerebellar stimulation may modulate ongoing firing patterns in frontal regions that are crucial for cognitive functions, such as planning and creativity [16, 39, 40].

(2) Anatomical and Molecular Mechanisms Mediating Cerebellar-Cognition Relationship. Our model focuses on BDNF and Nerve Growth Factor (NGF), which are related to learning and neural plasticity. Neurotrophins, initially synthesized as precursor proteins (proneurotrophins), can influence both developing and mature neural circuits, utilizing distinct receptors to mediate divergent neuronal actions [41, 42]. Thus, while proBDNF and NGF were shown to be related to learning, spatial cognition, and neuronal plasticity [43–46], proNGF was reported to play an important role in nociceptors, neuronal death, and neurodegeneration [47]. Importantly, BDNF is considered a key component mediating neuronal connectivity and movement dependent plasticity especially in the cerebellum [48, 49]. More specifically, motor training is accompanied by increased cerebellar BDNF mRNA amount [50, 51] and structural changes related to underlying cellular events, including synaptogenesis and dendritic arborisation [49, 52]. On the other hand, animal models have shown that severe deficiencies in motor coordination in BDNF knockout mice are linked to abnormal cerebellar development [53, 54]. In addition, sensorimotor training-induced functional

connectivity changes were found to be BDNF-dependent [55, 56].

Thus, we further present the possible effect induced by motor interventions in humans on the putative cerebellar-cognition relationship. Given the importance of the cerebellum in motor control, surprisingly few studies focused on cerebellar motor training effects in humans. In contrast, numerous animal models have consistently demonstrated training-induced effects on brain regions involved in locomotion such as the motor cortex, the basal ganglia, and the cerebellum (for review see [21, 22, 55, 56]). Nevertheless, human studies examining whole-body training-induced changes in executive functions have generally neglected motor-related areas. These studies have almost exclusively concentrated on frontal effects, generally reporting increased frontal alpha synchronization following training [39, 40, 57].

Interestingly, previous studies have found different procedures, such as transcranial direct current stimulation, to improve motor skill learning through augmentation of synaptic plasticity that requires BDNF-secretion [46]. Yet, noninvasive techniques, such as sensorimotor training paradigms, may serve as time and cost-efficient means of reaching similar effects, with no side effects. In line with this, while animal models of pharmacological treatment aimed at cerebellar compensation is largely unsatisfactory, exercise has been found to have some efficacy (for review see [21, 22]). For example, animal models of active training and enriched environment [58–60], as well as a few human studies [61, 62] have demonstrated cerebellar microstructural changes following sensorimotor training.

Consequently, we suggest that motor training in humans may serve as an optimal model to test the possible cerebellar-cognition relationship in two interrelated routes: (1) sensorimotor training may result in fast occurring, cerebellar and frontal low frequency oscillatory modulation [16], possibly leading to improved cognitive performance [40, 63]. (2) Changes in cerebellar function can be further stimulated through training by activating molecular mechanisms, mainly through the regulation of neurotrophins [48, 51].

Consequently, we review a series of sensorimotor training studies aimed at increasing our understanding of the possible link between cerebellar-induced change and cognitive improvement. This review will assist in supporting our presented model (Figure 1), providing evidence for training-induced alterations in alpha oscillation, anatomical, molecular, and cognitive change as a result of a specific sensorimotor training. The training method employed is the *Quadrato Motor Training* (QMT), a sensorimotor whole-body training.

2. Putting Theory into Practice: The Case of QMT

QMT is a new method for motor training, developed by Patrizio Paoletti, generally aiming at enhancing coordination, attention, and creativity [64, 65]. QMT involves following a structured set of simple oral instructions, by stepping to the instructed corner in a 50 × 50 cm square. See Figure 2.

The QMT requires a state of enhanced attention, as it combines dividing attention to the motor response and cognitive processing for producing the correct direction of movement to the next point in the Quadrato space [65, 70]. The QMT has the advantage of being a relatively short training (possibly several minutes) and can be relatively easily practiced in limited spaces. In addition, in comparison to other whole-body training paradigms, it can easily be quantified in terms of accuracy and reaction time. Together these unique aspects render the QMT a technique warranted of scientific exploration, with the future aim of implementing this technique in various health-promoting and educational setups. Next, we review results related to short-term effects of the QMT, that is, one practice of several minutes, as well as long-term effects, following a period of one-three months, in order to add several steps towards verifying our hypothesis.

2.1. Short-Term QMT-Induced Effects. Deficits in spatial cognition, creativity, and decreased cerebellar activity are reported in different developmental disorders and neurodegenerative diseases [71–74], emphasizing the importance of cerebellar oscillatory activity [1, 10, 13, 14, 75, 76]. While we could not study cerebellar electrophysiology directly, we studied the effect of one QMT session on low rhythm oscillations and connectivity, thought to mediate cerebellar function [66] and several cognitive skills, including creativity, spatial performance, reaction time, and reflectivity [64–68, 70].

2.1.1. Creativity, Reaction Time, Alpha Power, and Coherence. In the attempt to uncover the underlying mediating electrophysiological mechanism for movement-induced cognitive change, the effects of QMT were first examined in terms of EEG alpha power and coherence. In addition, changes in creativity and reaction time were examined [65]. Briefly, creativity was studied by means of the Alternate Uses Task (AU), measuring ideational fluency and ideational flexibility. In order to determine whether training-induced changes were driven by the cognitive or the motor aspects of the training, we used two control groups: *Verbal Training* (VT, identical cognitive training with verbal response) and *Simple Motor Training* (SMT, similar motor training with reduced choice requirements). Twenty-seven participants were randomly assigned to one of the groups, all practicing one session of 7 minutes. While reaction time was faster in both motor groups, only QMT enhanced interhemispheric and intrahemispheric alpha coherence, and increased ideational flexibility, which was not the case for either the SMT or VT groups (see Figure 3(a)). The different steps in model described in Figure 1 are further examined and detailed in Figure 4 describing specific QMT-induced changes.

Together these results indicate that the combination of the motor and cognitive aspects embedded in the QMT is important for increasing ideational flexibility and functional connectivity. In addition, a general decrease in alpha power was found following training, which may be related to the fact that decreased frontal alpha power is related to motor planning occurring at the contralateral side to the movement [77]. Faster reaction time was correlated with

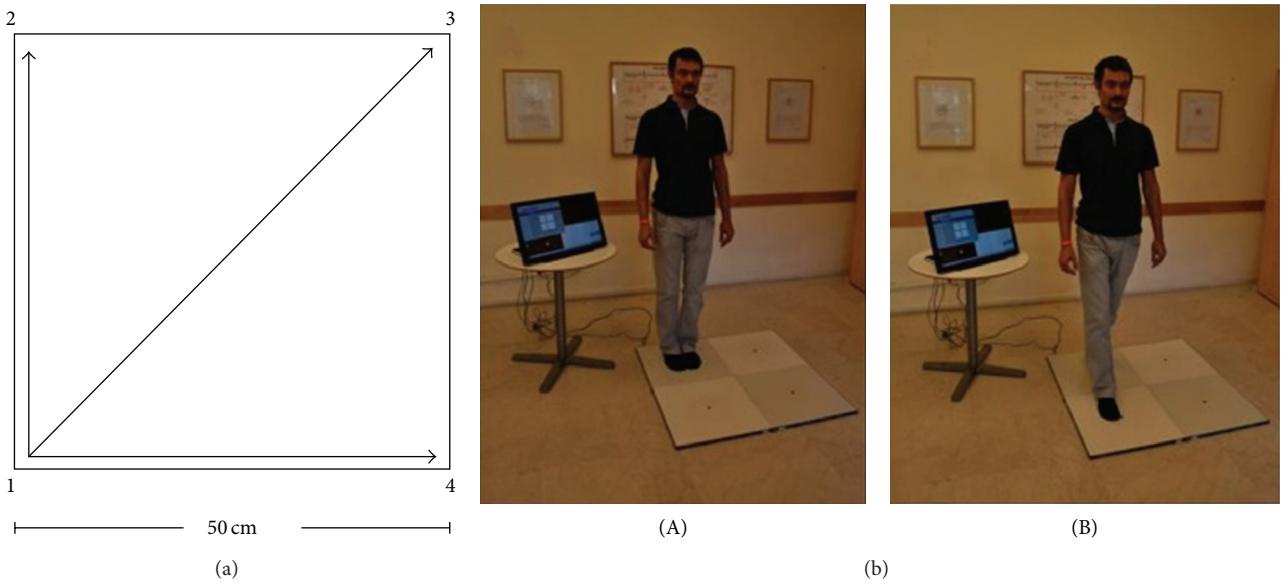

Figure 2: The Quadrato Motor Training (QMT). (a) A graphical illustration of the QMT. (b) A participant during the QMT while waiting for the next instruction (A) and following the instruction (B). Adapted from [64].

decreased frontal alpha power, providing initial support to arrows 2 and 4 in Figure 4, supporting the suggested link between training-induced alterations in alpha power and information processing. Importantly, increased frontal alpha coherence was significantly correlated with enhanced ideational flexibility, providing initial support to arrow 3 in Figure 4, supporting the suggested link between increased functional connectivity in the alpha range and enhanced creativity [65]. See Figure 3(a).

2.1.2. Spatial Performance, Reflectivity, and Electrophysiology. Another study examined the possible effect of QMT on spatial cognition and reflectivity, employing the Hidden Figures Test (HFT) [78]. HFT required locating a simple figure embedded within a complex figure. Spatial performance was measured by correct answers, whereas reflectivity, namely, the ability to exercise introspection by examining one's conscious thoughts and feelings, resulting in the inhibition of habitual thought and behavior, was interpolated from correct answers and reaction time (for details, see [64]). In this study, the participants ($n = 24$, females) were randomly allocated to either QMT, SMT, or VT.

One session of QMT was found to significantly improve HFT performance, compared to SMT and VT groups, demonstrating that QMT improves HFT performance above the pre-post expected learning. This study generally showed that QMT induces enhanced reflectivity and spatial performance. However, the possible mediating mechanism was not investigated. Thus, in another study reported in the same article we examined both reflectivity and electrophysiology [64]. In this study, thirty-seven participants (20 males) were examined for gender-related differences. While QMT-induced reflectivity and spatial cognition was reported in both genders (Figure 3(b)), a gender-dependent difference in functional connectivity was observed: while theta (4–7 Hz) and alpha intrahemispheric coherence was enhanced in females, the opposite pattern was found in males. These results are consistent with the idea that neural efficiency in males is reflected in local cortical oscillations, whereas neural efficiency in females is manifested in the functional coupling of several brain areas, as assessed by EEG coherence [79]. In the next section, we will examine the long-term effects on anatomical connectivity and neurotrophic level. These will be further linked to cognitive changes found following QMT.

2.2. Long-Term QMT-Induced Effects. Next, we turned to investigate the direct involvement of the cerebellum in cognitive improvement. To this end, we used MEG, molecular signals and MRI, in conjunction with various cognitive tests, including reading and creativity. Here, we tested long-term effects: 1–3 months of daily QMT sessions, to enable training-induced brain functional and structural modulation and reorganization.

2.2.1. QMT-Induced Effects on Reading and Cerebellar Electrophysiology. Due to the important role of the cerebellum and cerebellar alpha power in voluntary action [8–10] and its involvement in language and reading [33, 34, 38], it was hypothesized that QMT will increase cerebellar alpha power, which would in turn serve to improve reading. Thus, in the next study, the potential interactions between sensorimotor and reading systems and the role of the cerebellum oscillatory activity as a mediator [75, 76] were explored [66]. QMT was completed for a period of one month, in order to test its efficacy in inducing local and long-distance alpha oscillations. MEG was used due to its ability to localize the source of signals stemming from the cerebellum, thus enabling a direct investigation of the cerebellar role in reading

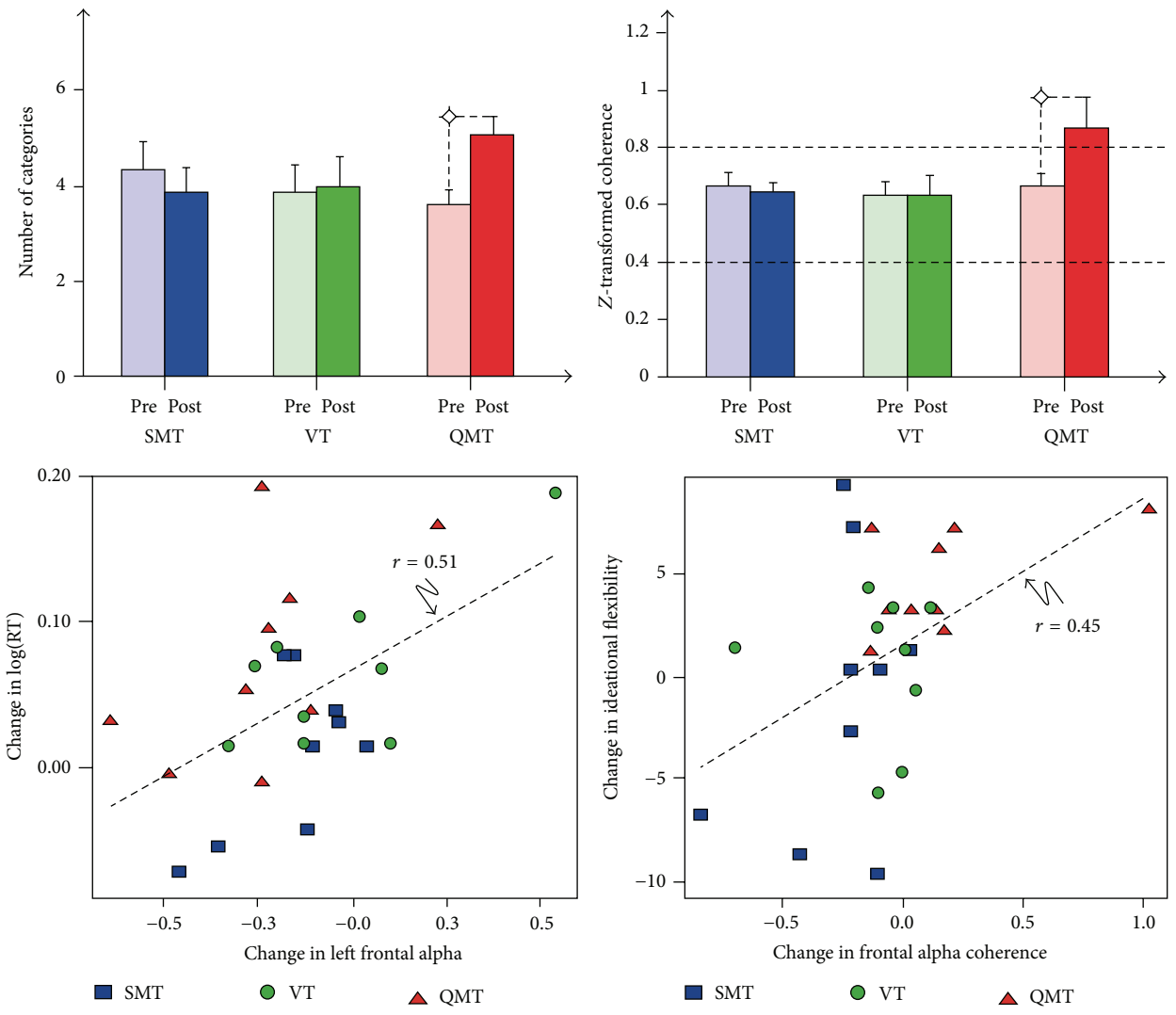

(a)

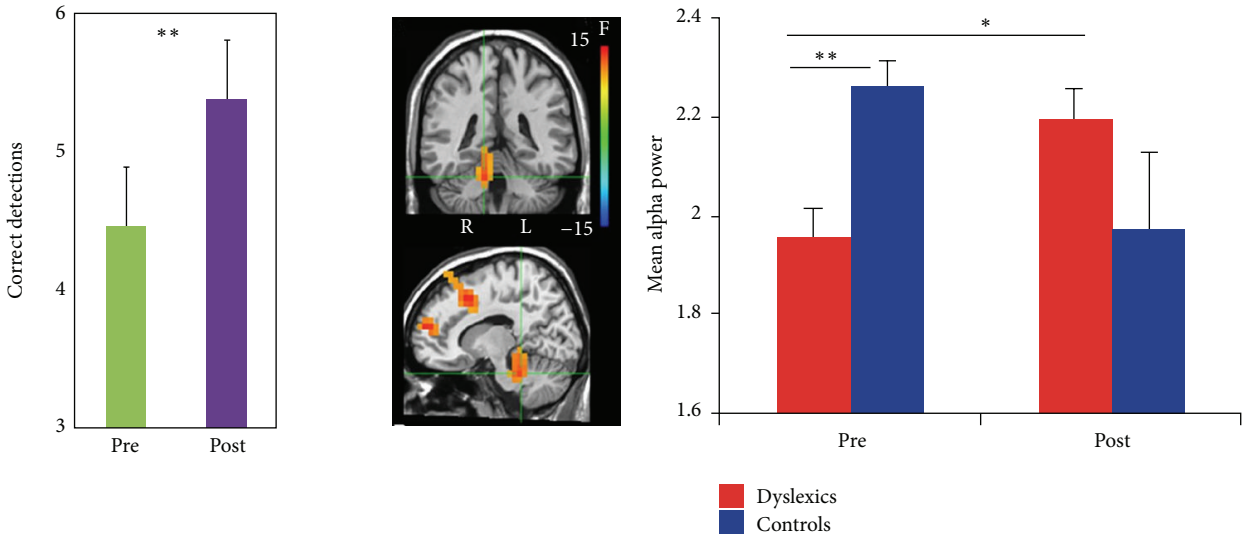

(b) (c)

Figure 3: Continued.

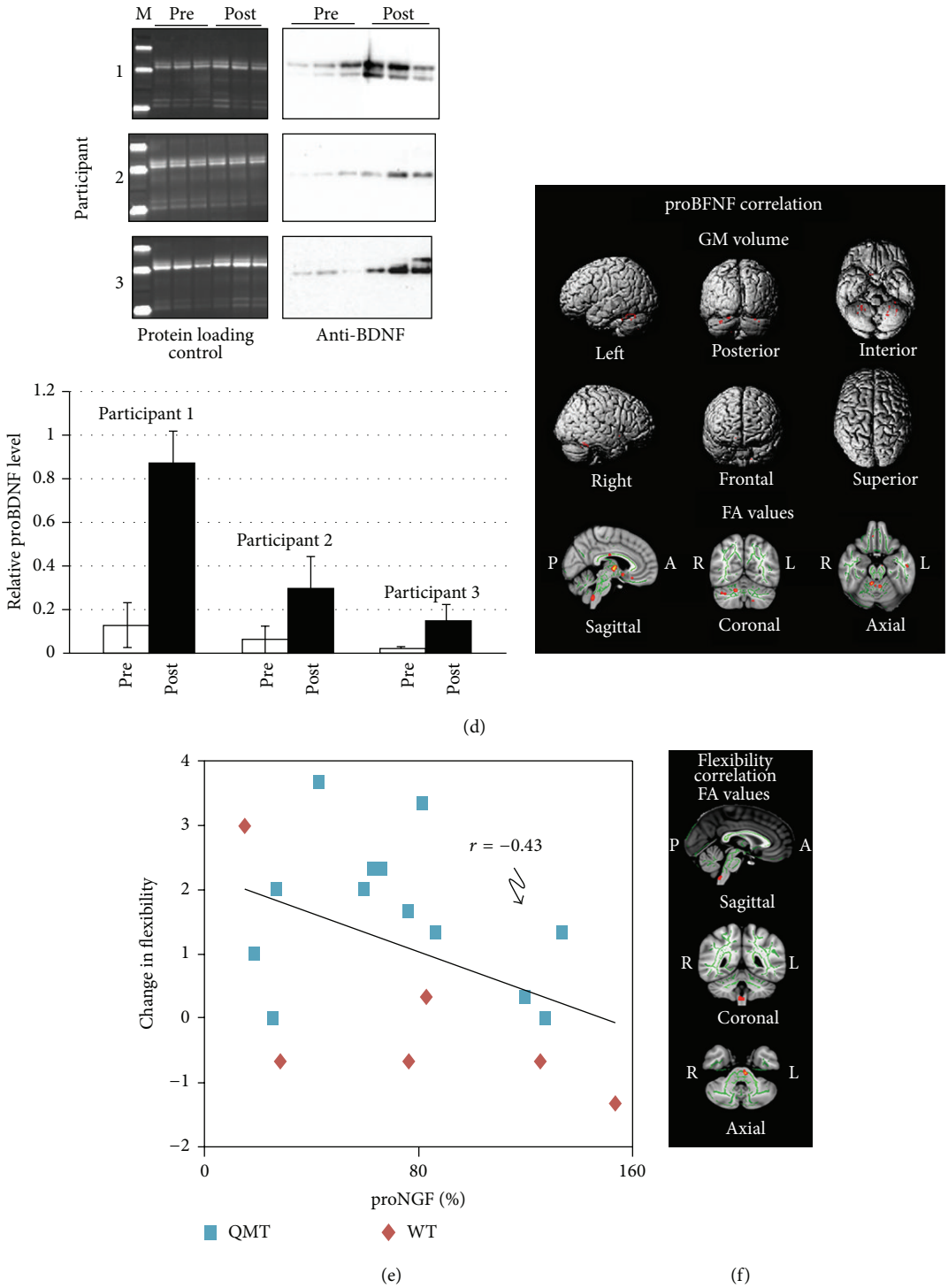

Figure 3: (a) Upper panel: change in ideational flexibility and z-transformed alpha coherence as a function of Group and Training ($^{*}p < 0.05$). Lower panel: correlation between change in frontal alpha activity and cognitive change following a session of QMT. Lower panel: correlations between change in frontal alpha power and log(RT) and frontal alpha coherence and ideational flexibility ($r = 0.51, 0.45$, $p < 0.01$, $n = 27$, resp.) [65]. (b) Spatial cognition. Pre-post difference in performance on the HFT task measured by the number of correct detections (mean ± SEM, $^{**}p < 0.005$) [64]. (c) Changes in alpha power. Left panel: significant clusters resulting from the group (dyslexics, controls) by training (pre, post) interaction. The focus point (green cross) is positioned in the right culmen. Right panel: the bar graph shows cerebellar alpha power as a function of Group and Training ($^{*}p = 0.01$; $^{**}p = 0.001$) [66]. (d) Changes in proBDNF and the cerebellum following 12 weeks of daily QMT practice. Left panel: Western blot analysis of proBDNF level. Histograms represent the average of the triplicate proBDNF values. Right panel: regions of GM volume and FA values positively correlated with proBDFN [67]. (e) Significant correlation between change in ideational flexibility and proNGF (beyond groups). Change in ideational flexibility, calculated by the subtraction of pre- from posttraining, was negatively correlated with the change in proNGF [68]. (f) Structural changes and creativity. A positive correlation ($p < 0.005$) between change in ideational flexibility and QMT-induced FA changes, mostly located in the middle cerebellar peduncles [69].

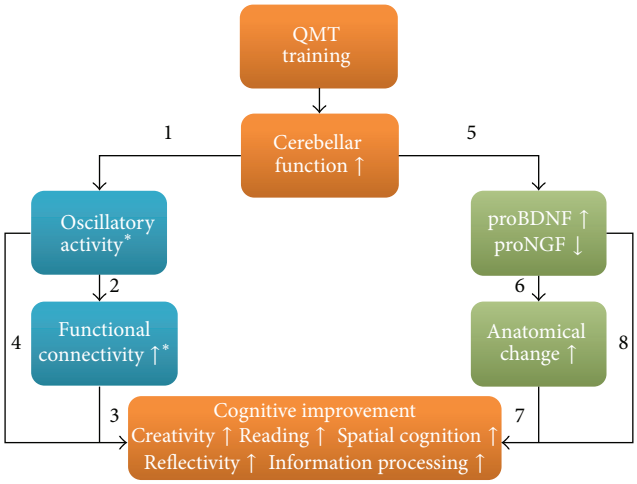

FIGURE 4: QMT-induced effects on cerebellar-cognition relationship. (∗) the alterations in the alpha activity and functional connectivity depending on population. While increased frontal and cerebellar alpha power were found in dyslexic adults following QMT [66], the opposite pattern, namely, decreased power, was observed in normal readers [64, 66]. In addition, while functional connectivity generally increased in females [64, 65] an opposite pattern was observed in males [64].

improvement. QMT-induced alterations in alpha power and coherence were examined in a group ($n = 12$) of adult dyslexics and matched controls ($n = 10$ normal readers) in addition to reading performance using a one-minute reading task.

The results demonstrate that one month of intensive QMT resulted in improved performance on the speeded reading task in both the dyslexic and control groups. See Figure 3(c). While the dyslexic group suffered from decreased cerebellar alpha power at baseline compared to the normal readers, they showed a significant increase in cerebellar oscillatory alpha power following a month of QMT training [66], located in the culmen, a region which has been previously reported to be related to language processing [33, 34]. As regards connectivity, interhemispheric alpha coherence was higher in the dyslexic group compared to the control group across both time points, suggesting that increased alpha coherence may reflect a compensation mechanism ([80]; and for additional details see [66]). These findings suggested that the combination of motor and language training embedded in QMT increases cerebellar oscillatory activity in dyslexics and improves reading performance in both groups. These results support the hypothesis that the cerebellum plays a role in skilled reading and begin to unravel the underlying mechanisms that mediate cerebellar contribution in cognitive and neuronal augmentation, supporting arrows 1 and 2 in Figure 4.

In addition, while there were no significant differences between the groups in these frontal areas prior to training, the healthy control group showed a significant decrease in alpha power in the left medial frontal gyrus (MFG), right superior frontal gyrus (SFG), and supplementary motor area (SMA) following 4 weeks of daily QMT. This is similar to the effects of a session of QMT [65]. On the other hand, the opposite pattern was observed in the dyslexic group in which alpha power increased in the right SFG.

2.2.2. QMT-Induced Effects on BDNF and Anatomy. As stated above, cerebellar changes are related to neurotrophic level, and specifically to BDNF [53, 54], reporting variations following training [58–62]. As the multidisciplinary studies combining the examination of training-induced neuronal and molecular changes in humans are scarce, the relationship between training-induced functional, anatomical, molecular, and cognitive change has yet to be established.

Consequently, in order to examine this relationship, proBDNF level was investigated following 3 months of daily QMT practice [67]. Briefly, a pilot MRI longitudinal study was conducted, which was designed to identify the possible link between anatomical and molecular effects of a long-term QMT. Structural high-resolution 3D T1-weighted (sMRI) and diffusion tensor imaging (DTI) data were acquired for three healthy female volunteers. For DTI, fractional anisotropy (FA) value, a marker of white matter (WM) integrity was used. Salivary BDNF was examined using Western blot analysis. The bands corresponding to proBDNF were quantified with Image Lab software and normalized to the most intense band visible on the membrane in the protein loading control. Following QMT, a significant GM volume increase in the cerebellum was found, especially in the culmen, which as stated has been previously reported to be related to language [33, 34], as well as in the right thalamus and limbic lobe. In addition, FA increases were mainly located in the corpus callosum, anterior thalamic radiations, corticospinal tracts, and cerebellar peduncles through which the cerebellum connects to the frontal cortex and other brain regions were reported. The correlation analysis revealed positive correlations between proBDNF values and GM and FA maps located in the cerebellum and cerebellar peduncle, respectively. See Figure 3(d).

This study, albeit exploratory in nature, provided important preliminary support to the relationship between sensorimotor training-induced anatomical and molecular changes (arrows 4 and 5 in Figure 4); it may shed light on the relationship between cerebellar activation and increased BDNF.

2.2.3. QMT-Induced Effects on NGF and Creativity. The previous study did not examine a direct or correlational relation between change in molecular and anatomical function with cognitive change. To study such a possible relationship between molecular and cognitive change, QMT-induced neurotrophic (NGF) change and creativity were examined following 4 weeks of daily training in two interrelated studies.

In the first study [68], the effects of motor training on NGF and creativity were measured, comparing QMT and walking training (WT) in healthy adults. Creativity was measured utilizing the AU task. In contrast with the WT, QMT resulted in increased creativity, emphasizing the importance of combining cognitive control with motor training. Importantly, the change in creativity negatively

correlated with the change in proNGF levels (see Figure 3(e)), supporting the negative relationship between neurotrophic factors and cognition (represented by arrow 8 in Figure 4).

In the second study, QMT-induced effects on creativity (measured by the Torrance Test of Creative Thinking (TTCT) task) and additional metacognitive functions were examined in children, using a nonintervention group as control. A total of twenty healthy children participated in this study. Following a month, 12 healthy children finished the training. Similar to the first study, a negative correlation of proNGF with QMT-induced creativity was found. Decreased proNGF further correlated with improved working memory updating and planning ability, as measured by the random number generation (RNG) and the Cognitive Assessment System (CAS) tasks, respectively. To sum up, creativity increased following a month of daily QMT practice, which further correlated with decreased proNGF level [68], supporting the negative relationship between proNGF and various cognitive functions, such as creativity [68] (arrow 6 in Figure 4).

A recent study demonstrated that increased creativity as measured by the AU task was correlated with increased cerebellar volume (under review). More specifically, a positive correlation was found between QMT-induced increased flexibility and GM increment in the right cerebellum (culmen) and the superior frontal gyrus (SFG). In addition, a positive correlation was found between increased flexibility and FA changes, mostly located in the middle cerebellar peduncles (Figure 3(f)), providing support for arrow 7 in Figure 4.

3. Summary and Conclusions

In our model, we propose a novel multimodal approach uniting training-induced electrophysiological changes, anatomical and neurotrophic changes, and suggest the cerebellar slow rhythm oscillations as the mediating mechanism allowing these effects to occur (Figure 4). Based on the literature, our model suggests that the importance of training-induced cerebellar changes for cognitive improvement may be based at least partly on two interrelated pathways the first being alterations in oscillatory activity, leading to changes in functional connectivity [35–37], and the second which takes longer periods to occur is mediated by neurotrophic factors, leading to anatomical changes [48].

While it has recently been suggested that sensorimotor training can result in neurotrophic-dependent changes in connectivity resulting in cognitive improvement [55, 56], the novelty of our current approach, presented in Figure 1, is in bringing forth a multimodal approach, linking cerebellum and cognition via electrophysiological fast occurring changes, anatomical and neurotrophic changes which require longer time to occur, and introduces cerebellar alpha oscillations as the mediating mechanism allowing these effects to occur. Together, although preliminary in their nature, the results presented in the current review support the hypothesis that sensorimotor training promotes alteration in cerebellar alpha oscillations which may mediate improved cognitive performance, such as enhanced creativity, faster information processing, reading, and reflectivity [64–66]. At the same time, sensorimotor training leads to anatomical and molecular changes, which are further supportive of cognitive change [67, 68].

In terms of functional connectivity, QMT practice increases inter- and intrahemispheric coherence in healthy adults [65]. Similar to studies demonstrating that frontal EEG coherence during tasks appears to be associated with improved cognitive functioning and creativity [81, 82], increased QMT-induced frontal connectivity is related to enhanced ideational flexibility [65]. Long-term QMT practice appears to further increase structural connectivity and cerebellar volume and altered cerebellar alpha activity [66]. QMT-induced anatomical changes in the cerebellum are correlated with increased BDNF level [67]. In turn, molecular change, especially proNGF decrease, is correlated with QMT-induced cognitive improvement in both children and adults [68]. Together, these findings support our proposition that cerebellar alpha oscillations may be the electrophysiological mechanism mediating neurotrophic-dependent connectivity changes resulting from sensorimotor training.

The current results are in line with previous studies demonstrating the relationship between healthy development, cerebellar activity, and BDNF [53, 54]. The cerebellum is known to be related to interoceptive accuracy reflecting explicit awareness of bodily processes [83]. Similar to the cerebellum, BDNF has also been associated with interoceptive awareness [84]. In fact, in parallel to suffering from deficient interceptive and motor awareness, Alzheimer's patients suffer from alterations in BDNF [85, 86].

The current QMT-related results found in healthy participants demonstrate increased amounts of proBDNF following 3 months of daily QMT practice [67], in addition to decreased proNGF following the training [68]. These results appear to be symmetrical to the ones conducted on the dementia patients [85–88], supporting previous claims for the inverse directionality of change in BDNF and proNGF following training [89]. Although limited indication is available on the influence of sensorimotor training paradigms on neurotrophin levels in the cerebellum, molecular change as measured by salivary proBDNF and proNG may serve an important cost-efficient benchmarks to help guide future research on the effects and the efficacy of different sensorimotor practices in both children and adults.

An important point that is raised from the reviewed studies is that Simple Motor Training which does not include a cognitive attention element could not induce such effects on creativity, as shown for the SMT group in one study [65] and by the walking training group in another study [68]. This indicates that the involvement of an attention-demanding task is necessary in order to induce these effects [65, 68]. Even though this still has to be verified, we hypothesize that such QMT effect on attention is still mediated through the cerebellum, which may in turn be affecting executive frontal regions [16]. This claim is partly supported by the fact that QMT resulted in similar changes in alpha power in both the cerebellum and frontal areas in healthy adults [66].

Undoubtedly, the model presented here is very preliminary, and much future research is required in order to sufficiently validate all its facets. However, it provides a

framework for future research and raises many scientifically testable predictions, important for guiding future directions.

4. Future Directions

The cerebellar deficits in development disorders may well explain the fact that, in a range of developmental disorders, such as ADHD, dyslexia, and autism, in parallel to the cognitive deficits, children suffer from deficient motor function and sensorimotor symptoms, thus having a higher probability of developing psychopathology [71, 72].

Since sensorimotor deficits are often observed in different developmental disorders, some researchers attributed their cognitive and motor deficiencies to abnormal development and functioning of the cerebellum [33–54]. In parallel to the cognitive deficits, both patients with different developmental disorders as well as neurodegeneration disease suffer from deficient sensorimotor function and emotional challenges [71, 72, 90] emphasizing the importance of efficient sensorimotor training paradigms for means of possible treatment. The examination of training-induced changes in functional and structural connectivity together with molecular change and their relations to cognition could greatly benefit from further studies in healthy and disabled populations. In order to verify whether cerebellar alpha oscillations are the underlying electrophysiological mechanism mediating change in cerebellar size, a combination of MRI and EEG should be implemented.

Conflict of Interests

The authors declare that there is no conflict of interests regarding the publication of this paper.

References

[1] K. Doya, "Complementary roles of basal ganglia and cerebellum in learning and motor control," *Current Opinion in Neurobiology*, vol. 10, no. 6, pp. 732–739, 2000.

[2] M. Kawato, "Internal models for motor control and trajectory planning," *Current Opinion in Neurobiology*, vol. 9, no. 6, pp. 718–727, 1999.

[3] V. B. Brooks, *The Neural Basis of Motor Control*, Oxford University Press, Cambridge, Mass, USA, 1986.

[4] M. Manto, J. M. Bower, A. B. Conforto et al., "Consensus paper: roles of the cerebellum in motor control—the diversity of ideas on cerebellar involvement in movement," *The Cerebellum*, vol. 11, no. 2, pp. 457–487, 2012.

[5] J. D. Schmahmann and J. C. Sherman, "The cerebellar cognitive affective syndrome," *Brain*, vol. 121, no. 4, pp. 561–579, 1998.

[6] J. D. Schmahmann, "Disorders of the cerebellum: ataxia, dysmetria of thought, and the cerebellar cognitive affective syndrome," *The Journal of Neuropsychiatry and Clinical Neurosciences*, vol. 16, no. 3, pp. 367–378, 2004.

[7] A. Diamond, "Close interrelation of motor development and cognitive development and of the cerebellum and prefrontal cortex," *Child Development*, vol. 71, no. 1, pp. 44–56, 2000.

[8] R. B. Ivry and S. W. Keele, "Timing functions of the cerebellum," *Journal of Cognitive Neuroscience*, vol. 1, no. 2, pp. 136–152, 1989.

[9] R. B. Ivry, R. M. Spencer, H. N. Zelaznik, and J. Diedrichsen, "The cerebellum and event timing," *Annals of the New York Academy of Sciences*, vol. 978, no. 1, pp. 302–317, 2002.

[10] C. D. Tesche and J. J. T. Karhu, "Anticipatory cerebellar responses during somatosensory omission in man," *Human Brain Mapping*, vol. 9, no. 3, pp. 119–142, 2000.

[11] B. K. Hölzel, J. Carmody, M. Vangel et al., "Mindfulness practice leads to increases in regional brain gray matter density," *Psychiatry Research: Neuroimaging*, vol. 191, no. 1, pp. 36–43, 2011.

[12] R. L. Buckner, "The cerebellum and cognitive function: 25 years of insight from anatomy and neuroimaging," *Neuron*, vol. 80, no. 3, pp. 807–815, 2013.

[13] S. P. Swinnen, "Intermanual coordination: from behavioural principles to neural-network interactions," *Nature Reviews. Neuroscience*, vol. 3, no. 5, pp. 348–359, 2002.

[14] C. I. de Zeeuw, F. E. Hoebeek, L. W. J. Bosman, M. Schonewille, L. Witter, and S. K. Koekkoek, "Spatiotemporal firing patterns in the cerebellum," *Nature Reviews Neuroscience*, vol. 12, no. 6, pp. 327–344, 2011.

[15] F. G. Andres, T. Mima, A. E. Schulman, J. Dichgans, M. Hallett, and C. Gerloff, "Functional coupling of human cortical sensorimotor areas during bimanual skill acquisition," *Brain*, vol. 122, no. 5, pp. 855–870, 1999.

[16] T. C. Watson, N. Becker, R. Apps, and M. W. Jones, "Back to front: cerebellar connections and interactions with the prefrontal cortex," *Frontiers in Systems Neuroscience*, vol. 8, no. 1, article 4, 11 pages, 2014.

[17] R. A. Chávez-Eakle, A. Graff-Guerrero, J.-C. García-Reyna, V. Vaugier, and C. Cruz-Fuentes, "Cerebral blood flow associated with creative performance: a comparative study," *NeuroImage*, vol. 38, no. 3, pp. 519–528, 2007.

[18] L. R. Vandervert, "Cognitive functions of the cerebellum explain how Ericsson's deliberate practice produces giftedness," *High Ability Studies*, vol. 18, no. 1, pp. 89–92, 2007.

[19] L. R. Vandervert, P. H. Schimpf, and H. Liu, "How working memory and the cerebellum collaborate to produce creativity and innovation," *Creativity Research Journal*, vol. 19, no. 1, pp. 1–18, 2007.

[20] H. Wilms, J. Sievers, and G. Deuschl, "Animal models of tremor," *Movement Disorders*, vol. 14, no. 4, pp. 557–571, 1999.

[21] F. Foti, D. Laricchiuta, D. Cutuli et al., "Exposure to an enriched environment accelerates recovery from cerebellar lesion," *The Cerebellum*, vol. 10, no. 1, pp. 104–119, 2011.

[22] D. P. Holschneider, J. Yang, Y. Guo, and J.-M. I. Maarek, "Reorganization of functional brain maps after exercise training: importance of cerebellar-thalamic-cortical pathway," *Brain Research*, vol. 1184, no. 1, pp. 96–107, 2007.

[23] W. Grodd, E. Hülsmann, M. Lotze, D. Wildgruber, and M. Erb, "Sensorimotor mapping of the human cerebellum: fMRI evidence of somatotopic organization," *Human Brain Mapping*, vol. 13, no. 2, pp. 55–73, 2001.

[24] J. E. Desmond, J. D. E. Gabrieli, A. D. Wagner, B. L. Ginier, and G. H. Glover, "Lobular patterns of cerebellar activation in verbal working-memory and finger-tapping tasks as revealed by functional MRI," *The Journal of Neuroscience*, vol. 17, no. 24, pp. 9675–9685, 1997.

[25] M. P. Kirschen, S. H. A. Chen, P. Schraedley-Desmond, and J. E. Desmond, "Load- and practice-dependent increases in cerebro-cerebellar activation in verbal working memory: an fMRI study," *NeuroImage*, vol. 24, no. 2, pp. 462–472, 2005.

[26] S. H. A. Chen and J. E. Desmond, "Cerebrocerebellar networks during articulatory rehearsal and verbal working memory tasks," *NeuroImage*, vol. 24, no. 2, pp. 332–338, 2005.

[27] H. Park, E. Kang, H. Kang et al., "Cross-frequency power correlations reveal the right superior temporal gyrus as a hub region during working memory maintenance," *Brain Connectivity*, vol. 1, no. 6, pp. 460–472, 2011.

[28] J. Wikgren, M. S. Nokia, and M. Penttonen, "Hippocampo-cerebellar theta band phase synchrony in rabbits," *Neuroscience*, vol. 165, no. 4, pp. 1538–1545, 2010.

[29] M. S. Nokia, H. M. Sisti, M. R. Choksi, and T. J. Shors, "Learning to learn: theta oscillations predict new learning, which enhances related learning and neurogenesis," *PLoS ONE*, vol. 7, no. 2, Article ID e31375, 2012.

[30] G. P. Dugué, N. Brunel, V. Hakim et al., "Electrical coupling mediates tunable low-frequency oscillations and resonance in the cerebellar Golgi cell network," *Neuron*, vol. 61, no. 1, pp. 126–139, 2009.

[31] M. J. Hartmann and J. M. Bower, "Oscillatory activity in the cerebellar hemispheres of unrestrained rats," *Journal of Neurophysiology*, vol. 80, no. 3, pp. 1598–1604, 1998.

[32] T. Martin, J. M. Houck, J. P. Bish et al., "MEG reveals different contributions of somatomotor cortex and cerebellum to simple reaction time after temporally structured cues," *Human Brain Mapping*, vol. 27, no. 7, pp. 552–561, 2006.

[33] C. Pernet, J. Andersson, E. Paulesu, and J. F. Demonet, "When all hypotheses are right: a multifocal account of dyslexia," *Human Brain Mapping*, vol. 30, no. 7, pp. 2278–2292, 2009.

[34] C. R. Pernet, J. B. Poline, J. F. Demonet, and G. A. Rousselet, "Brain classification reveals the right cerebellum as the best biomarker of dyslexia," *BMC Neuroscience*, vol. 10, article 67, 2009.

[35] R. B. Silberstein, F. Danieli, and P. L. Nunez, "Fronto-parietal evoked potential synchronization is increased during mental rotation," *NeuroReport*, vol. 14, no. 1, pp. 67–71, 2003.

[36] S. Palva and J. M. Palva, "New vistas for alpha-frequency band oscillations," *Trends in Neurosciences*, vol. 30, no. 4, pp. 150–158, 2007.

[37] J. M. Palva, S. Monto, S. Kulashekhar, and S. Palva, "Neuronal synchrony reveals working memory networks and predicts individual memory capacity," *Proceedings of the National Academy of Sciences of the United States of America*, vol. 107, no. 16, pp. 7580–7585, 2010.

[38] J. Kujala, K. Pammer, P. Cornelissen, A. Roebroeck, E. Formisano, and R. Salmelin, "Phase coupling in a cerebro-cerebellar network at 8–13 Hz during reading," *Cerebral Cortex*, vol. 17, no. 6, pp. 1476–1485, 2007.

[39] A. Fink, B. Graif, and A. C. Neubauer, "Brain correlates underlying creative thinking: EEG alpha activity in professional vs. novice dancers," *NeuroImage*, vol. 46, no. 3, pp. 854–862, 2009.

[40] A. Dietrich, "Transient hypofrontality as a mechanism for the psychological effects of exercise," *Psychiatry Research*, vol. 145, no. 1, pp. 79–83, 2006.

[41] S. Cohen-Cory, A. H. Kidane, N. J. Shirkey, and S. Marshak, "Brain-derived neurotrophic factor and the development of structural neuronal connectivity," *Developmental Neurobiology*, vol. 70, no. 5, pp. 271–288, 2010.

[42] B. Lu, P. T. Pang, and N. H. Woo, "The yin and yang of neurotrophin action," *Nature Reviews Neuroscience*, vol. 6, no. 8, pp. 603–614, 2005.

[43] J. M. Conner, K. M. Franks, A. K. Titterness et al., "NGF is essential for hippocampal plasticity and learning," *The Journal of Neuroscience*, vol. 29, no. 35, pp. 10883–10889, 2009.

[44] R. J. Mandel, F. H. Gage, and L. J. Thal, "Spatial learning in rats: correlation with cortical choline acetyltransferase and improvement with NGF following NBM damage," *Experimental Neurology*, vol. 104, no. 3, pp. 208–217, 1989.

[45] F. Angelucci, P. De Bartolo, F. Gelfo et al., "Increased concentrations of nerve growth factor and brain-derived neurotrophic factor in the rat cerebellum after exposure to environmental enrichment," *The Cerebellum*, vol. 8, no. 4, pp. 499–506, 2009.

[46] B. Fritsch, J. Reis, K. Martinowich et al., "Direct current stimulation promotes BDNF-dependent synaptic plasticity: potential implications for motor learning," *Neuron*, vol. 66, no. 2, pp. 198–204, 2010.

[47] R. A. Y. A. Al-Shawi, A. Hafner, S. Chun et al., "ProNGF, sortilin, and age-related neurodegeneration," *Annals of the New York Academy of Sciences*, vol. 1119, no. 1, pp. 208–215, 2007.

[48] C. W. Cotman and N. C. Berchtold, "Exercise: a behavioral intervention to enhance brain health and plasticity," *Trends in Neurosciences*, vol. 25, no. 6, pp. 295–301, 2002.

[49] J. M. Gatt, S. A. Kuan, C. Dobson-Stone et al., "Association between BDNF Val66Met polymorphism and trait depression is mediated via resting EEG alpha band activity," *Biological Psychology*, vol. 79, no. 2, pp. 275–284, 2008.

[50] M. E. Morrison and C. A. Mason, "Granule neuron regulation of Purkinje cell development: striking a balance between neurotrophin and glutamate signaling," *The Journal of Neuroscience*, vol. 18, no. 10, pp. 3563–3573, 1998.

[51] S. A. Neeper, F. Gómez-Pinilla, J. Choi, and C. W. Cotman, "Physical activity increases mRNA for brain-derived neurotrophic factor and nerve growth factor in rat brain," *Brain Research*, vol. 726, no. 1-2, pp. 49–56, 1996.

[52] J. Scholz, M. C. Klein, T. E. J. Behrens, and H. Johansen-Berg, "Training induces changes in white-matter architecture," *Nature Neuroscience*, vol. 12, no. 11, pp. 1370–1371, 2009.

[53] P. Ernfors, K. F. Lee, and R. Jaenisch, "Mice lacking brain-derived neurotrophic factor develop with sensory deficits," *Nature*, vol. 368, no. 6467, pp. 147–150, 1994.

[54] P. M. Schwartz, P. R. Borghesani, R. L. Levy, S. L. Pomeroy, and R. A. Segal, "Abnormal cerebellar development and foliation in $BDNF^{-/-}$ mice reveals a role for neurotrophins in CNS patterning," *Neuron*, vol. 19, no. 2, pp. 269–281, 1997.

[55] M. W. Voss, R. S. Prakash, K. I. Erickson et al., "Plasticity of brain networks in a randomized intervention trial of exercise training in older adults," *Frontiers in Aging Neuroscience*, vol. 2, no. 1, Article ID Article 32, p. 17, 2010.

[56] M. W. Voss, K. I. Erickson, R. S. Prakash et al., "Neurobiological markers of exercise-related brain plasticity in older adults," *Brain, Behavior, and Immunity*, vol. 28, pp. 90–99, 2013.

[57] J. B. Crabbe and R. K. Dishman, "Brain electrocortical activity during and after exercise: a quantitative synthesis," *Psychophysiology*, vol. 41, no. 4, pp. 563–574, 2004.

[58] M. Bose, P. Muñoz-Llancao, S. Roychowdhury et al., "Effect of the environment on the dendritic morphology of the rat auditory cortex," *Synapse*, vol. 64, no. 2, pp. 97–110, 2010.

[59] L. Macgillivray, K. B. Reynolds, P. I. Rosebush, and M. F. Mazurek, "The comparative effects of environmental enrichment with exercise and serotonin transporter blockade on serotonergic neurons in the dorsal raphe nucleus," *Synapse*, vol. 66, no. 5, pp. 465–470, 2012.

[60] J.-L. Yang, Y.-T. Lin, P.-C. Chuang, V. A. Bohr, and M. P. Mattson, "BDNF and exercise enhance neuronal DNA repair by stimulating CREB-mediated production of apurinic/apyrimidinic endonuclease 1," *NeuroMolecular Medicine*, vol. 16, no. 1, pp. 161–174, 2014.

[61] M. Carbon, M. Argyelan, C. Habeck et al., "Increased sensorimotor network activity in DYT1 dystonia: a functional imaging study," *Brain*, vol. 133, no. 3, pp. 690–700, 2010.

[62] M. Carbon, P. B. Kingsley, C. Tang, S. Bressman, and D. Eidelberg, "Microstructural white matter changes in primary torsion dystonia," *Movement Disorders*, vol. 23, no. 2, pp. 234–239, 2008.

[63] D. J. L. G. Schutter and J. van Honk, "An electrophysiological link between the cerebellum, cognition and emotion: frontal theta EEG activity to single-pulse cerebellar TMS," *NeuroImage*, vol. 33, no. 4, pp. 1227–1231, 2006.

[64] T. D. Ben-Soussan, A. Berkovich-Ohana, J. Glicksohn, and A. Goldstein, "A suspended act: increased reflectivity and gender-dependent electrophysiological change following Quadrato Motor Training," *Frontiers in Psychology*, vol. 5, article 55, 2014.

[65] T. D. Ben-Soussan, J. Glicksohn, A. Goldstein, A. Berkovich-Ohana, and O. Donchin, "Into the square and out of the box: the effects of Quadrato Motor Training on creativity and alpha coherence," *PLoS ONE*, vol. 8, no. 1, Article ID e55023, 2013.

[66] T. D. Ben-Soussan, K. Avirame, J. Glicksohn, A. Goldstein, Y. Harpaz, and M. Ben-Shachar, "Changes in cerebellar activity and inter-hemispheric coherence accompany improved reading performance following Quadrato Motor Training," *Frontiers in Systems Neuroscience*, vol. 8, article 81, 2014.

[67] T. D. Ben-Soussan, C. Piervincenzi, S. Venditti, L. Verdone, M. Caserta, and F. Carducci, "Increased cerebellar volume and BDNF level following quadrato motor training," *Synapse*, vol. 69, no. 1, pp. 1–6, 2015.

[68] S. Venditti, L. Verdone, C. Pesce, T. Tocci, M. Caserta, and T. D. Ben-Soussan, "Creating well-being: increased creativity and proNGF decrease following quadrato motor training," *BioMed Research International*. In press.

[69] T. D. Ben-Soussan, A. Berkovich-Ohana, C. Piervincenzi, J. Glicksohn, and F. Carducci, "Interoception-related neuroplasticity and increased creativity following quadrato motor training," Under review.

[70] T. D. Ben-Soussan and P. Paoletti, "Plasticity in the Square—from a philosophical model to neurocognitive applications," in *Proceedings of the World Congress on the Square of Oppositions*, J.-Y. Béziau and K. Gan-Krzywoszyńska, Eds., pp. 21–22, Pontifical Lateran University, Vatican City, 2014.

[71] H. Yamaguchi, S. Hirai, M. Morimatsu, M. Shoji, and Y. Nakazato, "Diffuse type of senile plaques in the cerebellum of Alzheimer-type dementia demonstrated by β protein immunostain," *Acta Neuropathologica*, vol. 77, no. 3, pp. 314–319, 1989.

[72] N. Levit-Binnun, M. Davidovitch, and Y. Golland, "Sensory and motor secondary symptoms as indicators of brain vulnerability," *Journal of Neurodevelopmental Disorders*, vol. 5, article 26, 2013.

[73] N. Levit-Binnun and Y. Golland, "Finding behavioral and network indicators of brain vulnerability," *Frontiers in Human Neuroscience*, vol. 6, no. 1, article 10, 9 pages, 2012.

[74] E. Courchesne, J. Townsend, N. A. Akshoomoff et al., "Impairment in shifting attention in autistic and cerebellar patients," *Behavioral Neuroscience*, vol. 108, no. 5, pp. 848–865, 1994.

[75] U. Goswami, "A temporal sampling framework for developmental dyslexia," *Trends in Cognitive Sciences*, vol. 15, no. 1, pp. 3–10, 2011.

[76] H. T. Hunt, "'Dark Nights of the Soul': phenomenology and neurocognition of spiritual suffering in mysticism and psychosis," *Review of General Psychology*, vol. 11, no. 3, pp. 209–234, 2007.

[77] M. M. Pangelinan, F. A. Kagerer, B. Momen, B. D. Hatfield, and J. E. Clark, "Electrocortical dynamics reflect age-related differences in movement kinematics among children and adults," *Cerebral Cortex*, vol. 21, no. 4, pp. 737–747, 2011.

[78] J. Glicksohn and Z. Kinberg, "Performance on embedded figures tests: profiling individual differences," *Journal of Individual Differences*, vol. 30, no. 3, pp. 152–162, 2009.

[79] A. C. Neubauer and A. Fink, "Fluid intelligence and neural efficiency: effects of task complexity and sex," *Personality and Individual Differences*, vol. 35, no. 4, pp. 811–827, 2003.

[80] M. Arns, S. Peters, R. Breteler, and L. Verhoeven, "Different brain activation patterns in dyslexic children: evidence from EEG power and coherence patterns for the double-deficit theory of dyslexia," *Journal of Integrative Neuroscience*, vol. 6, no. 1, pp. 175–190, 2007.

[81] F. Travis and A. Arenander, "Cross-sectional and longitudinal study of effects of transcendental meditation practice on interhemispheric frontal asymmetry and frontal coherence," *International Journal of Neuroscience*, vol. 116, no. 12, pp. 1519–1538, 2006.

[82] R. Horan, "The relationship between creativity and intelligence: a combined yogic-scientific approach," *Creativity Research Journal*, vol. 19, no. 2-3, pp. 179–202, 2007.

[83] H. D. Critchley, S. Wiens, P. Rotshtein, A. Öhman, and R. J. Dolan, "Neural systems supporting interoceptive awareness," *Nature Neuroscience*, vol. 7, no. 2, pp. 189–195, 2004.

[84] J. M. Mercader, F. Fernández-Aranda, M. Gratacòs et al., "Correlation of BDNF blood levels with interoceptive awareness and maturity fears in anorexia and bulimia nervosa patients," *Journal of Neural Transmission*, vol. 117, no. 4, pp. 505–512, 2010.

[85] E. J. Dhurandhar, D. B. Allison, T. van Groen, and I. Kadish, "Hunger in the absence of caloric restriction improves cognition and attenuates Alzheimer's disease pathology in a mouse model," *PLoS ONE*, vol. 8, no. 4, Article ID e60437, 2013.

[86] C. Xu, Z. Wang, M. Fan et al., "Effects of BDNF val66met polymorphism on brain metabolism in Alzheimer's disease," *NeuroReport*, vol. 21, no. 12, pp. 802–807, 2010.

[87] S. Peng, J. Wuu, E. J. Mufson, and M. Fahnestock, "Increased proNGF levels in subjects with mild cognitive impairment and mild Alzheimer disease," *Journal of Neuropathology and Experimental Neurology*, vol. 63, no. 6, pp. 641–649, 2004.

[88] M. Fahnestock, B. Michalski, B. Xu, and M. D. Coughlin, "The precursor pro-nerve growth factor is the predominant form of nerve growth factor in brain and is increased in Alzheimer's disease," *Molecular and Cellular Neuroscience*, vol. 18, no. 2, pp. 210–220, 2001.

[89] F. Angelucci, E. Ricci, L. Padua, A. Sabino, and P. A. Tonali, "Music exposure differentially alters the levels of brain-derived neurotrophic factor and nerve growth factor in the mouse hypothalamus," *Neuroscience Letters*, vol. 429, no. 2-3, pp. 152–155, 2007.

[90] C. Pesce and T. D. Ben-Soussan, "'Cogito ergo sum' or 'ambulo ergo sum'? New perspectives in developmental exercise and cognition research," in *Exercise-Cognition Interaction: Neuroscience Perspectives*, T. McMorris, Ed., Elsevier, New York, NY, USA, 2014.

Hindawi Publishing Corporation
BioMed Research International
Volume 2015, Article ID 248724, 11 pages
http://dx.doi.org/10.1155/2015/248724

Research Article

FC-NIRS: A Functional Connectivity Analysis Tool for Near-Infrared Spectroscopy Data

Jingping Xu,[1,2] Xiangyu Liu,[3] Jinrui Zhang,[4] Zhen Li,[1,2] Xindi Wang,[1,2] Fang Fang,[5,6,7,8] and Haijing Niu[1,2]

[1] *State Key Laboratory of Cognitive Neuroscience and Learning and IDG/McGovern Institute for Brain Research, Beijing Normal University, Beijing 100875, China*
[2] *Center for Collaboration and Innovation in Brain and Learning Sciences, Beijing Normal University, Beijing 100875, China*
[3] *Department of Neurology, Jilin Oil Field General Hospital, Jilin 138000, China*
[4] *Circulating Department of Internal Medicine, Jilin Oil field General Hospital, Jilin 138000, China*
[5] *Department of Psychology and Beijing Key Laboratory of Behavior and Mental Health, Peking University, Beijing 100871, China*
[6] *Key Laboratory of Machine Perception, Ministry of Education, Peking University, Beijing 100871, China*
[7] *Peking-Tsinghua Center for Life Sciences, Peking University, Beijing 100871, China*
[8] *PKU-IDG/McGovern Institute for Brain Research, Peking University, Beijing 100871, China*

Correspondence should be addressed to Haijing Niu; niuhjing@bnu.edu.cn

Received 27 March 2015; Accepted 18 June 2015

Academic Editor: Roberto Sotero

Functional near-infrared spectroscopy (fNIRS), a promising noninvasive imaging technique, has recently become an increasingly popular tool in resting-state brain functional connectivity (FC) studies. However, the corresponding software packages for FC analysis are still lacking. To facilitate fNIRS-based human functional connectome studies, we developed a MATLAB software package called "functional connectivity analysis tool for near-infrared spectroscopy data" (FC-NIRS). This package includes the main functions of fNIRS data preprocessing, quality control, FC calculation, and network analysis. Because this software has a friendly graphical user interface (GUI), FC-NIRS allows researchers to perform data analysis in an easy, flexible, and quick way. Furthermore, FC-NIRS can accomplish batch processing during data processing and analysis, thereby greatly reducing the time cost of addressing a large number of datasets. Extensive experimental results using real human brain imaging confirm the viability of the toolbox. This novel toolbox is expected to substantially facilitate fNIRS-data-based human functional connectome studies.

1. Introduction

Functional near-infrared spectroscopy (fNIRS), a promising noninvasive imaging technique, has become an increasingly popular neuroimaging technique for brain function research in recent years [1–4]. This technique holds several advantages relative to functional magnetic resonance imaging (fMRI), namely, its instrument portability, high temporal sampling rate, and ability to perform long data acquisitions. Given the technique's specific strengths, fNIRS has been extensively used to localize brain activation during task states [5–10] and to identify functional connectivity (FC) during resting states in both normal and diseased populations [4].

For the study of resting-state fNIRS, one of its promising advances is the detection of resting-state FC [6, 11] and the characterization of the topological organization of the brain connectivity network [12]. The approaches of seed-based correlation analysis [6, 13, 14], whole-brain correlation analysis [15–17], and graph-theoretical topological analysis [12, 18] were primarily used to derive the resting-state FC and the brain network. Particularly, the seed correlation analysis calculates the resting-state FC by predefining a seed region and

subsequently computing the temporal correlation between it and other regions. With seed-based correlation analysis, researchers have observed a strong FC between the bilateral sensorimotor [11, 13], auditory [13], and visual system [19] in adults and connectivity changes during the normal development of early infancy [5, 15] and in neurological disorders [19, 20]. Similarly, whole-brain correlation analysis calculates resting-state FC by examining the temporal correlation of a time series between any two measurement regions in the whole-brain range. Using this approach, Homae et al. [15] found that the cerebral FC changed dynamically in infants from several days old to months old. Additionally, using this method, Zhang et al. [17] showed that the dominant frequency of FC within one functional system in adults can be identified by introducing a priori anatomical information. In contrast to the previous two methods, the graph-theoretical topological analysis models the brain as a complex network and then provides a straightforward but powerful mathematical framework for characterizing the topological properties of the brain networks. With the graph-theoretical network analysis approach, our group constructed the first whole-brain FC network using fNIRS brain data [12] and found that the fNIRS brain network was topologically organized in a nontrivial fashion, for example, with a small-world and modular architecture. Furthermore, our study [18] also showed that the graph theory metrics of the fNIRS brain network were reliable across different scanning sessions. In summary, this progress in FC and network analysis demonstrates the increasing interests in the study of functional brain connectivity and network organization using the fNIRS technique.

As an emerging analysis strategy for fNIRS data and considering the complexity of FC and network analysis, it is necessary and important to develop an easy-to-use and efficient FC toolbox to facilitate fNIRS researchers. There are already several available fNIRS toolkits, such as Homer [21], NIRS-SPM [22], fOSA [23], NINPY [24], and NAP [25], which have greatly assisted with the preprocessing of fNIRS data and activation detection based on task data. However, it must be noted that toolkits for assessing the FC and network analysis of resting-state fNIRS data are still lacking.

In this study, to facilitate human functional connectome studies in the fNIRS field, we developed a MATLAB software package for fNIRS-based connectivity analysis, which is called FC-NIRS (functional connectivity analysis for near-infrared spectroscopy data) and can be downloaded freely from the website http://www.nitrc.org/projects/fcnirs/ as an open-source package. The package's functions include preprocessing, quality control, FC calculation, and network analysis. Although the fNIRS collection has a chainless feature, it also easily leads to motion-head artifacts. At the same time, there are usually many sources and detectors placed on the head that are used for a whole-brain network study, which thus inevitably lead to a loss of contact between certain optodes and the scalp. Therefore, the two primary types of noise (i.e., motion artifacts [26, 27] and a low signal-to-noise ratio due to poor contact between the optodes and scalp [24]) need to be checked before performing FC and network analysis.

2. Materials and Methods

2.1. Toolbox Development

2.1.1. Development Environment. FC-NIRS was developed using MATLAB 2010b in a 64-bit Windows 7 environment. The data preprocessing and network analysis modules include two established packages, Hemodynamic Evoked Response (Homer) and Graph-Theoretical Network Analysis (Gretna), for fNIRS data processing and graph theory-based network analysis, respectively. This FC-NIRS toolbox has been successfully tested under different operating systems with MATLAB installed, such as Windows and Linux (Ubuntu and CentOS).

2.1.2. Data Format. Currently, FC-NIRS can process two file types: one type is in the .nirs format from the CW5/6 system (TechEn, Inc.) and the other type is in the .csv format from ETG4000/7000 (Hitachi Inc.). In fact, the .csv files can be easily transformed into.nirs files. Thus, in the following description, we mainly introduce the parameters that were included in .nirs files. (1) d: this variable was the actual raw data that were variable. This variable had the dimensions of ⟨number of measurements⟩×⟨number of time points⟩. The rows in d were mapped by the measurement list (the mL variable described below). The d variable could be complex (as in the case of sine-cosine demodulation for laser carrier frequencies). (2) t: this is a time variable describing the time length of the data collection. (3) SD: this variable was a structured variable that described the configuration of the probe (source-detector) geometry. Furthermore, during the stage of "processing," a ".proc" file could be brought out for each participant after clicking the "RUN" button. The ".proc" file was a MATLAB file with four fields: (1) RawData, which recorded the raw optical density information as in the .nirs file; (2) OD, which recorded optical density changes; (3) Conc, which recorded the time series of the relative concentration variations in oxyhemoglobin (HbO), deoxyhemoglobin (HbR), and the total hemoglobin (HbT); and (4) SD, which recorded the configurations of the sources, detectors, and measurement channels between the sources and detectors. The abundant information in the ".proc" file provided the convenience of processing batches for the subsequent FC calculation and network analysis in the toolbox.

2.1.3. FC-NIRS Analysis Procedure. The main procedure of FC-NIRS is shown in Figure 1, and it included four main function modules: (1) preprocessing, (2) quality control, (3) FC calculation, and (4) network analysis.

2.2. Preprocessing. FC-NIRS provides a series of preprocessing methods in the panel of "Preprocessing Methods" (Figure 3), from which some methods can be selected and displayed in the panel of "Selected Methods." Pressing the "≫" button selects a preprocessing method to the "Selected Methods" box, while pressing the "≪" button cancels the corresponding selected method. The "Up" and "Down" buttons were used to adjust the order of the selected methods. In the "input directory," the users need to set a directory in advance

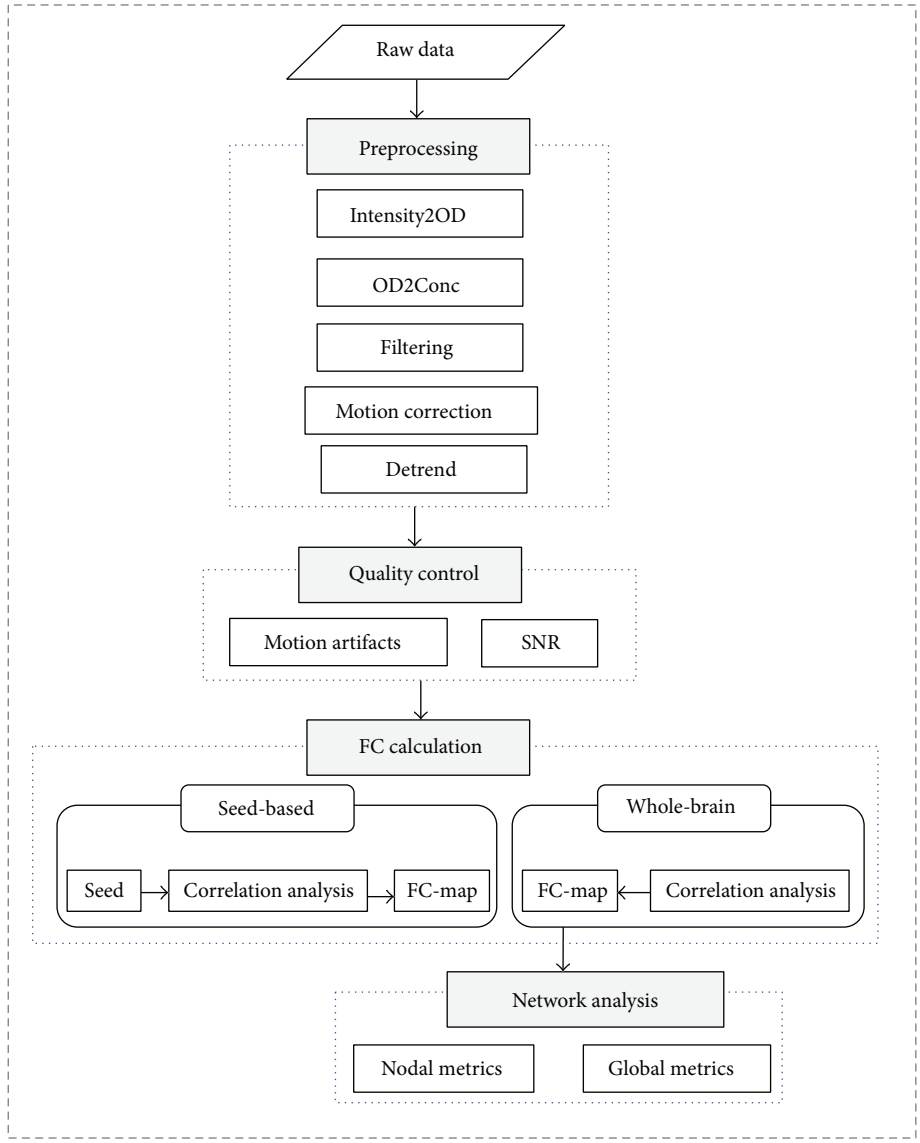

Figure 1: The main procedures for the processing of fNIRS datasets in FC-NIRS. The procedures contain four parts: (1) preprocessing, (2) quality control, (3) FC calculation, and (4) network analysis.

to read the raw data. Similarly, in the "out directory," the user also needs to provide an output directory to save the generated data. FC-NIRS also generated log files and kept track of the processing. After the operations and pressing the "RUN" button, FC-NIRS generated a ".proc" file for each subject in the output directory. For simplicity, FC-NIRS also provided some default preprocessing methods, which mainly included optical signal conversion, filtering, motion correction, and detrend. The details of the methods are as follows.

2.2.1. Optical Signal Conversion. Similar to Homer software [21], the raw optical intensity was first normalized as the optical density (OD) to provide a relative (percent) concentration change by dividing by the mean of the intensity. Then, the OD data were further converted to HbO, HbR, and HbT based on the modified Beer-Lambert law [28].

2.2.2. Filtering. FC-NIRS uses a band-pass filter with third-order Butterworth, zero-phase digital filtering for low-pass and fifth-order Butterworth, zero-phase digital filtering for high-pass to remove low-frequency noise, and physiological interference sources. The filtering range for the band-pass filter could be defined by the users themselves according to their study objectives. In the FC-NIRS toolbox, for convenience, we provided a default band-pass range from 0.01 to 0.1 Hz, which represents the frequency range of hemodynamic signals that are thought to emanate from spontaneous neural activity.

2.2.3. Motion Correction. To reduce the motion-induced artifacts, FC-NIRS provided a spline interpolation method [29] and a correlation-based signal improvement (CBSI) method [30], respectively. Specifically, the spline interpolation method detected the motion-induced artifacts by

calculating the moving standard deviation (MSD) within sliding time windows in a window length set by the user (default: 2 seconds). MSD values larger than the threshold defined by the user (default: five standard deviations away from the mean of the MSD) are regarded as artifacts. Next, the time series that represented the motion artifacts was further modeled via a cubic spline interpolation, which was subtracted from the original signal of the time series. The resulting signal was considered to be free of motion artifacts. By contrast, the CBSI was a type of channel-by-channel method that was based on the hypothesis that HbO and HbR should be negatively correlated during functional activation, while at the same time they should be more positively correlated when a motion artifact occurred. These approaches have demonstrated an improvement in the data quality through reducing motion artifacts [29, 30].

2.2.4. Detrend. Previous studies demonstrated that systematic signal increases or decreases occurred over time due to long-term physiological shifts, with movement-related noise remaining. The linear trend is usually removed during fNIRS data preprocessing. Similar to the previous operation [4], FC-NIRS also estimated the linear trend with a least-square fit of a straight line and then subtracted it from the hemoglobin concentration signals.

2.3. Quality Control. To guarantee high quality data for the FC calculation and network analysis, a quality control module was designed to control the motion-induced artifacts and to lower the signal-to-noise ratio (SNR) that arose from poor contact between the optodes and scalp. For the head motion check, we calculated the sliding standard deviation of the time series of concentration signal to quantify the signal fluctuations within a series of sliding windows. The resulting time series of the sliding standard deviation was cut by a predefined threshold value T, and the values above the threshold value T were regarded as motion artifacts. FC-NIRS offers two types of display windows for the motion check at selected channels by clicking "Selected Channels" and the total channels by clicking "All Channels." For the SNR check of the hemodynamic signal, FC-NIRS primarily examined the signal quality from the SNR optical intensity values and the signal correlation values in the concentration signal among all of the measurement channels. Because a low SNR value (equal to the mean signal intensity divided by the standard deviation of the signal intensity over time) in fNIRS measurements represents poor contact between the optodes and scalp, the quantification of the SNR values at all of the measurement channels allowed for the examination and identification of the measurement channels with poor quality. At the same time, we assumed that low SNR signals did not reflect real brain activity (similar to noise) and that, as a result, low SNR signals should have the smallest correlation with other measurement signals. Therefore, by performing a whole-brain correlation analysis, the correlation coefficients with nearly zeros between one measurement channel and the other channels were found to represent low SNR measurements. By double-checking the motion artifacts and the SNR, high quality data were identified for the subsequent FC calculation and network analysis.

2.4. FC Calculation. FC-NIRS provides two types of approaches for the FC calculation: a seed-based correlation method and a whole-brain correlation method. Specifically, the seed-based correlation method calculated FC by estimating the strength of the pairwise relationships between the seed regions and all of the other regions in the brain [4]. The whole-brain correlation analysis calculated FC by computing the connectivity strength between any two measurement channel pairs within the entire cerebral cortex. For each method, we provided three different correlation strategies, Pearson's correlation, Cross-correlation, and Spearman's correlation, based on three different hemoglobin concentration signals. The analysis can be performed at both the individual level and group level. For the group analysis, FC-NIRS offers several statistical correlation maps, such as the R map, the Z map, the Z to R map, and the T map. The R values in the R map represent the average of the correlation coefficients across participants; the Z values in the Z map represent the average of the Z-score of the FC; the R values in the Z to R map represent the correlation coefficients that were back-transformed from the average Z values; and the t values (uncorrected) in the T map represent the t statistical values after the one-sample t-test.

2.5. Network Analysis. FC-NIRS calculated the topological properties of the brain network based on a modern graph-theoretical approach [4, 12, 18]. The graph-theory approach is a straightforward and powerful tool for characterizing the topological architecture of brain networks. In the study of the fNIRS brain network, the channels are considered to be vertices and the FCs between any two channels are considered to be edges. Therefore, fNIRS data with N nodes forms an $N \times N$ correlation matrix and each value in the correlation matrix represents the FC strength. FC-NIRS calculated the global and local network metrics based on the Gretna package (http://www.nitrc.org/projects/gretna). Specifically, the global network metrics included small-world properties (clustering coefficient, characteristic path length, normalized clustering coefficient, and normalized characteristic path length), efficiency parameters (global and local efficiency), hierarchy, and modularity coefficients. These metrics were used to characterize the global topological organization of the whole-brain network. The nodal network metrics included the nodal degree, nodal efficiency, and nodal betweenness, which were used to examine the regional characteristics of the functional brain network. Of note, the diagonal elements in the correlation matrix were automatically set to "0" before network analysis. For more details about the graph metrics, see the report from Rubinov and Sporns [31].

2.6. Experimental Validation

2.6.1. Subjects. Twenty-one healthy right-handed subjects (17 males and 4 females, aged 21 to 27 years) were recruited, and written informed consent was obtained from all of the participants prior to the experiment. This study was approved by

the Institutional Review Board of Beijing Normal University Imaging Center for Brain Research. Of note, the data used in this study were obtained from a previous experiment that examined the test-retest reliability of the graph metrics of the resting-state fNIRS brain network [18].

2.6.2. Data Acquisition. A continuous-wave (CW) near-infrared optical imaging system (CW6, TechEn Inc., MA, USA) was used to measure the variations of the HbO and HbR concentration. The system generated two wavelengths (690 and 830 nm) of near-infrared light and collected the hemoglobin-dependent signals at a sampling rate of 25 Hz. Twelve light sources (each with two wavelengths) and 24 detectors were designed to configure 46 measurement channels to allow for the whole brain (i.e., frontal, temporal, parietal, and occipital lobes) to be covered bilaterally (Figure 8(a)). The spatial separation between any adjacent source and detector pair was 3.2 cm. The positioning of the probes was set according to the international 10–20 system.

2.6.3. Data Preprocessing. The default procedures were used for data processing and analysis. These procedures included the conversion of the optical density to the hemoglobin concentration, band-pass filtering, detrending, and motion correction using CBSI. For each method, default parameters were used for data preprocessing.

2.6.4. Quality Control. We checked the quality of the fNIRS data by examining the motion artifacts and SNR. We discarded the data from 3 participants that had large motion artifacts and low SNRs.

2.6.5. FC Calculation. We adopted the seed-based correlation method to calculate the FC map in which the seed region was located in the right visual cortex region. Pearson's correlation was adopted to measure the FC strength between the seed and the other brain regions.

2.6.6. Network Analysis. Graph-theoretical approaches were used to characterize the topological properties of the fNIRS brain networks. For simplicity, we only examined the small-world feature to verify the validity of the network analysis in FC-NIRS.

3. Results

3.1. Toolbox Development

3.1.1. Download and Installation. The FC-NIRS toolbox is an open-source package, and its source code is freely available at the website http://www.nitrc.org/projects/fcnirs/. The toolbox can run under both Windows and Linux operating systems with MATLAB installed. The installation of FC-NIRS is similar to that of most MATLAB software packages. To run the package, type "FC-NIRS" in the command window of MATLAB after adding the FC-NIRS folder in the MATLAB search path. To facilitate users who do not have MATLAB installed, we generated an actual binary executable file (FC_NIRS.exe) for windows users. As shown in Figure 2, the four buttons preprocessing (Figure 3), quality control

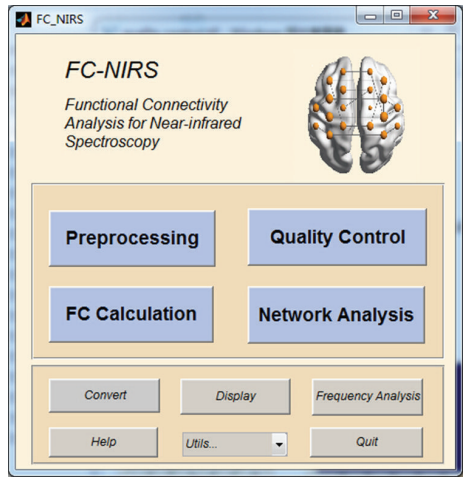

Figure 2: The main window of FC-NIRS. The four blue buttons are linked to four different functional modules, that is, preprocessing, quality control, FC calculation, and network analysis, which are shown in Figures 3, 4, 5, and 6, respectively.

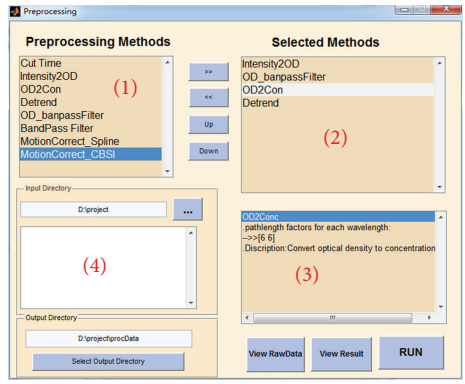

Figure 3: The preprocessing module of FC-NIRS. (1) Preprocessing methods provided by FC-NIRS; (2) preprocessing methods selected by users for data preprocessing; (3) parameter settings for selected methods; and (4) the input directory and output directory settings.

(Figure 4), FC calculation (Figure 5), and network analysis (Figure 6) are linked to four primary functional modules. In addition, a user-friendly manual is available within the packages, which provides a detailed guide for using FC-NIRS.

3.1.2. Quality Control. Figure 4(a) shows the GUI of the motion artifact check, which includes two panels that display the probe geometry (Figure 4(a)(1)) and the moving standard deviation of the concentration signals at the selected measurement channels (Figure 4(a)(2)). The window length and the threshold of the moving standard deviation in the panel can be set by clicking the "Refresh" button. FC-NIRS also offers a quick way to check the time series in all of the channels by clicking the "View TimeSeries" button. Figure 4(b) shows the GUI of the SNR check, which also includes two panels that display the SNR values at all of the measurement channels (Figure 4(b)(1)) and the correlation matrix map calculated from the whole-brain time signals (Figure 4(b)(2)).

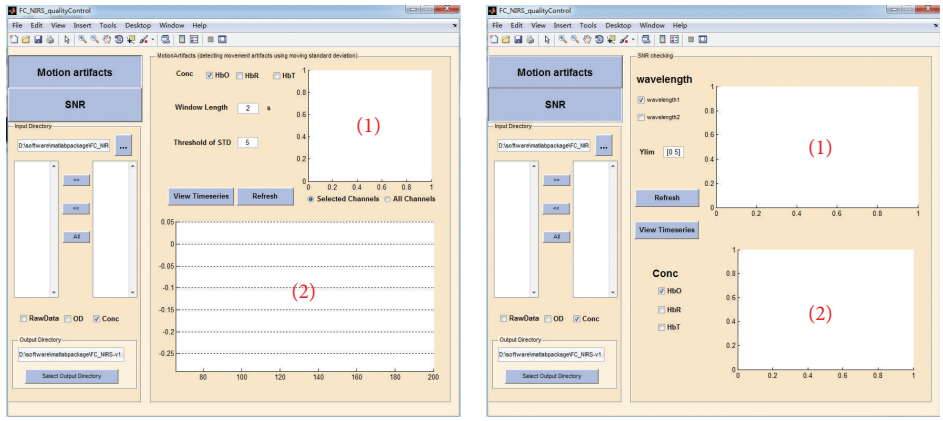

FIGURE 4: The quality control module of FC-NIRS. (a) The motion check, in which "(1)" shows the probe geometry for the imaging pad and "(2)" shows the time series of the moving standard deviation for the selected channels. (b) The SNR check, in which "(1)" shows the SNR values of all of the channels and "(2)" shows the correlation coefficients calculated from any two measurement channels.

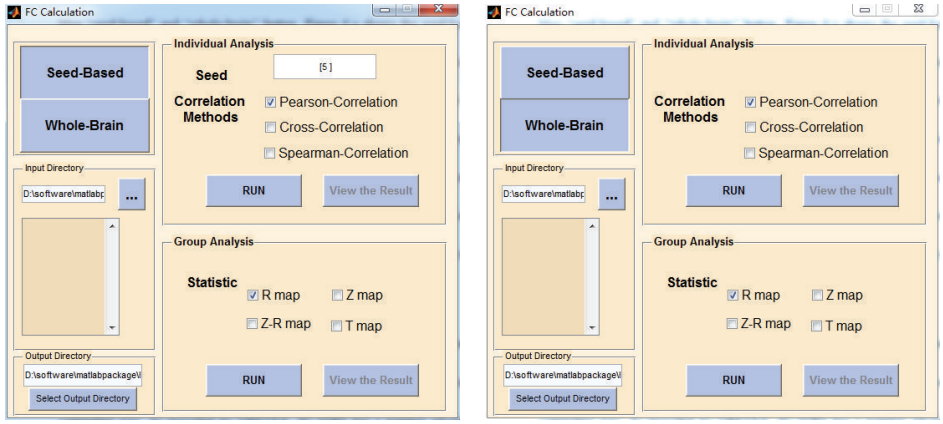

FIGURE 5: The FC calculation module of FC-NIRS. (a) The seed-based correlation analysis and (b) the whole-brain correlation analysis.

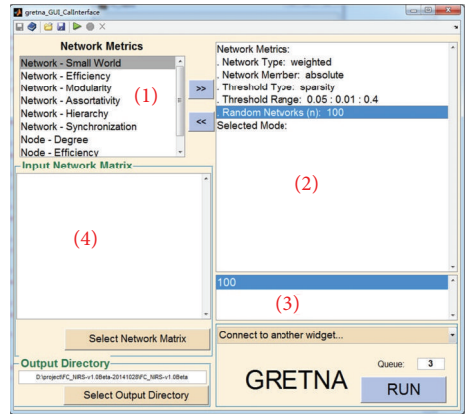

FIGURE 6: The network analysis module of FC-NIRS. Here, (1) shows the network metrics provided by FC-NIRS, (2) shows the network parameters (e.g., weight or binary network) and the selected network metrics, (3) shows the parameter settings for the selected network and network metrics, and (4) shows the input and output directory settings.

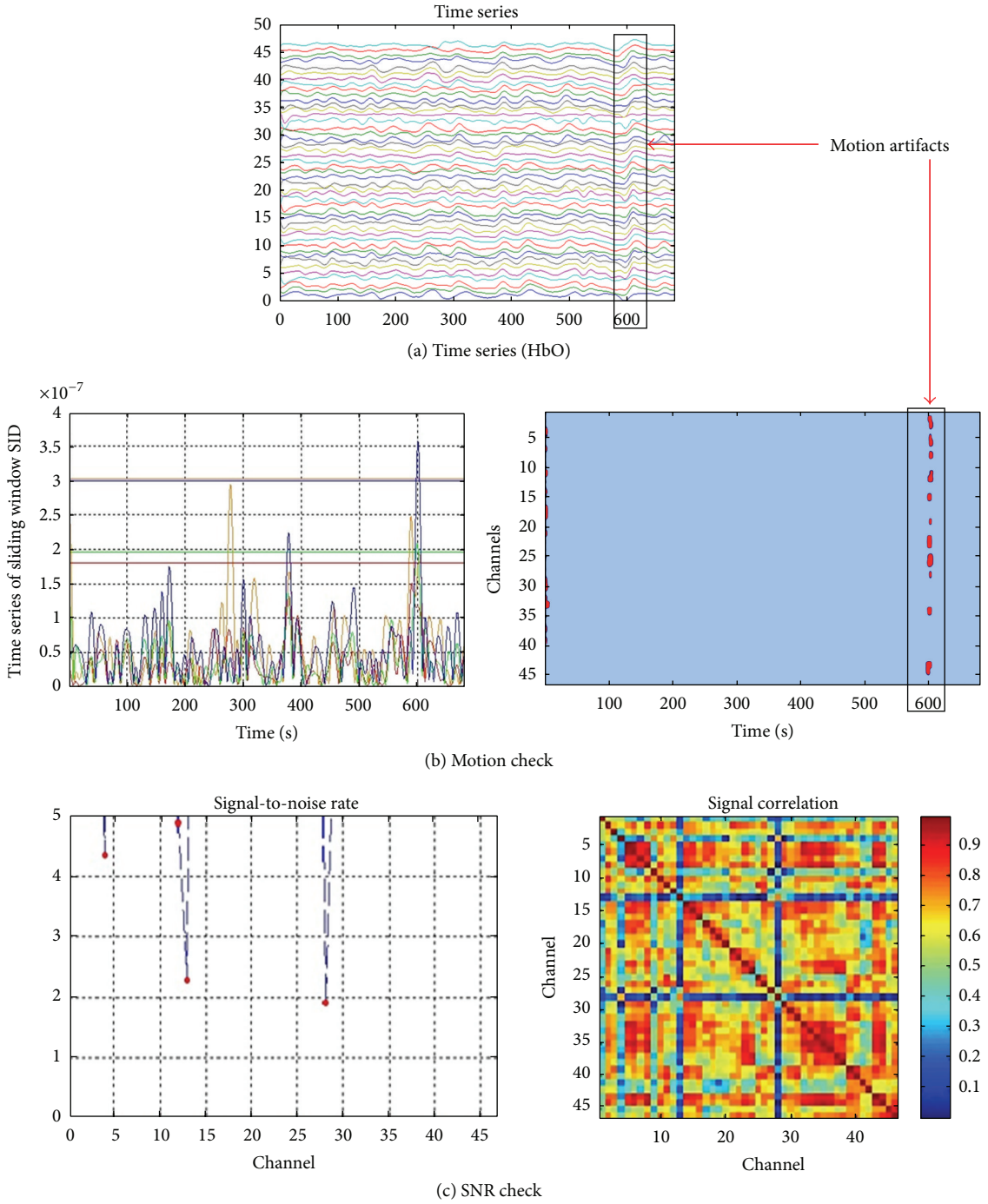

FIGURE 7: The experimental example for quality control of human brain data. (a) The time series of the hemoglobin concentration signals. A large fluctuation can be found at approximately 600 seconds. (b) The motion artifacts check. The window length is set to 2 s. The threshold is set to 5, which means that the values larger than five standard deviations from the mean are considered to be motion artifacts. (c) The SNR check. Channel 13 and channel 28 both have very low SNRs, which are computed as the mean signal intensity divided by the SD of the signal intensity over time compared with the other channels, and the corresponding signal correlation is very low. The low SNR of two channels can be caused by poor contact between the optodes and the scalp.

3.1.3. FC Calculation. Seed-based (Figure 5(a)) and whole brain-based (Figure 5(b)) FC calculation methods can be selected by pressing the "Seed-based" or "Whole-brain" button. Figure 5(a) shows the GUI of the seed-based FC calculation. Within the panel, similar to the preprocessing procedure, the users must also set the input directory and the output directory in advance. To perform individual analyses, the user must input a seed channel and select a correlation

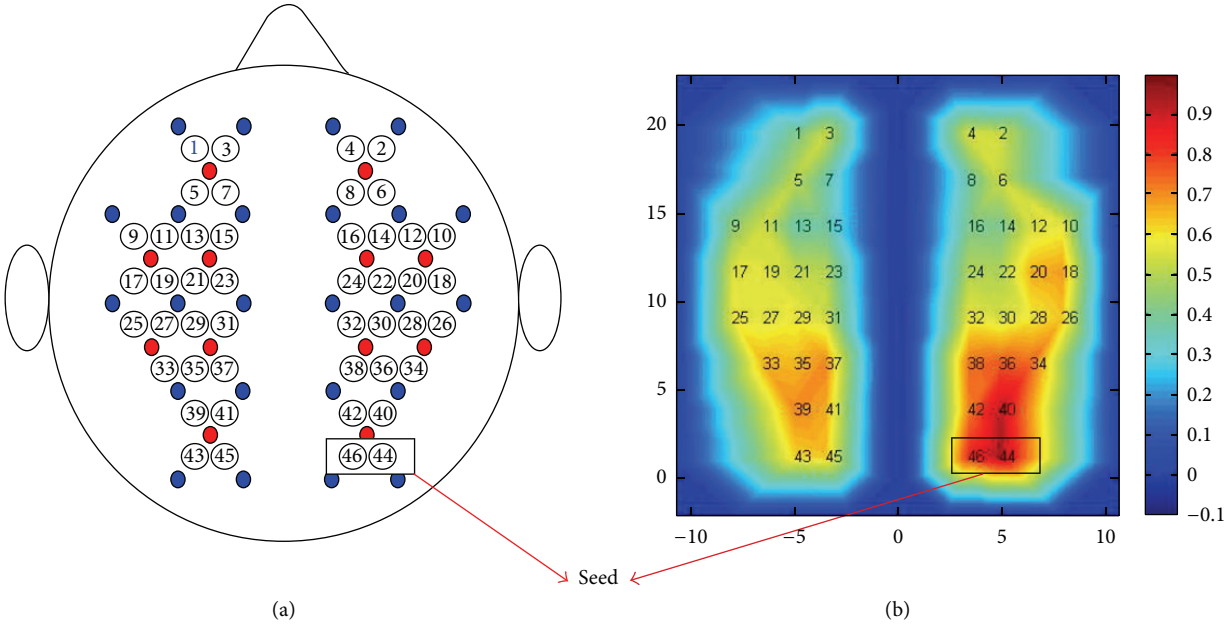

Figure 8: The results of the seed-based FC map. (a) The arrangement of the whole-brain 46-measurement channels on a brain template. (b) FC map (R map). Two channels in the black rectangle are used for the seed regions.

method in advance. Afterward, the user can click the "RUN" button to obtain the individual analysis of the seed-based FC calculation. The user can view the correlation results by clicking the "View the Result" button. For the group analysis (Figure 5(a)), several different statistical maps (i.e., the correlation R map, the Z map, the R-Z map, and the T map) are generated by pressing the "RUN" button within the group analysis panel. All of the results from both the individual and group analyses are saved in the output directory.

3.1.4. Network Analysis. Figure 6 shows the GUI of the network analysis. The network analysis must use the results of the whole-brain FC analysis as its input data (Figure 6). The module enables users to calculate the global and nodal network properties in parallel. FC-NIRS has a number of advantages for network analysis: for example, (1) it can run jobs in parallel either on a single computer with multiple cores or in a computing cluster; (2) it can generate log files and keep track of the pipeline execution; and (3) the jobs will run in the background and FC-NIRS and MATLAB can be closed after clicking the "RUN" button.

3.2. Validation

3.2.1. Quality Control. Figure 7(a) shows an example of the hemoglobin time series from a subject in which clear head motion was visually observed. With the motion detection method (i.e., the moving standard deviation method), the head motion was identified (Figure 7(b)). Notably, the moving window length was two seconds and the threshold for head motion was five times larger than the standard deviation of the moving standard deviation. In contrast, for the SNR check of the participant data, the SNR values of all of the channels are shown in Figure 7(c), from which two obviously low SNR channels (i.e., channels 13 and 28) were identified. Similarly, based on the whole-brain signal correlation analysis, we also identified two channels that had much lower correlation coefficients between them and the other measurement channels. The low correlation could be attributed to poor contact between the optodes and scalp. Based on this analysis, the subject data must be removed from the group data.

3.2.2. FC Analysis. Adopting the seed-correlation method (the seed point in the right visual cortex, Figure 8(a)), we observed bilateral FC patterns between the left and right visual regions (Figure 8(b)). The results are consistent with those of previous fNIRS investigations [11].

3.2.3. Network Analysis. Figure 9 shows the small-world properties (clustering coefficients and characteristic path lengths) of the fNIRS brain network. Compared to matched random networks, we found that the real brain network has larger clustering coefficients, C_p, and numerically similar characteristic path lengths, L_p. These results are typical features of small-world topology and are also similar to our previous results [12].

4. Discussion

In this study, we developed a MATLAB software package called FC-NIRS for analyzing brain FC and networks from fNIRS data. The toolbox includes several major functions, such as data preprocessing, quality control, FC calculation, and network topological analysis. Furthermore, FC-NIRS allows for individual analysis of a group of participants using the module "quality control" and batch processing analysis

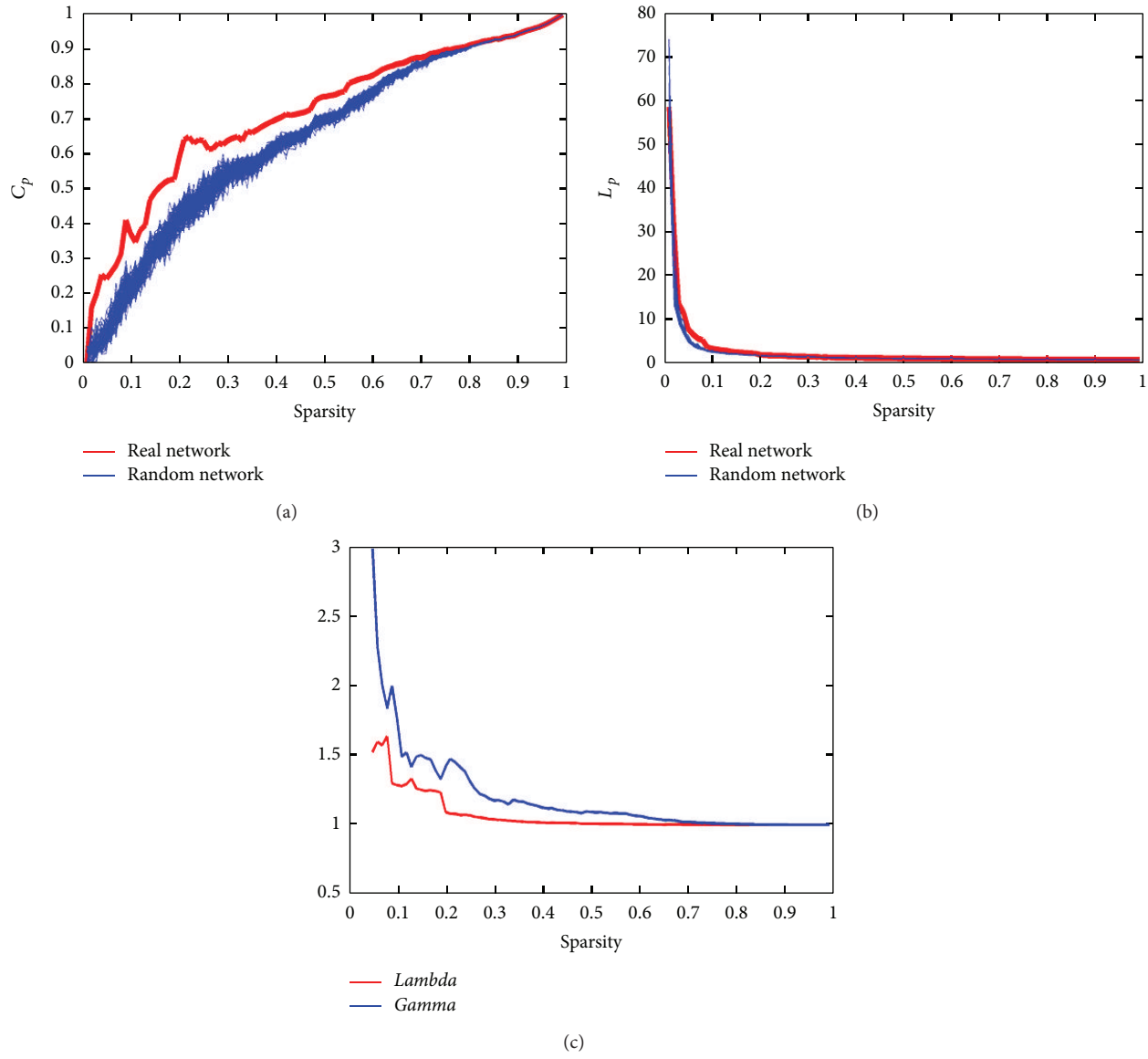

FIGURE 9: The results of the network analysis. (a) C_p is the clustering coefficient; the red line is the C_p of the real network, and the blue lines are the C_p of the random network. (b) L_p is the characteristic path length; the red line is the L_p of the real network, and the blue lines are the L_p of the random network. (c) *Lambda* is the normalized clustering coefficient, which is plotted with a red line; *Gamma* is the normalized characteristic path length, which is plotted with a blue line.

in the other modules (i.e., preprocessing, FC calculation, and network analysis), which facilitates the calculation of the FC and network matrices with both high quality control and high efficiency using FC-NIRS.

Notably, different software packages for fNIRS data processing and analysis exist, for example, the widely used Homer [21] and the recently developed NIRS-SPM [22] packages. Of note, these two tools have a focus on activation detection during task states. Different from the Homer or NIRS-SPM, our FC-NIRS tool primarily aims at FC calculation and network analysis during task free or resting states. This work fills a gap in brain network research, specifically, the previous lack of software for fNIRS data. Furthermore, FC-NIRS provides different file formats (e.g., .nirs from TechEn, Inc., and .csv from Hitachi Inc.) for data importation and analysis, which facilitates the use of different fNIRS imaging systems for FC calculation and network analysis. The ability to convert .csv files to .nirs files is also provided by FC-NIRS.

In its FC calculation and network analysis, FC-NIRS has great applicability in the field of connectivity neuroscience. For example, this tool can be applied to fNIRS datasets that are collected to study different connectivity hypotheses. Additionally, the evaluation of the effect of fNIRS imaging duration, correlation strategies, and frequency-band selection on the graphic metrics of brain network can be easily tested using FC-NIRS. Currently, the concept of "connectome" [32, 33] has been proposed to advance our understanding of comprehensively mapping and analyzing brain

FC and networks [33], and fNIRS has been considered to be a promising technique for the study of functional connectome [4], especially during early childhood development and in unconscious patients. To handle the fNIRS-based connectome dataset, FC-NIRS has unique advantages, as it can process a large number of datasets in an efficient manner because of its batch processing strategies. Therefore, FC-NIRS can potentially make contributions to the study of the functional brain connectome in the future.

In the present study, we applied FC-NIRS to generate results for testing the resting-state FC in the bilateral visual cortex as well as network topological analysis at the whole-brain scale. Symmetrical FC was found in the bilateral visual system, which is highly compatible with previous findings [11, 34]. In addition, significant small-world features were observed in the whole-brain fNIRS network, which is also highly consistent with our previous results using the same dataset [12]. The present findings confirm the usability and validity of the FC-NIRS package.

In summary, FC-NIRS can facilitate and simplify the FC and network analysis in fNIRS-related studies and can provide optional FC definitions and network topological measures. However, some improvements in the software, such as providing statistical analysis for multiple comparisons and corrections for T-maps, are still required. Because FC-NIRS includes an extendable design framework, new functions for statistical analysis or new utilities can and will be added to future releases of the software.

Conflict of Interests

The authors declare that no conflict of interests exists.

Acknowledgments

The authors sincerely thank the developers of Homer and Gretna, the functions of which are partially used by FC-NIRS. This study is supported by the Natural Science Foundation of China (Grant nos. 81201122 and 81571755), the Fundamental Research Funds for the Central Universities (Grant no. 2012LYB06), the Specialized Research Fund for the Doctoral Program of Higher Education, and the Open Research Fund of the State Key Laboratory of Cognitive Neuroscience and Learning.

References

[1] M. Ferrari and V. Quaresima, "A brief review on the history of human functional near-infrared spectroscopy (fNIRS) development and fields of application," *NeuroImage*, vol. 63, no. 2, pp. 921–935, 2012.

[2] F. Scholkmann, S. Kleiser, A. J. Metz et al., "A review on continuous wave functional near-infrared spectroscopy and imaging instrumentation and methodology," *NeuroImage*, vol. 85, part 1, pp. 6–27, 2014.

[3] S. Tak and J. C. Ye, "Statistical analysis of fNIRS data: a comprehensive review," *NeuroImage*, vol. 85, pp. 72–91, 2014.

[4] H. Niu and Y. He, "Resting-state functional brain connectivity: lessons from functional near-infrared spectroscopy," *The Neuroscientist*, vol. 20, no. 2, pp. 173–188, 2014.

[5] T. Nakano, H. Watanabe, F. Homae, and G. Taga, "Prefrontal cortical involvement in young infants' analysis of novelty," *Cerebral Cortex*, vol. 19, no. 2, pp. 455–463, 2009.

[6] H. Niu, S. Khadka, F. Tian et al., "Resting-state functional connectivity assessed with two diffuse optical tomographic systems," *Journal of Biomedical Optics*, vol. 16, no. 4, Article ID 046006, 2011.

[7] G. Taga, K. Asakawa, A. Maki, Y. Konishi, and H. Koizumi, "Brain imaging in awake infants by near-infrared optical topography," *Proceedings of the National Academy of Sciences of the United States of America*, vol. 100, no. 19, pp. 10722–10727, 2003.

[8] J. Gervain, F. Macagno, S. Cogoi, M. Peña, and J. Mehler, "The neonate brain detects speech structure," *Proceedings of the National Academy of Sciences of the United States of America*, vol. 105, no. 37, pp. 14222–14227, 2008.

[9] L. Sugiura, S. Ojima, H. Matsuba-Kurita et al., "Sound to language: different cortical processing for first and second languages in elementary school children as revealed by a large-scale study using fNIRS," *Cerebral Cortex*, vol. 21, no. 10, pp. 2374–2393, 2011.

[10] B. W. Zeff, B. R. White, H. Dehghani, B. L. Schlaggar, and J. P. Culver, "Retinotopic mapping of adult human visual cortex with high-density diffuse optical tomography," *Proceedings of the National Academy of Sciences of the United States of America*, vol. 104, no. 29, pp. 12169–12174, 2007.

[11] B. R. White, A. Z. Snyder, A. L. Cohen et al., "Resting-state functional connectivity in the human brain revealed with diffuse optical tomography," *NeuroImage*, vol. 47, no. 1, pp. 148–156, 2009.

[12] H. Niu, J. Wang, T. Zhao, N. Shu, and Y. He, "Revealing topological organization of human brain functional networks with resting-state functional near infrared spectroscopy," *PLoS ONE*, vol. 7, no. 9, Article ID e45771, 2012.

[13] C.-M. Lu, Y.-J. Zhang, B. B. Biswal, Y.-F. Zang, D.-L. Peng, and C.-Z. Zhu, "Use of fNIRS to assess resting state functional connectivity," *Journal of Neuroscience Methods*, vol. 186, no. 2, pp. 242–249, 2010.

[14] Y.-J. Zhang, C.-M. Lu, B. B. Biswal, Y.-F. Zang, D.-L. Peng, and C.-Z. Zhu, "Detecting resting-state functional connectivity in the language system using functional near-infrared spectroscopy," *Journal of Biomedical Optics*, vol. 15, no. 4, Article ID 047003, 2010.

[15] F. Homae, H. Watanabe, T. Otobe et al., "Development of global cortical networks in early infancy," *The Journal of Neuroscience*, vol. 30, no. 14, pp. 4877–4882, 2010.

[16] S. Sasai, F. Homae, H. Watanabe, and G. Taga, "Frequency-specific functional connectivity in the brain during resting state revealed by NIRS," *NeuroImage*, vol. 56, no. 1, pp. 252–257, 2011.

[17] Y.-J. Zhang, L. Duan, H. Zhang, B. B. Biswal, C.-M. Lu, and C.-Z. Zhu, "Determination of dominant frequency of resting-state brain interaction within one functional system," *PLoS ONE*, vol. 7, no. 12, Article ID e51584, 2012.

[18] H. Niu, Z. Li, X. Liao et al., "Test-retest reliability of graph metrics in functional brain networks: a resting-state fNIRS study," *PLoS ONE*, vol. 8, no. 9, Article ID e72425, 2013.

[19] B. R. White, S. M. Liao, S. L. Ferradal, T. E. Inder, and J. P. Culver, "Bedside optical imaging of occipital resting-state functional connectivity in neonates," *NeuroImage*, vol. 59, no. 3, pp. 2529–2538, 2012.

[20] M. Imai, H. Watanabe, K. Yasui et al., "Functional connectivity of the cortex of term and preterm infants and infants with

Down's syndrome," *NeuroImage*, vol. 85, part 1, pp. 272–278, 2014.

[21] T. J. Huppert, S. G. Diamond, M. A. Franceschini, and D. A. Boas, "HomER: a review of time-series analysis methods for near-infrared spectroscopy of the brain," *Applied Optics*, vol. 48, no. 10, pp. D280–D298, 2009.

[22] J. C. Ye, S. Tak, K. E. Jang, J. Jung, and J. Jang, "NIRS-SPM: statistical parametric mapping for near-infrared spectroscopy," *NeuroImage*, vol. 44, no. 2, pp. 428–447, 2009.

[23] P. H. Koh, D. E. Glaser, G. Flandin et al., "Functional optical signal analysis: a software tool for near-infrared spectroscopy data processing incorporating statistical parametric mapping," *Journal of Biomedical Optics*, vol. 12, no. 6, Article ID 064010, 2007.

[24] G. E. Strangman, Q. Zhang, and T. A. Zeffiro, "Near-infrared neuroimaging with NinPy," *Frontiers in Neuroinformatics*, vol. 3, article 12, 2009.

[25] T. Fekete, D. Rubin, J. M. Carlson, and L. R. Mujica-Parodi, "The nirs analysis package: noise reduction and statistical inference," *PLoS ONE*, vol. 6, no. 9, Article ID e24322, 2011.

[26] B. Molavi and G. A. Dumont, "Wavelet-based motion artifact removal for functional near-infrared spectroscopy," *Physiological Measurement*, vol. 33, no. 2, pp. 259–270, 2012.

[27] S. K. Piper, A. Krueger, S. P. Koch et al., "A wearable multi-channel fNIRS system for brain imaging in freely moving subjects," *NeuroImage*, vol. 85, pp. 64–71, 2014.

[28] L. Kocsis, P. Herman, and A. Eke, "The modified Beer-Lambert law revisited," *Physics in Medicine and Biology*, vol. 51, no. 5, pp. N91–N98, 2006.

[29] F. Scholkmann, S. Spichtig, T. Muehlemann, and M. Wolf, "How to detect and reduce movement artifacts in near-infrared imaging using moving standard deviation and spline interpolation," *Physiological Measurement*, vol. 31, no. 5, pp. 649–662, 2010.

[30] X. Cui, S. Bray, and A. L. Reiss, "Functional near infrared spectroscopy (NIRS) signal improvement based on negative correlation between oxygenated and deoxygenated hemoglobin dynamics," *NeuroImage*, vol. 49, no. 4, pp. 3039–3046, 2010.

[31] M. Rubinov and O. Sporns, "Complex network measures of brain connectivity: uses and interpretations," *NeuroImage*, vol. 52, no. 3, pp. 1059–1069, 2010.

[32] C. Kelly, B. B. Biswal, R. C. Craddock, F. X. Castellanos, and M. P. Milham, "Characterizing variation in the functional connectome: promise and pitfalls," *Trends in Cognitive Sciences*, vol. 16, no. 3, pp. 181–188, 2012.

[33] O. Sporns, G. Tononi, and R. Kötter, "The human connectome: a structural description of the human brain," *PLoS Computational Biology*, vol. 1, no. 4, article e42, 2005.

[34] H. Zhang, Y.-J. Zhang, C.-M. Lu, S.-Y. Ma, Y.-F. Zang, and C.-Z. Zhu, "Functional connectivity as revealed by independent component analysis of resting-state fNIRS measurements," *NeuroImage*, vol. 51, no. 3, pp. 1150–1161, 2010.